The isotopic evolution of the British lithosphere

Thesis

THE ISOTOPIC EVOLUTION OF THE BRITISH LITHOSPHERE

A thesis presented for the degree of

Doctor of Philosophy

by

GARETH REES DAVIES

B.Sc. Hons. University of Leicester 1979

Department of Earth Sciences

The Open University

November 1983

PAGE NUMBERING AS ORIGINAL

I confirm that I am willing for my thesis to be made available to readers and may be photocopied, subject to the discretion of the Librarian.

S R Davies

8.5.84

Abstract

A Sm-Nd mineral isochron obtained from an olivine gabbro yields an age of 375 $\pm$ 34 Ma (M.S.W.D. = 0.006) and represents the formation age of the Lizard Igneous Complex. Two magmatic suites are recorded in the complex, an early trace element enriched (εNd_{375} = + 8.9 - + 10.1) and a late MORB-like (εNd_{375} = + 9.2 - + 11.7). The early magmatic suite records a decoupling between low Sm/Nd and high $(^{143}Nd/^{144}Nd)_{375}$ ratios and indicates that the low Sm/Nd ratios were generated immediately prior to the petrogenesis of the early magmatic suite, due to either i) L.REE enrichment of the source or ii) enrichment processes during magma genesis.

The marked L.REE depletion of the spinel lherzolites, which comprise the majority of the Lizard peridotite, reflects multiple, small percentage (<10%), melt extraction from the rocks while in the garnet stability field. The petrology and Sm-Nd isotope systematics of the plagioclase and pargasite peridotites record the local infiltration of a melt. Significantly the Sm-Nd isotope systematics of the "metasomatised" peridotites are the same as the calculated sources of the dolerite dyke suites and are probably equivalent to these, at depth, sources.

Two suites of metabasaltic rocks occur in the Mona Complex (Anglesey), the Gwna Group ($(Ce/Yb)_N$ = 0.6 - 2.1) and New Harbour Group ($(Ce/Yb)_N$ = 0.3 - 0.5). The Gwna Group yield a whole-rock Sm-Nd isochron of 595 $\pm$ 86 Ma (M.S.W.D. = 1.5) with an initial ratio equivalent to εNd of 7.1 $\pm$ 1.0. This isochronous relationship and large variation in the degree of L.REE enrichment indicates, as in the case of the early magmatic suite of the Lizard Complex, that the low Sm/Nd ratios were generated immediately prior to the petrogenesis of the metabasalts.

Nd model ages of the Mona gneisses, a sediment and the Coedana Granite, in conjunction with the age of the Gwna Group, argue for an origin of the entire Mona Complex during the late Precambrian.

The Lower Palaeozoic subduction related volcanism of south east Ireland occurs in 2 distinct suites, north and south of the Leinster Granite. The southern suite has trace element, Sr and Nd isotope systematics equivalent to the present day calc alkaline volcanism of Java. It is estimated that 80% of the Sr and 50% of the Nd in these rocks are slab derived. The northern tholeiitic suite is markedly trace element enriched, and the rocks show a correlation between their Sm/Nd and $(^{143}Nd/^{144}Nd)_I$ ratios, and the % of slab derived Nd. The calculated Sr/Nd ratio of the slab component is 19, such that mixing lines between slab and mantle wedge components are straight lines on an εSr vs εNd diagram. It is not possible to distinguish between an ancient LILE and L.REE enrichment event, circa 1100 Ma, or sediment subduction to account for the isotopic systematics of the slab component.

The dioritic primary magma to the Leinster Granite is predominantly derived from juvenile lower crust. The maximum mantle component involved in the diorites' petrogenesis is 30% and the maximum T_{CHUR} age of the lower crust is 720 Ma. The primary dioritic magma assimilated Lower Palaeozoic sediments and fractionated a plagioclase, K feldspar and biotite assemblage, resulting in the production of granitic rocks with more and less radiogenic Sr and Nd isotope ratios respectively.

Lower curstal xenoliths from central Ireland and the Midland Valley of Scotland indicate that crustal accretion occurred during both Grenvillian and Late Precambrian times. The N.E. Ox Mountains inlier also provides evidence of a Late Precambrian crust forming event (605 $\pm$ 39 Ma). (No evidence of Archaean crust is found in these regions.) The lower crustal garnet granulite xenoliths from Ireland and the Midland Valley represent possible crustal components involved in the petrogenesis of both the pre and post-tectonic Caledonian granites of Central Scotland.

The majority of basement rocks of southern Britain formed during the Late Precambrian with only the Rushton Schists and Rosslare Complex having Nd and Sr isotope systematics characteristics of old, >1300 Ma, crust. Late Precambrian and Cambro-Ordovician sediments have Nd isotope systematics equivalent to the majority of the Late Precambrian basement rocks. Subsequent to the closure of the Iapetus Ocean the sedimentary pile within southern Britain records the gradual introduction of an "ancient" crustal component, presumably from the mixed Archean/Proterozoic terrains of northern Europe. A steady state is reached by Jurassic times such that present day coastal sediments have equivalent Nd isotope systematics to those of Jurassic sediments.

Acknowledgements

I would like to express my thanks to everyone at the Open University and the following individuals in particular:

My supervisor, Chris Hawkesworth, for helpful guidance and constructive criticism of early drafts of this work. Other members of the Isotope Research Group, particularly Andy Gledhil and Peter van Calsteren who organised the smooth functioning of both the mass spectometer and the chemistry laboratories, most of the time!

Members of the Department of Earth Sciences for their help; Andy Tindle and Phil Potts for electron microprobe instruction, Ian Chaplin and Moira Staerck for the rapid production of thin sections, John Taylor, Helen Boxall and Jenny Munn for cartographic advice, Nick Rogers, Martin Menzies, Julian Pearce, Paul Browning, Steve Roberts and Steve Lippard for stimulating discussions and advice.

I am greatly indebted to the following people who supplied samples and unpublished data; Fred Frey, Brian Upton, Peda Aspen, Rob Barnes, Peter Strogen, Mike Max, J. Winchester, Richard Thorpe, Chris Stillman, Bob Beckinsale, Jane Evans, Steve Daly, Ian Sanders, John Watson, Andy Gledhill, P. Bruck , Steve Richardson , Padrig Kennan and Andy Tindle.

Joy Clark for typing this thesis and the Open University for funding.

My parents for their unfailing support and encouragement, and finally Joanne who drew all the maps and complicated diagrams, compiled the reference list and provided mental, financial and physical support, most of the time!

CONTENTS

LIST OF FIGURES

Chapter I

Introduction

Combined Nd and Sr isotope studies have been widely used over the past 10 years to examine the petrogenesis of basaltic rocks and hence to infer the nature of physical and chemical processes occurring within the mantle (DePaolo and Wasserburg, 1976a and b, O'Nions et al., 1977 and 1979). Similar studies, combined with trace element analyses, are carried out in this work to constrain the nature of the mantle beneath Britain.

The Rb-Sr decay system has been used extensively to date crustal rocks and to study the Earths crustal evolution (Moorbath, 1978). Recent Nd isotope studies of crustal rocks have suggested, due to the lack of fractionation in the Sm/Nd ratios of crustal rocks by crustal processes (i.e. weathering, metamorphism, and intra-crustal melting (McCulloch and Wasserburg, 1978)), that it may be possible to see back through the effects of regional metamorphism. In particular it should be possible to ascertain the periods of major crustal accretion within an area and to trace the evolution of crustal material through the sedimentary cycle significantly more precisely than using Rb-Sr isotope systematics. This work aims to constrain the crustal evolution of southern Britain.

1:1 The Chondritic Earth model. The isotopic data reported in this thesis are discussed with respect to a model based on the chondritic evolution of the whole Earth. U-Th Pb and Rb-Sr ages of circa 4.55 Ga have been obtained from chondritic and achondritic meteorites (Tatsumoto et al., 1976 and Manhes et al., 1978). It is assumed that the solar nebula was homogeneous with respect to its $^{143}Nd/^{144}Nd$ ratio and hence the chondrites define the Earths' initial $^{143}Nd/^{144}Nd$ ratio. Sm and Nd are not volatile and have similar physical and chemical properties such that during condensation of the solar nebula there should be little variation in the Sm/Nd ratios between the protoplanets. This hypothesis is

substantiated by the work of Jacobsen and Wasserburg (1980) who demonstrated that there is only a circa 4% range in the majority of the Sm/Nd ratios determined on 64 chondritic meteorites. The chondrites studied by Jacobsen and Wasserburg (op. cit.) have indistinguishable initial $^{143}Nd/^{144}Nd$ ratios (.506609 calculated at 4.6 Ga). All $^{143}Nd/^{144}Nd$ ratios quoted in this thesis are normalised to a $^{146}Nd/^{144}Nd$ ratio of 0.7219. This initial ratio and the average Sm/Nd ratio from the Jacobsen and Wasserburg study, 0.325, are used in this study to define the Nd isotope evolution of the whole earth. Significantly, as shown in Figure 3:4, most Archean rocks analysed to date have initial ratios close to the chondritic evolution curve defined by Jacobsen and Wasserburg suggesting that a chondritic Sm/Nd ratio for the whole earth is probably a valid assumption.

DePaolo and Wasserburg (1976) and O'Nions et al. (1977) demonstrated that present day oceanic basaltic rocks have anticorrelated $^{143}Nd/^{144}Nd$ and $^{87}Sr/^{86}Sr$ ratios. The intersection of this "mantle array" with the postulated bulk earth $^{143}Nd/^{144}Nd$ ratio is used to define the present bulk earth $^{87}Sr/^{86}Sr$ ratio, 0.7047. Having made this assumption the bulk earth $^{87}Rb/^{86}Sr$ ratio may be calculated using the initial ratio of chondrites/achondrites at 4.6 Ga; $(^{87}Sr/^{86}Sr)_I$ = 0.69898 (Papanastassiou and Wasserburg, 1969). The calculated $^{87}Rb/^{86}Sr_{BE}$ = 0.0847, is significantly lower than in chondrites.

1:2 Crust - Mantle Evolution. In marked contrast to the approximate chondritic initial $^{143}Nd/^{144}Nd$ ratios of Archean rocks, younger rocks show significant variations. In order to compare directly the initial ratios of rocks of different ages Nd and Sr isotope results are often reported relative to the bulk earth values using the εNd and εSr notation introduced by DePaolo and Wasserburg (1976). The initial isotope ratio of a sample formed t million years ago is presented as fractional deviations from the isotope ratio of a uniform reservoir (UR) at

the same time.

Neodymium

$$\varepsilon_{Nd}^{UR} = \left[\frac{^{143}Nd/^{144}Nd \text{ sample } (t)}{^{143}Nd/^{144}Nd_{UR}\ (t)} - 1 \right] \times 10^4$$

Strontium

$$\varepsilon_{Sr}^{UR} = \left[\frac{^{87}Sr/^{86}Sr \text{ sample } (t)}{^{87}Sr/^{86}Sr_{UR}\ (t)} - 1 \right] \times 10^4$$

In practice terrestrial samples are considered relative to the estimated bulk earth values and the UR postscript is omitted.

The εNd values of recent basalts are illustrated in Figure 1:1 and demonstrate that the majority are derived from sources depleted relative to bulk earth values. In contrast Figure 1:1 shows that the majority of crustal rocks are enriched relative to bulk earth values. This is the result of the relative enrichment of Nd compared to Sm in crustal rocks and hence low Sm/Nd ratios. A significant aspect of the Sm/Nd systematics of crustal rocks is that the major fractionation in their Sm/Nd ratios occurs during mantle derivation and subsequent crustal processes have minimal effect (McCulloch and Wasserburg, 1978). The Nd model age of a crustal rock can therefore be used to examine its mantle derivation age, provided it has not undergone mixing with other rock types. Nd model ages, T_{UR}^{Nd}, are an expression of how long a rock has had a Sm/Nd ratio different from that of a uniform reservoir (see Figure 1:2)

Figure 1:1

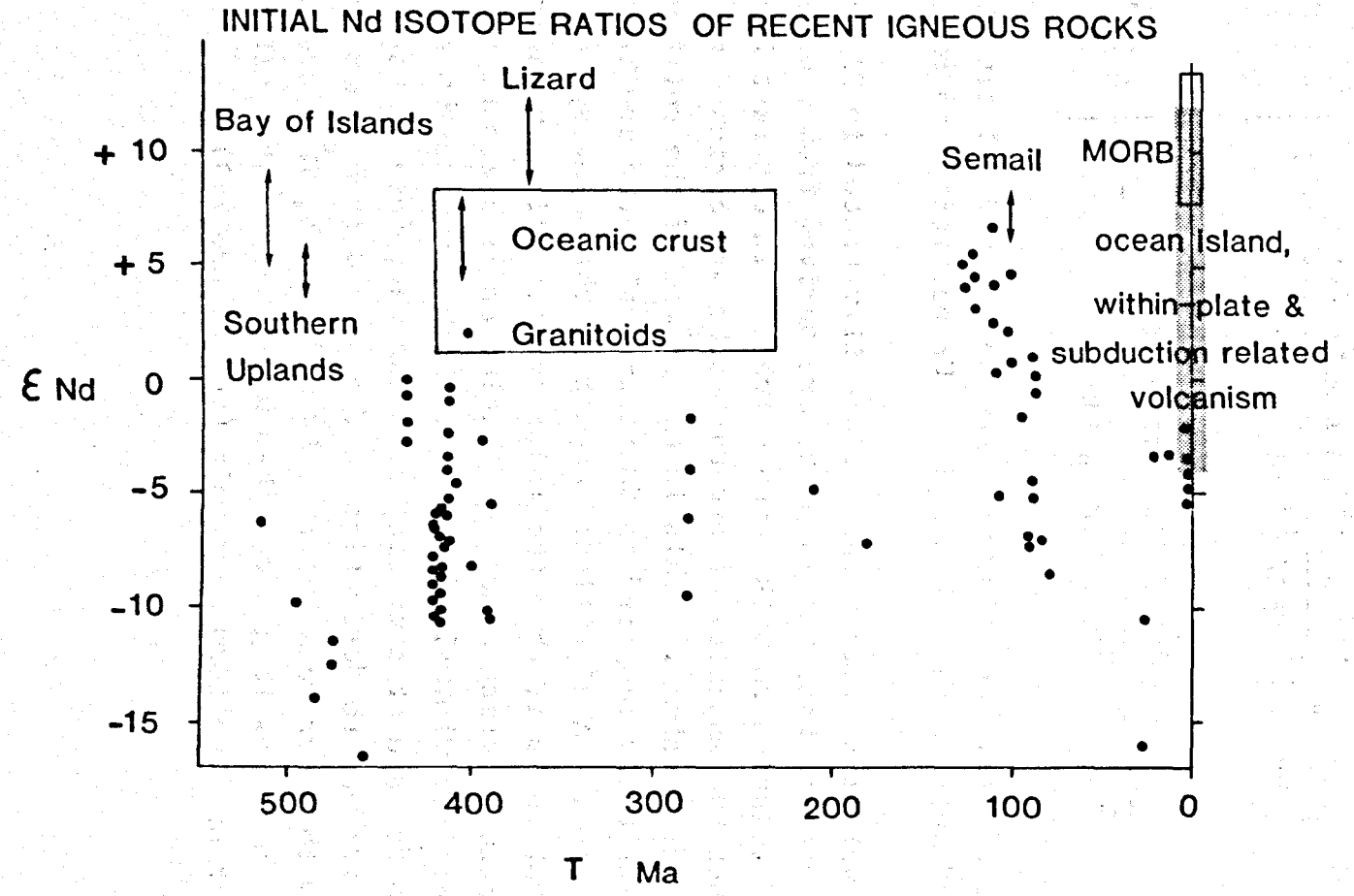

Data sources: DePaolo and Wasserburg (1976a, b), Richard et al (1976), O'Nions et al (1977), Carter et al (1978), Jacobsen and Wasserburg (1979b), Allegre and Othman (1980), Hamilton et al (1980a), McCulloch et al (1980), DePaolo (1981b), Hawkesworth et al (1981), Hooker etal (1981), Duyverman et al (1982), McCulloch and Chappell (1982).

Figure 1:2a

Sm-Nd ISOTOPE EVOLUTION DIAGRAM

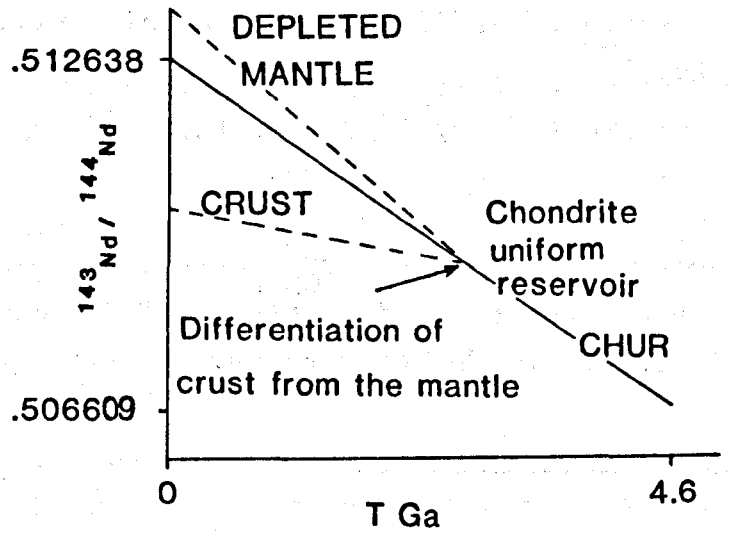

Figure 1:2b

Sm-Nd ISOTOPE EVOLUTION DIAGRAM EXPRESSED IN TERMS OF ε Nd

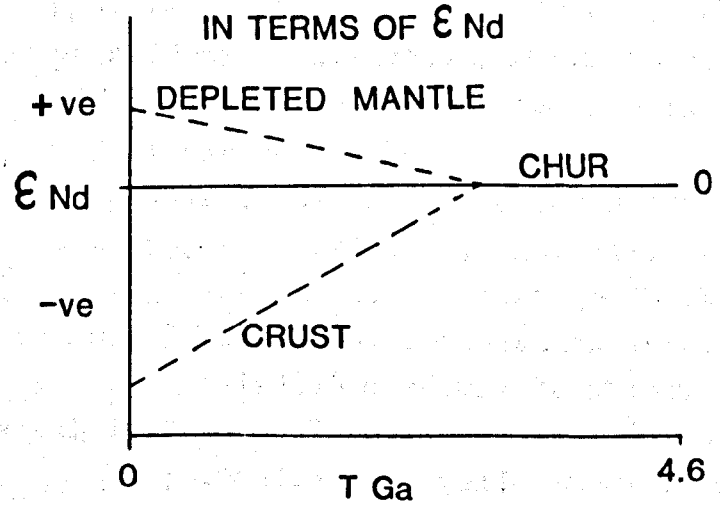

$$T_{UR}^{Nd} = \ln\left[\frac{(^{143}Nd/^{144}Nd)_S - (^{143}Nd/^{144}Nd)_{UR} + 1}{(^{147}Sm/^{144}Nd)_S - (^{147}Sm/^{144}Nd)_{UR}}\right]$$

Two uniform reservoirs are considered in this work;

i) chondritic, T_{CHUR}^{Nd}

ii) depleted mantle ($^{143}Nd/^{144}Nd = 0.51310$ $^{147}Sm/^{144}Nd = 0.2282$, T_{DM}^{Nd}

In order to distinguish between T_{CHUR}^{Nd} ages of L.REE enriched and depleted rocks the term "depletion age" is used in this thesis for isotopically depleted rocks.

1:3 Objectives of this thesis

The main objectives of this thesis are to study two aspects of the British Lithosphere.

i) The trace element and isotopic characteristics of the mantle beneath southern Britain and to establish the nature of mantle processes responsible for the depletion/enrichment events.

ii) The age of the major crustal accretion events in Britain and the degree of subsequent crustal reworking.

To this aim the following complexes and rock types are studied for Nd and Sr isotopes;

i) Lizard Complex

ii) Precambrian basement complexes of southern Britain

iii) Granitoids of southern Britain

iv) Lower crustal xenoliths from central Ireland and the Midland Valley of Scotland.

v) Precambrian to Jurassic sedimentary rocks of southern Britain.

Chapter 2

Trace Element and Nd Isotope Evolution of the Lizard Complex

The Lizard peridotite represents the largest exposed fragement of mantle in Britain (Figure 2:1). This chapter presents a combined geochemical and Nd isotope study of the peridotites and the associated igneous and metamorphic lithologies with the aim of establishing their age, origin and inter-relationships.

2:1 General Geology

The Lizard Complex forms a peninsular on the south coast of Cornwall with an aerial extent of circa 40 sq. miles. Inland exposure is poor, consequently most research has concentrated on the coastal sections. Peridotites comprise over half the complex; gabbro and various types of amphibolite the remainder (Figure 2:1). Recent boreholes (Styles and Kirby, 1980) and seismic experiments (Brooks et al., 1981) have established that the peridotite body is a relatively thin sheet (< 1km) as originally proposed by Sanders (1955).

Recent authors have interpreted the association of peridotite, gabbro and the sheeted dykes at Porthoustock as part of an ophiolite sequence (Bromley, 1976, Strong et al., 1975, Badham and Kirby, 1976 and Styles and Kirby, 1980). The ophiolitic assemblages occur in two tectonic units (see Figure 2:1 and 2:2) associated with amphibolites. There are two forms of amphibolite found within the Lizard Complex, i) Traboe Schists and ii) Landewednack Schists (Figure 2:1 and 2:2). Characteristically the Traboe Schists are coarse grained amphibolites with a pronounced,but folded, foliation. The rocks are variably deformed and within low strain regions relict igneous textures and cumulate layering are found (e.g. north of Porthoustock). This suggests a gabbroic precursor for the Traboe Schists. In marked contrast the Landewednack Schists

Figure 2:1 GEOLOGICAL MAP OF THE LIZARD COMPLEX

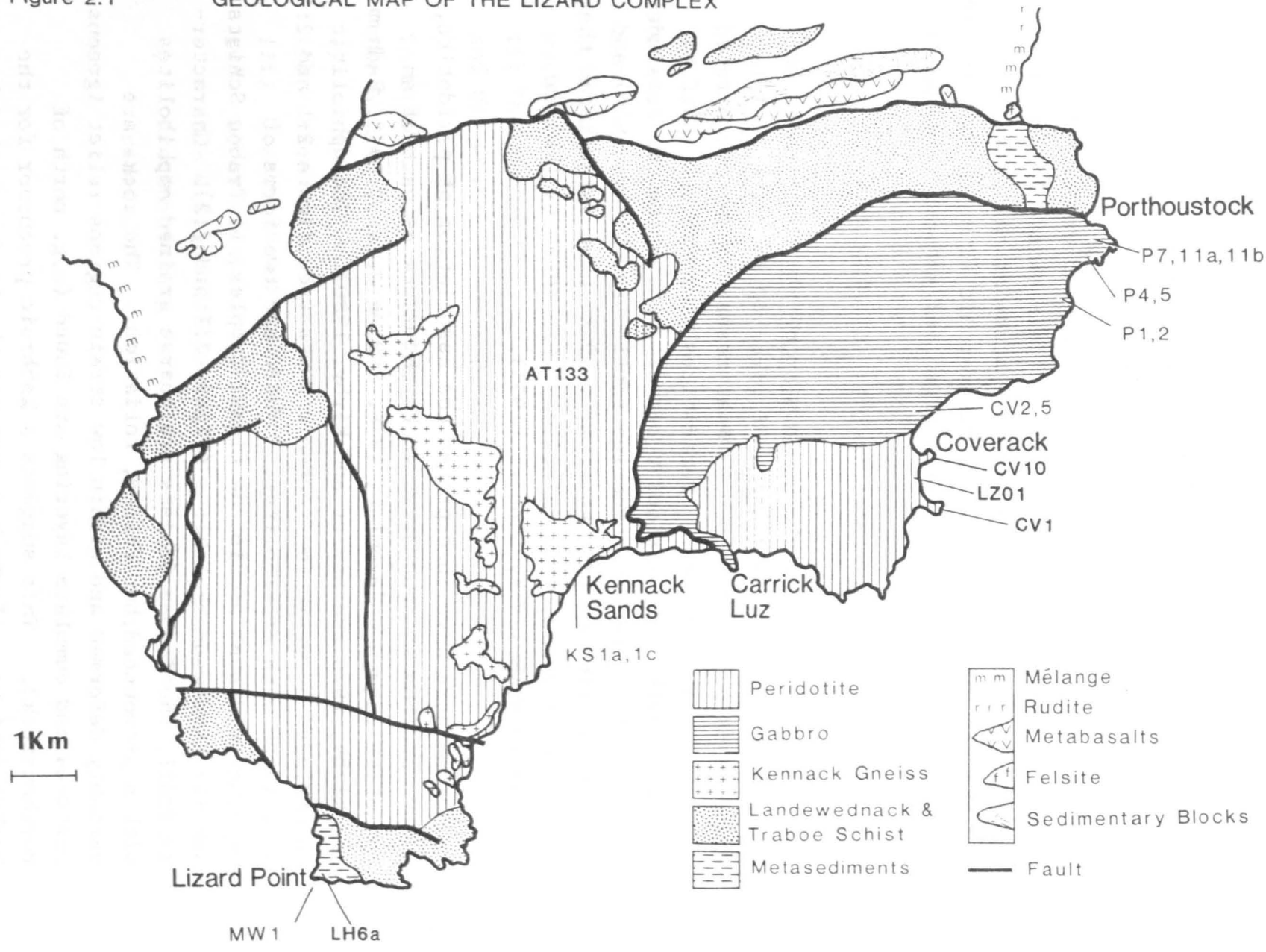

Figure 2:2 SKETCH GEOLOGICAL CROSS-SECTION OF THE LIZARD COMPLEX

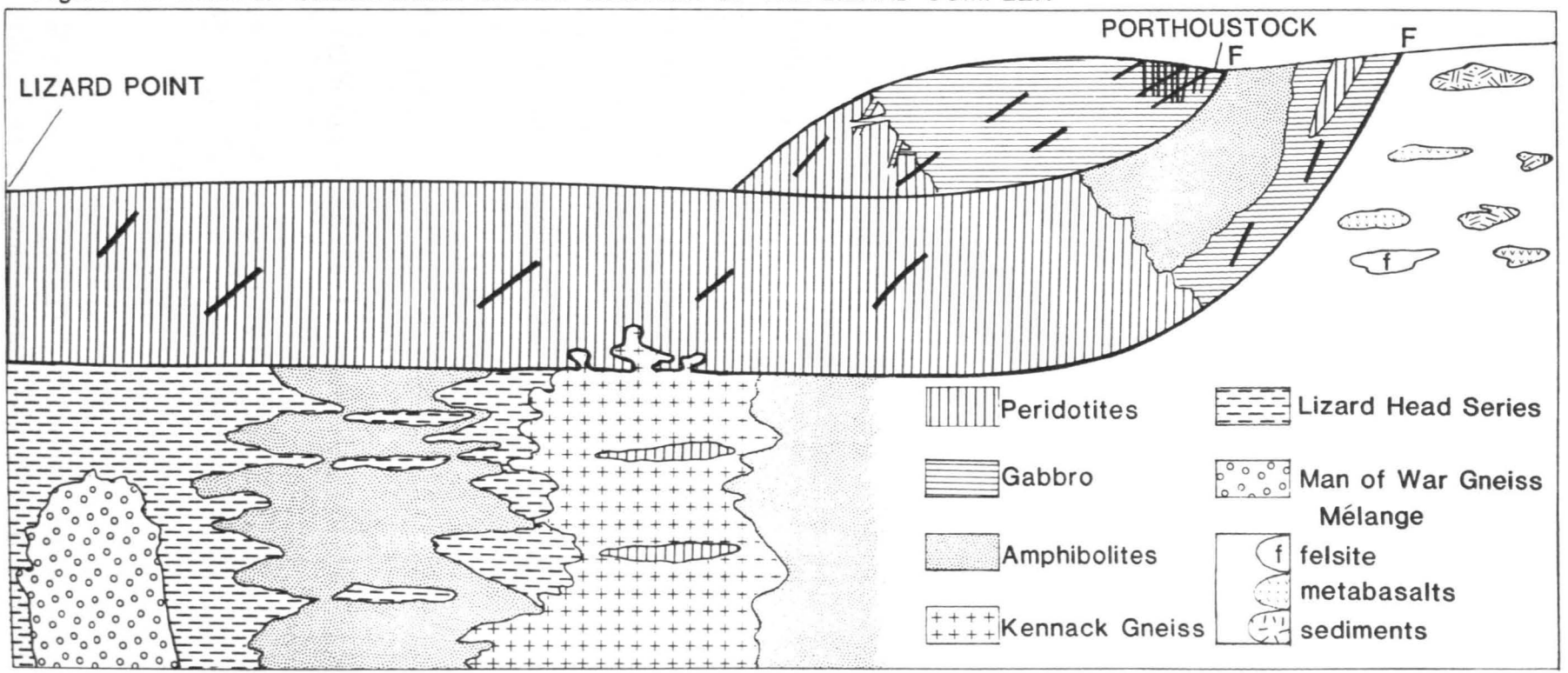

are fine grained, massive, black rocks with a well developed mineral lineation. From a geochemical study Kirby (1979) interpreted this rock type, which occurs both within and beneath the ophiolitic units, as of a metavolcanic origin (basalts or basaltic tuffs).

Structurally beneath the ophiolitic units three other rock types are recognised; i) Lizard Head Series, ii) Man of War Gniess, iii) Kennack Gneiss. The Lizard Head series is comprised of a group of predominantly pelitic sediments with subordinate volcanics. The rocks have suffered moderate to high temperature metamorphism, garnet being ubiquitous, and have a flat lying fabric apparently parallel to the original bedding. Locally small quartzo feldspathic segregations, that cross cut the fabric, are developed indicating that the metasediments reached partial melting conditions. The second rock unit, the Man of War Gneiss, is a dioritic gneiss that has a deformed but intrusive contact with the Lizard Head metasediments (Flett and Hill, 1914). The foliation within the gneiss is parallel to that within the metasediments. Thirdly the Kennack Gneiss is an extremely heterogeneous suite of metamorphic rocks ranging in composition from amphibolite to granite. The rocks are intimately associated with the base of the ophiolitic units and in places the granitic gneisses cross cut the basal thrust. A borehole at Kennack Sands demonstrated that in that area the gneisses are > 155m thick and they contain numerous peridotite bodies (Styles and Kirby, 1980). Several hypotheses have been proposed for the origin of the Kennack Gneiss including;

i) Archean migmatites predating the peridotites (Bonney, 1877)

ii) Composite basic and acid intrusions post dating the peridotites (Flett, 1946 and Green, 1964a)

iii) Migmatites derived from the amphibolites (Sanders, 1955).

Recent authors have argued that the gneisses reflect anatexis of a mixed volcano-sedimentary pile (Lizard Head Series and Landewednack Schists) during and subsequent to the emplacement of the ophiolitic assemblage (Kirby, 1979, Bromley, 1979 , Vernacombe, 1980, Styles and Kirby, 1980).

Anatexis is only rarely found associated with the emplacement of ophiolites, e.g. in Oman, where temperature estimates of the metamorphic conditions within the amphibolitic metamorphic sole are between 765 and 900°C (Searle and Malpas 1980, Ghent and Stout, 1981). Although not high enough to cause large scale partial melting of basic amphibolites these temperatures could result in extensive melting of wet sediments as my have been present in the precursors to the Kennack Gneiss.

North of the Lizard Complex (boundary marked by the Lizard Boundary Fault) there are a succession of low grade metasediments. The rocks comprise a group of arenaceous slump breccias with a variety of lithological blocks incorporated within a shale matrix. The blocks (some up to 2 km long) include basaltic pillow lavas, acid volcanics and limestones, the latter vary from Ordovician to Middle Devonian in age. Leveridge (1977) reports Upper Givetian (Middle Devonian) fossils preserved in the shale matrix. The association has been interpreted as a mélange and correlated with similar rocks in the Roseland/Dodman Point area of Cornwall (Barnes and Andrews, 1981).

In order to establish a possible genetic relationship between the mélange and the Lizard Complex, the pillow lavas and gneissose clasts from conglomerate beds within the mélange have been analysed. Significantly the metamorphic grade recorded in the mélange (both in the shale matrix and the basaltic blocks) only reached 300°C and 2 to 4 Kb (Barnes and Andrews in press), which is significantly lower than that recorded by the metasediments of the Lizard Complex. There is no evidence of the Lizard Complex overprinting the low grade regional metamorphic assemblage suggesting that either;

i) The Lizard Complex had cooled prior to emplacement (Barned and Andrews in press) or

ii) The thermal aureole developed by the emplacement of the Lizard Complex was of a very local extent.

However, due to the possible large and late movement of the Lizard Boundary Fault, relative to the emplacement of ophiolitic sequence into the crustal rocks, the two formations may not have been juxtaposed until significantly after the formation of the Kennack Gneiss during ophiolite obduction.

This chapter is principally concerned with the geochemical and Nd isotope nature of the ophiolite rocks and their source regions. Detailed petrological descriptions of the major rock types within the ophiolitic units are therefore given below.

2:2 Peridotites

Flett and Hill (1914) originally mapped the peridotite body as 3 concentric serpentinite intrusions; tremolite serpentinite, dunite serpentinite, and bastite serpentinite. Green (1964b) concluded that this classification roughly reflected a zonation in grain size, degree of mylonitisation and recrystallisation, and subdivided the ultramafic rocks into one primary and two recrystallised (hydrous and anhydrous) assemblages. In order to by pass the genetic implications of Green's terminology, the standard Streckeisen nomenclature will be used in this study;

	Green's Terminology
Spinel Lherzolite	- Primary Peridotite
Plagioclase Lherzolite	- Recrystallised anydrous Peridotite
Pargasite Lherzolite / Harzburgite	- Recrystallised hydrous Peridotite

2:2:1 Spinel Lherzolite. The composition of the spinel lherzolite varies within certain limits, 65 to 75% olivine 15 to 24% enstatite, 6 to 10% clinopyroxene and 1 to 3% spinel. The texture of this rock type, where not extensively sheared and recrystallised, is porphyroclastic being characterised by large (>0.5 cm), usually strained, porphyroclasts of enstatite,

olivine and rarely diopside in a fine grained matrix (< 1mm) of unstrained (polygonal) grains (Figure 2:3a to c). Interestingly the porphyroclastic texture is that most commonly found in ultramafic xenoliths and alpine type peridotites (Mercier and Nicholas, 1974, Neilson and Schwarzman, 1976). Due to the extensive serpentinisation, the size, shape and deformation state of the porphyroclastic olivines are difficult to establish. The enstatite porphyroclasts have irregular ovoid outlines with curved grain boundaries. Deformation of these porphyroclasts is marked, kink bands are common, often curved (Figure 2:3b), locally possibly of 2 generations. Exsolution lamellae of clinopyroxene are ubiquitous. Significant re-equilibration is indicated by the absence of exsolution and kink bands at the edge of the porphyroclasts. The most striking feature of the enstatite porphyroclasts is that they enclose, or are embayed by, rounded olivine grains (Figure 2:3b and 2:4b). Dick (1977) suggested that a similar texture in the Josephene Peridotite was produced by the breakdown of orthopyroxene to olivine plus melt during partial melting. If this is the case it should be noted that the porphyroclasts have undergone a complex deformational history subsequent to the melting episode.

The matrix is composed of equant unstrained olivines and enstatites, the latter have no clinopyroxene exsolutions. Diopsides generally forms small clusters of grains (< 0.3 mm) that are interstital to olivine. These grains tend to be concentrated at triple junctions and may extend as narrow septa along grain boundaries. This suggests interstitial crystallisation, presumably from trapped liquid remaining after inefficient melt extraction.

The spinel phase within the spinel lherzolite is generally olive green and occurs in two forms;

i) small (< 1mm) anhedral and interstitial
ii) large (5mm) subhedral almost porphyroclastic (Figure 2:3c)

Photomicrographs of Spinel Lherzolites

Figure 2:3a; Sample 2553 x.p.l. field of view = 6 mm

Extensively serpentinised polygonal olivine porphyroclasts, circa 1 mm. The rock shows variable deformation which results in local recrystallisation of enstatite porphyroclasts, e.g. area A - A.

Figure 2:3b; Sample 2553 x.p.l. field of view = 6 mm

Enstatite porphyroclast (1 cm) showing undulose extinction as the result of curved kink bands. Clinopyroxene exsolution lamallae are thin and also curved. Note the lack of exsolution lamallae and kink bands at the edges of the porphyroclasts indicating re-equilibration. Small rounded olivines are enclosed within the enstatite porphyroclast, (A).

Figure 2:3c; Sample 2553 p.p.l. field of view = 6 mm

Subhedral almost porphyroclastic olive green spinel, sensu stricto.

Figure 2:3d; Sample CV1 p.p.l. field of view = 6 mm

Skeletal spinel (chromite) surrounded by altered plagioclase in a region of high deformation and serpentinisation.

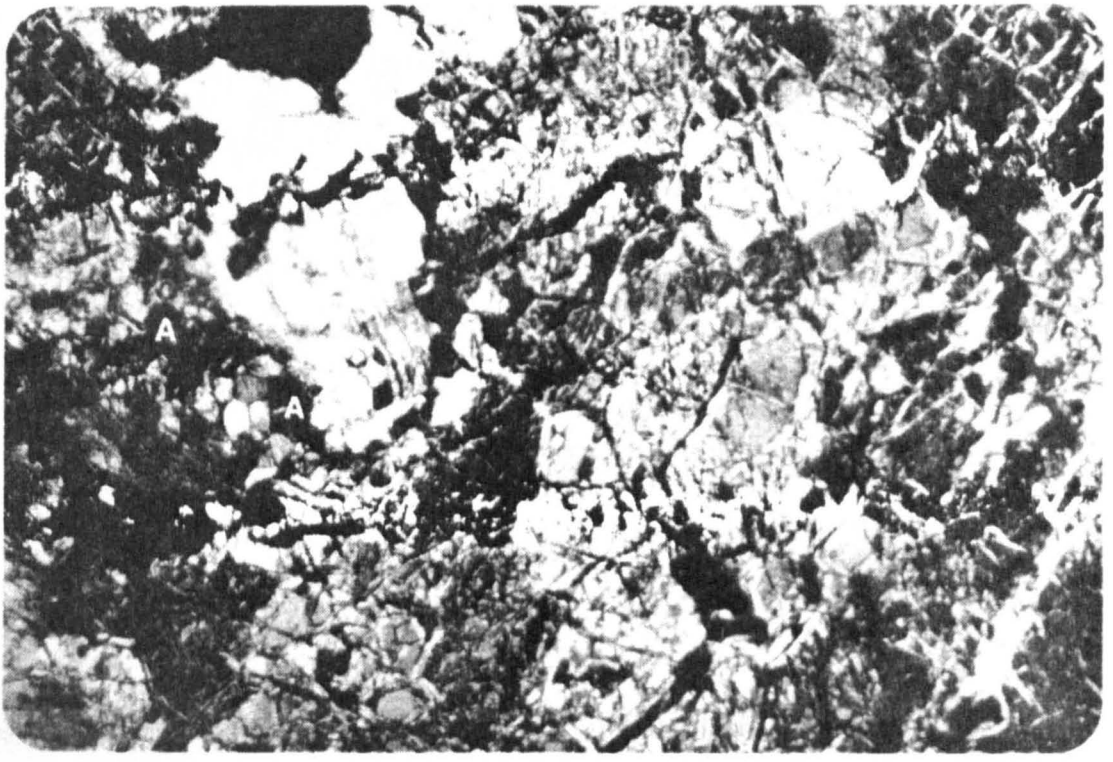

Figure 2:3a Spinel Lherzolite 2553

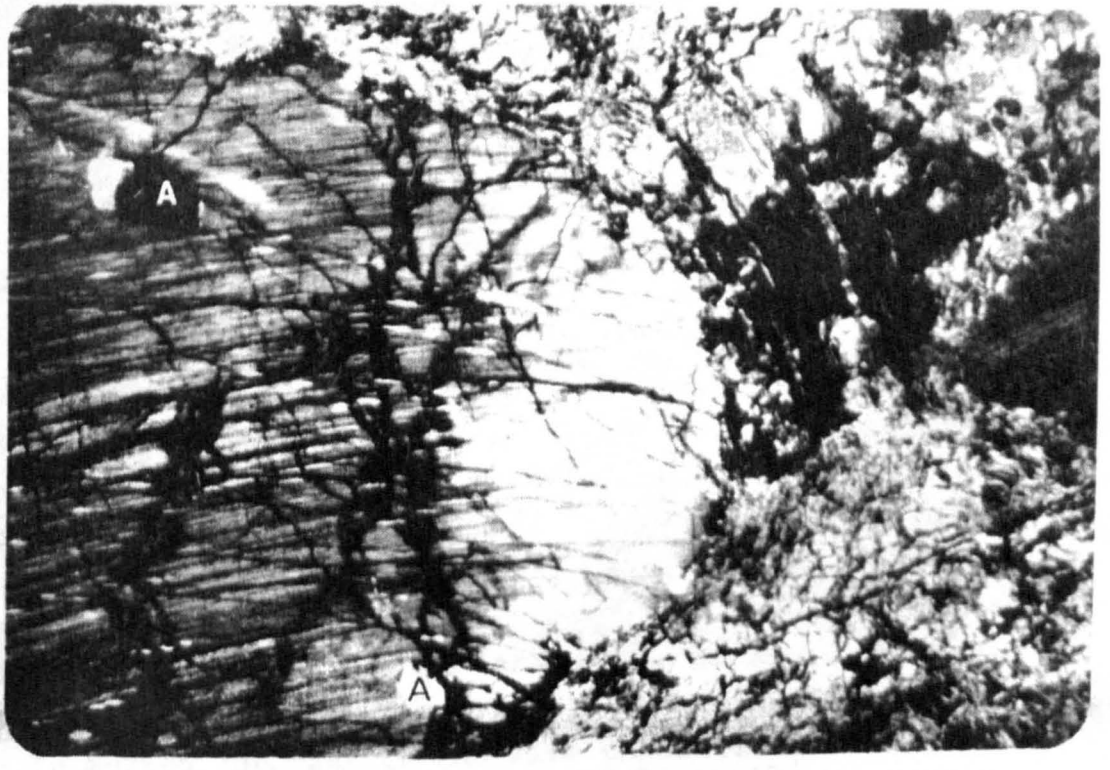

Figure 2:3a Spinel Lherzolite

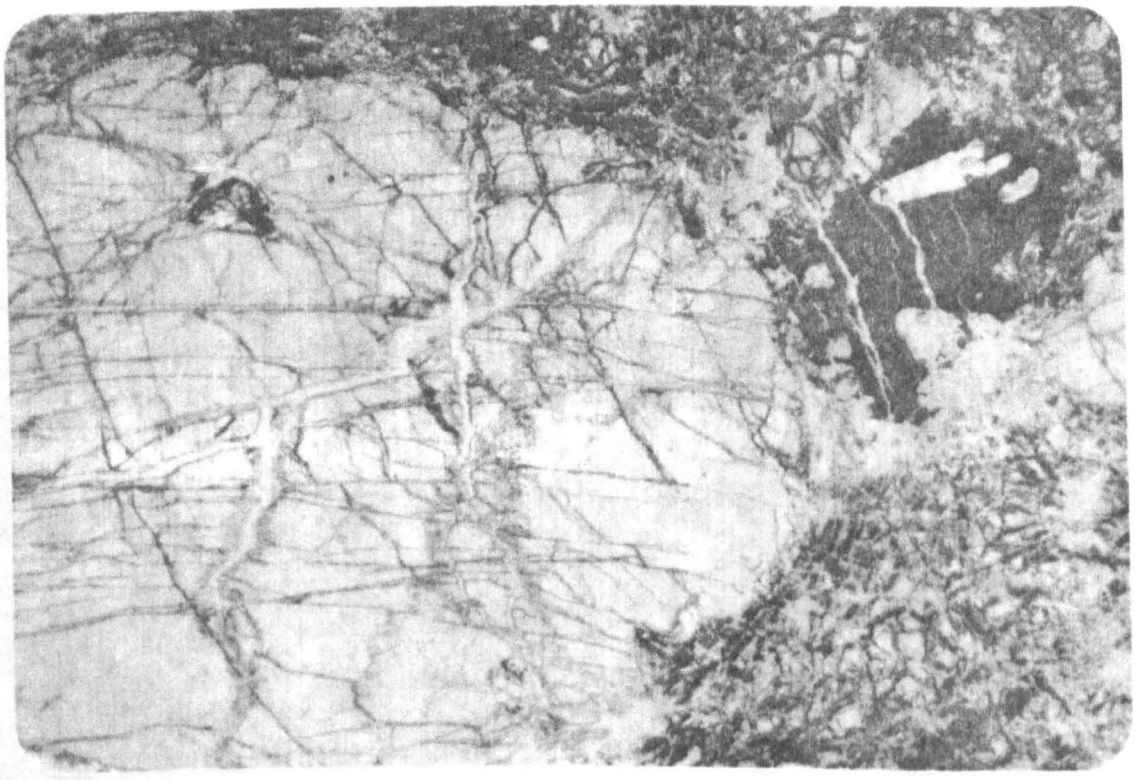

Figure 2:3c Spinel lherzolite 2553

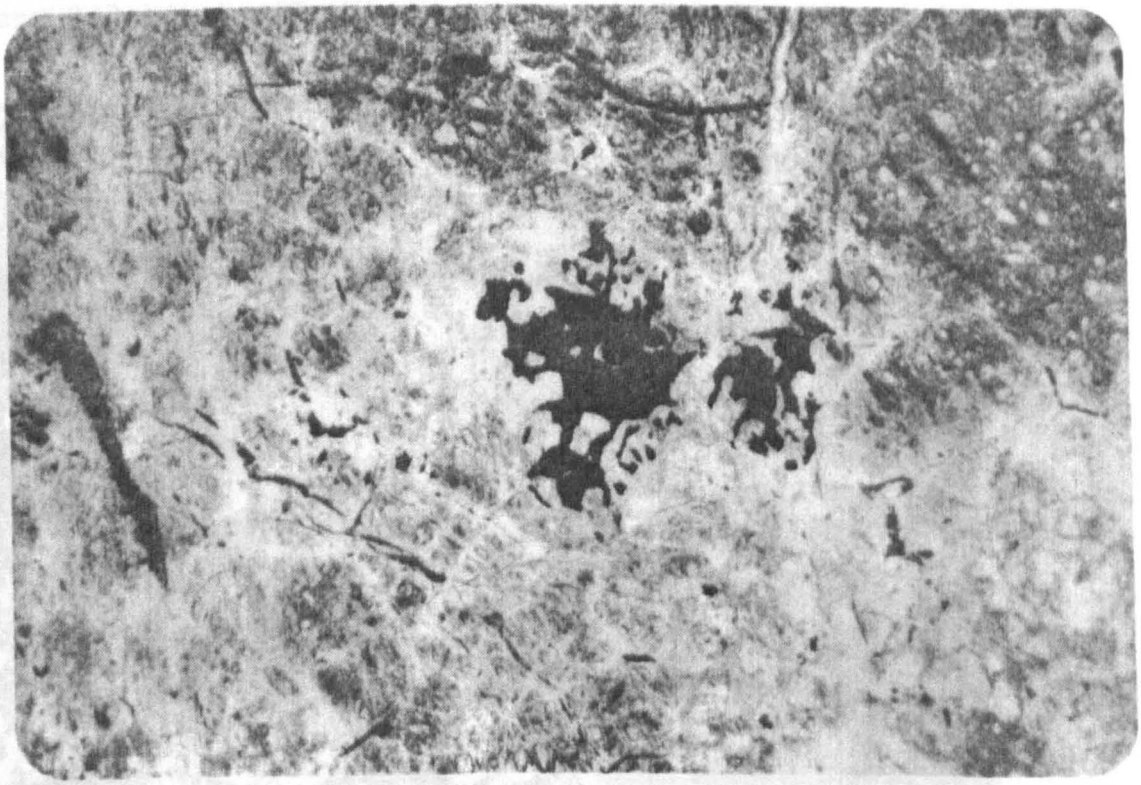

Figure 2:3d Spinel lherzolite CV1

In the more deformed rocks the spinel occurs in a skeletal form, chromite, surrounded by plagioclase (Figure 2:3d).

In outcrop the spinel lherzolite is usually amorphous but occasionally shows mineralogical banding on a 1 to 20 cm scale. The banding is formed by modal variations in the pyroxene content. Dunite pods, with significant amounts of chromite, 2 to 20%, and pyroxenite bands and dykes are also found within the spinel lherzolite.

2:2:2 Plagioclase Lherzolite. The plagioclase lherzolite occurs in two distinct forms, generally being fine grained with a marked foliation. In outcrop weathering picks out the foliation and a crude mineral lineation. Altered plagioclase is often visible in outcrop. In thin section the rock can be seen to have been intensely sheared forming a fine grained foliated matrix in which enstatite augen (0.1 to 0.5cm) are commonly recrystallised parallel to the foliation. The composition of the rock is difficult to establish due to the intense shearing and serpentinisation but it is approximately 75% olivine, 15% enstatite, 5 to 8% diopside, 2 to 5% plagioclase, 1 to 3% chromite and 0 to 2% pargasite. Plagioclase, which usually encloses small subhedral chromites (1mm), forms interstitial patches that are usually extensively altered. Occasionally these altered patches can be seen to be partially replaced by pargasite (Figure 2:5d). However, there are regions of relatively undeformed plagioclase lherzolite (70% olivine, 20% enstatite, 7 to 10% diopside, 5% plagioclase and 1 to 3% chrome rich spinel). The texture is similar to that of the spinel lherzolites i.e. porphyroclastic (Figure 2:4a). The enstatite porphyroclasts are distinctly more anhedral than in the spinel lherzolite but they still enclose, or are embayed by, rounded olivines. Kink bands are less well developed in the enstatite porphyroclasts of this rock type but again the porphyroclasts have no exsolution or sign of deformation at their margins. Clinopyroxene exsolution lamellae are irregular forming anhedral blobs in marked contrast to the fine exsolution lamellae in the spinel lherzolites (Figure 2:4b). Enstatite porphyroclasts

Photomicrographs of Plagioclase Lherzolites

Figure 2:4a; Sample LZ01 x.p.l. field of view = 6mm

Enstatite prophyroclasts embayed by, or enclosing, rounded olivines. Interstitial plagioclase is marked with a "p" and generally shows albitic twinning. A plagioclase rich vein (2:4 d) lies to the left of this photograph.

Figure 2:4b; Sample LZ01 x.p.l. field of view = 6 mm

As above but showing the extensive plagioclase and clinopyroxene exsolution caused by melt infiltration. The clinopyroxene exsolutions are more anhedral compared to those within the spinel lherzolites. Again note no exsolution at the margins of the porphyroclasts.

Figure 2:4c; Sample LZ01 x.p.l. field of view = 3 mm

Anhedral plagioclase and subhedral chromite exsolved in an enstatite porphyroclast in a region of melt infiltration.

Figure 2:4d Sample LZ01 x.p.l. field of view = 4 mm

Part of a large region of plagioclase, 1 cm, running to the N.E. and S.E. of the photograph. The plagioclase shows albite twinning and poikilitically encloses euhedral chromite and rounded olivines which in turn may enclose euhedral chromite.

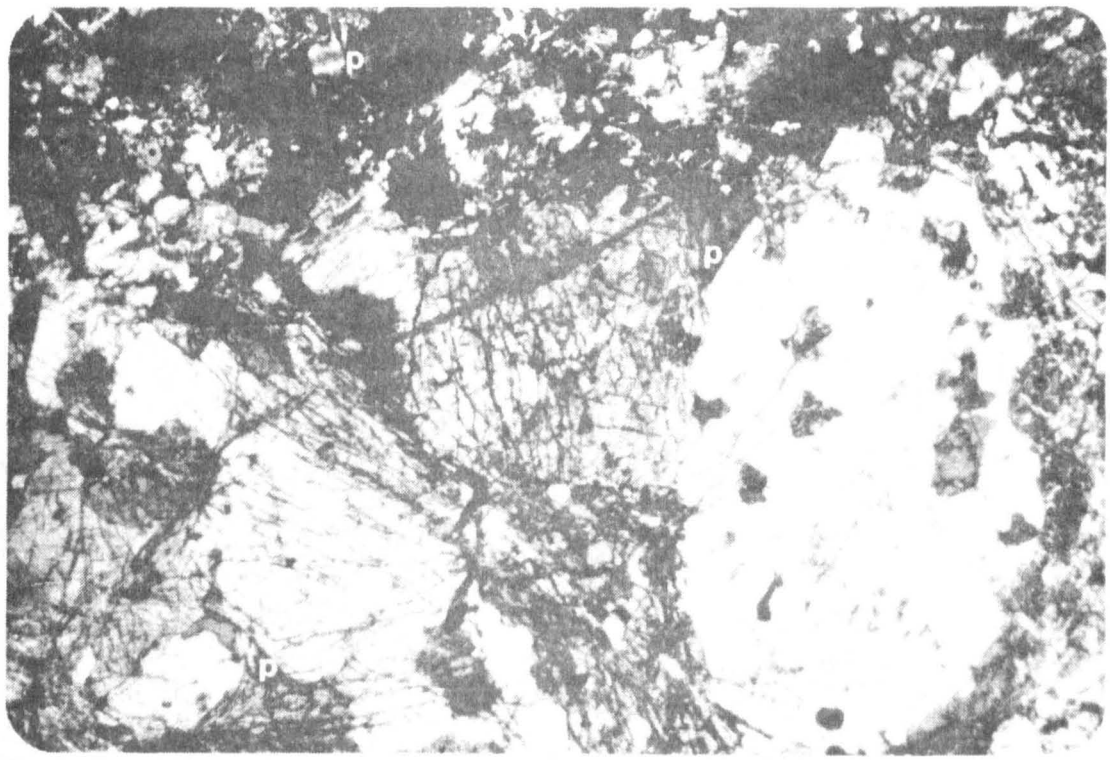

Figure 2:4a Plagioclase lherzolite LZ01

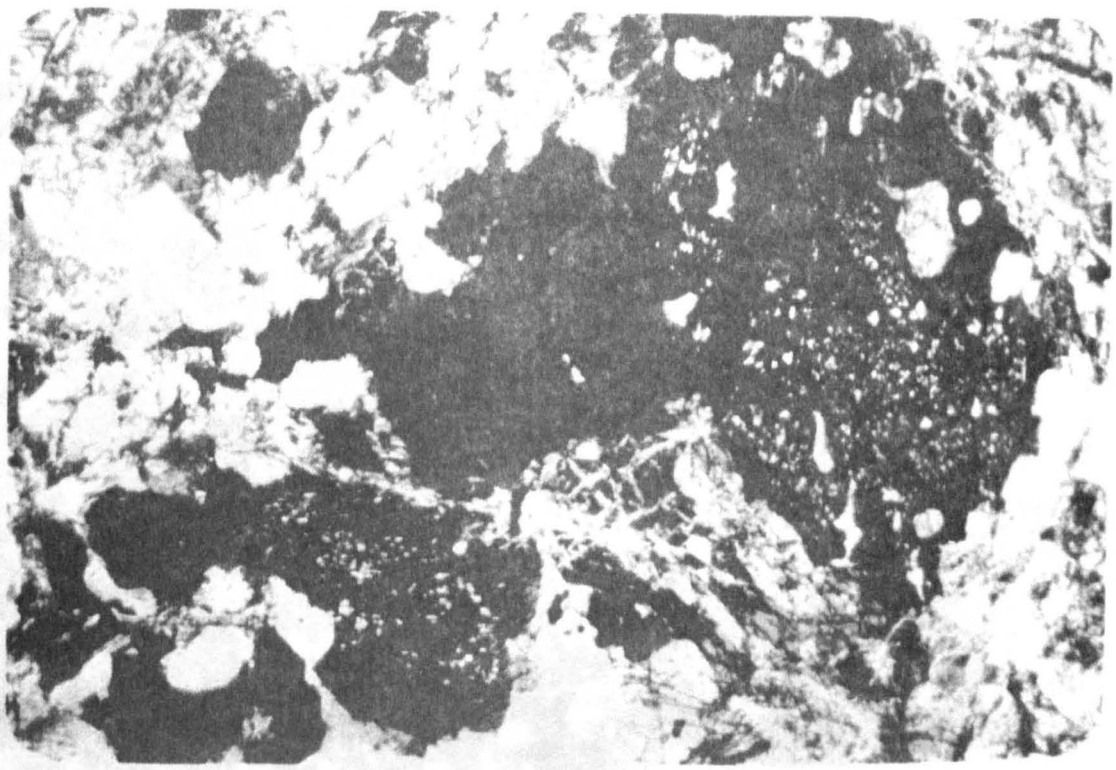

Figure 2:4b Plagioclase lherzolite LZ01

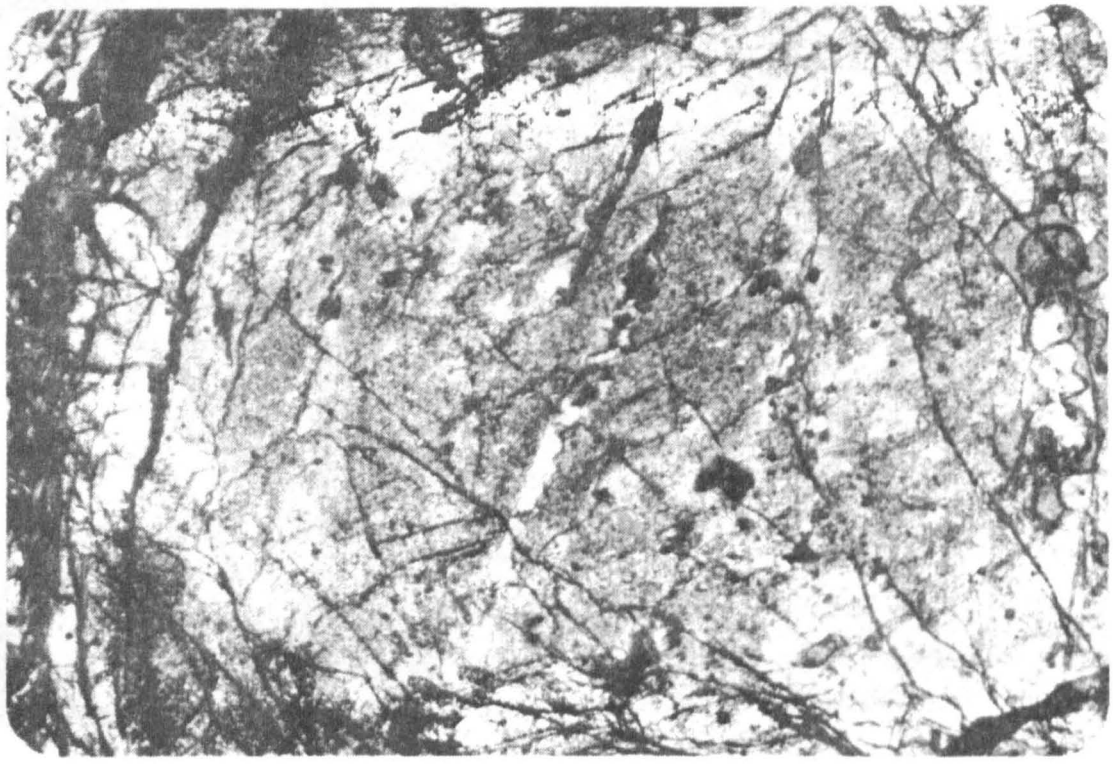

Figure 2:4c Plagioclase lherzolite LZ01

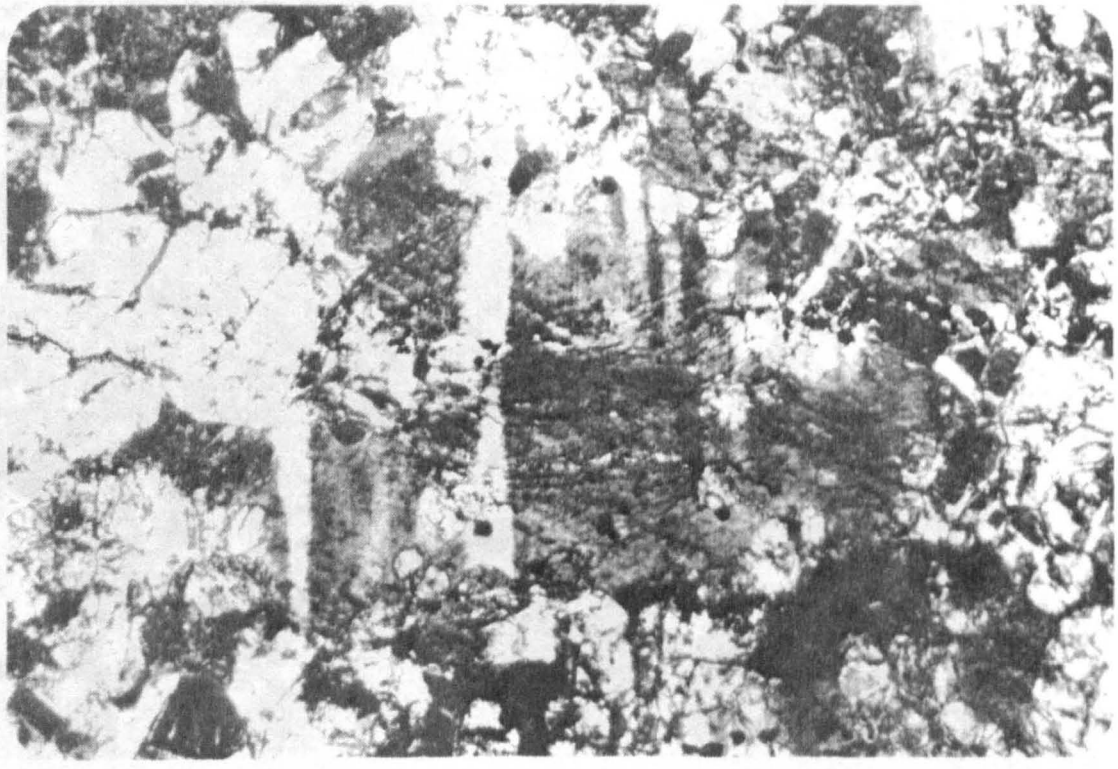

Figure 2:4d Plagioclase lherzolite LZ01

adjacent to plagioclase rich regions have exsolved plagioclase and small (0.001mm) euhedral chromite grains (Figure 2:4c) suggesting that the enstatites have undergone considerable re-equilibration resulting in the exsolution of aluminous rich phases.

The matrix is composed predominantly of equant olivines and enstatites. As in the spinel lherzolites, diopside occurs as small clusters of grains with septa between olivine grain boundaries. Chrome spinel occurs in two forms; i) large skeletal grains (up to 2 mm) generally surrounded by plagioclase (Figure 2:3d). This form apparently originated as the result of the re-equilibration of the porphyroclastic olive green spinels found within the spinel lherzolites with the associated exsolution of plagioclase. ii) The second chrome spinel form occurs as small enhedral grains (0.05 mm) poikilitically enclosed in plagioclase or within olivines within the plagioclase (Figure 2:4d). Plagioclase forms elongate patches, up to 1cm in length, interstitial to the pyroxene porphyroclasts and encloses small (0.02mm) rounded olivines and euhedral enstatites (0.03mm). Albite twinning is common (Figure 2:4d) and the large patches show some zonation.

From purely petrological evidence the texture of the undeformed plagioclase lherzolites is interpreted as the result of interstitial crystallisation of a liquid within a spinel lherzolite resulting in extensive re-equilibration and the exsolution of aluminous phases within the enstatite porphyroclasts. It is calculated that the least deformed plagioclase lherzolite (LZ01) contains 5% of the introduced liquid. The effects of the fluid infiltration on the mineral chemistry are considered in a following section.

No inter-relationship has been found between the two forms of plagioclase lherzolite, but the fine grained variety appears

to represent the deformed and re-equilibrated coarse grained form. Transitional zones are, however, found between the deformed plagioclase lherzolite and the pargasite peridotites.

2:2:3 Pargasite lherzolite and harzburgite. The pargasite peridotites occur in two forms: i) fine grained pargasite harzburgite showing evidence of high deformation with a marked fabric (Figure 2:5a) ii) coarse grained pargasite lherzolite with a granular texture (1 to 2 mm grain size) (Figure 2:5b). The two forms are often interbanded with each other and deformed plagioclase lherzolite on a 1 to 10cm scale (Figure 2:6). The bands of the coarser grained pargasite lherzolite rarely exceed 1 cm in width and comprise of 35% olivine, 35% pargasite and 30% diopside with 1 to 2% enstatite and chromite. Spray (1982) postulated that these thin bands represent crystallised picritic fluid introduced into the ultramafic body while still within the mantle. The only available chemical analysis (Green 1964a) of a coarse pargasite lherzolite band is consistent with this interpretation.

The pargasiteharzburgite is always intensely sheared and generally intimately associated with the coarse granular pargasite lherzolite. The mineralogy of the harzburgite is variable but predominantly consists of 60% olivine and 35% pargasite $\pm$ clinopyroxene, orthopyroxene, chromite and plagioclase. A foliation is caused by the alignment of pargasite and rare orthopyroxenes which can have length/aspect ratios up to 100 (Figure 2:5c). Rounded inclusions of chromite often occur within pargasite.

In the transition zone between the sheared plagioclase lherzolite and pargasite harzburgite, pargasite replaces plagioclase and encloses the associated chromite (Figure 2:5d) The original relationships between the pargasite and plagioclase peridotites are obscured by extensive deformation and re-equilibration. However, the following model is envisaged;

Photomicrographs of Pargasite Peridotites

Figure 2:5a; Sample 2555 x.p.l. field of view = 4 mm

Fine grained pargasite harzburgite with a E - W fabric.

Figure 2:5b; Sample AT 133 p.p.l. field of view = 6 mm

Granular coarse grained pargasite lherzolite band above fine grained deformed pargasite harzburgite. Pargasite, brown, olivine, high relief and serpentinised, clinopyroxene, v. pale brown.

Figure 2:5c; Sample AT 133 x.p.l. field of view = 6 mm

Deformed and recrystallised enstatite with high length/aspect ratio.

Figure 2:5d; Sample AT 133 p.p.l. field of view = 2 mm

Plagioclase enclosing chromite being partially replaced by pargasite in a transition zone between plagioclase lherzolite and pargasite harzburgite.

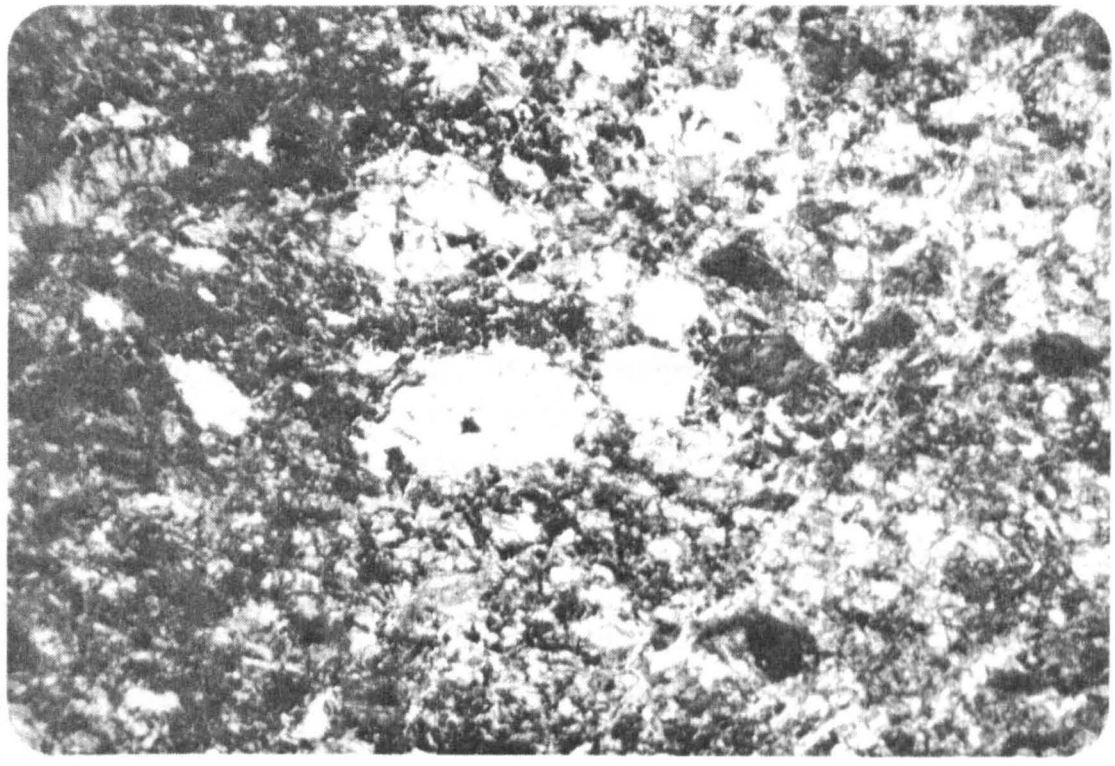

Figure 2:5a Pargasite harzburgite 2555

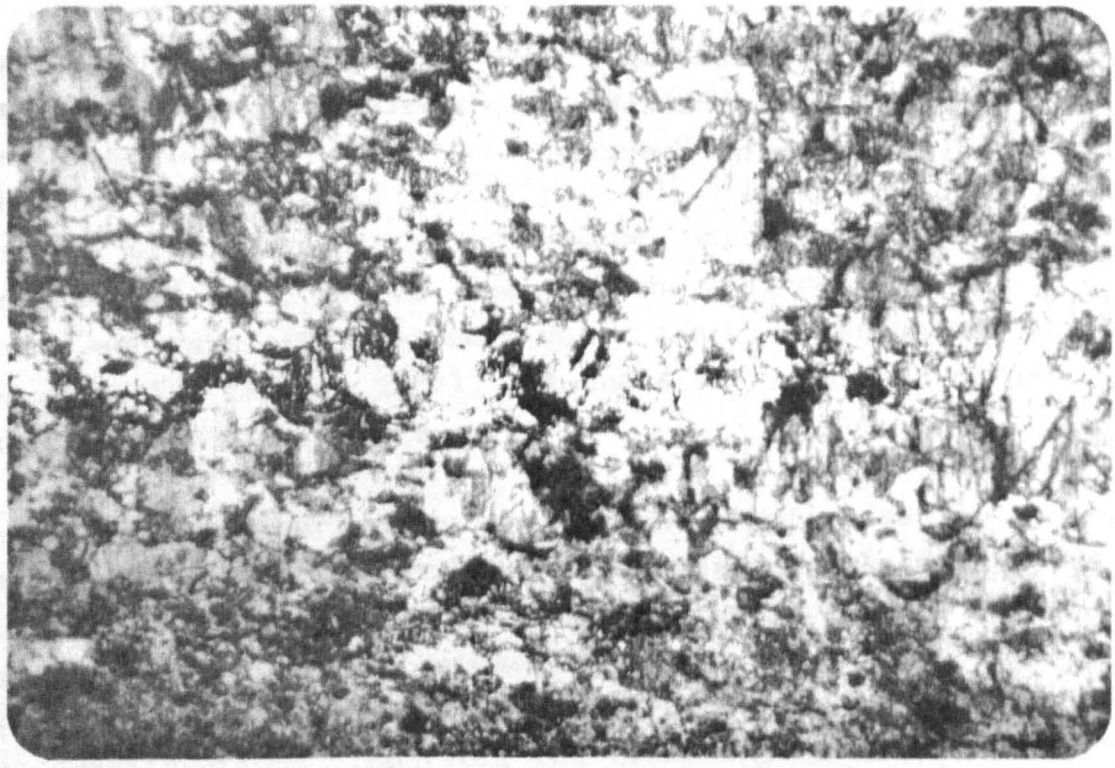

Figure 2:5b Pargasite lherzolite AT 133

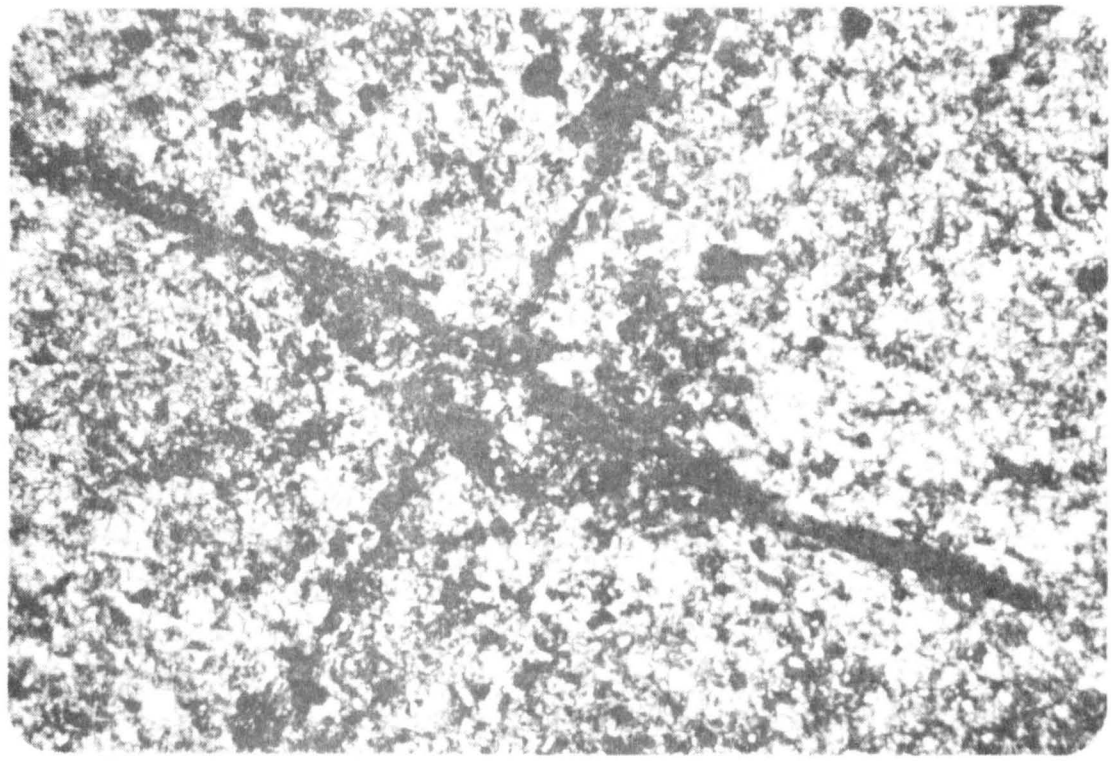

Figure 2:5c Pargasite harzburgite AT 133

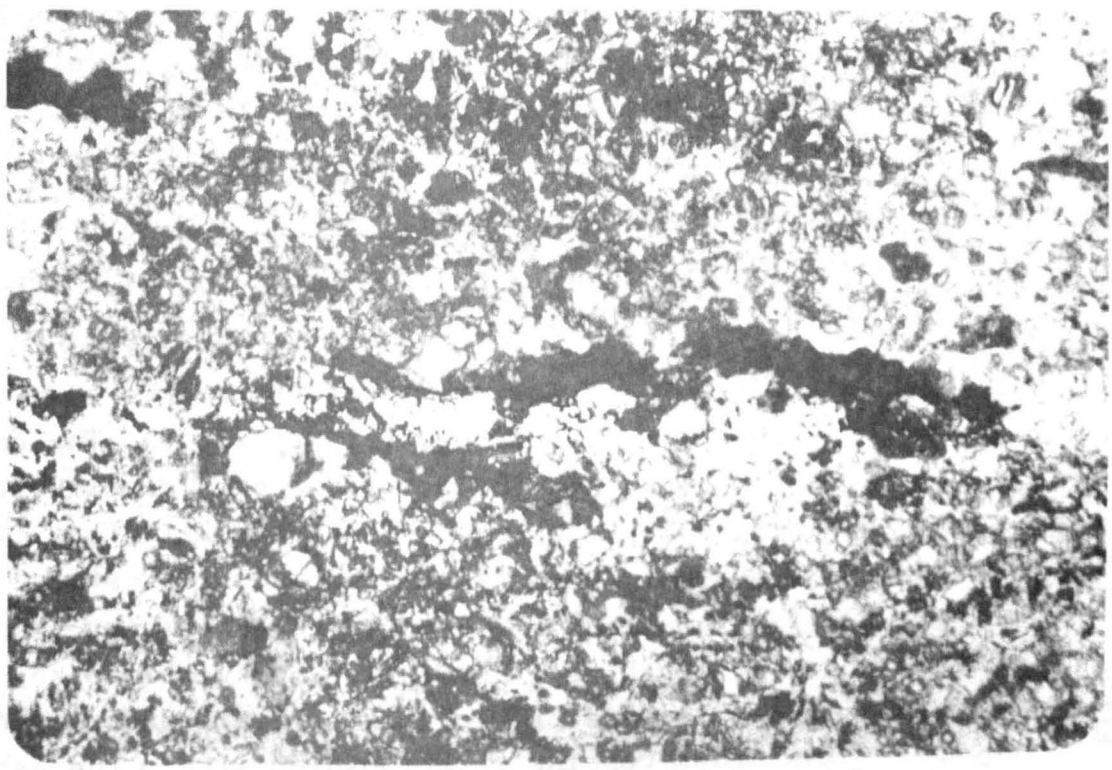

Figure 2:5d Pargasite harzburgite AT 133

Porphyroclastic spinel lherzolite (with a complex history of deformation and melt extraction) is intruded by a picritic fluid that is trapped in interstitial patches or forms centimetre wide bands or dykes. The melt crystallises as a plagioclase lherzolite assemblage. Subsequent re-equilibration results in pargasite replacing a combination of plagioclase, orthopyroxene and olivine to form pargasite peridotites.

Due to the frequent fine scale interbanding of the plagioclase and pargasite peridotites, sampling and hence chemical analysis of purely one rock type is difficult. The chemical analysis of the typical peridotite assemblages are presented in Table 2:1 along with data of Green (1964b) and Kirby (1979). Significantly the Al_2O_3 content of the spinel lherzolite 2553 reported by Green (op. cit.) is much greater than that obtained on the same rock powder in this study. The possibility of analytical errors plus relatively large variations in Al_2O_3 and CaO within the spinel lherzolites (2.1 to 2.5% and 1.5 to 2.2% respectively in this study) makes the evaluation of the fluid infiltration hypothesis difficult from purely the major element data. However, the data show an overall increase in CaO and Al_2O_3 contents from the spinel lherzolite to the pargasite harzburgite and plagioclase lherzolite to the pargasite lherzolite.

2:3 Gabbros and Dolerites

The gabbro mass forms a 7 sq. mile crescent shaped body in the north east of the Lizard Peninsula (Figure 2:1). The contact between the peridotites and the gabbro is only exposed in two areas, Coverack and Carrick Luz. Flett and Hill (op. cit.) described the numerous large ($\leqslant$45m) gabbro dykes at the latter locality and remarked upon the complex relationships found at Coverack where at least four generations of gabbro dykes are found (rock types include troctolites, olivine gabbro and gabbro). The cross cutting relationships within the gabbro

Table 2:1

Calculated anhydrous chemical analyses of Lizard Peridotites

	spinel lherzolite					plagioclase lherzolite			pargasite harzburgite	pargasite lherzolite
	2553	2553+	2554	Au 31*	S30 B*	LZ01	2559	2560+	2555+	90692+
SiO_2	44.76	44.60	45.63	49.7	46.83	44.82	44.07	45.12	44.89	44.26
TiO_2	0.07	0.16	0.07	0.04	0.16	0.20	0.19	0.23	0.28	0.52
Al_2O_3	2.10	4.18	2.46	2.02	2.08	2.34	4.18	4.96	3.99	13.95
Fe_2O_3	9.61	--	9.64	8.77	9.30	9.39	9.14	--	--	--
FeO	--	8.30	--	--	--	--		7.87	8.49	4.49
MnO	0.14	0.09	0.14	--	--	0.13	0.13	0.09	0.11	0.08
MgO	41.31	40.45	39.72	33.56	36.2	40.47	37.2	37.97	38.62	23.04
CaO	1.45	1.72	2.19	1.43	2.38	2.05	3.23	3.10	2.82	12.94
Na_2O	ND	0.11	ND	0.65	0.19	0.11	ND	0.24	0.35	0.46
K_2O	ND	0.02	ND	0.06	0.01	ND	ND	0.06	0.05	0.11
Cr_2O_3	0.37	0.37	0.40	0.40	.28	0.49	0.37	0.36	0.40	0.15
NiO	0.26	0.28	0.29	0.27	0.20	0.29	0.26	.16	.28	0.07

\+ Green (1964a)

* Kirby (1979)

ND Not detected

-- Not analysed

Figure 2:6a; Banded Pargasite Peridotite

Sample AT 133 interbanded pargasite lherzolite, pale, and pargasite harzburgite. The thin section is cm long.

Figure 2:6b; Sample CV 5 x.p.l. field of view = 6 mm

Olivine gabbro CV 5 comprises partially serpentinised olivine, subpoikilitic plagioclase and interstitial clinopyroxene.

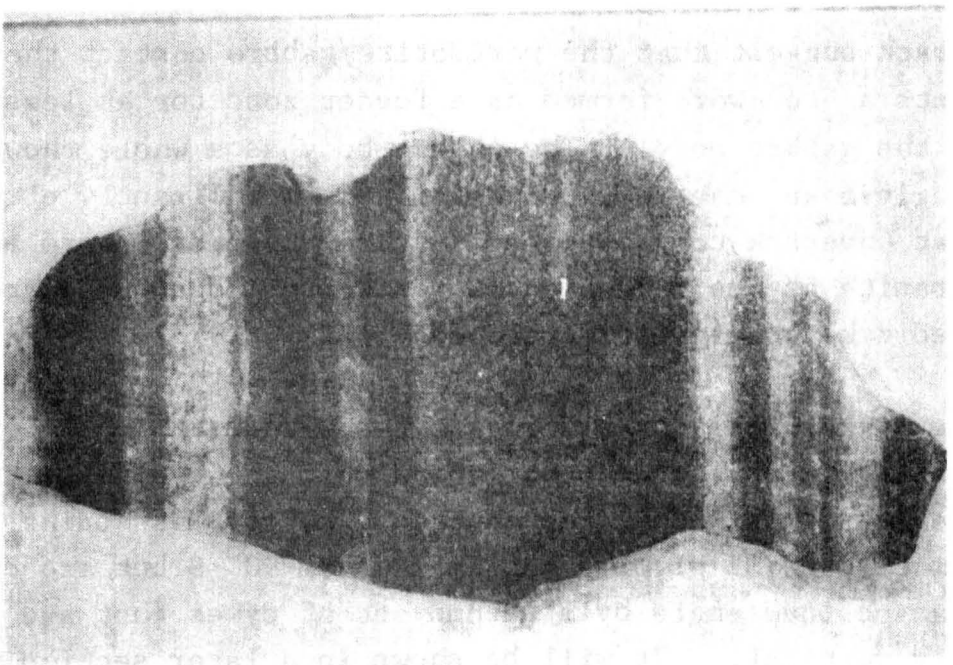

Figure 2:6a Pargasite Peridotite AT 133

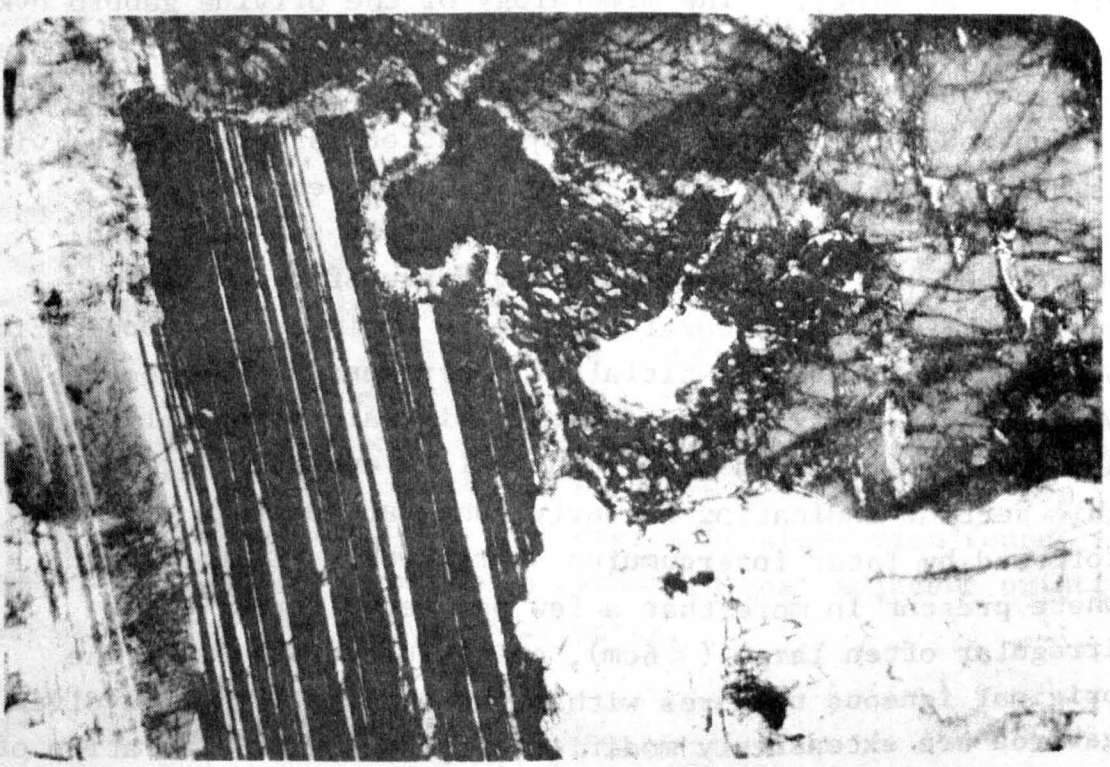

Figure 2:6b Olivine Gabbro CV5

at Coverack suggest that the peridotite/gabbro contact there represents a stockwork formed as a feeder zone for at least part of the gabbro body. The gabbro body as a whole shows a mineralogical and chemical progression from dominantly olivine gabbro at Coverack to gabbro and then horn blende gabbro and plagiogranite as one moves northwards to Porthoustock where a sheeted dyke complex is developed(Bromley, 1973).

Dolerite dykes cross cut all rock types within the ophiolitic units and are also found, deformed, within the Traboe schists. The dolerite dykes within the sheeted dyke complex strike approximately NW/SE dipping between 60 and 90° S but are cross cut at an oblique angle by a second set of dykes that are generally vertical. It will be shown in a later section that the two dyke suites are chemically distinct and that only the younger suite cross cut the stratigraphically lower parts of the ophiolite sequence such as the peridotite.

2:3:1 Petrology. The mineralogy of the olivine gabbro dykes at Coverack varies from troctolite (less than 10% clinopyroxene, plagioclase ≏ olivine) to an olivine gabbro with up to 30% clinopyroxene. The degree of alteration is variable, olivine is ubiquitously serpentinised but to different degrees, plagioclase may be unaltered to completely saussuritised. The gabbros often show textural evidence of a partially cumulate origin; subhedral olivine is enclosed by subpoikilitic plagioclase with interstitial clinopyroxene. Plagioclase, which is generally the predominant mineral, is usually zoned, and frequently varies from subhedral to euhedral within one thin section indicating an early euhedral cumulate origin followed by later intercumulus overgrowth. Clinopyroxene, where present in more than a few per cent, forms very irregular often large (<6cm), poikilitic crystals. The original igneous textures within the chemically more evolved gabbros are extensively modified by greenschist alteration of

all the phases. The alteration probably reflects a combination of the chemical composition, i.e. more susceptible to alteration, and the fact that this portion of the ophiolitic sequence would have been nearer to the sea floor and hence more liable to the effects of hydrothermal circulation.

The most distinctive rock type in the Coverack region is an almost black olivine gabbro that is found adjacent to the gabbro-peridotite contact. This rock is relatively fresh, comprising 30% serpentinised olivine, 20% clinopyroxene and 50% labradorite (Figure 2:6). The dark nature of the rock is caused by numerous microscopic inclusions of titaniferous iron oxide in the labradorite which is patchily saussuritised ($\simeq$10%) appearing white in hand specimen. A sample of this rock type was chosen for a mineral isochron determination (Sample CV5).

The majority of the dolerite dykes have ophitic to sub-ophitic textures (Figure 2:7a). However, 20% are fine grained with large (< 1cm) plagioclase phenocrysts (Figure 2:7b). Microprobe analyses of these phenocrysts show them to be more albitic than the groundmass plagioclase and their resorbed margins implies that they may have been xenocrysts, presumably derived from the gabbro (see Table 2:2). Olivine, where present in the dolerites, is totally psuedomorphed. Clinopyroxene is generally unaltered, locally rimmed with chlorite and actinolite and only wholly psuedomorphed in the rare dykes that now have a greenschist mineralogy. Petrologically it is not possible to distinguish the two dyke generations within the sheeted dyke complex. The degree of alteration found within the dykes is apparently random in that adjacent pristine and greeschist dykes frequently occur.

2:4 Peridotite Mineral Chemistry

This particular section describes the mineral chemistry of the Lizard peridotites with the aim of evaluating their petrogenesis

Table 2:2 Average microprobe Plagioclase compositions

Dolerite P5 groundmass		Dolerite P5 xenocryst	Olivine Gabbro CV 5
n =	8	4	12
SiO_2	51.61±.42	53.53±.24	53.16±.40
Al_2O_3	30.07±.33	28.85±.24	29.78±.32
FeO*	0.63±.04	0.55±.03	0.31±.05
CaO	13.21±.13	12.36±.15	12.60±.11
Na_2O	3.78±.11	4.65±.10	4.38±.14
K_2O	0.01±.01	0.02±.01	0.04±1
Total	99.30	99.96	100.27
An	66	59	61

Figure 2:7a; Sample CV2 x.p.l. field of view = 6 mm

Partially amphibolitised sub-ophitic dolerite. The majority of clinopyroxene and plagioclase are unaltered.

Figure 2:7b; Sample P5 x.p.l. field of view = 6 mm

Altered plagioclase xenocryst in a fine grained dolerite.

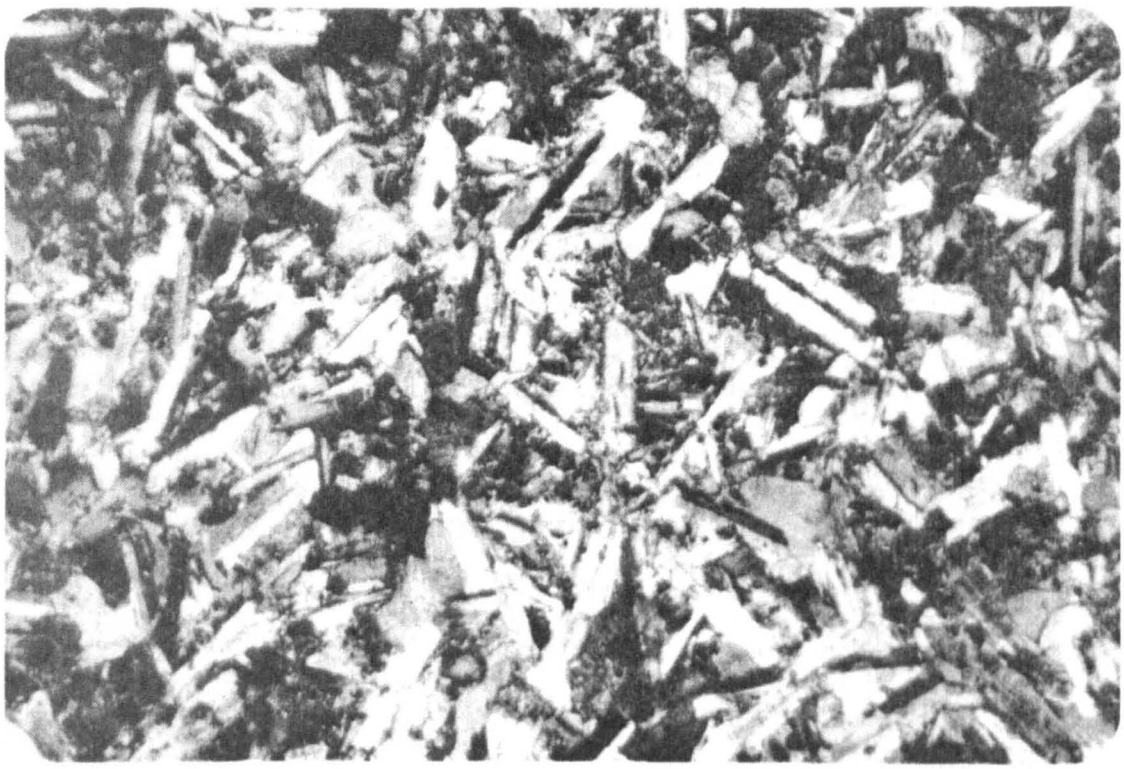

Figure 2:7a Dolerite CV2

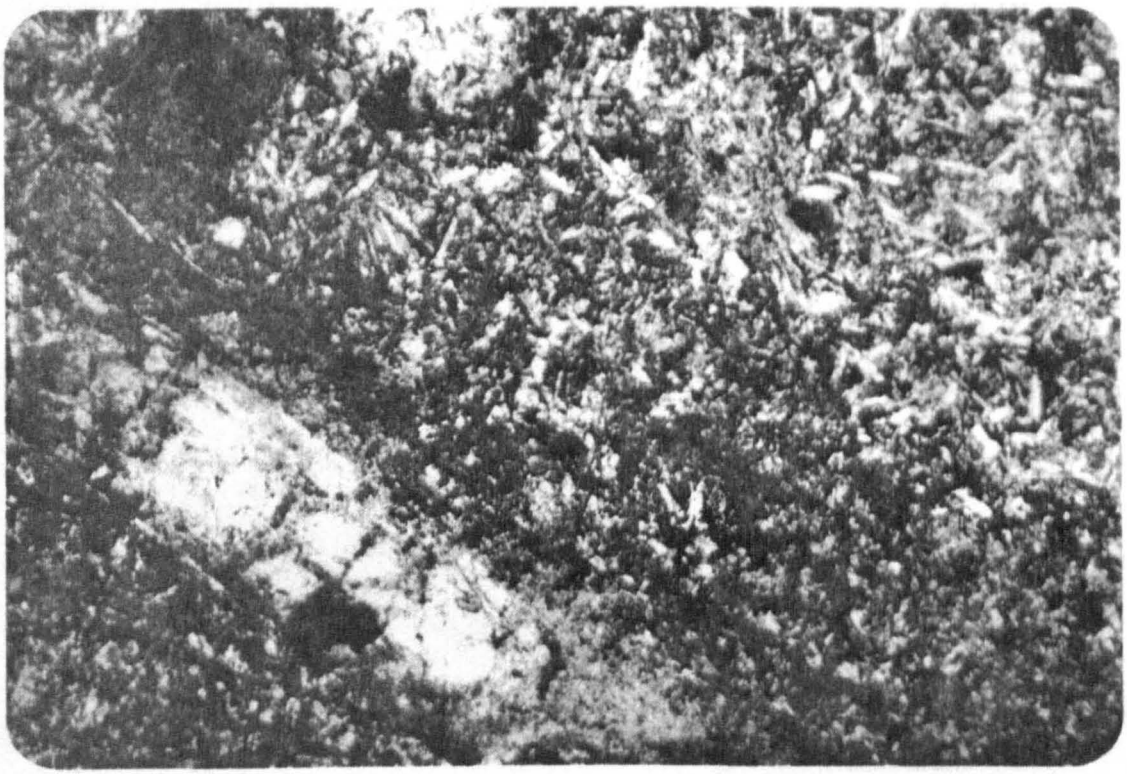

Figure 2:7b Dolerite P5

and inter-relationship. Analytical procedure and errors are discussed in Appendix II.

Mineral analyses were obtained from 9 spinel lherzolites, 4 plagioclase lherzolites and 3 pargasite harzburgites/lherzolites, but for clarity data for just nine samples are discussed and presented in the following diagrams. The four spinel lherzolite samples considered span the entire mineralogical range from 6 to 10% modal clinopyroxene. Samples 2560 and LZ01 are deformed and undeformed plagioclase lherzolites respectively. AT133 comprises interbanded pargasite harzburgite and lherzolite.

2:4:1 Olivines. Average olivine analyses for each representative sample are presented in Table 2:3. The olivines are all Mg rich (Fo_{88} to 90.5) lying in the range of olivines from mantle derived peridotites, (Fo_{88} to Fo_{92}). Olivine is unzoned throughout and, with the exception of the plagioclase lherzolite LZ01, each sample shows very little variation in Fo content (typically $\pm$ 0.1 of the mean). Minor element contents (CaO = 0.04%, MnO = 0.017% and NiO = 0.36%) are relatively constant in all the lithologies except for the low CaO content of the olivines in the pargasite peridotites, 0.01%. The Fo contents of olivines in the plagioclase and spinel lherzolite show little variation (90.3 to 89.7) whereas those in pargasite lherzolite have Fo = 89.1 and in pargasite harzburgite Fo = 88.2. The 2 generations of olivine in LZ01 have different Fo contents, 90.3 in rounded olivines in plagioclase and 90.0 in the porphyroclasts and groundmass. However, this difference is within analytical error $\pm$ 0.3 (see Appendix II) and therefore cannot be interpreted as significant.

2:4:2 Orthopyroxenes. As with the olivines the orthopyroxenes in the Lizard peridotites are Mg rich (Figure 2:8a and b and Table 2:4) with compositions comparable to orthopyroxenes from mantle derived peridotites. As a whole there is relatively

Table 2:3 Average microprobe analyses of olivines from Lizard Peridotites.

Spinel lherzolites

	2553 n = 12	2554 14	CV 1 8	CV 10 9
SiO_2	41.14 ± 0.31	41.35 ± 0.28	41.43 ± 0.29	41.38 ± 0.26
MgO	49.21 ± 0.27	49.58 ± 0.26	48.94 ± 0.28	48.81 ± 0.2
CaO	0.04 ± 0.02	0.04 ± 0.02	0.06 ± 0.02	0.06 ± 0.02
MnO	0.16 ± 0.02	0.14 ± 0.02	0.14 ± 0.03	0.17 ± 0.03
FeO*	9.50 ± 0.09	10.05 ± 0.09	10.05 ± 0.10	10.04 ± 0.11
NiO	0.36 ± 0.03	0.38 ± 0.04	0.39 ± 0.03	0.36 ± 0.03
Total	100.41	101.54	101.01	100.82
Fo	90.2	89.8	89.7	89.7

	Plagioclase Lherzolite			Pargasite Peridotites	
	2560 n = 6	LZ01 n = 8	LZ01 enclosed in plag. n = 10	AT 133 n = 5	n = 7
SiO_2	41.36 ± 0.29	41.09 ± 0.28	41.13 ± 0.33	40.83 ± 0.27	40.83 ± 0.29
MgO	48.28 ± 0.27	49.27 ± 0.25	49.43 ± 0.29	48.10 ± 0.26	47.85 ± 0.28
CaO	0.03 ± 0.01	0.03 ± 0.01	0.06 ± 0.02	0.01 ± 0.01	0.01 ± .01
MnO	0.17 ± 0.02	0.16 ± 0.02	0.17 ± 0.02	0.17 ± 0.02	0.17 ± 0.02
FeO*	10.26 ± 0.10	9..3 ± 0.08	9.74 ± 0.09	10.54 ± 0.11	11.45 ± 0.09
NiO	0.33 ± 0.03	0.38 ± 0.3	0.36 ± 0.3	0.36 ± 0.03	0.32 ± 0.04
Total	100.43	100.36	100.87	100.01	100.63
Fo	89.3	90.3	90.0	89.1	88.2

Table 2:4 Average microprobe analyses of orthopyroxenes from Lizard Peridotites.

	2553 core n = 10	2553 rim 6	2554 C 9	2554 R 5	CV 10 C 11	CV 10 R 7
SiO_2	54.26 ± 0.23	55.38 ± 0.32	54.35 ± 0.25	55.13 ± 0.27	55.2 ± 0.28	56.17 ± 0.29
TiO_2	0.15 ± 0.03	0.11 ± 0.02	0.09 ± 0.02	0.09 ± 0.02	0.10 ± 0.03	0.11 ± 0.02
Al_2O_3	5.41 ± 0.10	4.11 ± 0.11	5.29 ± 0.17	4.89 ± 0.15	3.64 ± 0.18	3.09 ± 0.16
Cr_2O_3	0.61 ± 0.07	0.43 ± 0.05	0.73 ± 0.09	0.61 ± 0.07	0.72 ± 0.08	0.65 ± 0.06
MgO	31.42 ± 0.32	32.33 ± 0.29	30.91 ± 0.25	31.95 ± 0.31	31.83 ± 0.26	32.[illegible] ± 0.33
CaO	1.72 ± 0.07	0.98 ± 0.05	2.62 ± 0.09	1.56 ± 0.06	1.96 ± 0.08	1.35 ± 0.06
MnO	0.16 ± 0.02	0.16 ± 0.02	0.14 ± 0.02	0.16 ± 0.03	0.11 ± 0.02	0.12 ± 0.02
FeO*	6.21 ± 0.18	6.50 ± 0.21	6.34 ± 0.15	6.49 ± 0.20	6.29 ± 0.19	6.42 ± 0.21
Na_2O	0.07 ± 0.02	0.02 ± 0.01	0.04 ± 0.01	0.01 ± 0.01	0.02 ± 0.01	0.02 ± 0.01
Total	100 [illegible]	100.02	100.53	100.88	99.88	100.51
En	86.9	88.1	85.0	87.0	86.6	87.7
Fs	9.6	9.9	9.8	9.9	9.6	9.7
Wo	3.4	1.9	5.2	3.1	3.8	2.6
Mg	90.0	89.9	89.7	89.8	90.0	90.0

CV 1 C 12	CV 1 R 6	2560 C 5	LZ01 C 15	LZ01 R 7	AT 133 C 5
55.21 ± 0.25	56.50 ± 0.31	56.29 ± 0.27	56.79 ± 0.28	56.91 ± 0.29	57.03 ± 0.24
0.09 ± 0.02	0.07 ± 0.02	0.15 ± 0.03	0.35 ± 0.04	0.44 ±	0.15 ± 0.02
3.07 ± 0.18	2. ± 0.09	2.07 ± 0.09	1.36 ± 0.06	1.16 ±	1.39 ± 0.08
0.[illegible] ± 0.07	0.65 ± 0.05	0.41 ± 0.05	0.53 ± 0.06	0.44 ±	0.24 ± 0.04
32.[illegible] ± 0.29	32.85 ± 0.33	32.52 ± 0.28	33.28 ± 0.33	33.47 ± 0.25	33.26 ± 0.27
1.36 ± 0.09	1.67 ± 0.0	0.82 ± 0.05	1.65 ± 0.0	1.37 ± 0.0	0.48 ± 0.0
0.17 ± 0.02	.17 ± 0.03	0.16 ± 0.02	0.17 ± 0.03	0.17 ± 0.02	0.19 ± 0.04
6.31 ± 0.17	[illegible] ± 0.21	6.88 ± 0.18	6.34 ± 0.17	6.42 ± 0.23	7.13 ± 0.24
0.01 ± 0.01	0.[illegible] ± 0.01	0.01 ± 0.01	0.04 ± 0.01	0.01 ± 0.01	0.01 ± 0.01
99.67	100.39	99.31	100.51	100.39	100.08
86.9	87.5	88.0	87.5	88.0	88.1
9.5	9.4	10.4	9.4	9.5	10.6
3.6	3.1	1.6	[illegible]	2.6	1.3
90.1	90.3	88.9	90.3	90.3	89.3

little compositional variation with a total range from $En_{88.1}\ Wo_{1.3}\ Fs_{10.6}$ to $En_{85}\ Wo_{5.2}\ Fs_{9.8}$. However, there is a small but significant compositional range within a single thin section. The cores of the enstatite porphyroclasts are generally more MgO, CaO and Al_2O_3 rich than the porphyroclast rims and groundmass grains (Figure 2:8b and Table 2:4). This chemical trend between porphyroclast cores and rims is also apparent between lithologies in that the orthopyroxenes in the plagioclase and pargasite peridotites have lower MgO, CaO and Al_2O_3 contents compared with those of the spinel lherzolites. The enstatites of LZ01 are notable in that they have the greatest TiO_2 contents (0.4% compared to typical values of 0.15%).

2:4:3 Clinopyroxenes. The clinopyroxenes from the spinel lherzolites display a narrow compositional range from $En_{51.5}\ Wo_{42.6}\ Fs_{5.9}$ to $En_{47.2}\ Wo_{47.9}\ Fs_{5.0}$ (Figure 2:8a and b and Table 2:5). There is considerable compositional overlap between the clinopyroxenes of the different spinel lherzolites but the Al_2O_3 contents of the clinopyroxenes tend to be higher, and the CaO lower, in rocks with more modal clinopyroxene. The porphyroclasts again show zonation with lower MgO, Al_2O_3 and higher CaO in the rims (Figure 2:8b). The clinopyroxenes in the plagioclase lherzolites LZ01 show equivalent zonations but as in the case of the orthopyroxenes they contain less Al_2O_3 and more TiO_2 compared to the clinopyroxenes of the spinel lherzolites ($En_{53.7}\ Wo_{40.9}\ Fs_{5.4}$).

There are significant compositional variations in the clinopyroxenes of the pargasite peridotites. Clinopyroxenes from the coarse bands (circa 1cm) of pargasite lherzolite $En_{46.2}\ Wo_{46.5}\ Fs_{7.3}$ are more FeO, TiO_2 and Al_2O_3 rich compared to those of the narrow bands $En_{46.7}\ Wo_{47.6}\ Fs_{5.6}$ and those of the associated deformed harzburgites $En_{48.2}\ Wo_{46.8}\ Fs_5$ (TiO_2, 0.89 to 0.38% Al_2O_3, 4.02 to 2.89%).

Table 2:5 Average microprobe analyses of clinopyroxenes from Lizard Peridotites.

	2553 C n = 10	2553 R 6	2554 C 11	2554 R 5	CV 10 C 10	CV 10 R 5
SiO_2	51.63 ± 0.26	51.84 ± 0.24	51.91 ± 0.29	51.84 ± 0.27	51.38 ± 0.25	51.93 ± 0.33
TiO_2	0.36 ± 0.04	0.40 ± 0.05	0.25 ± 0.04	0.25 ± 0.05	0.25 ± 0.06	0.28 ± 0.05
Al_2O_3	7.00 ± 0.21	5.88 ± 0.19	6.04 ± 0.18	5.71 ± 0.23	5.51 ± 0.09	3.72 ± 0.21
Cr_2O_3	0.96 ± 0.09	0.93 ± 0.08	0.87 ± 0.07	0.80 ± 0.06	1.11 ± 0.12	1.26 ± 0.14
MgO	16.31 ± 0.17	15.71 ± 0.21	17.32 ± 0.19	16.42 ± 0.22	17.50 ± 0.21	16.87 ± 0.25
CaO	20.62 ± 0.25	22.18 ± 0.28	20.48 ± 0.23	22.22 ± 0.27	20.15 ± 0.26	22.04 ± 0.29
MnO	0.11 ± 0.03	0.11 ± 0.02	0.11 ± 0.02	0.09 ± 0.02	0.11 ± 0.01	0.13 ± 0.03
FeO*	3.33 ± 0.15	2.96 ± 0.19	3.40 ± 0.16	3.10 ± 0.14	3.59 ± 0.17	3.12 ± 0.18
Na_2O	0.76 ± 0.08	0.84 ± 0.10	0.31 ± 0.07	0.28 ± 0.07	0.33 ± 0.05	0.41 ± 0.07
Total	101.08	100.85	100.69	100.71	99.93	99.96
En	49.4	47.2	51.0	48.1	51.5	48.9
Fs	5.7	5.0	5.6	5.1	5.9	5.1
Wo	44.9	47.9	43.4	46.8	42.6	46.0
Mg	89.7	90.4	90.1	90.4	89.7	90.6

	CV 1 C n = 8	2560 C 5	LZ 01 C 10	LZ 01 R 6	Coarse band parg. Lhz. AT 133 C 10	Thin band parg. Lhz. AT 133 C 10	Parg. Hz. AT 133 C 8
SiO_2	52.65 ± 0.29	53.09 ± 0.33	52.93 ± 0.26	53.36 ± 0.28	51.61 ± 0.21	52.09 ± 0.25	53.46 ± 0.24
TiO_2	0.25 ± 0.07	0.35 ± 0.08	0.55 ± 0.07	0.40 ± 0.06	0.40 ± 0.09	0.80 ± 0.08	0.38 ± 0.05
Al_2O_3	3.22 ± 0.16	2.95 ± 0.17	2.61 ± 0.15	2.38 ± 0.16	4.02 ± 0.24	3.62 ± 0.22	2.89 ± 0.21
Cr_2O_3	1.44 ± 0.15	1.21 ± 0.12	1.34 ± 0.09	1.33 ± 0.10	0.49 ± 0.05	0.59 ± 0.07	0.77 ± 0.08
MgO	17.35 ± 0.28	18.15 ± 0.27	18.39 ± 0.25	18.33 ± 0.31	15.79 ± 0.22	16.07 ± 0.26	16.69 ± 0.21
CaO	21.66 ± 0.29	19.64 ± 0.28	19.52 ± 0.26	20.03 ± 0.28	22.14 ± 0.29	22.78 ± 0.26	22.52 ± 0.24
MnO	0.13 ± 0.02	0.10 ± 0.01	0.09 ± 0.01	0.11 ± 0.02	0.14 ± 0.04	0.09 ± 0.03	0.11 ± 0.12
FeO*	3.01 ± 0.21	3.65 ± 0.18	3.28 ± 0.15	3.22 ± 0.17	4.45 ± 0.22	3.45 ± 0.18	3.11 ± 0.12
Na_2O	0.39 ± 0.05	0.59 ± 0.07	0.61 ± 0.11	0.54 ± 0.09	0.51 ± 0.13	0.52 ± 0.12	0.53 ± 0.14
Total	99.80	99.73	99.32	99.69	100.04	100.01	100.46
En	50.1	52.9	53.7	53.1	46.2	46.7	48.2
Fs	4.9	6.0	5.4	5.2	7.3	5.6	5.0
Wo	45.0	41.1	40.9	41.7	46.5	47.6	46.8
Mg	91.1	89.9	90.9	91.0	86.3	89.2	90.5

Figure 2:8a LIZARD PERIDOTITE PYROXENE COMPOSITION

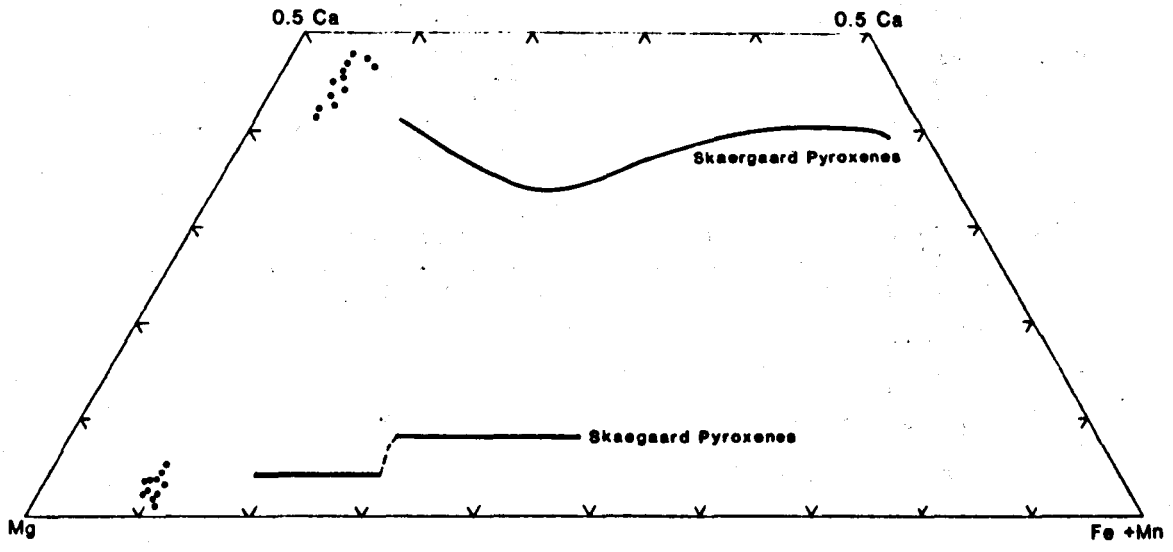

Figure 2:8b

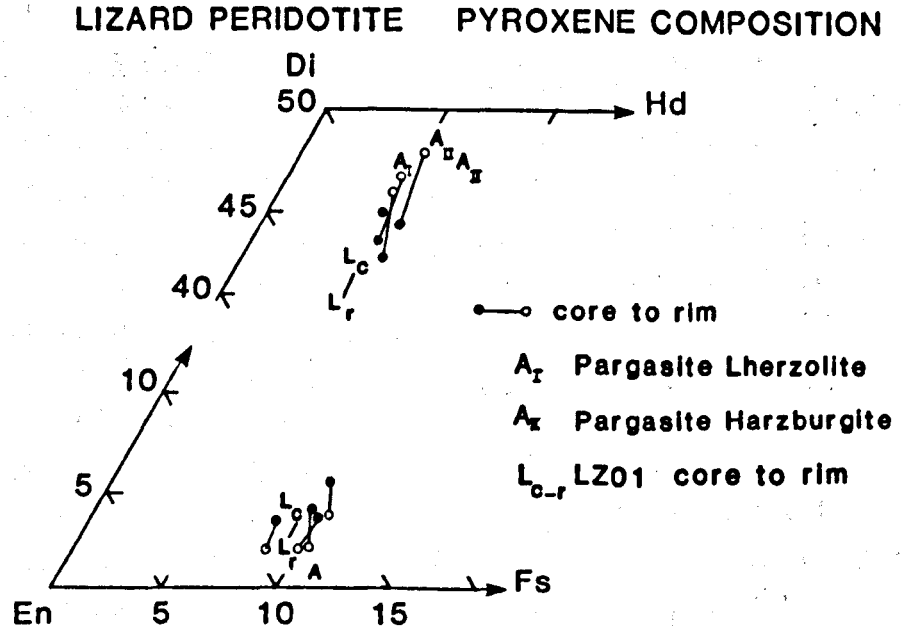

2:4:4 Pargasite. The pargasites within the banded pargasite peridotites show marked compositional variation from $Mg_{60.4}$ $Ca_{29.5}$ $Fe_{10.2}$ in the coarse lherzolite bands to $Mg_{55.8}$ $Ca_{30.5}$ $Fe_{13.7}$ in the associated deformed harzburgites (see Table 2:6). All the pargasites contain high TiO_2, 2.98 to 4.54% and Cr_2O_3, 1.50 to 0.79%.

2:4:5 Spinels. Spinels in the Lizard peridotites display systematic variations in Al_2O_3, 55.42 to 14.34%, Cr_2O_3, 12.47 and 45.77%, MgO, 18.79 to 9.24% and FeO, 13.42 to 27.87% (Table 2:7, Figure 2:9). High MgO and Al_2O_3 contents are associated with low Cr_2O_3 and FeO in olive green spinels, sensu stricto, and vice versa in opaque chromites.

Spinels in all the lithologies show zonation with relatively MgO and Al_2O_3 rich core and Cr_2O_3 and FeO rich rims. Significantly Talkington and Malpas (1979) predict that during re-equilibration pyroxenes would loose Tschermak's molecules ($Mg\ Al_2\ SiO_6$ and $Ca\ Al_2SiO_6$) which would equilibrate with spinels and yield relatively MgO and Al_2O_3 rich rims, the opposite to that observed here. This is probably due to at least partial re-equilibration in the plagioclase lherzolite stability field (see next section) during which the reaction plagioclase and orthopyroxene $\rightleftharpoons$ clinopyroxene + spinel would result in plagioclase formation and hence a loss of Al from the original spinels.

The Cr/Cr + Al ratios of the cores of spinels from spinel lherzolites show a correlation with the modal % clinopyroxene in the rock and the Al_2O_3 contents of the associated orthopyroxenes and clinopyroxenes (Figure 2:10). Similar relationships have been recorded in peridotites by several workers; ultramafic xenoliths (Frey and Prinz, 1978) and ophiolites (Allen 1975, Talkington and Malpas 1979). The relationship reflects changes in the bulk rock Cr/Al ratio which varies with the modal abundance of clinopyroxene.

Table 2:6 Average microprobe analyses of pargasites and plagioclase from Lizard Peridotites

	Pargasite			Plagioclase			
	AT 133 P. Lherz. coarse band 10	AT 133 P. Lherz. thin band 10	AT 133 P. Lherz. 5		2560 core 5	LZ01 core 5	LZ01 margins 5
SiO_2	43.29 ± 0.21	42.99 ± 0.25	42.41 ± 0.24	SiO_2	48.12 ± 0.29	48.11 ± 0.32	48.54 ± 0.36
TiO_2	2.98 ± 0.15	4.05 ± 0.19	4.54 ± 0.21	Al_2O_3	32.10 ± 0.24	32.69 ± 0.22	32.15 ± 0.27
Al_2O_3	12.25 ± 0.24	12.30 ± 0.269	12.30 ± 0.21	CaO	16.22 ± 0.19	16.57 ± 0.21	16.00 ± 0.26
Cr_2O_3	1.50 ± 0.09	1.36 ± 0.11	0.79 ± 0.07	FeO*	0.13 ± 0.02	0.08 ± 0.01	0.10 ± 0.02
MgO	7.09 ± 0.31	15.79 ± 0.25	15.59 ± 0.27	Na_2O	2.43 ± 0.9	2.16 ± 0.11	2.48 ± 0.10
CaO	11.60 ± 0.22	11.94 ± 0.18	11.86 ± 0.21	K_2O	0.00	0.00	0.00
MnO	0.06 ± 0.01	0.06 ± 0.01	0.11 ± 0.02				
K_2O	0.41 ± 0.07	0.07 ± 0.03	0.07 ± 0.05				
FeO*	5.12 ± 0.21	5.75 ± 0.26	6.84 ± 0.29				
Na_2O	2.70 ± 0.12	2.03 ± 0.15	1.97 ± 0.15				
Total	97.00	96.28	96.85	Total	99.00	99.61	99.27
MgO	60.4	57.2	55.8	Ab	21.3	19.1	21.9
FeO*	10.2	11.7	13.7	An	78.7	80.9	78.1
Ca	29.5	31.1	30.5	Or	0.0	0.0	0.0

Table 2:7 Average microprobe analyses of spinels from lizard Peridotites

	2553 C. Subh	2553 R. Subh	CV 1 C. Skel	CV 1 R. Skel	2554 C. Skel
	n = 7 ± 1 G	n = 4 ± 1 G	n = 5 ± 1 G	n = 3 ± 1 G	n = 8
SiO_2	0.06 ± 0.02	0.09 ± 0.03	0.12 ± 0.04	0.17 ± 0.03	0.14 ± 0.03
TiO_2	0.10 ± 0.02	0.10 ± 0.02	0.07 ± 0.03	0.06 ± 0.02	0.08 ± 0.02
Al_2O_3	55.42 ± 0.29	54.21 ± 0.43	27.42 ± 0.23	25.28 ± 0.37	52.93 ± 0.21
Cr_2O_3	12.47 ± 0.31	13.13 ± 0.32	38.08 ± 0.26	39.33 ± 0.39	13.60 ± 0.17
FeO*	13.42 ± 0.18	13.82 ± 0.28	22.93 ± 0.20	23.89 ± 0.21	13.88 ± 0.26
MnO	0.10 ± 0.01	0.10 ± 0.02	0.11 ± 0.02	0.10 ± 0.02	0.10 ± 0.02
NiO	0.37 ± 0.05	0.39 ± 0.03	0.33 ± 0.04	0.17 ± 0.03	0.36 ± 0.03
MgO	18.79 ± 0.20	18.49 ± 0.17	10.37 ± 0.21	10.41 ± 0.15	18.88 ± 0.21
Total	100.73	100.33	99.43	99.41	99.97
$100Mg/Mg+Fe^{2+}$	73.6	72.9	47.7	47.9	74.7
$100Cr/Cr+Al$	13.1	14.0	48.2	51.1	14.7
$Fe^{3+}/Cr+Al+Fe^{3+}$	1.5	1.8	3.4	4.9	2.7

	2554 R. Skel	2554 C Isolate & small	2554 R Isolate & small	CV 10 C Subheldral	2560 anhedral in plag.
	n = 6	n = 4	n = 1	n = 5	n = 5
SiO_2	0.11 ± 0.04	0.09 ± 0.03	0.10	0.07 ± 0.02	0.08 ± 0.02
TiO_2	0.07 ± 0.02	0.05 ± 0.01	0.07	0.09 ± 0.02	0.35 ± 0.04
Al_2O_3	51.29 ± 0.33	52.84 ± 0.18	51.85	30.47 ± 0.21	30.80 ± 0.25
Cr_2O_3	14.54 ± 0.24	13.81 ± 0.22	14.73	35.64 ± 0.23	33.27 ± 0.34
FeO*	15.46 ± 0.41	13.59 ± 0.22	14.66	20.35 ± 0.18	22.40 ± 0.21
MnO	0.09 ± 0.01	0.13 ± 0.01	0.14	0.11 ± 0.02	0.35 ± 0.03
NiO	0.30 ± 0.04	0.32 ± 0.03	0.34	0.32 ± 0.03	0.10 ± 0.02
MgO	18.46 ± 0.23	18.83 ± 0.24	18.61	12.63 ± 0.09	11.26 ± 0.11
Total	100.32	99.66	100.50	99.68	98.61
$100Mg/Mg+Fe^{3+}$	7?.4	74.8	73.8	56.5	50.9
$100Cr/Cr+Al$	16.0	14.9	16.0	44.0	42.0
$Fe^{3+}/Cr+Al+Fe^{3+}$	3.9	2.6	3.2	3.8	3.9

	LZ 01 Resorbed	LZ 01 Subh. in plag.	LZ 01 Subh. in ol.	LZ 01 Euh. ox. in opx.	AT 133 (Hz.) Subh. in parg.
	n = 3	n = 8	n = 6	n = 10	n = 4
SiO_2	0.11 ± 0.03	0.15 ± 0.02	0.16 ± 0.03	0.05 ± 0.02	0.15 ± 0.02
TiO_2	0.28 ± 0.05	2.03 ± 0.08	2.22 ± 0.10	2.30 ± 0.11	1.03 ± 0.09
Al_2O_3	21.33 ± 0.23	16.75 ± 0.16	14.34 ± 0.21	16.25 ± 0.14	23.49 ± 0.27
Cr_2O_3	45.77 ± 0.32	44.96 ± 0.24	44.12 ± 0.33	44.65 ± 0.27	40.53 ± 0.33
FeO*	22.04 ± 0.27	24.33 ± 0.23	27.87 ± 0.15	24.12 ± 0.24	23.62 ± 0.25
MnO	0.20 ± 0.03	0.21 ± 0.03	0.27 ± 0.03	0.20 ± 0.02	0.27 ± 0.03
NiO	0.10 ± 0.02	0.17 ± 0.03	0.16 ± 0.03	0.17 ± 0.04	0.15 ± 0.02
MgO	10.06 ± 0.18	10.61 ± 0.23	9.24 ± 0.26	11.70 ± 0.25	10.65 ± 0.12
Total	99.89	99.21	98.38	99.44	99.89
$100Mg/Mg+Fe^{2+}$	47.1	48.8	43.3	53.1	48.3
$100Cr/Cr+Al$	59.0	64.3	67.4	64.8	53.6
$Fe^{3+}/Cr+Al+Fe^{3+}$	2.5	6.4	9.2	8.0	4.4

During partial melting the K_D of $Cr_{residue-melt}$ is significantly greater than the K_D of $Al_{residue-melt}$ such that increasing degrees of partial melting will result in residues with higher Cr/Al bulk rock ratios and lower clinopyroxene contents.

Spinels from plagioclase lherzolites show a large range in their Cr/Cr + Al ratio from values similar to those in the clinopyroxene poor (6 modal %) spinel lherzolites to those in stratiform ultrabasic bodies (Figure 2:9). The data also plot on an extension of the (Cr/Cr + Al) vs (Al_2O_3 content of clinopyroxene) relationship defined by the spinel lherzolites (Figure 2:10).

The plagioclase lherzolite LZ01 (undeformed) is significant in that it has 2 spinel morphologies; i) anhedral/porphyroclastic (2.0 to 0.1 mm) and enclosed in plagioclase (apparently originating as a result of re-equilibration of the olive green spinels found in the spinel lherzolites, Green 1964b (op. cit.)) ii) Euhedral small (0.005 mm) poikilitically enclosed in plagioclase and in olivines within the plagioclase. Spinels are also found exsolved within orthopyroxene porphyroclasts adjacent to plagioclase rich patches.

The two morphologies have different compositions with the euhedral form having higher Cr/Cr + Al ratios (Table 2:7, Figure 2:9). The euhedral form also shows some chemical variation apparently dependant upon the enclosing phase. For example the highest Al_2O_3 contents and lower Cr/Cr + Al ratio are found in spinels in plagioclase whereas the spinels in olivines have the lowest Mg/Mg + Fe^{2+} ratios (Figure 2:9). Similar relationships within the Rhum layered intrusion were ascribed by Henderson (1975) and Henderson and Suddaby (1971) to subsolidus re-equilibration between spinels and the associated silicate phases.

Perhaps the most significant chemical difference between the two spinel morphologies is in their TiO_2 content; greater than 2.00% in the euhedral form and less than 0.3% in the anhedral

Figure 2: 9 Cr/Cr+Al vs Mg/Mg+Fe^{2+} DIAGRAM FOR SPINELS

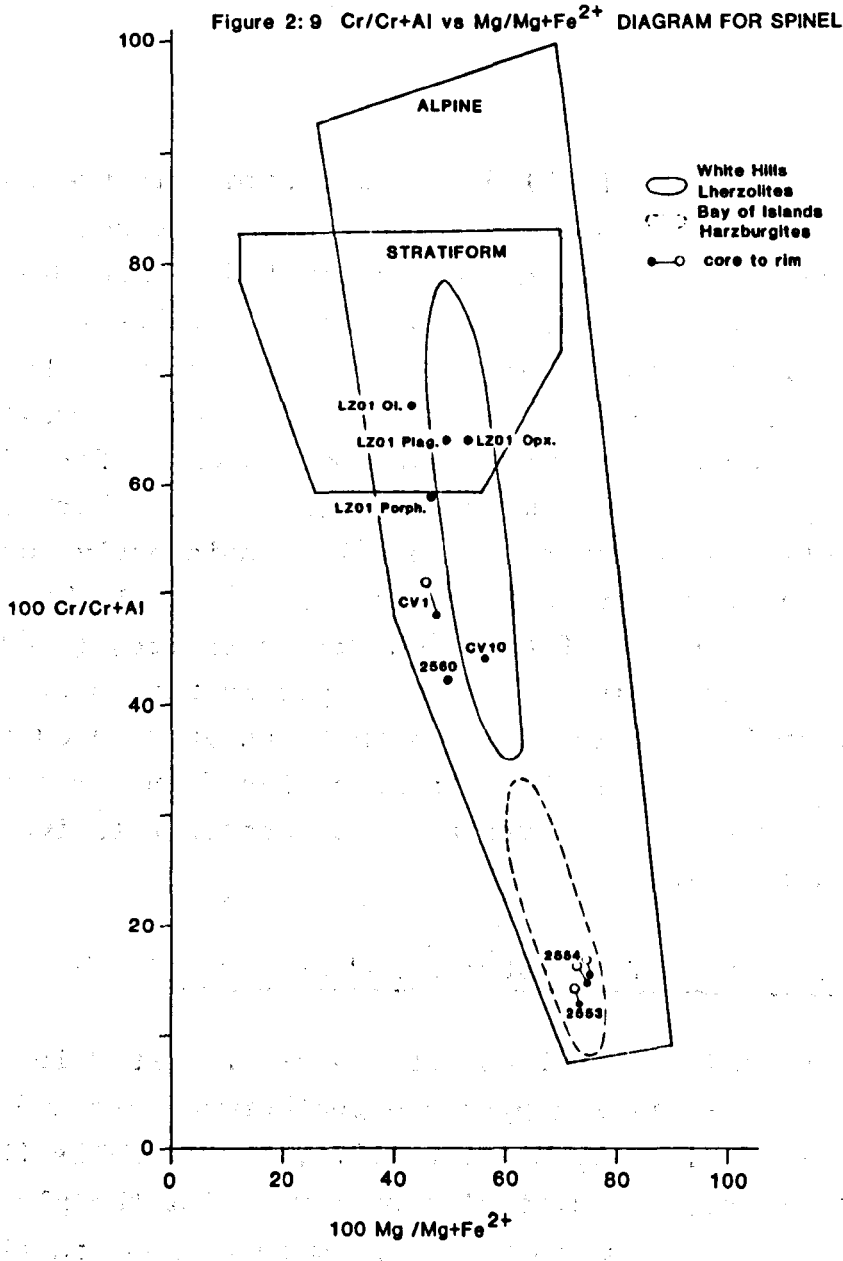

Figure 2:10 Al_2O_3 CPX wt % vs Cr/(Cr+Al) Spinel in the LIZARD PERIDOTITES

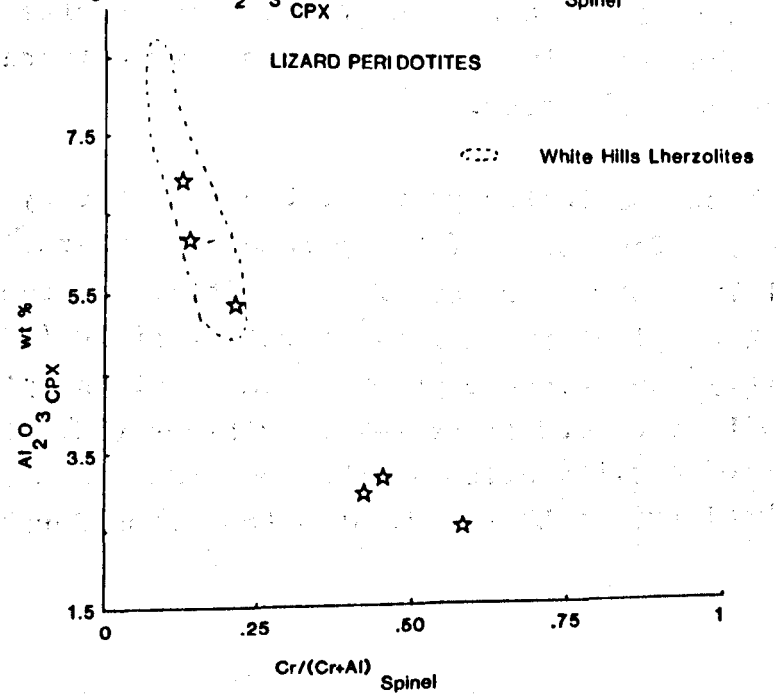

Data from Talkington and Malpas 1980

form. Henderson (1975) does not record evidence for TiO_2 re-equilibration between spinels and their adjacent silicate phases and it is therefore concluded that the high TiO_2 contents are primary. Disseminated spinels in alpine type lherzolites and harzburgites typically contain low TiO_2 contents ($<0.4\%$) and TiO_2 is only found to exceed 0.4% in spinels from dunites and massive chromites which formed as early precipitates from a magma (e.g. Auge and Roberts, 1982). TiO_2 contents greater than 1% are only consistently found in spinels in layered ultrabasic bodies e.g. Bushweld (Cameron, 1975) The high TiO_2 contents of the subhedral chromites ($>2.00\%$) are therefore indicative of chromite precipitation from a relatively undifferentiated magma that was introduced into the lherzolite. Interestingly spinels enclosed in pargasite within the pargasite harzburgite also contain relatively high TiO_2 (circa 1.00%).

2:4:6 Equilibration Temperatures and Pressures

Calculated equilibrium P-T conditions are reported in Table 2:8, based on co-existing pyroxene geothermometers and geobarometers derived by Mercier (1976, 1980), Wells (1977) and Powell (1978). Equilibrium pressures for the plagioclase lherzolites were estimated using the method of Obata (1976). The cores of pyroxene porphyroclasts record P-T conditions 4 to 6 Kb and 100 to 140°C higher than the porphyroclast rims indicating that the rims have suffered down temperature and pressure re-equilibration.

Figure 2:11 schematically portrays the P-T history of the Lizard peridotites. The cores of the pyroxene porphyroclasts within the spinel lherzolites record P-T conditions at the uppermost limits of the spinel lherzolite stability field (19 Kb, 1100°C). Significantly the pyroxene porphyroclasts of the plagioclase lherzolite LZ01 record lower P-T conditions (5Kb, 1075°C) indicative of equilibration in the upper most mantle. The mineral chemistry of LZ01 indicates that considerable

Table 2:8 Calculated P-T conditions for the Lizard Peridotites

2553		2554		CV 10		CV 1	
C	R	C	R	C	R		
15.4 Kb	9.7 Kb	19.2 Kb	12.1 Kb	20.7 Kb	16.5 Kb	18.7 Kb	Mercier
1083°C	953°C	1134°C	1007°C	1157°C	1043°C	1081°C	
1043°C		1138°C		1076°C		991°C	Wells
10 Kb 1119°C		1316°C		1146°C		1167°C	
15 Kb 1145°C		1350°C		1179°C		1185°C	Powell
20 Kb 1175°C		1384°C		1212°C		1203°C	

LZ01	2560	AT 133	
1076°C	1098°C	889°C	Wells
5 Kb 1066°C	874°C	5 Kb 862°C	
10 Kb 1101°C	893°C	870°C	
15 Kb 1136°C	922°C	879°C	Powell
20 Kb 1171°C	951°C	887°C	
5 Kb	5 Kb	5 Kb	Obata

re-equilibration occurred as a result of melt infiltration into a spinel lherzolite and that it is this event recorded by the P-T estimates. The data therefore suggest that the Lizard spinel lherzolites had risen adiabatically from the spinel lherzolite stability field to the base of the crust (see Figure 2:11). The deformation and recrystallisation of the pargasite and plagioclase lherzolites occurred after essentially isobaric cooling, i.e. within the uppermost mantle at approximately 900°C.

2:4:7 Conclusions

The mineral chemistry of the spinel lherzolites reflect differing degrees of melt extraction followed by down temperature and pressure re-equilibration. The formation of the plagioclase and pargasite peridotites can be related to the introduction of a picritic melt into the spinel lherzolites (Spray, 1982) that had undergone an adiabatic rise to the uppermost mantle (5Kb, 1075°C). Extensive equilibration accompanied the melt infiltration and was followed by deformation and re-crystallisation at lower temperatures (900°C).

Figure 2:11 INFERRED P–T TRAJECTORY OF THE LIZARD PERIDOTITES

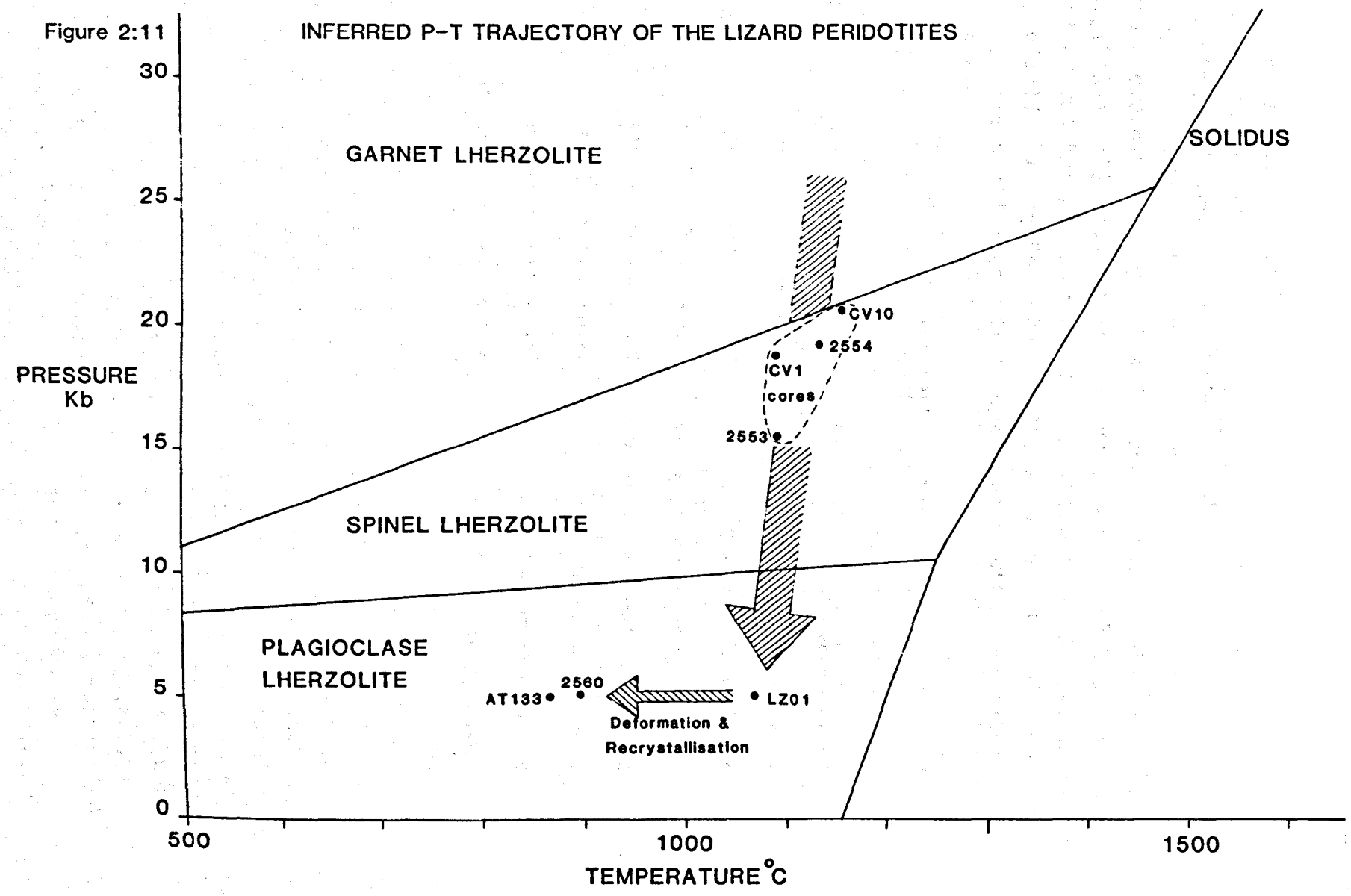

2:5 Geochronology

2:5:1 Previous work. Several K/Ar age determinations have been reported for parts of the Lizard Complex (Table 2:9) and they suggest a metamorphic age of between 350 and 400 Ma for the rocks beneath the ophiolitic units but provide little constraint as to the actual age of the ophiolitic rocks.

Table 2:9 K/Ar ages for the Lizard Complex

Kennack Gneiss (biot)	Miller and Green (1961a)	Av of 2	391 ± 7
Kennack Gneiss (Hbl)	Miller and Green (1961b)		366 ± 20
Old Lizard Head Series (Musc)	Miller and Green (1961a)		356 ± 4
Llanderednack Hornblende Schist (Hbl)	Miller and Green (1961b)		371 ± 20
Llanderednack Hornblende Schist (Hbl)	Miller and Green (1961b)		442 ± 24
Hornblende Amphibolite (WR)	Miller and Green (1961b)		357 ± 20
Hornblende Granulite (WR)	Miller and Green (1961b)		492 ± 26
Dolerite dykes (11 WR)	Halliday and Mitchell (1977)		131 - 403

2:5:2 Sm-Nd Mineral Isochron. Clinopyroxene, plagioclase, olivine and magnetite fractions were separated by magnetic and hand picking techniques from a fresh sample of black olivine gabbro CV5. Analytical techniques are described in Appendix II and the results presented in Table 2:10. A second whole rock analysis was carried out 4 months later to check the reproducibility of the data and the homogeneity of the powder. The two analyses were found to be within analytical error.

The data are presented on a Sm-Nd isochron diagram (Figure 2:12). The "olivine" analysis is deviant from a regression line through the remaining points and, due to its partially serpentinised and oxidised nature, has been omitted from the isochron calculations. The data were processed on a computer program using the least squares approximation method following York (1966), and yielded an age of 375 $\pm$ 34 Ma with M.S.W.D. of 0.006. The exceedingly small M.S.W.D. could be taken to indicate that the analytical errors used in the calculations were too great. However, the within run errors for $^{143}Nd/^{144}Nd$, circa 0.002%, and Sm/Nd, 0.1%, represent the likely minimum errors. The initial ratio of 0.51265 $\pm$ 2 indicates that the gabbro CV5 was derived from a depleted source with an εNd_I value of 9.8 $\pm$ 0.4.

Before discussing the significance of the age determination it is interesting to compare the precision of this age to that of previously published Sm-Nd mineral isochrons. Some published Sm-Nd mineral ages appear to be much more precise than that presented here (Table 2:11). However, when those ages are recalculated using a standard least squares program based on York (1966) several would appear to have been reported with underestimated errors (see Table 2:11). The most spectacular example is for the Bay of Island ophiolite for which Jacobson and Wasserburg (1979) reported an age of 508 $\pm$ 6 Ma in contrast to the age of 508 $\pm$ 58 Ma calculated here. Since the M.S.W.D. is 0.01 one can only conclude that even though the M.S.W.D. is less than 1 Jacobson and Wasserburg have effectively multiplied their calculated error by $\sqrt{\text{M.S.W.D.}}$. This procedure is clearly untenable, and if applied to the data from the Coverack gabbro would yield an age of 375 $\pm$ 2 Ma.

Figure 2:12

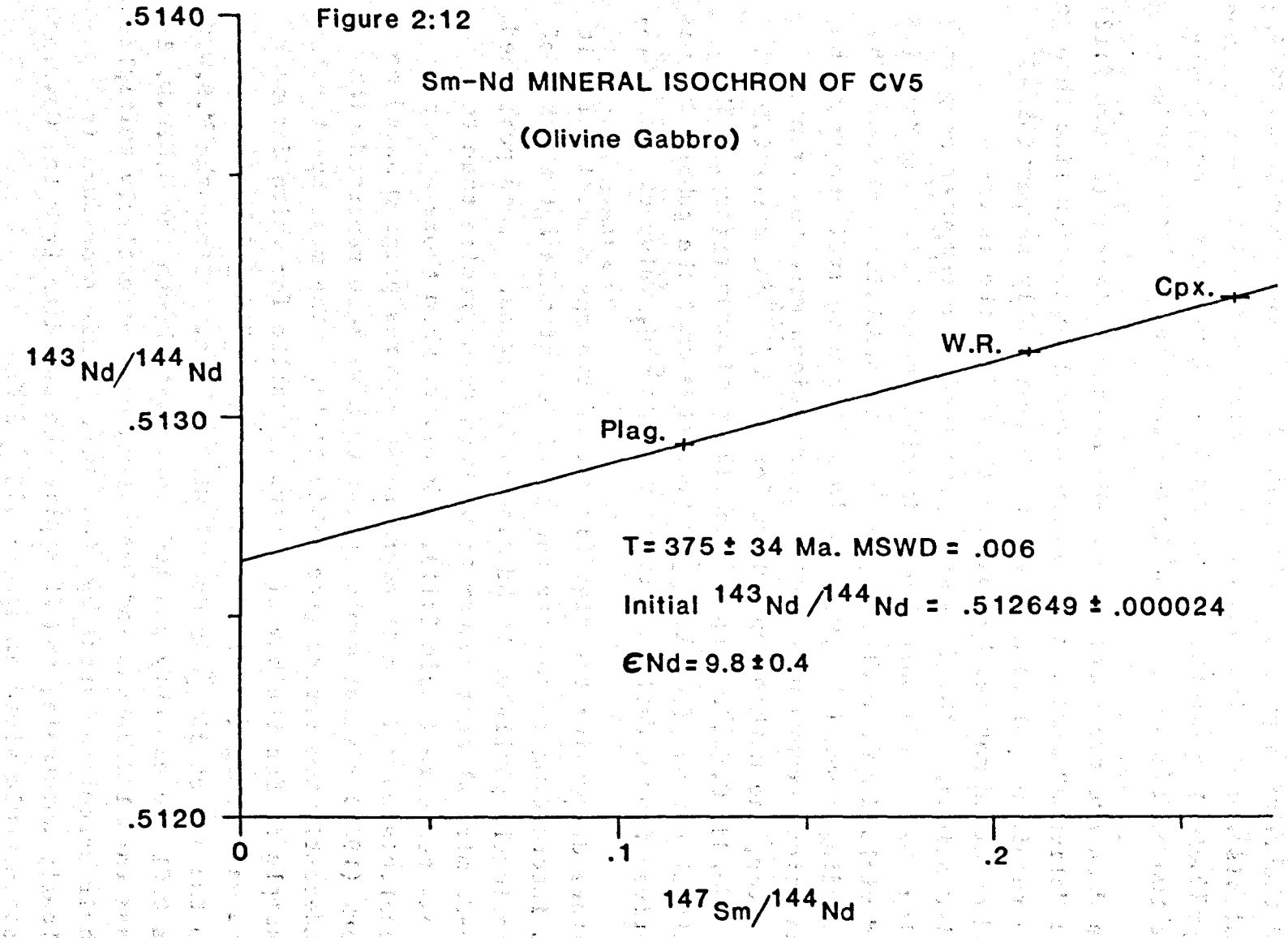
Sm-Nd MINERAL ISOCHRON OF CV5
(Olivine Gabbro)
.5140
.5130
.5120
143Nd/144Nd
0
.1
.2
147Sm/144Nd
Cpx.
W.R.
Plag.
T= 375 ± 34 Ma. MSWD = .006
Initial 143Nd/144Nd = .512649 ± .000024
εNd= 9.8 ± 0.4

Table 2:11

Sm-Nd mineral Isochrons

			Recalculated	M.S.W.D.
Stillwater				
Depaolo and Wasserburg (1979)				
2 Pyroxene gabbro	Age;	2701 $\pm$ 8	2699 $\pm$ 39	2.2
Bay of Islands				
Jacobson and Wasserburg (1979)				
		508 $\pm$ 6	508 $\pm$ 58	0.01
Oman				
McCulloch et al. (1980)				
		128 $\pm$ 20	127 $\pm$ 26	1.6
Lizard Complex				
			375 $\pm$ 34	0.006

In conclusion it is noted that although several Sm-Nd mineral isochrons have been published it is not always clear which parameters have been used in the isochron calculations, what the M.S.W.D. value is, and at which sigma levels errors are quoted. Standardisation following Rb-Sr isochron procedures would be desirable. The age from the Lizard Complex is of comparable precision to other published Sm-Nd mineral ages.

2:5:3 Discussion. The 375 $\pm$ 34 Ma age obtained for the olivine gabbro from Coverack lies within the range of the K-Ar dates obtained from the metamorphic assemblages in the Lizard Complex (see Table 2:9). It is therefore important to ascertain if this new date represents; i) a primary igneous cooling age or ii) a metamorphic age.

At present there is little direct evidence for the blocking temperatures of REE in the major rock forming minerals and it is therefore difficult to evaluate the conditions under which the original igneous age of the gabbro CV5 would be reset. Humphries and Cliff (1982) suggested that the blocking temperature of the Sm-Nd system in garnets, which upon thermodynamic considerations is expected to be in excess of 1000°C, may be as low as 500°C under very slow cooling rates ($1^{\circ}C\ Myr^{-1}$). The effective Sm-Nd blocking temperature for a particular mineral depends upon its size, the diffusion coefficients for Sm and Nd and the cooling rate. (The faster the cooling rate the higher the blocking temperature.) Although no specific data are available for REE diffusion in plagioclase Hart (1981) suggested from a study of available experimental diffusion data on feldspars (O, Ar, K, Na, Sr and Rb) that for cooling rates in the range of 10 to 10^5 $^{\circ}C\ myr^{-1}$ all element species can be expected to "freeze-in" simultaneously at temperatures in the range 400 to 600°C. Clinopyroxene, the other major constituent mineral in the gabbro is a high temperature mineral and would be expected to have a higher

blocking temperatures for REE compared to plagioclase.

It is not possible to establish the exact cooling rate for the gabbro body as the original size is unknown. However, a cooling rate of 10^3 to 10^4 $^{o}C\ Myr^{-1}$ would be appropriate for a body the size of the Lizard Complex (Hart, 1981). Under such cooling rates the Sm-Nd systematics of the gabbro body would be "frozen-in" above 500°C and the age obtained from this rock would represent the period of geological activity and not an age subsequent to a long cooling history (i.e. less than 1 Ma after event). It is therefore concluded that temperatures in excess of 500°C are probably required to reset the original igneous Sm-Nd isotope systematics of the gabbro body.

Barnes and Andrews (in press) established that during the regional metamorphism in S.W. England (365 to 345 Ma, Dodson and Rex, 1971) temperatures did not exceed 300°C suggesting that the Sm-Nd mineral age is not the result of the regional metamorphism. However, temperatures generated during the emplacement of the ophiolitic units were sufficiently high to cause partial melting and the generation of the Kennack Gneiss (>600°C) and hence could have reset the Sm-Nd systematics of the gabbro. Significantly, however, the gneisses are only locally developed and they are always associated with the base of the lower ophiolite unit. Thus there is at least 500 m of peridotite between the gabbro and the zone of high temperatures in the possibly underlying Kennack Gneiss. Very high thermal gradients (1100°C/Km Jamieson, 1980) are characteristic of such emplacement metamorphism and so it is unlikely that at that time the temperatures in the gabbro were high enough to reset the Sm-Nd systematics. However, perhaps the most convincing evidence that the igneous Sm-Nd systematics of the gabbro have not been reset is provided by the petrology of the gabbro itself. Olivine is partially serpentinised

indicating that water was present in the rock but amphibole and chlorite (minerals that would be associated with low and high temperature hydrous alteration of the clinopyroxene) are rare, only being found associated with joints. It is therefore concluded that the 375 $\pm$ 34 Ma age of the olivine gabbro at Coverack is a primary igneous cooling age and represents the age of the crustal portion of the ophiolitic units.

The Kennack Gneiss cross cuts the basal thrust of the ophiolitic units and thus records an event post or synchronous with the emplacement of the ophiolitic units. Styles and Rundle (in press) recently obtained a Rb-Sr whole-rock age of 369 $\pm$ 12 Ma for the Kennack Gneiss, and since this is analytically indistinguishable from the age of the Coverack gabbro it precludes a lengthy history for the ophiolitic rocks prior to their emplacement. Similarly short histories have been reported from ophiolite complexes such as that in Oman where the formation age 98 to 95 $\pm$ 1 Ma (Tilton et al., 1979) and emplacement ages of 89 $\pm$ 3 Ma.

2:5:4 Interim Summary of Geological events in S.W. England. The formation and emplacement of the Lizard ophiolite complex are analytical indistinguishable at circa 370 Ma. The mélange to the north of the Lizard Complex is Middle Devonian, circa 370 Ma and hence may have a genetic link with the Lizard Complex. S.W. England suffered a low grade regional metamorphic event associated with the Hercynian Orogeny circa 365 to 345 Ma (Dodson and Rex, 1971) prior to the emplacement of the Cornwall Granites at 270 Ma.

2:6 RE and Trace Element Geochemistry of the Ophiolitic Rock Types

2:6:1 Igneous Rocks. Trace and R.E. element determinations are reported in Table 2:12 and Appendix III for a total of 7 dolerite dykes, a plagiogranite and 3 metabasalts from the mélange. The REE data are presented as chondrite normalised patterns in Figure 2:13. The dolerites and metabasalts record significant

variations in the degree of incompatible element enrichment ($Zr/Y = 2.5$ to 6.1 and $(Ce/Yb)_N = 0.8$ to 2.2). The late dolerite suite and mélange metabasalts have similar trace element characteristics and in marked contrast to the late dykes they are incompatible element enriched, $Zr/Y = 4.1$ to 6.1 and $(Ce/Yb)_N = 1.4$ to 2.1). All the basaltic rocks show moderately fractionated H.REE patterns with $(Dy/Yb)_N$ ratios of 1.1 to 1.3 (Figure 2:13a to c).
The plagiogranite, P7, is notable for very high trace element contents (Zr = 705 ppm, $(Ce)_N = 101$ and $(Yb)_N = 28.5$) and marked incompatible element enrichment ($Zr/Y = 9$ and $(Ce/Yb)_N = 3.5$). The REE profile also shows flat H.REE and a marked Eu anomaly, $Eu/Eu^* = 0.82$ (Figure 2:13a). In contrast the basaltic rocks have only minor Eu anomalies, $Eu/Eu^* = 0.92$ to 1.07. Significantly the 2 rocks with positive Eu anomalies, CV2 and P5, contain large resorbed plagioclase xenocrysts that are more albitic than the groundmass plagioclose (see Table 2:2). It is therefore possible that the positive Eu anomalies are the result of plagioclase accumulation:- probably from the gabbro body.

The present of negative Eu anomalies in the plagiogranite and the majority of the basaltic rocks suggest that plagioclase fractionation may have played a significant role in their petrogenesis. Rayleigh fractionation modelling has been performed to establish if the variations between, and within, each rock suite, and the formation of the plagiogranite, can be accounted for by purely fractional crystallisation. Olivine gabbro (30% olivine, 40% plagioclase and 30% clinopyroxene) was taken as the probable fractionating assemblage due to the presence of plagioclase, olivine and clinopyroxene as phenocryst phases within the dolerite dykes.

The Rayleigh fractionation calculations demonstrate that in excess of 40% fractionation is required to account for the variations in the H.REE contents within each rock suite.

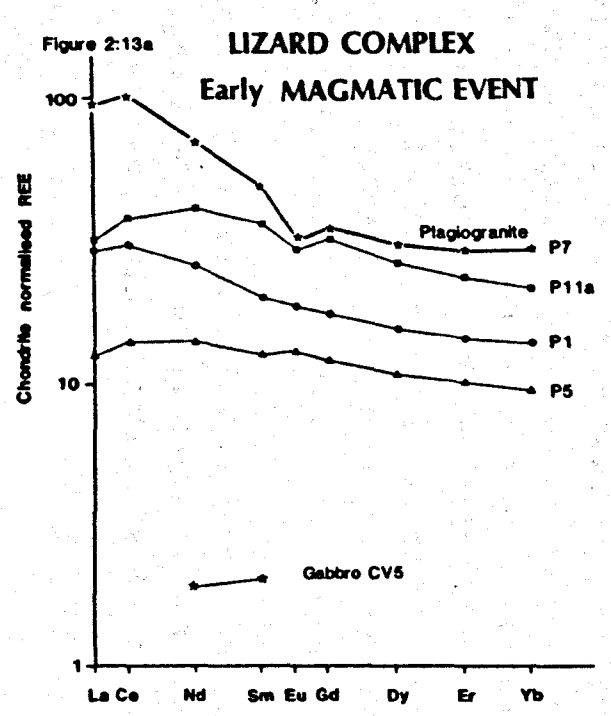

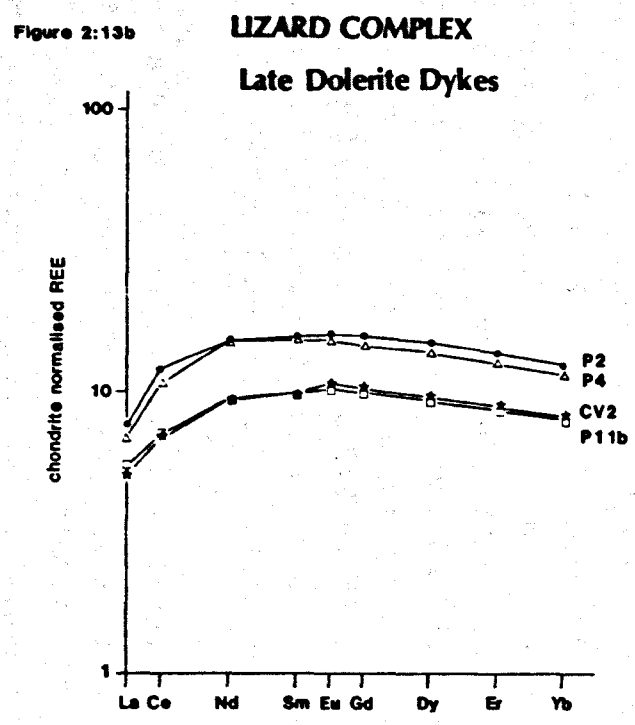

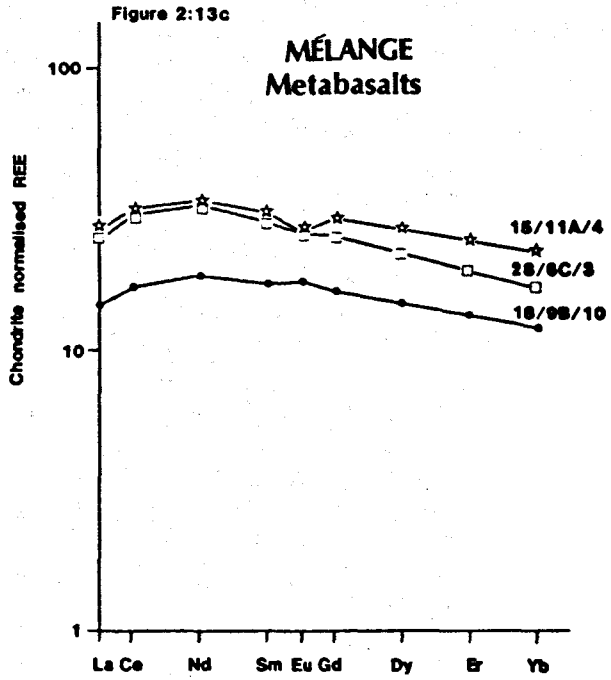

Figure 2:13

REE data for igneous rocks from the Lizard Complex
All samples are dolerite dykes unless otherwise stated

However, significantly greater degrees of fractionation are required to explain the L.REE variations. 40% fractional crystallisation of a gabbroic assemblage from the chemically most primitive basaltic liquids recorded in the Lizard Complex (MgO = 10% and SiO_2 = 48%) would result in liquids more evolved than any of the dolerites (MgO < 5% and SiO_2 > 54%). Even higher degrees of fractional crystallisation are required to explain the inter-suite REE variations. It therefore appears that although fractional crystallisation has occurred, it cannot account for the overall range in REE abundances.

It is significant to note that the tholeiitic nature of the basaltic rocks (Kirby, op. cit.) argues for large percentage partial melting, > 10%, of their respective mantle source regions and hence the REE patterns of the magmas will not be significantly fractionated compared to their sources. The $(Ce/Yb)_N$ variations between and within basaltic suites are therefore probably indicative of heterogeneous source regions.

The extremely high trace element contents of the plagiogranite (e.g. Zr = 705 ppm) suggest that, if they are genetically related to the gabbroic and basaltic rocks (Zr < 300 ppm), that fractional crystallisation has played a major role in its petrogenesis (see Chapter 4 for a discussion on the role of fractional crystallisation and crustal melting in the petrogenesis of highly evolved rocks). In excess of 90% fractionation of a gabbroic assemblage is required to produce the trace element content of the plagiogranite from a basaltic liquid equivalent to a dolerite, P1. Interestingly the REE pattern of the plagiogranite, P7, does not show the L.REE depletion typical of most MORB and ophiolite derived plagiogranites (Figure 2:14).

Average MORB normalised trace element patterns for the early and late dyke suites are presented in Figure 2:15. The early dyke suite shows relative enrichment in all elements except Ti and Yb with the greatest enrichment in Ba. This style of

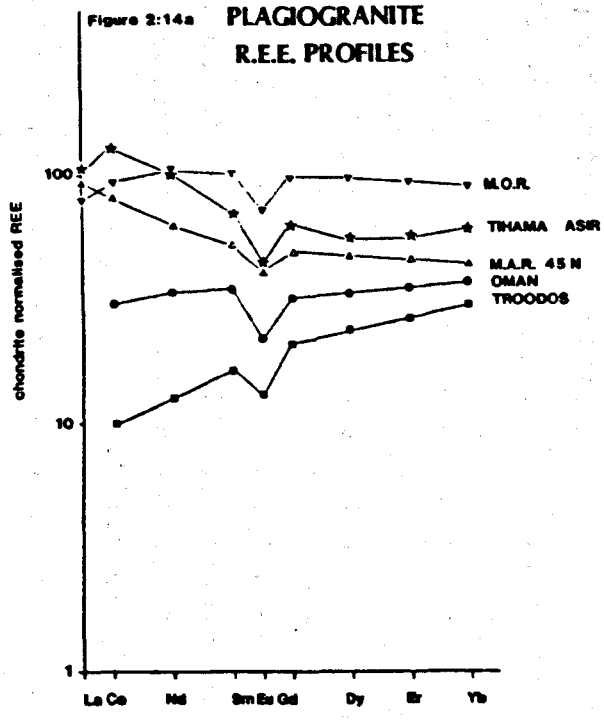

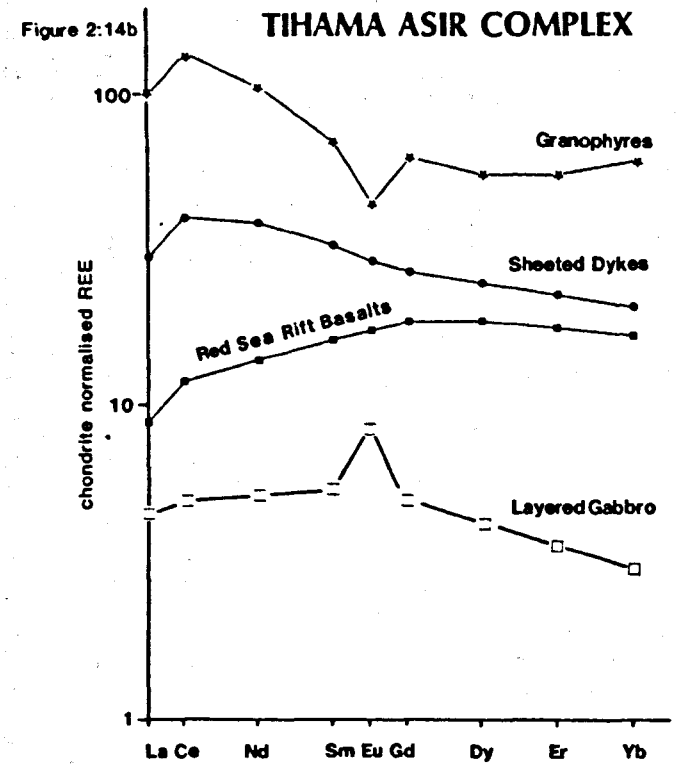

REE data for;

a) oceanic and ophiolitic plagiogranites

Data sources; Aldiss,1981,Chase,1969,Coleman et al.,1979

b) the Tihama Asir Ophiolite Complex which shows an evolution in igneous activity equivalent to that of the Lizard Complex i.e. early L.REE enriched, followed by MORB like, magmas.

trace element enrichment is typical of "within plate" and "E type MORB" volcanism, e.g. Hawaii and the Gulf of Aden (Figure 2:15). The mélange metabasalts are not shown in Figure 2:15 but have similar trace element characteristics to the early dyke suite. In contrast the geochemistry of the late dykes shows MORB-like characteristics, but again has relative LILE and Nb enrichment with the greatest relative enrichment recorded in Ba suggesting a possible genetic relationship between the source regions of the early and late dyke suites. Although LILE enrichment is characteristic of subduction related volcanism, such rocks also have relative Nb depletion (Figure 2:15). LILE enrichment and Nb depletion are also characteristic of volcanism in some marginal basins (see Pearce et al., 1981). It is therefore probable that the Lizard ophiolitic rocks did not form in a subduction related environment.

Interestingly the trace element characteristics and evolution recorded in the Lizard Complex is comparable to that of the Red Sea. The Miocene Tihama Asir Ophiolite complex, which formed during the initial rifting of the Red Sea, contains L.REE enriched dolerite dykes associated with layered gabbros and plagiogranites (Coleman et al., 1979) (Figure 2:14). The plagiogranites are significant in that, as in the case of the Lizard plagiogranites, they show no evidence of L.REE depletion typical of most MORB and ophiolite derived plagiogranites (Figure 2:14). Unfortunately no trace element data are available for the dolerite dykes. However, tholeiitic basalts forming islands within the Red Sea have similar major element compositions to those of the dolerite dykes. The trace element characteristics of these tholeiitic basalts are equivalent to those of the early dyke suite (Figure 2:15a and e) and the late dyke suite are comparable to the basalts of the Gulf of Aden.

It is concluded from the trace element data that there are two volcanic suites within the Lizard Complex and that they are derived from heterogeneous source regions. The

Figure 2:15a TRACE ELEMENT PATTERNS FOR LIZARD BASALTIC VOLCANISM

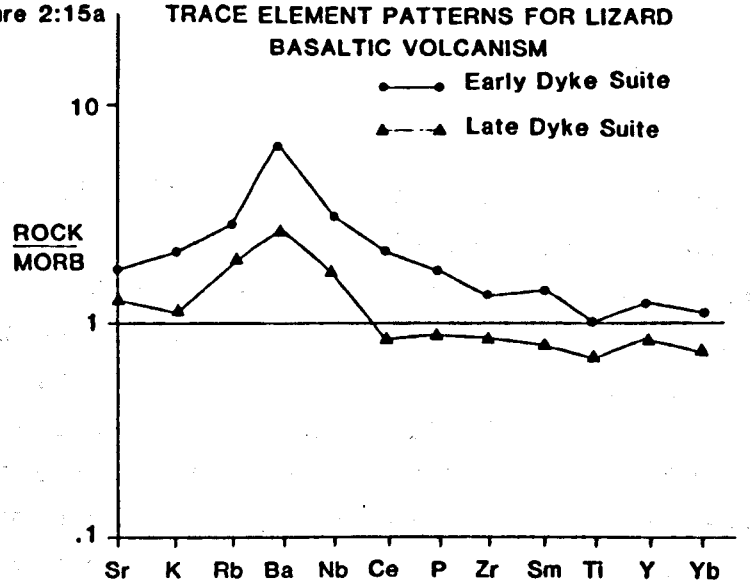

Figure 2:15b MORB variations

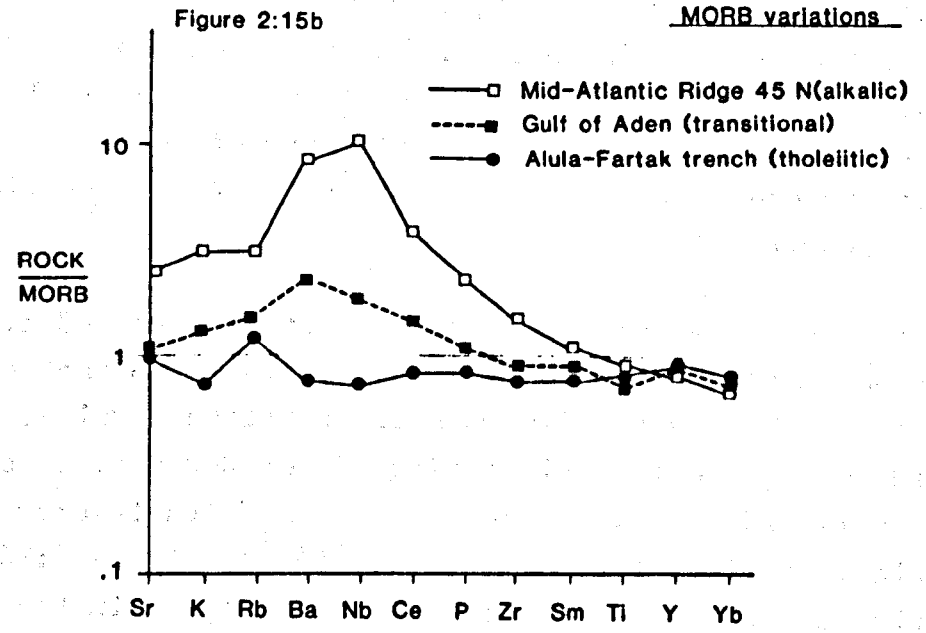

Figure 2:15c Intra-plate Volcanism

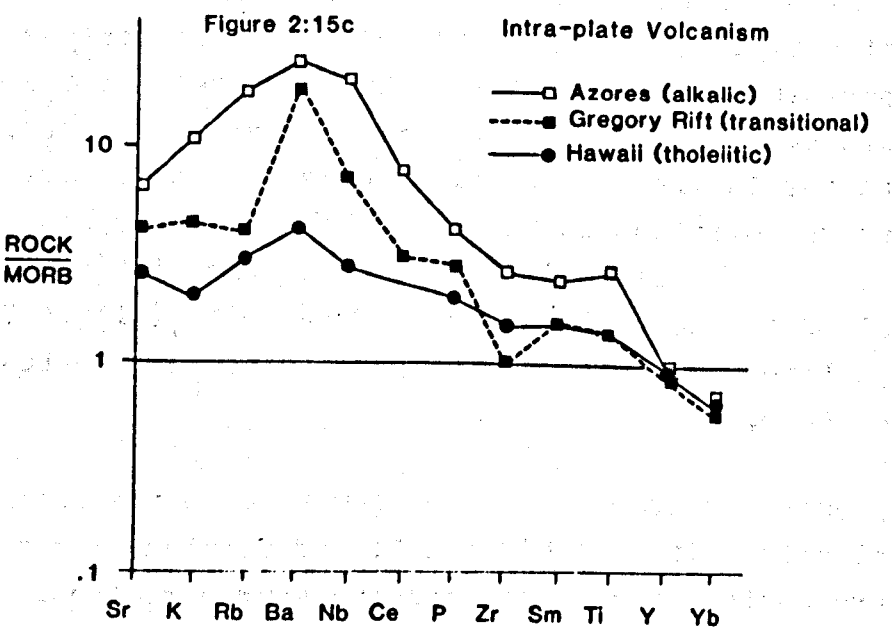

Figure 2:17 $(Ce)_N$ - $(Yb)_N$ VARIATION DIAGRAM FOR PERIDOTITES

REE data for all three Lizard Peridotite types are plotted along with those from several ultramafic complexes. The solid line represents an unfractionated chondritic source.

Calculated residue trajectories are shown for melt extraction, under batch melting conditions, from a 2.5 times chondritic source. Each residue trajectory is marked with 1, 5, 10 and 20% melting.

Trend A	Spinel lherzolite	portion coefficients	Hanson, 1977
B	"	"	Loubet et al., 1975
C	"	"	Frey et al., 1978
D	Garnet lherzolite	"	Hanson, 1977
E	Garnet lherzolite residue (10%)	"	Hanson, 1977

Initial Mode: spinel lherzolite:- 55% olivine, 25% cpx, 15% opx, 5% spinel

garnet lherzolite:- 55% olivine, 25% opx, 10% cpx, 10% gnt.

Melting proportions:

spinel lherzolite:- cpx:opx:ol = 0.6 : 0.2 : 0.2

garnet lherzolite:- cpx:gnt:Opx:Ol = 0.4:0.4:0.1:0.1

Figure 2:15d

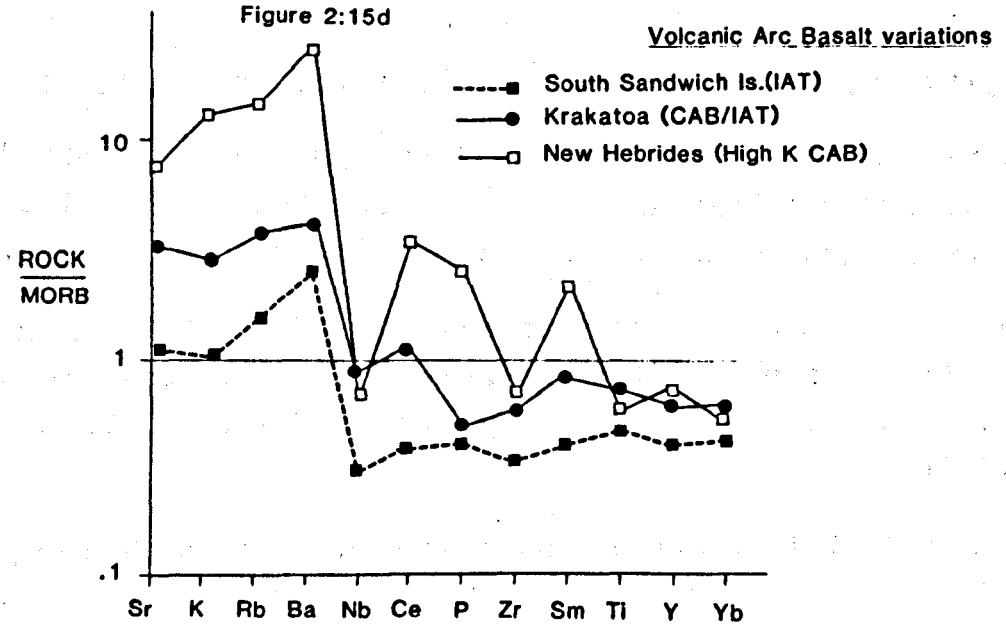

Figure 2:15e TRACE ELEMENT PATTERNS OF RED SEA VOLCANISM

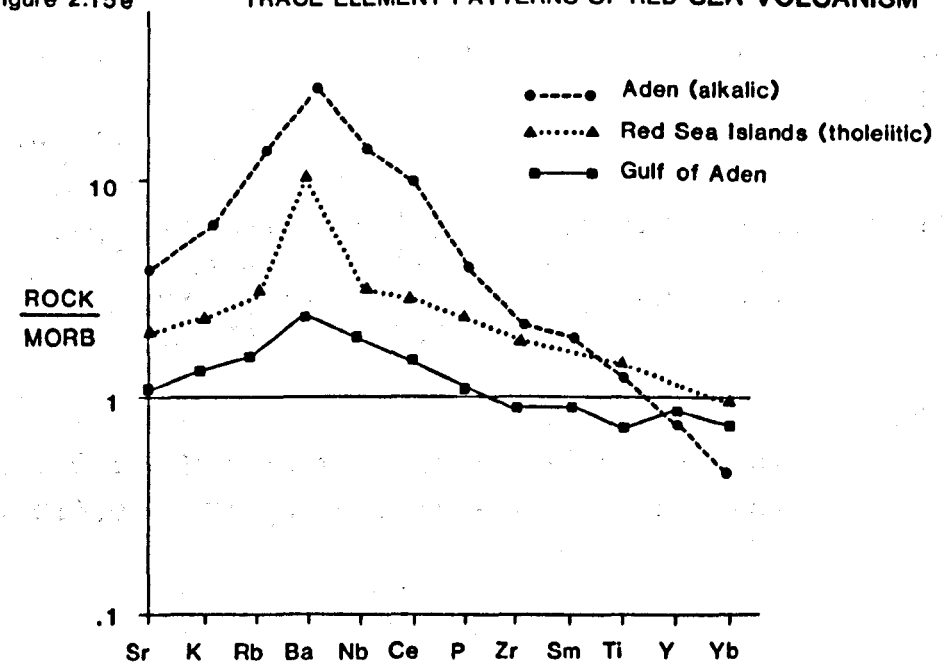

Data sources; Pearce, 1982
Gass et al., 1973

plagiogranites within the Lizard Complex are apparently derived by large degrees of fractional crystallisation >90%. The magmatic evolution of the Lizard Complex is comparable to the initial rifting of the Red Sea, in that early incompatible element enriched magmas were succeeded by more MOR3-like magmas.

2:7 Nd Isotope Systematics of the Lizard Complex

2:7:1 Peridotites. The Nd isotope data of the peridotites are presented in Table 2:13, the basaltic rocks Table 2:12 and the gneisses Table 2:14. The range in present day $^{143}Nd/^{144}Nd$ ratios of the peridotites and the mineral separates, 0.51301 to 0.51414 is partially a consequence of the large range in their Sm/Nd ratios, 0.289 to 1.188. In each case the high values are among the most depleted yet recorded. The initial ratios of the peridotites (considered at 375 Ma the formation and emplacement age of the Lizard Complex) range from 0.51238 to 0.51282 equivalent to εNd_I values of + 4.8 $\pm$ 1.6 to + 13.3 $\pm$ 1.0 (Figure 2:16). These data therefore exhibit more diversity than present day MORB, ε Nd + 8 to + 13. The mineral separates and LZ01 were leached overnight in 6 MHCL to remove any possible alteration. LZ01 showed a 40% weight loss, consistent with the dissolution of a large proportion of the serpentinised olivine leaving a pyroxene enriched residue.

Due to the highly serpentinised nature of the majority of the peridotites, Sr isotope analyses were only carried out on mineral separates and the freshest whole-rock, LZ01. Unfortunately the small quantity of clinopyroxene separated from the spinel lherzolite 2553 and the extremely low Rb and Sr contents of the rock is reflected in the larger errors in its $^{87}Sr/^{86}Sr$ and Rb/Sr ratios. Clinopyroxene is the phase within plagioclase and spinel lherzolites that will contain most of the REE and LILE, such that the analysis of clinopyroxene is likely to provide the best estimate of the isotope composition of the unaltered whole rock. The present

Table 2 : 12 Trace Element and Isotope Data for the Basaltic Rocks of the Lizard Complex

Sample	Rock Type	Locality	Zr/Y +	La	Ce	Nd	Sm	Eu	Gd	Dy	Er	Yb	$(Ce/Yb)_N$	$^{147}Sm/^{144}Nd$	$^{143}Nd/^{144}Nd$	$\varepsilon_{Nd_{375}}$
P2	dolerite	S. Porthoustock	3.3	2.46	10.4	9.53	3.11	1.17	4.10	4.71	2.83	2.52	1.0	0.198	0.513095 ± 14	+ 9.2 ± 0.3
P4	dolerite	S. Porthoustock	3.4	2.21	9.15	9.46	3.17	1.22	4.36	5.12	3.11	2.77	0.8	0.203	0.513216 ± 16 0.513241 ± 20	+ 11.7 ± 0.4
P116	dolerite	Porthoustock	3.0	1.78	6.02	5.94	1.99	0.804	2.80	3.21	1.92	1.73	0.9	0.203	0.513157 ± 24	+ 10.2 ± 0.5
CV2	dolerite	Coverack	3.0	1.7	5.9	6.0	2.02	0.835	2.82	3.29	1.99	1.8	0.8	0.202	0.513206 ± 20	+ 11.2 ± 0.4
P1	dolerite	S. Porthoustock	6.1	9.78	26.8	16.7	4.17	1.46	4.95	5.43	3.31	3.08	2.2	0.151	0.512966 ± 14	+ 8.9 ± 0.3
P5	dolerite	S. Porthoustock	4.1	4.13	12.2	8.96	2.57	1.01	3.32	3.80	2.30	2.11	1.5	0.174	0.513035 ± 14	+ 9.0 ± 0.3
P11a	dolerite	Porthoustock	5.1	10.4	33.4	26.5	7.52	2.33	9.28	8.15	4.71	4.30	1.98	0.171	0.513038 ± 12	+ 10.1 ± 0.2
P7	plagiogranite	Porthoustock	9.0	31.3	87.8	44.7	9.6	2.41	9.42	10.2	6.34	6.27	3.5	0.130	0.512955 ± 12	+ 9.5 ± 0.2
15/IIS/4	metabasalt	Melange	2.5*	8.63	26.7	21.3	6.15	2.03	7.88	9.06	5.37	4.72	1.4	0.175	0.512987 ± 16	+ 8.2 ± 0.3
18/9B/10	metabasalt	Melange	4.1*	4.8	14.1	11.5	3.40	1.32	4.40	4.97	2.93	2.61	1.4	0.180	0.512998 ± 16	+ 8.2 ± 0.3
28/6C/3	metabasalt	Melange	4.6*	8.27	25.8	20.2	5.68	1.97	6.87	7.37	4.11	3.59	1.8	0.171	0.512987 ± 8	+ 8.3 ± 0.2

+ XRF Nottingham

* XRF Southampton (Barnes perscom)

Table 2:13 Isotope data for the LIZARD PERIDOTITES

Sample	Rock Type	Locality	Sm	Nd	Sm/Nd	$^{143}Nd/^{144}Nd$	$\varepsilon_{Nd_{375}}$	Rb	Sr	$Rb/_{Sr}$	$^{87}Sr/^{86}Sr$	$\varepsilon_{Sr_{375}}$
2553	spinel lherzolite	Gwenter Goonhilly Downs	0.9489	1.342	0.7070	0.513870 ± 54	+13.3 ± 1.0					
2553 cpx.			1.311	1.641	0.7989	0.514022 ± 46	+ 13.6 ± 1.0	0.09 ± 1	8.15 ± 6	0.01117	0.70178 ± 10	- 37.5 ± 3
2554	spinel lherzolite	Gwenter Goonhilly Downs	0.04198	0.03535	1.1876	0.514143 ± 80	+ 4.8 ± 1.6					
2555	pargasite harzburgite	Kernewas Goonhilly Downs	0.2770	0.8450	0.3278	0.513102 ± 26	+ 9.3 ± 0.5					
2555 amph.			1.560	4.598	0.3393	0.513099 ± 22	+ 8.9 ± 0.4	1.428	29.41	0.04855	0.70399 ± 4	- 14.3 ± 0.6
2559	plagioclase lherzolite	Kernewas Goonhilly Downs	0.2905	0.7169	0.4052	0.513090 ± 28	+ 6.9 ± 0.6					
2560	plagioclase lherzolite	Kernewas Goonhilly Downs	0.2321	0.5495	0.4224	0.513323 ± 32	+ 10.9 ± 0.6					
LZ01*	plagioclase lherzolite	S. Coverack	0.5586	1.936	0.2885	0.513008 ± 30	+ 8.6 ± 0.6					
LZ01	plagioclase lherzolite					0.512958 ± 28		0.4201	18.61	0.02257	0.70396 ± 3	- 9.0 ± 0.4

*unleached sample

See section A:2:2 for a discusion of the Nd blank.

Figure 2:16

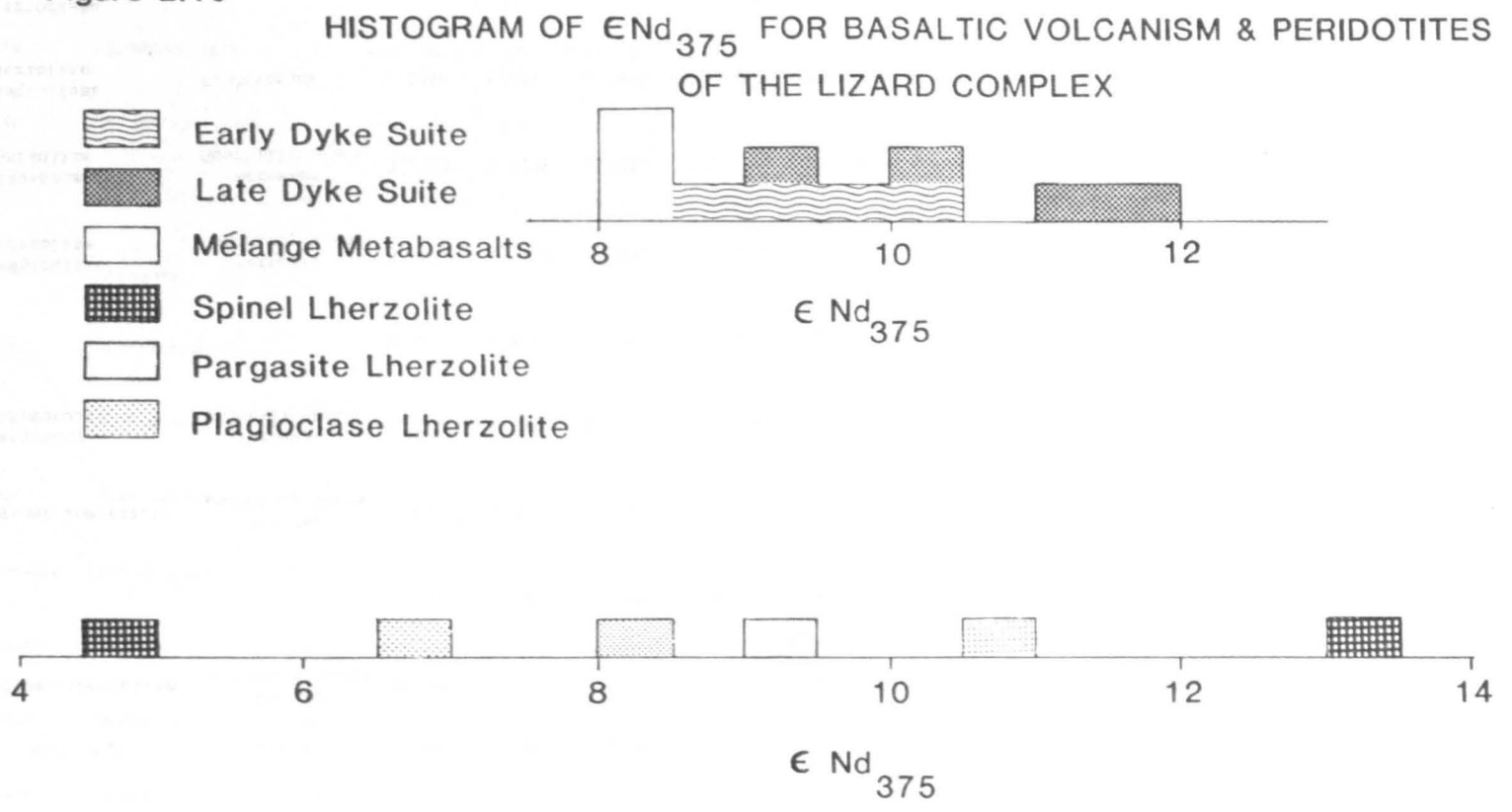
HISTOGRAM OF ϵNd375 FOR BASALTIC VOLCANISM & PERIDOTITES OF THE LIZARD COMPLEX
Early Dyke Suite
Late Dyke Suite
Mélange Metabasalts
Spinel Lherzolite
Pargasite Lherzolite
Plagioclase Lherzolite
8
10
12
ϵ Nd375
4
6
8
10
12
14
ϵ Nd375

day $^{143}Nd/^{144}Nd$ ratio of the clinopyroxene from 2553 and the pyroxene rich residue of LZ01 are more and less radiogenic than the whole-rock samples respectively. However, the $(^{143}Nd/^{144}Nd)_{375}$ ratios of the clinopyroxene and whole-rock of 2553 are within error. The Sm/Nd and Rb/Sr ratios were not determined for both the whole-rock and residue of LZ01, but the differences in the present day $^{143}Nd/^{144}Nd$ and $^{87}Sr/^{86}Sr$ ratios between the whole-rock and residue are relatively small and may be explained by small differences in Sm/Nd and Rb/Sr or minor alteration effects.

2:7:2 Petrogenesis of the spinel lherzolites. Spinel lherzolites comprise the majority of the Lizard Peridotite body and this section considers the petrogenesis of these rocks which show no evidence of the melt infiltration event recorded in the plagioclase lherzolite, LZ01.

Frey (1969) reported REE analyses for the 2 spinel lherzolites analysed for the Nd isotopes in this study. These samples possess $(Ce/Yb)_N$ ratios of 0.01 and are the most L.REE depleted peridotites yet analysed (Figure 2:17, 2:24). REE data for all 3 Lizard peridotite types and from several other ultramafic complexes, are plotted in a $(Ce)_N$ vs $(Yb)_N$ diagram (Figure 2:11). The peridotites from the Lizard Complex encompass the entire recorded range in $(Ce)_N$ values within Alpine type ultramafic bodies. The Lizard spinel lherzolites are notable in that they have the lowest Ce contents while having Yb contents comparable with many other peridotites.

In order to evaluate the conditions under which the Lizard spinel lherzolites could have been generated, batch melting calculations ere performed using a number of different sets of published REE distribution coefficients (K_D's) (see Figure 2:17 for details). Trends A, B and C on Figure 2:17 (different K_D's) show the progressive evolution of the residue of a spinel lherzolite undergoing increasing degrees of batch melting, assuming a source with undifferentiated REE at 2.5 x chondrite

Figure 2:17 $(Ce)_N - (Yb)_N$ VARIATION DIAGRAM FOR PERIDOTITES

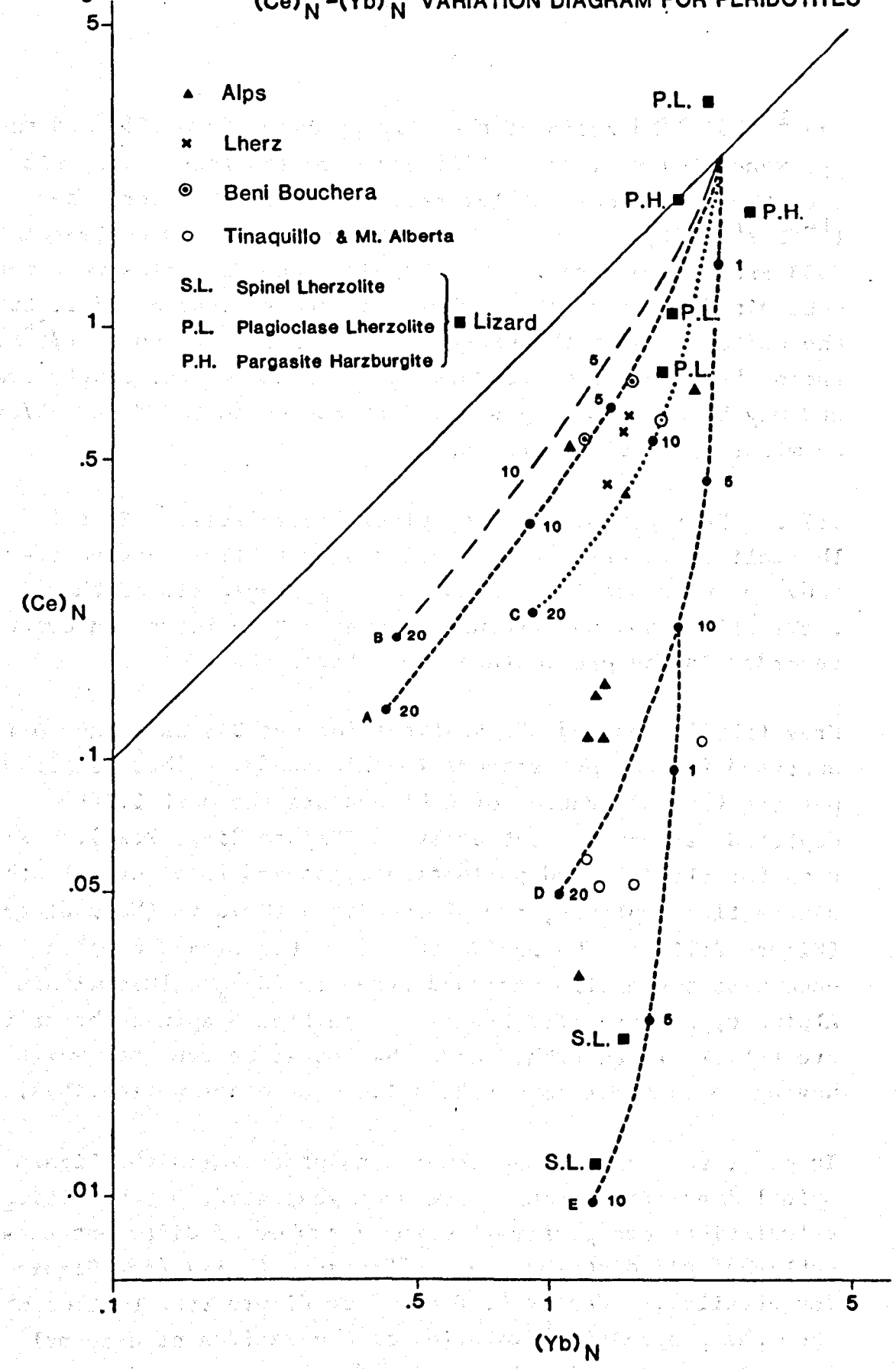

Data sources; Frey, 1969, Loubet and Allegre, 1982, Loubet et al., 1975, Menzies et al., 1977.

abundances. In all the calculations the residue undergoes significant depletion in both Ce and Yb, possessing a $(Ce/Yb)_N$ ratio of about 0.3 after 20% melting. Trend D illustrates the evolution of the residue from a garnet lherzolite undergoing increasing degrees of batch melting. This produces a more marked L.REE depleted residue with a $(Ce/Yb)_N$ ratio of 0.05 after 20% partial melting. However, it is clear from Figure 2:17 that none of these models are capable of reproducing the extreme L.REE depletion shown by the Lizard Spinel lherzolites. The depletion can be reproduced, however, if a multi-stage melting event of a garnet lherzolite is postulated. For example, a two stage model is illustrated in Figure 2:17 (trend E). Note that in each stage of melting, only a relatively small fraction of melt is extracted. In this way, the residue becomes strongly L.REE depleted whilst loosing only a relatively small fraction of its basaltic constituents, i.e. the residue remains of lherzolite composition rather than being reduced to a harzburgite, as in the single stage models. This prediction is compatible with the composition of the spinel lherzolites, which, as their name implies contain >5% cpx and are therefore relatively CaO-rich. It is therefore suggest that the depleted trace element and isotopic characteristics of the spinel lherzolites reflect multiple, small percentage, melt extraction while in the garnet stability field. This conclusion is not incompatible with P-T estimates for these rocks which indicate equilibration within spinel lherzolite stability field but very close to the limits of the garnet lherzolite stability field (Figure 2:11). It is therefore suggested that subsequent to melt extraction in the garnet lherzolite stability field the rock re-equilibrated within the spinel lherzolite stability field.

The combined εNd_{375} and εSr_{375} data of a clinopyroxene from the spinel lherzolite 2553 lie within the mantle array at slightly higher εNd values than present day MORB (Figure 2:18). An implication of the REE data (i.e. multiple depletion events) is that the Sm-Nd isotope systematics of the spinel lherzolites cannot be interpreted as a simple 2 stage model (i.e. chondritic evolution followed by one depletion event), and consequently

Figure 2:18 ε_{Nd} vs ε_{Sr} DIAGRAM FOR LIZARD PERIDOTITES

The diagram depicts the Lizard peridotites (★) relative to present day MORB and Ocean Island Basalts (i.e. the mantle array, marked by dashed lines) and various forms of metasomatised peridotites;

Diopsides from South African garnet lherzolites record ancient LILE and L.REE enrichment (Menzies and Murthy 1979)

In contrast diopsides from Ataq spinel lherzolites record L.REE enrichment but LILE depletion. However, the metasomatic kaersutites from Ataq are displaced to more radiogenic Sr values than the mantle array (Menzies and Murthy 1980).

Apatite pyroxenites from Kiama (Australia) have similar isotope systematics to the Ataq diopsides, (Menzies and Wass in press).

The spinel lherzolites, 2553, lies within the mantle array to more radiogenic ε_{Nd} values than MORB. A mixing line is shown between the spinel lherzolite and the calculated metasomatic fluid which has isotopic systematics equivalent to the hydrous Ataq xenoliths. Interestingly with time, 1000 Ma, the "metasomatised" Lizard peridotites will evolve across the mantle array to values equivalent to the present day values of Kiama and Ataq.

Figure 2:18 ϵ_{Nd} vs ϵ_{Sr} DIAGRAM OF LIZARD PERIDOTITES

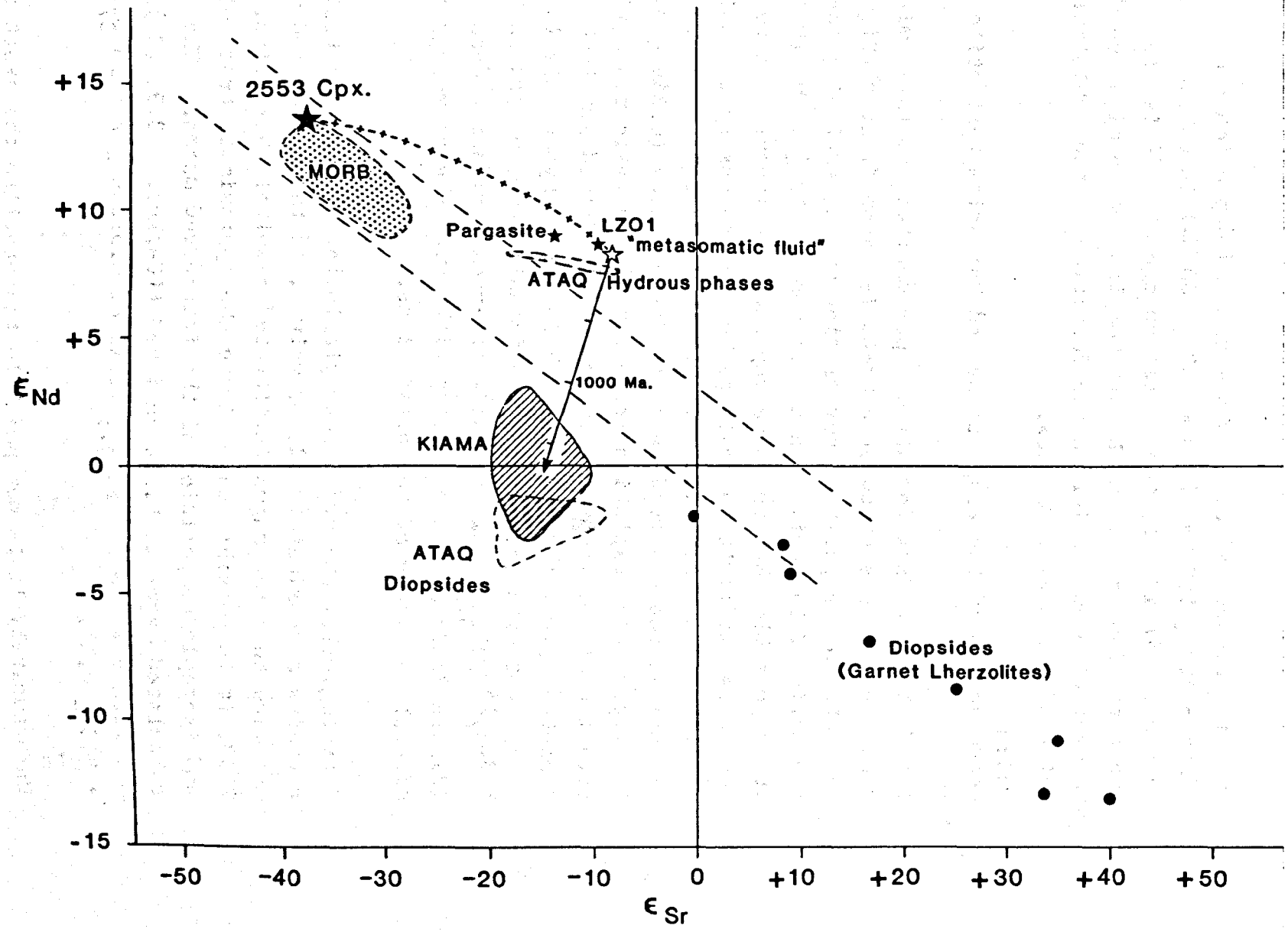

the significance of their whole rock Nd depletion ages (2554 = 420 $\pm$ 160 Ma, 2553 = 830 $\pm$ 100 Ma) is unknown. However, coincidently the depletion age of 2554 is close to the formation age of the Lizard Complex and so might be due to depletion just prior to the formation of the ophiolitic units of the Lizard Complex.

2:7:3
Petrogenesis of the Plagioclase and Pargasite Peridotites

The Nd isotope data for all the peridotites and their mineral separates are presented on a Sm-Nd isochron diagram (Figure 2:19). The data show a positive correlation which, excluding the spinel lherzolite 2554, define an errorchron of 510 $\pm$ 42 Ma (M.S.W.D. = 5) It is possible that the data represent an isochronous relationship but it is difficult to envisage how the necessary isotopic equilibrium was achieved while at the same time maintaining, or producing, the observed range in Sm-Nd ratios (0.259 - 0.707). The alternative explation is that the data reflect a mixing relationship between an introduced magma/fluid and isotopically depleted spinel lherzolites. This latter hypothesis is consistent with the linear relationship between 1/Nd and $^{143}Nd/^{144}Nd)_{375}$ shown by the whole-rock peridotite data (Figure 2:20) and is more compatible with the petrology and mineral chemistry of the peridotites.

Petrologically the undeformed plagioclase lherzolite LZ01 contains approximately 5%, by volume, of the introduced magma. Assuming that the magma infiltrated a spinel lherzolite, e.g. 2553, it is possible to estimate the approximate trace element and isotopic composition of the introduced magma. The calculated magma is L.REE enriched ($(Ce/Yb)_N$ = 3.9, $(Ce)_N$ = 66) with a $(^{143}Nd/^{144}Nd)_{375}$ ratio of 0.51256 $\pm$ 2 (εNd_{375} = + 8.3 $\pm$ 0.4).

Unfortunately it is not possible to establish the exact time of the mixing event. However, the decoupling shown between the low Sm-Nd and high $^{143}Nd/^{144}Nd_{375}$ ratios of LZ01 probably

Figure 2:19

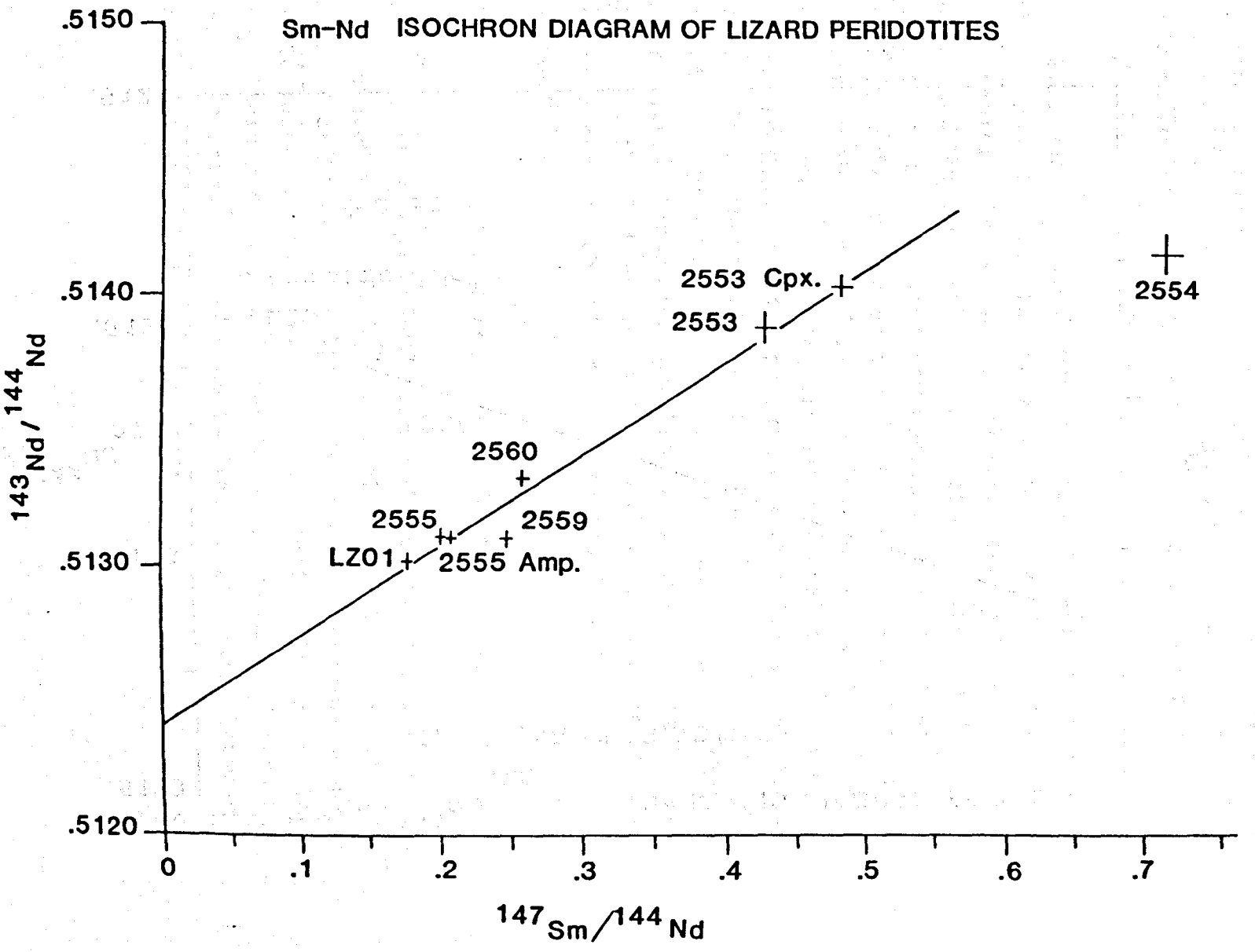
Sm-Nd ISOCHRON DIAGRAM OF LIZARD PERIDOTITES
.5150
.5140
.5130
.5120
143Nd/144Nd
0
.1
.2
.3
.4
.5
.6
.7
147Sm/144Nd
2553 Cpx.
2553
2554
2560
2555
2559
LZ01
2555 Amp.

Figure 2:20 $^{143}Nd/^{144}Nd_{375}$ vs 1/Nd MIXING DIAGRAM FOR THE LIZARD PERIDOTITES

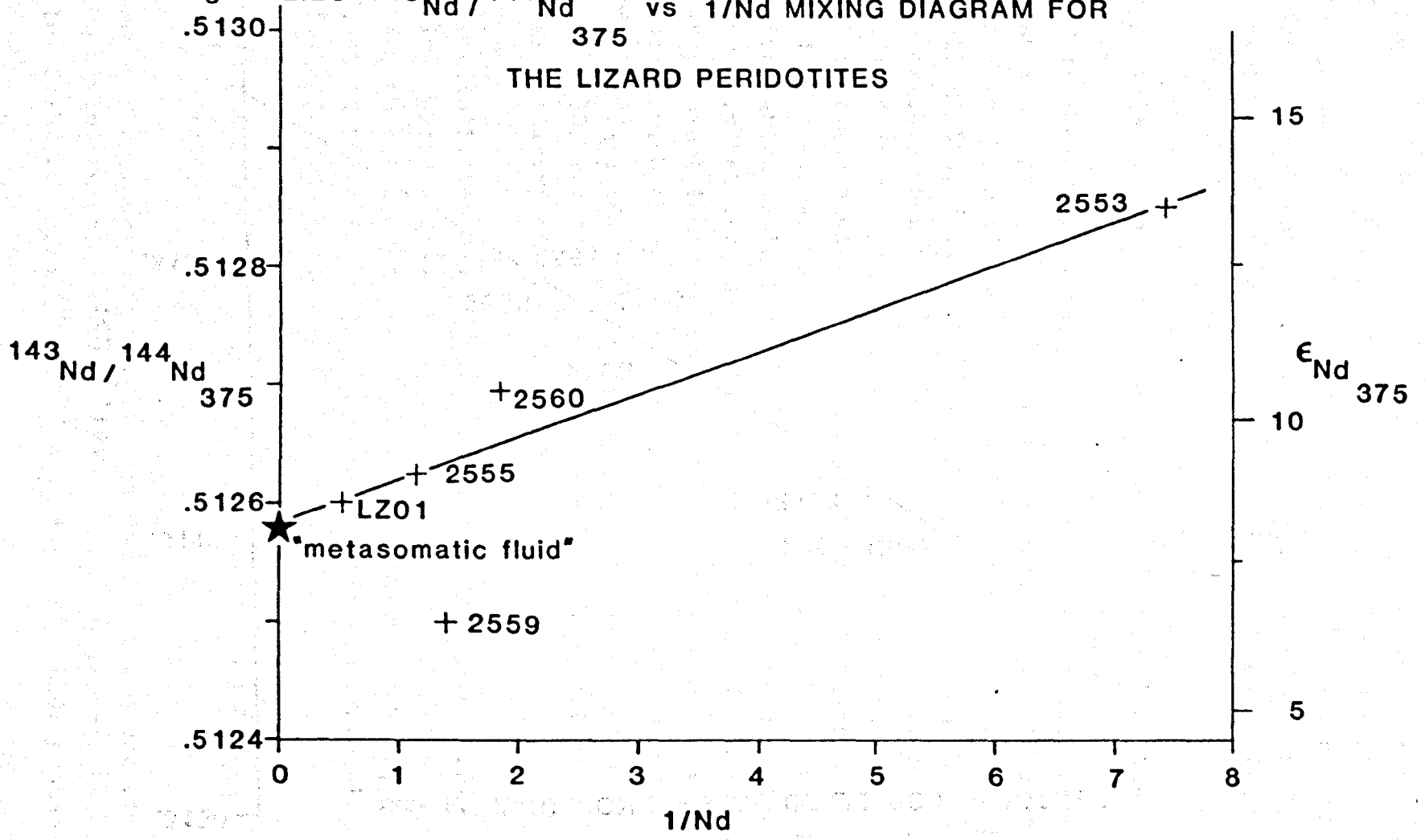

occurred shortly before the formation of the Lizard Complex (<200 Ma prior). Unlike the Sm-Nd systematics the Rb-Sr systematics of the calculated magma show a coherent relationship with a $^{87}Sr/^{86}Sr_{375}$ ratio of 0.7036 (εSr_{375} = -9) and a Rb-Sr ratio less than that of bulk earth (Rb = 8.2 ppm, Sr = 360 ppm, Rb-Sr = 0.023).

Figure 2:21 shows that the "metasomatised" peridotites plot slightly above the mantle array on an εNd vs εSr diagram in a similar position to metasomatised xenoliths from Ataq (Menzies and Murthy 1980). Due to the low Sm-Nd and Rb-Sr ratios of both these peridotite suites they would, with time (>1000 Ma) evolve across the mantle array to plot below it whereupon the observed isotope characteristics would be similar to those of the Ataq diopsides (Menzies and Murthy, op cit.) and Kiama apatite pyroxenites (Menzies and Wass, in press). It is interesting to note that the mantle derived peridotites with similar εNd, εSr, Sm/Nd and Rb/Sr to the "metasomatised" Lizard peridotites are from the South Yeman, adjacent to the Red Sea consistent with earlier arguments that the development of the Lizard Complex may be comparable to that of the Red Sea.

2:7:4 Nd Model Ages of the Gneissic Rocks

This brief study was undertaken on the gneissic rocks within, or associated with, the Lizard Complex to establish the age of the rocks or their crustal precursors and to examine possible genetic relationships. The aim is specifically to examine if the gneissic pebbles within the mélange are derived from the Kennack Gneisses?and hence assess the relationship between the mélange and the Lizard Complex.

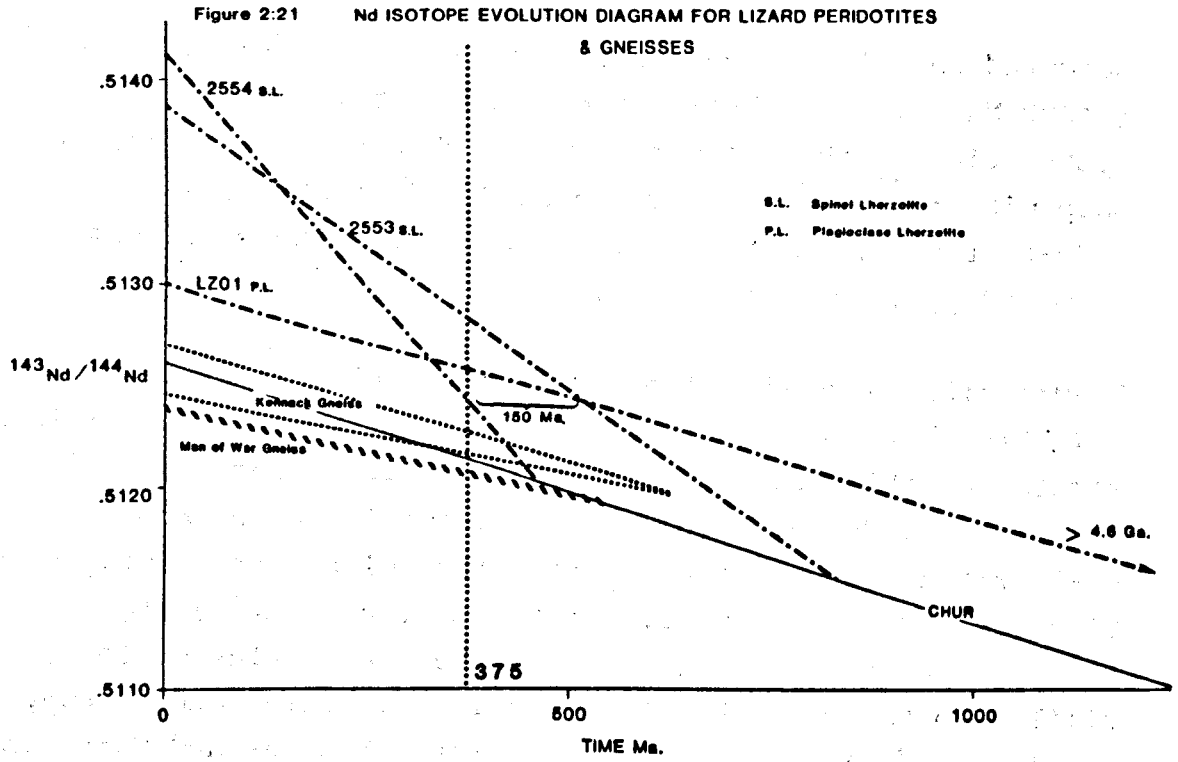

The Nd isotope evolution paths of spinel lherzolite 2553 and plagioclase lherzolite LZ01 intersect at 525 Ma suggesting "metasomatism" of the hydrous peridotites occurred post 525 Ma. Note that the evolution path of LZ01 would not intersect with that of CHUR.

The Nd isotope data for the gneissic rocks are presented in Table 2:14 along with T_{CHUR} and T_{MORB} ages. All the T_{MORB} ages are less than 1000 Ma and thus none of the gneissic rocks contain a significant Archean/Proterozoic crustal component. Moreover, both the Man of War and the Kennack Gneiss have T_{CHUR} ages which are younger than the emplacement age of the Lizard Complex emphasising that they were derived from a high εNd source rocks and that T_{CHUR} ages are not applicable (Figure 2:21). The εNd_{375} variation of the Kennack Gneiss + 0.7 $\pm$ 0.3 to + 2.7 $\pm$ 0.3 indicates that the rocks did not suffer Nd isotope homogenisation (as they did for Sr) during the deformation and metamorphism associated with ophiolite emplacement. The above data suggest that the oldest the precursors to the gneiss could be was circa 800 Ma, i.e. Late Precambrian. The Rb-Sr isotope systematics of the Kennack Gneiss are also interpreted as indicative of a relatively short crust residence (Styles and Rundle, in press).

Significantly the gneiss pebbles from the mélange have lower $^{143}Nd/^{144}Nd$ ratios and hence older T_{CHUR} and T_{MORB} ages (av. 485 and 960 Ma respectively) than either the Kennack or the Man of War Gneisses (Figure 2:21). Thus they were presumably not derived from the Lizard Complex and these data do not support a genetic relationship between the mélange and the Lizard Complex.

2:7:5 Petrogenesis of the Basaltic Rocks

Present day $^{143}Nd/^{144}Nd$ ratios of the basaltic and related rocks are presented in Table 2:12 and on a Sm/Nd vs $^{143}Nd/^{144}Nd$ diagram Figure 2:22. The 375 Ma reference line is from the olivine gabbro mineral isochron in Figure 2:12. The 3 rock suites (early and late dyke suites and mélange metabasalts) plot in different fields in Figure 2:22 suggesting that all three suites are not genetically related. The εNd values of the suites at 375 Ma (Table 2:12 and Figure 2:16) show limited

TABLE 2:14

Nd Isotope results for the Crustal Rocks associated with the Lizard Complex.

sample	Sm	Nd	Sm/Nd	$^{143}Nd/^{144}Nd$	εNd_{375}	T^{Nd}_{CHUR}	T^{Nd}_{CHUR}
KS1A Kennack Gneiss	4.06	21.59	0.1878	.512457±30	+0.7	330	860
KS1C Kennack Gneiss	4.77	16.56	0.2882	.512702±20	+2.7	-	1130
18/4c/1 melange pebble	4.01	21.42	0.1872	.512356±14	-1.5	520	990
28/6b/2 melange pebble	4.01	21.90	0.1830	.512383±20	-0.9	450	930
Man of War Gneiss	5.89	29.63	0.1987	.512580±14	+2.5	120	740
Eddystone Rock	5.96	32.03	0.1861	.512295±12	-2.7	620	1060

TABLE 2:15

Trace Element Ratios for some typical Basaltic Igneous Rocks

	MORB	Hawaiian tholeiite	Hawaiian alkali basalt	Hawaiian nephelinite	Lizard metasomatic fluid
K/Rb	1060	525	380	300	350
Rb/Sr	0.008	0.02	0.03	0.04	0.025
Zr/Y	2.7	5.5	7.0	8.5	6.0
$(Ce/Yb)_N$	0.8	2.8	8.0	25.0	6.0

Data from; Hanson 1977
Chen & Frey 1983
Pearce & Norry 1979

Figure 2:22

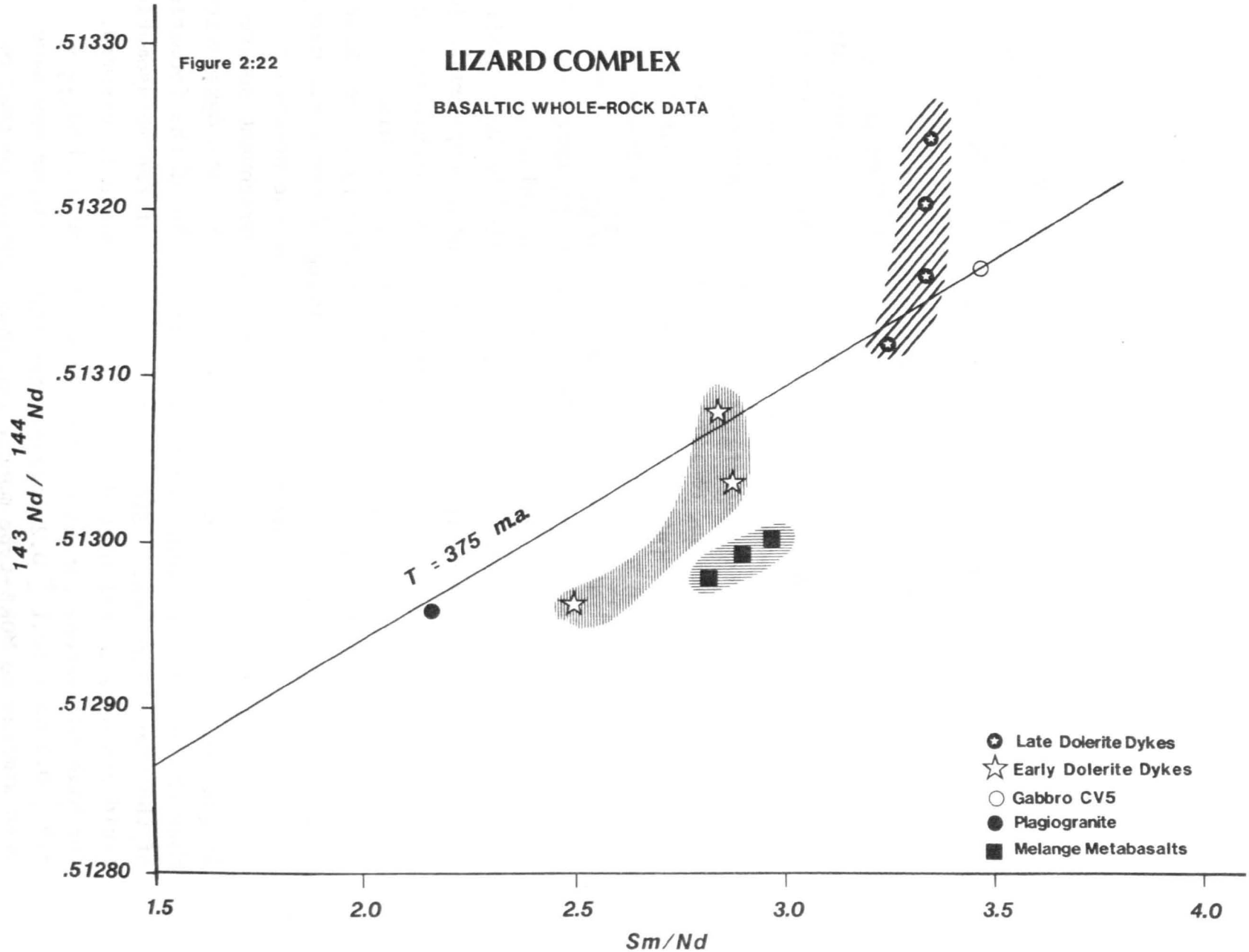
LIZARD COMPLEX
BASALTIC WHOLE-ROCK DATA
.51330
.51320
.51310
.51300
.51290
.51280
143 Nd / 144 Nd
T = 375 ma
1.5
2.0
2.5
3.0
3.5
4.0
Sm/Nd
Late Dolerite Dykes
Early Dolerite Dykes
Gabbro CV5
Plagiogranite
Melange Metabasalts

overlap. The mélange metabasalts have restricted εNd_{375} values + 8.2 $\pm$ 0.3 whereas the εNd_{375} values of the early, + 8.9 $\pm$ 0.3 to 10.1 $\pm$ 0.2, and late + 9.2 $\pm$ 0.3 to 11.7 $\pm$ 0.4, dyke suites are both higher and more variable. Interestingly there is a large overlap in the εNd_{375} values of the peridotites and basaltic rocks of the Lizard Complex (Figure 2:16). The high εNd values, all within the range of present day MORB, indicate that the basaltic rocks were derived from sources that had been depleted for a long period of time. However, there is a decoupling between the Sm/Nd and $^{143}Nd/^{144}Nd$ ratios of the rocks with high $^{143}Nd/^{144}Nd$ and low Sm/Nd ratios. The Sm/Nd ratio of the basalts will presumably be slightly lower than that of their source rocks, but since the rocks are tholeiites and are likely to represent reasonably large degrees of partial melting, the Sm/Nd ratio may only have fractionated by circa 10-15%. Batch melting calculations suggest that the Sm/Nd ratios of the sources of the basalts ranged from 0.285 - 0.430 (Figure 2:24). Applying these values, with the $^{143}Nd/^{144}Nd_{375}$ ratios gives T^{Nd}_{CHUR} depletion ages of between 1 and 1.7 Ga for the source of the late dyke suit (Figure 2:23). In marked contrast the calculated sources of the early dyke suite show a decoupling between their Sm/Nd and $^{143}Nd/^{144}Nd$ ratios such that their Nd isotope evolution paths would not intersect with that of bulk earth within the age of the Earth (Figure 2:23). Therefore, to explain this decoupling it is necessary to advocate a relatively recent L.REE enrichment of the source region. The timing of the enrichment event can only be constrained if the nature of the precursor source is assumed. For example, if the pre-enrichment source is assumed to be equivalent to the source of the late dyke suite then the enrichment event occurred within 250 Ma of the formation of the Lizard Complex. Similarly the nature of the metasomatic fluid can only be calculated if a precursor source is assumed. The high Nd isotope ratios of the early dyke suite, εNd_{375} + 8.9 $\pm$ 0.3 to + 10.1 $\pm$ 0.2 suggest that the precursor may have been similar to MORB-type mantle and thus similar to that of

Figure 2:23 Nd ISOTOPE EVOLUTION DIAGRAM FOR THE LIZARD DYKE SUITES

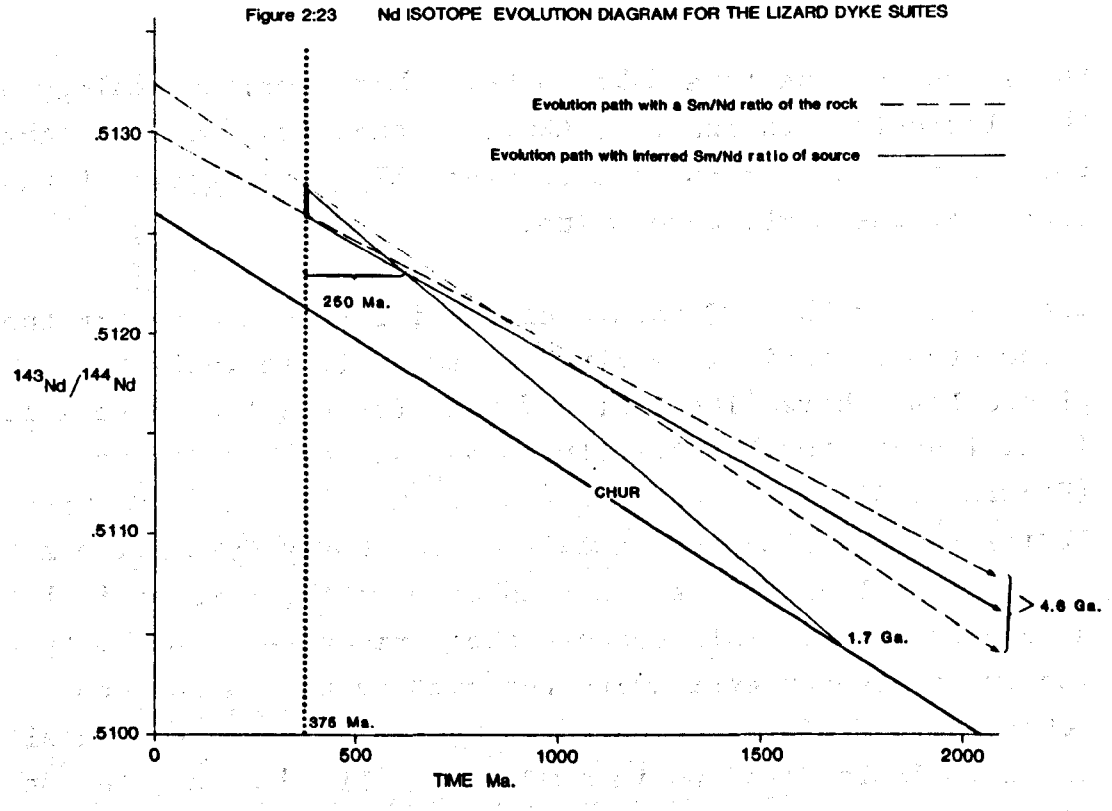

The Nd isotope evolution paths of the sources of the 2 dyke suites intersect at 625 Ma suggesting "metasomatism" of the source of the early dyke suite post 625 Ma. Note that the source of early dyke suite would not intersect with that of CHUR.

the source of the late dyke suite. Moreover, by analogy with the plagioclase lherzolite, LZ01, of the Lizard Complex the enrichment event could have involved 5% metasomatism of the source of the early dyke suite.

Interestingly the REE nature of the inferred source for the trace element enriched early dyke suite is equivalent to the plagioclase lherzolite LZ01 and that for the late dyke suite is similar to the L.REE depleted pargasite harzburgites (Figure 2:24). The REE pattern of the calculated "metasomatic" fluids involved in petrogenesis of the early dyke suite and the plagioclase lherzolites are also comparable, further implying a genetic relationship between the peridotites and the dykes. The trace element enrichment recorded by the calculated metasomatic fluid is compared to typical present day basaltic rocks in Table 2:15 and in a MORB normalised trace element diagram, Figure 2:25. The fluid is more trace element enriched than typical within plate tholeiites (e.g. Hawaii), but it is comparable to many alkali basalts.

The similarity between the trace element and Nd isotope nature of the calculated sources of the dyke suites and the chemically fertile ($CaO > 2\%$, $Al_2O_3 > 3\%$) "metasomatised" Lizard peridotites presents an interesting dilemma, are the peridotites equivalent to the source of the dykes at depth? Or has the volcanism that generated the ophiolitic units interacted with the peridotites and caused the metasomatism?

The fact that some of the metasomatised peridotites record evidence for extensive high temperature and moderate pressure deformation and re-crystallisation ($900^{\circ}C$, 5Kb) argues for the former possibility; i.e. the Lizard peridotites are equivalent to the sources, at depth, of the volcanism.

Figure 2:24

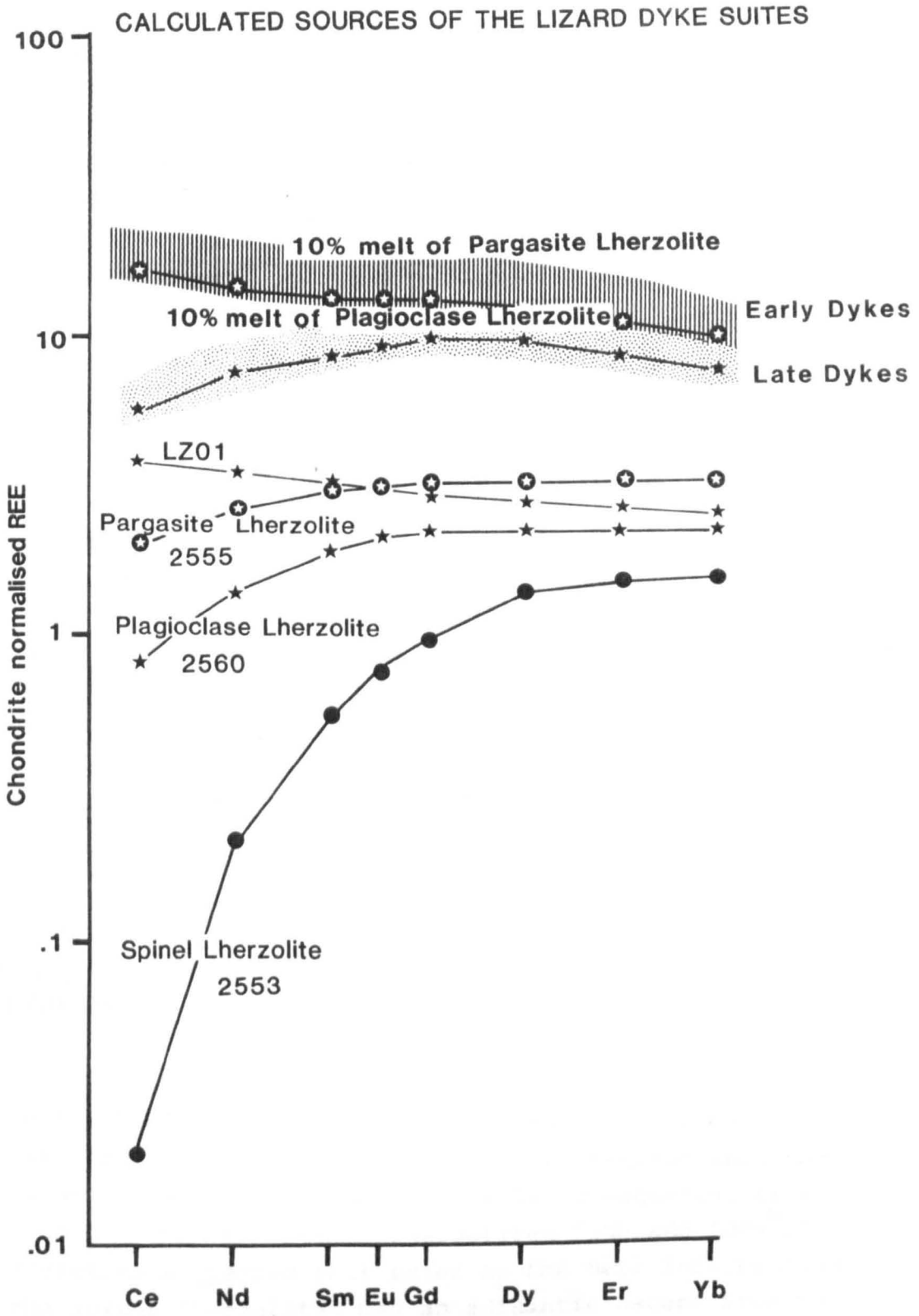
CALCULATED SOURCES OF THE LIZARD DYKE SUITES
100
10
1
.1
.01
Chondrite normalised REE
10% melt of Pargasite Lherzolite
10% melt of Plagioclase Lherzolite
Early Dykes
Late Dykes
LZ01
Pargasite Lherzolite
2555
Plagioclase Lherzolite
2560
Spinel Lherzolite
2553
Ce
Nd
Sm
Eu
Gd
Dy
Er
Yb

Figure 2:25 TRACE ELEMENTS PATTERNS OF THE LIZARD "METASOMATIC FLUID" COMPARED WITH PRESENT DAY TRACE ELEMENT ENRICHED BASALTIC VOLCANISM

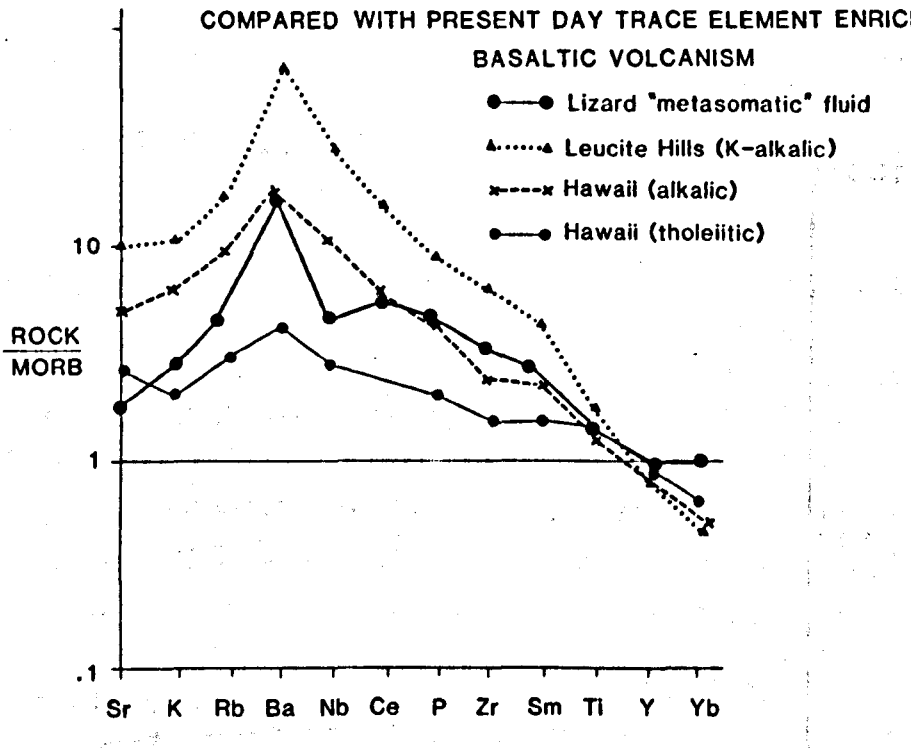

Data sources; Pearce, 1982
Kay and Gast, 1973

2:8 Conclusions

The formation and emplacement of the ophiolitic rocks of the Lizard Complex are analytical indistinguishable at circa 370 Ma. It is argued that the igneous evolution of the Lizard Complex is equivalent to the early development of the Red Sea with early trace element enriched basic magmatism followed by MORB-like magmas. These latter magmas record MORB-like Sm-Nd isotope systematics that indicate 1.0 to 1.7 Ga depletion of their source regions. The early magmatism shows a decoupling between trace elements and Nd isotopes, in that these L.REE enriched rocks originated from an heterogeneously and isotopically depleted source, εNd_{375} = 8.9 $\pm$ 0.3 to 10.1 $\pm$ 0.2. A relatively recent trace element enrichment of their source region is therefore indicated (<250 Ma prior to eruption).

The majority of the peridotites in the Lizard Complex are spinel lherzolite. Their mineral chemistry indicates equilibration at 20 Kb and 1150°C within the spinel lherzolite stability field. The extreme L.REE depletion of these rocks ($(Ce/Yb)_N$ = 0.01, Frey, 1969) is accounted for by multiple melt extraction while within the garnet stability field. The variable Sm-Nd isotope systematics of the spinel lherzolites, εNd_{375} = +4.8 $\pm$ 1.6 to + 13.6 $\pm$ 1.0, indicate complex and different depletion histories for the 2 samples analysed. However, a depletion event just prior to the emplacement of the Lizard Complex is indicated by sample 2554 (T_{CHUR} =420 $\pm$160Ma). The εSr_{375} and εNd_{375} values of the clinopyroxene from 2553 lie on the mantle array at slightly more depleted values than MORB.

The mineral chemistry and petrology of the plagioclase lherzolite LZ01 are indicative of melt infiltration into the spinel lherzolite and associated extensive re-equilibration at lower pressure than the spinel lherzolites (5Kb and 1075°C) It is therefore suggested that prior to the melt infiltration event the spinel lherzolites had an adiabatic ascent from the spinel lherzolite stability field to the upper most mantle (15 km depth). Other plagioclase lherzolites and the

pargasite peridotites have mineral chemistry indicative of melt infiltration but have suffered deformation and re-crystallisation at 5 kb and 900°C. The Sm-Nd isotope systematics of the plagioclase and pargasite peridotites show a mixing relationship exists between the spinel lherzolites and the introduced melt. Interestingly the plagioclase and pargasite peridotites have trace element and isotopic compositions equivalent to the source of the early enriched magmatism of the Lizard Complex. Due to the relatively high temperature deformation recorded by the peridotites it is concluded that their "metasomatism" is not a result of the interaction of the Lizard magmas with the peridotites during the formation of the ophiolitic sequence and that the peridotites are probably equivalent to the sources of the magmas at depth. The Sm-Nd and Rb-Sr isotope systematics of the "metasomatic" fluid and the plagioclase and pargasite peridotites are similar to those of the metasomatised Ataq xenolith suite (Margin of the Red Sea, Menzies and Murthy, 1980) plotting slightly to the right of the mantle array. With time, due to their low Rb/Sr ratios, the xenoliths would evolve to a position below the mantle array, similar to that now occupied by the Kiama xenolith suite (Menzies and Wass, in press). The "metasomatic" fluid appears to be analogous to the style of trace element enrichment recorded by many alkali basalts.

Chapter 3

Mona Complex

3:1 Introduction

The Mona Complex, Anglesey, represents the largest outcrop of Precambrian rock within southern Britain and comprises 3 major units; i) The Bedded Succession
ii) Mona Gneisses
iii) Coedona Granite and related hornfels (Figure 3:1) (Greenly, 1919, Shackleton, 1969, Barber and Max, 1979).

The Bedded Succession comprises 4 major units (South Stack Group(oldest),New Harbour Group,Skerries Group and Gwna Group) and forms a thick sequence (7000m) of flysch-type sediments. The youngest rocks of the Bedded Succession, the Gwna Group, contain blocks of chert,manganiferous shale,mafic and ultramafic rocks and are interpreted as an olistostrome(Shackleton, 1969).This assemblage in conjunction with the presence of glaucophane schists,is interpreted by Wood(1974) as evidence for an early Caledonian subduction event in North Wales with the obduction and dismembering of oceanic crust within an ocean trench.

During the last century the ages and inter-relationship between the Bedded Succession and the Mona gneisses have been the subject of considerable debate. Greenly (1919) and Barber and Max (1979) consider that the gneisses represent "ancient continental basement" upon which the Bedded Succession was deposited. Barber and Max (op. cit.) and Barber et al. (1980) correlate them with the gneissic rocks of the Rosslare Complex and propose an age of circa 2.4 Ga. Citing the palaeontological evidence of Muir et al. (1979), Barber and Max (1980) further suggest a Cambrian age for the entire Bedded Succession. Notably, however, the Late Precambrian stromatolitic limestones within the Gwna Group (Wood and Nicholls, 1973) and the presence of Monian lithologies in the Lower Cambrian sediments on the mainland of North Wales

Figure 3:1 GEOLOGICAL MAP OF ANGLESEY

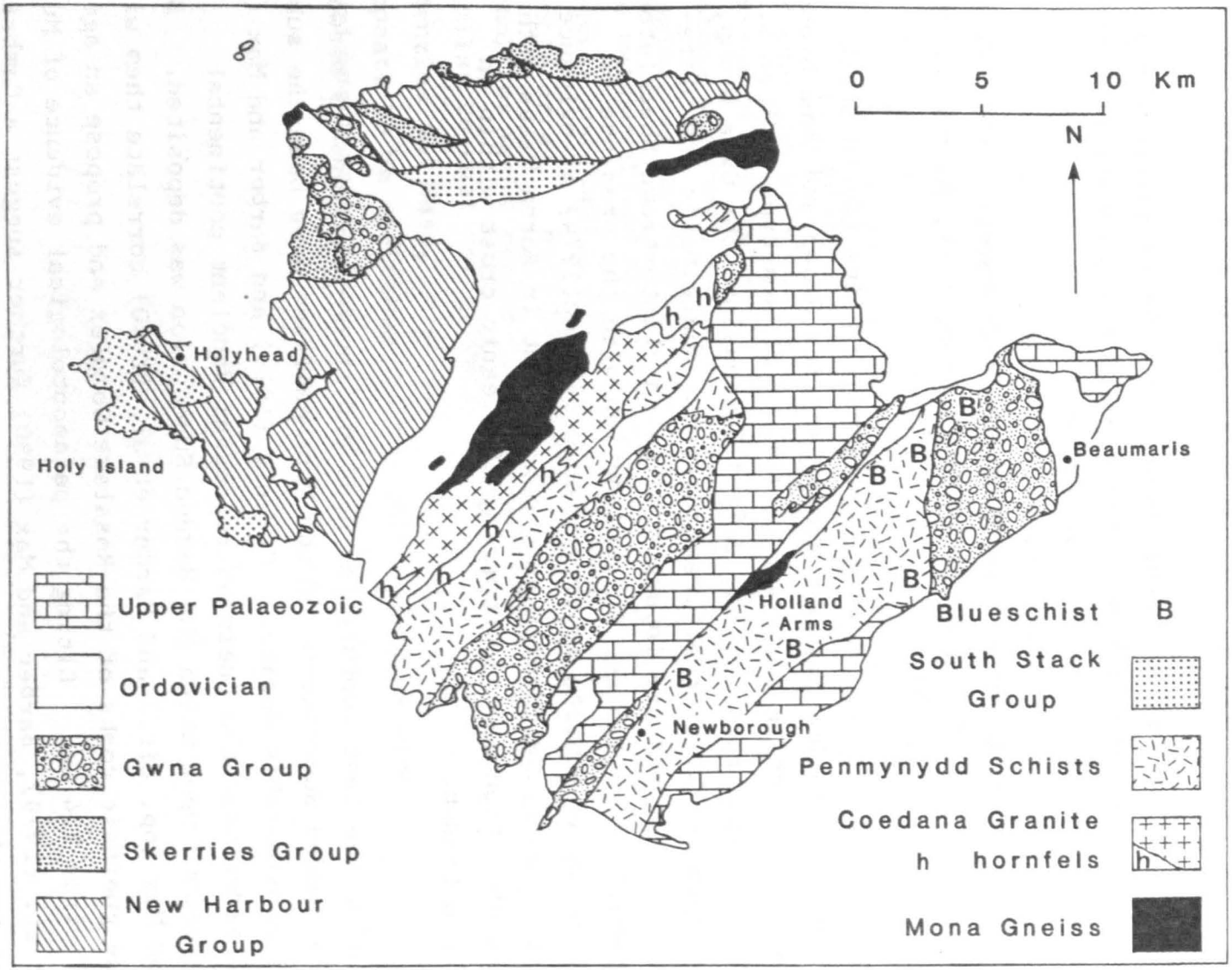

indicate a Precambrian age for the entire Mona Complex.

In contrast Shackleton (1954, 1969) proposed that the gneisses were the result of high grade metamorphism of the Bedded Succession and that the Coedona Granite originated by anatexis during the peak of metamorphism. Shackleton's hypothesis is based on the indentification of prograde transitions between the gneisses and the metasediments. However, Baker (1969) and Gibbons (1983) dispute the existence of such prograde transitions. No unconformity is found between the two units and therefore their inter-relationship remains enigmatic.

Beckinsale and Thorpe (1979) report whole-rock Rb/Sr ages for the Coedona Granite, 603 $\pm$ 34 Ma and Mona Gneisses from Hollands Arms, 595 $\pm$ 12 Ma. The relatively low initial ratios of these rocks, 0.7086 and 0.7061 respectively, are interpreted by Beckinsale and Thorpe (op. cit.) to preclude a long crustal residence time for their precursors, <200 Ma.

The aims of this particular study were i) to obtain Nd whole rock ages from metabasalts within the Bedded Succession and to examine their petrogenesis and ii) to obtain Nd model ages for the gneisses, sediments and the Coedona Granite to see if they are genetically related and to constrain the mantle derivation ages of their precursors.

3:2 Samples

The metabasaltic samples analysed in this study are from the New Harbour and Gwna Groups, the latter show good pillow structures. The geochemistry of these samples is reported by Thorpe et al. (in press). The metabasalts from the Gwna Group have MORB like trace element contents whereas the New Harbour Group samples are similar to island arc tholeiites (Figure 3:2a). The New Harbour metabasalts are consistently L.REE depleted $(Ce/Yb)_N = 0.3$ to 0.5 with the Gwna Group samples showing considerable variation from L.REE depleted, $(Ce/Yb)_N = 0.6$, to L.REE enriched, $(Ce/Yb)_N = 2.1$ (Figure 3:2b).

Figure 3:2a Zr/Y vs Y DIAGRAM FOR MONA BASALTS

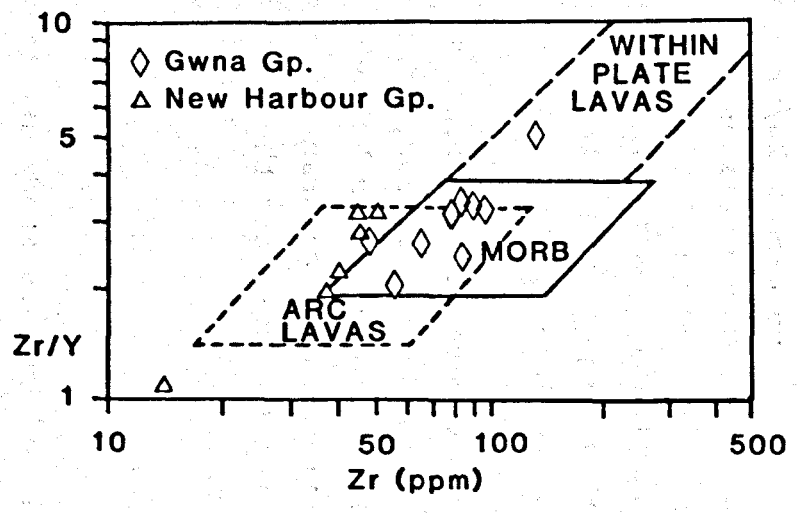

Data from Thorpe et al. in press.

Figure 3:2b REE PATTERNS OF MONA BASALTS

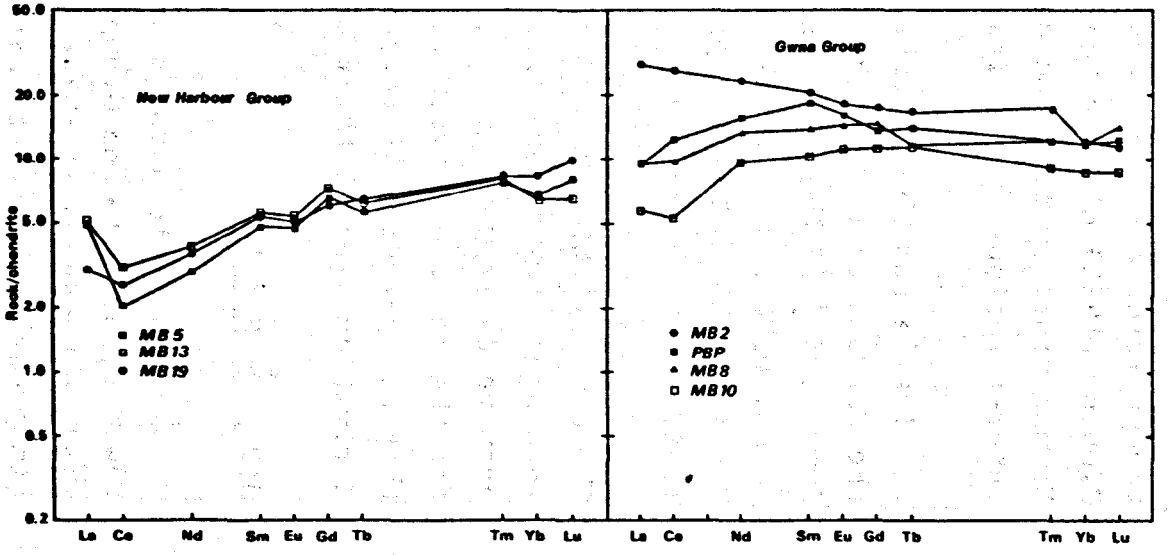

The gneiss and granite samples were taken from the isochron suites of Beckinsale and Thorpe (1979) and a single pelite from the New Harbour Group was also analysed.

3:3 Nd Isotope Data

The Nd isotope data are presented in Table 3:1. The Monian metabasalts have a significant range in both Sm/Nd and $^{143}Nd/^{144}Nd$ ratios 0.263 to 0.429 and 0.51287 to 0.51316 respectively. The gneiss, granite and sediment samples show a limited range in both Sm/Nd and $^{143}Nd/^{144}Nd$ ratios, 0.175 to 0.198 and 0.51211 to 0.51224 respectively. The granites have the least radiogenic $^{143}Nd/^{144}Nd$ ratios and the sediment the most radiogenic.

3:4 Discussion

3:4:1 Nd Model Ages. The Nd model ages (T_{CHUR}) of the gneisses and granites of the Mona Complex are between 860 $\pm$ 30 Ma and 955 $\pm$ 25 Ma (Table 3:1). These data therefore preclude a major Mid Proterozoic or Archean component being involved in the petrogenesis of these rocks, as proposed by Barber et al. (1980). Significantly the Nd model ages of the Mona Complex gneisses are less than those of the Rosslare Complex (see Chapter 7) suggesting that the two complexes are not genetically related.

The 680 $\pm$ 30 Ma Nd model age of the New Harbour Group sediment is less than those of the gneisses suggesting that the gneisses may not represent the metamorphic equivalents of the Bedded Succession as proposed by Shackleton (1956, 1969). The sediment also records the addition of a significant proportion of juvenile mantle derived material to the crust subsequent to the formation of the gneisses (εNd_I gneisses, 2.7 $\pm$ 0.3 to 3.6 $\pm$ 0.4 compared to εNd_I 1.5 $\pm$ 0.3 for the sediment. Taken as a whole the Nd model ages indicate that the Mona Complex formed during the Late Precambrian (see Chapter 7).

Table 3:1 Nd isotope results for the Mona Complex

Sample		Sm	Nd	Sm/Nd	$^{143}Nd/^{144}Nd$	εNd_I	T^{Nd}_{CHUR}
MB2	Gwna Group metabasalt	4.112	15.285	0.2702	0.512865 ±18	+7.0± 0.4	
MB4	Gwna Group metabasalt	3.872	12.885	0.3005	0.512930 ±18	+6.8± 0.4	
MB6	Gwna Group metabasalt	4.100	11.992	0.3419	0.513052 ±12	+7.3± 0.2	
MB8	Gwna Group metabasalt	2.929	8.479	0.3454	0.513052 ±14	+7.2± 0.3	
MB10	Gwna Group metabasalt	2.005	5.008	0.4004	0.513164 ±18	+6.8± 0.4	
PBG	Gwna Group metabasalt	3.018	9.380	0.3217	0.513017 ±12	+7.5± 0.2	
MB5	New Harbour Group metabasalt	0.906	2.113	0.4288	0.513144 ±22	+5.1± 0.4	
MB13	New Harbour Group metabasalt	0.968	2.506	0.3862	0.512985 ±24	+3.9± 0.5	
MB19	New Harbour Group metabasalt	1.131	3.066	0.3689	0.513127 ±24	+7.5± 0.5	
2601	Coedana Granite	2.14	11.92	0.1795	0.512109 ±12	-3.9± 0.3	920
2609	Coedana Granite	3.788	19.34	0.1959	0.512149 ±10	-3.6± 0.2	955
AS16	Holland Arms Gneiss	6.09	30.995	0.1965	0.512198 ±16	-2.7± 0.3	860
2622	Holland Arms Gneiss	5.820	29.428	0.1978	0.512171 ±18	-3.6± 0.4	925
2585	New Harbour Group sediment	11.688	66.638	0.1754	0.512237 ±16	-1.5± 0.3	680

Age of sediment assumed to be 550Ma

3:4:2 Age of the metabasalts. The Nd isotope data of the Gwna Group metabasalts show a positive correlation on a Sm-Nd isochron diagram (Figure 3:3) equivalent to an age of 595 $\pm$ 86 Ma. The scatter in the data (M.S.W.D. = 1.5) is just outside analytical error. The initial $^{143}Nd/^{144}Nd$ ratio of 0.51224 $\pm$ 0.00006 is equivalent to an εNd_I value of + 7.1 $\pm$ 1. The age obtained is analytically indistinguishable from that of the Late Precambrian age of 595 $\pm$ 12 Ma reported by Beckinsale and Thorpe (1979) for the Holland Arms gneisses. The data therefore indicate a Late Precambrian age for the metabasaltic blocks within the Gwna olistostrome. However, due to the exotic nature of the metabasalts and the relatively large error in the age determination (595 $\pm$ 86 Ma) a Lower Cambrian age for the Bedded Succession cannot be ruled out.

The New Harbour metabasalts do not show a positive correlation on a Sm-Nd isochron diagram (Figure 3:3) and have a considerable range in εNd_{595} values + 3.9 $\pm$ 0.5 to +7.5 $\pm$ 0.5.

3:4:3 Petrogenesis of the metabasalts. The Gwna Group metabasalts record a large range in Sm/Nd ratio (0.263 to 0.4) despite being derived from an isotopically homogenous source. There are three processes that could be important in the generation of this range in Sm/Nd ratios; i) fractional crystallisation ii) partial melting iii) source heterogeneity. It is apparent that the first possible mechanism, fractional crystallisation, has not played a major role from the relatively high MgO ($>6\%$) and low Zr contents (<130 ppm) of the metabasalts (Thorpe et al., in press). Batch melting calculations demonstrate that between 0.5 and 25% partial melting of a source similar to that of MORB (Sm/Nd = 0.4) is required to produce the observed range in Sm/Nd ratios. Due to the altered nature of the metabasalts, it is not possible to use their major element contents to ascertain their tholeiitic or alkalic character. However, their MORB like trace element characteristics (Zr/Y ratios circa 3 Figure 3:2a) suggest a tholeiitic affinity and hence relatively large degrees

Figure 3:3 Nd ISOTOPE DIAGRAM FOR THE MONA BASALTS

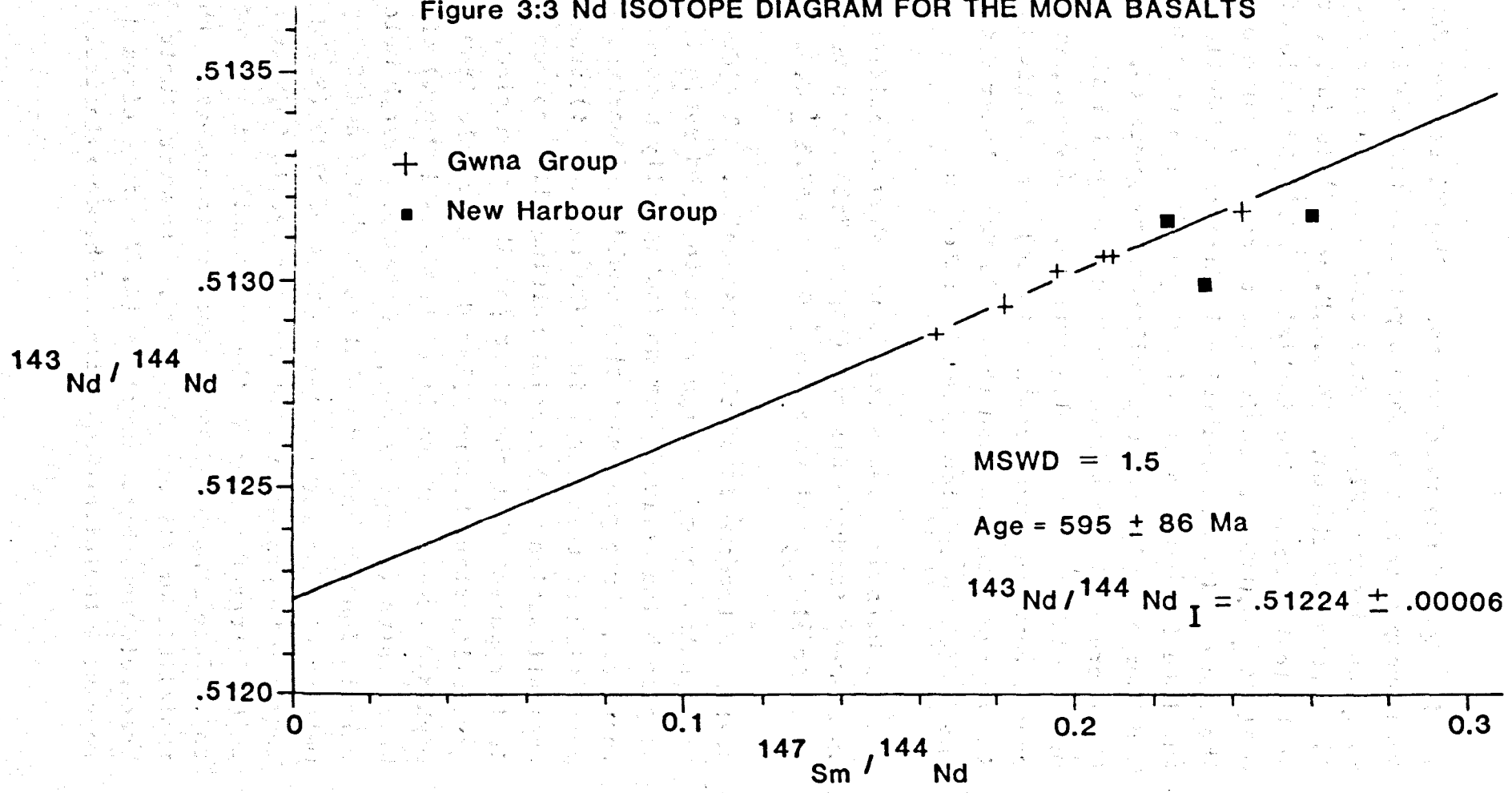

of partial melting (>10%) in their petrogenesis. The entire range in the Sm/Nd ratios of the Gwna Group metabasalts cannot, therefore, be accounted for by variations in the degree of partial melting which in turn implies that the source region was heterogeneous with respect to REE. However, because of the Sm-Nd isochronous relationship shown by the Gwna Group metabasalts their source region must be homogeneous with respect to $^{143}Nd/^{144}Nd$. These data therefore imply that the low Sm/Nd ratios were generated immediately prior to the petrogenesis of the metabasalts due either to i) recent L.REE enrichment of the source or ii) enrichment processes during magma genesis, e.g. zone refining and dynamic melting as proposed for the famous basalts by Langmuir et al. (1977).

3:5 Nd Isotope evolution of the Mantle; Significance of Mona and Lizard basalts. The initial $^{143}Nd/^{144}Nd$ ratios of the basaltic rocks studied in this thesis (Mona and Lizard Complexes) are plotted in εNd_I form on a Nd isotope evolution diagram (Figure 3:4) together with selected data from basaltic and crustal rocks of different ages. Figure 3:4 shows that the Anglesey basalts are less depleted than present day MORB and the Lizard basalts. The diagram also shows that the εNd_I value recorded by mantle derived volcanics increases with time. The maximum εNd_I values plot below an Nd isotope evolution line for a Sm/Nd ratio of 0.36 from 4.6 Ga. Significantly, however, the source of MORB like rocks have Sm/Nd ratios greater than 0.36 (0.37 to 0.42 DePaolo 1981) which raises the intriguing question; why are no present day magmas, derived from sources isotopically more depleted than $\varepsilon Nd + 13$?

A MORB evolution line (Sm/Nd = 0.41) is shown in Figure 3:4 and demonstrates that a MORB like source would evolve to an εNd value of + 13 within 2.0 Ga. Several lines of evidence suggest that rocks within the mantle should have εNd values greater than + 13. Firstly, Archean and Proterozoic Greenstone belts record significant Nd isotope source depletion (see Figure 3:4 for references) in rocks that range from L.REE enriched to those that are more L.REE

Figure 3:4 Nd Isotope Evolution Diagram

Two possible MORB evolution lines (dashed) illustrate that present day MORB sources have not existed for 2·0 Ga and suggest that depleted MORB like mantle formed during the Archean has been destroyed or isolated such that it is not sampled by recent volcanism.

Data sources; Bokhari and Kramers (1981), Chauvel et al. (1983), DePaolo and Wasserburg (1976a, b, 1979), Grau et al. (1983), Hamilton et al. (1977, 1978a, b, 1979), Hooker et al. (1981), Jacobsen and Wasserburg (1979a), McCulloch and Compston (1981), McCulloch et al. (1982), Memuge (1982), Zindler et al. (1978) and this work.

Wherever possible the data have been normalised to a $^{143}Nd/^{144}Nd$ ratio of 0.51262 for BCR-1.

Figure 3:4 Nd ISOTOPE EVOLUTION DIAGRAM

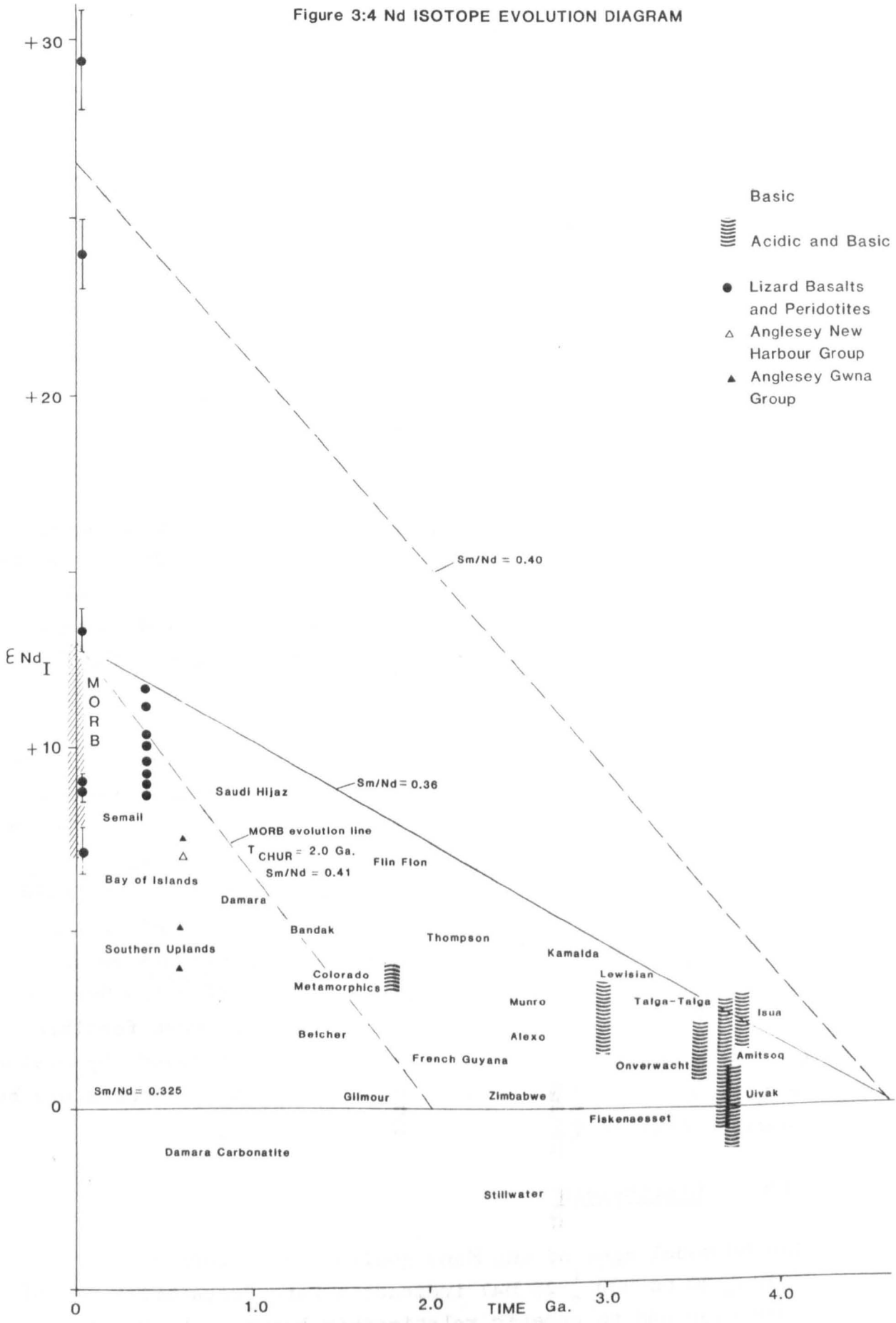

depleted than MORB (John et al., 1982 and references therein). The sources of some of these basalts/komatiites would therefore be expected to have evolved present day εNd values greater than + 20. Secondly the Lizard Peridotites (see Chapter 2) have present day εNd values of between + 7.2 $\pm$ 0.6 and +29.4 $\pm$ 1.5, despite being chemically fertile (5 to 15% clinopyroxene,> 3% CaO and >4% Al_2O_3).

Subjected to large degrees of partial melting (>10%) these lherzolites would yield tholeiitic MORB like magmas with εNd values from less than, to significantly greater than those of MORB.

Interestingly present day MORB record Pb/Pb and Rb/Sr psuedo-isochrons of between 2.0 and 1.6 Ga (Tatsumoto, 1978 and Brooks et al., 1976) suggesting that their source regions suffered a major depletion event circa 2.0Ga. The Nd isotope data therefore preclude the existence of present day MORB like sources for significantly greater than 2.0 Gyr.

The above discussion therefore implies that the source reservoir for present day MORB formed circa 2.0 Ga and that pre-existing depleted reservoirs are destroyed or at least removed from the parts of the mantle sampled by subsequent volcanism. A second implication is that reservoirs with Sm/Nd ratios > 0.4 (MORB frequently have Sm/Nd ratios >0.4) must also be effectively isolated or destroyed quickly within the mantle otherwise εNd values > + 13 would be produced within circa 1.0 Gyr (see Figure 3:4). Mantle convection provides the most feasible mechanism whereby depleted sources may be destroyed, by mixing with less depleted material, or isolated due to temperature and density contrasts.

3: 6 Conclusions

The Nd model ages of the Mona gneisses and granite (840 $\pm$ 30 to 930 $\pm$ 25 Ma) indicate a Late Precambrian age of formation and no genetic relationship between the Rosslare and Mona Complexes. The younger Nd model age of the New

Harbour Group sediment 680 $\pm$ 30 Ma suggests that the gneisses do not represent metamorphic equivalents of the Bedded Succession.

The Gwna Group metabasalts record an Sm-Nd age of 595 $\pm$86 Ma with an initial ratio equivalent to εNd + 7.1 $\pm$ 1. A Late Precambrian age is therefore inferred for the entire Mona Complex but a Lower Cambrian age for the Bedded Succession cannot be ruled out. The low Sm/Nd ratios of some of the Gwna Group metabasalts must have been generated immediately prior to their petrogenesis (due either to i) L.REE enrichment of the source or ii) enrichment during magma genesis) in order to maintain the Sm-Nd isochron relationship of the entire suite.

The New Harbour Group metabasalts do not record an Sm-Nd isochron relationship, having a significant range in εNd_{595} values + 3.9 $\pm$ 0.5 to + 7.5 $\pm$ 0.5.

A consideration of the Nd isotope systematics of mantle derived volcanic rocks of all ages suggests that sources with present day εNd values greater than those of MORB should exist unless depleted mantle reservoirs are destroyed or effectively isolated within the mantle. The Pb/Pb, Rb-Sr and Sm-Nd isotope systematics of MORB imply their source regions have not existed for greater than 2.0 Ga.

Chapter 4

The Caledonian Volcanism of South East Ireland

4:1 Introduction

The Lower Palaeozoic volcanic rocks of south east Ireland are thought to have been erupted in a subduction zone environment (Stillman and Williams, 1978, Phillips et al., 1976). The igneous rocks range in age from Llanvirnian to Ashgillian and are succeeded by the intrusive phases of the Leinster Granite Batholith, which has been dated at 404 $\pm$ 24 Ma (M.S.W.D. = 36), by O'Connor and Bruck (1977). Associated sediments vary from sandstones, siltstones and shales in the south to predominantly pelagic material further north, and are of Lower-Cambrian to Silurian age.

4:1:1 The volcanic rocks may be subdivided into two areas, north and south of the Leinster Granite (Figure 4:1). In the north the earliest volcanism is recorded in a suite of highly altered, predominantly basaltic rocks erupted in the Llanvirn. These are followed by voluminous Caradocian basalts and andesites, many of which were erupted from isolated seamounts. For example, the Lambay Island Succession has been interpreted by Stillman et al. (1974) as a well established island vent subsequently sealed by contact with seawater. There is evidence for spatter deposits and compound lava flows of blocky or aa type, consistent with weakly gas charged Hawaiian type eruptions. Interspersed are sub-plinian pyroclastic deposits in the form of vitric and crystal-lithic tuffs. Throughout the build up of such seamounts, magmas appear to have evolved from basalt to andesite and, rarely, dacite.

South of the Leinster Granite the volcanic rocks are much more extensive, forming an almost continuous outcrop from Wicklow along strike to Dungarvan (140 km) (Figure 4:1). Locally the outcrop pattern is controlled by Caledonian folding, resulting in narrow elongate bodies between Wicklow and

Figure 4:1 GEOLOGICAL MAP OF SOUTHEAST IRELAND

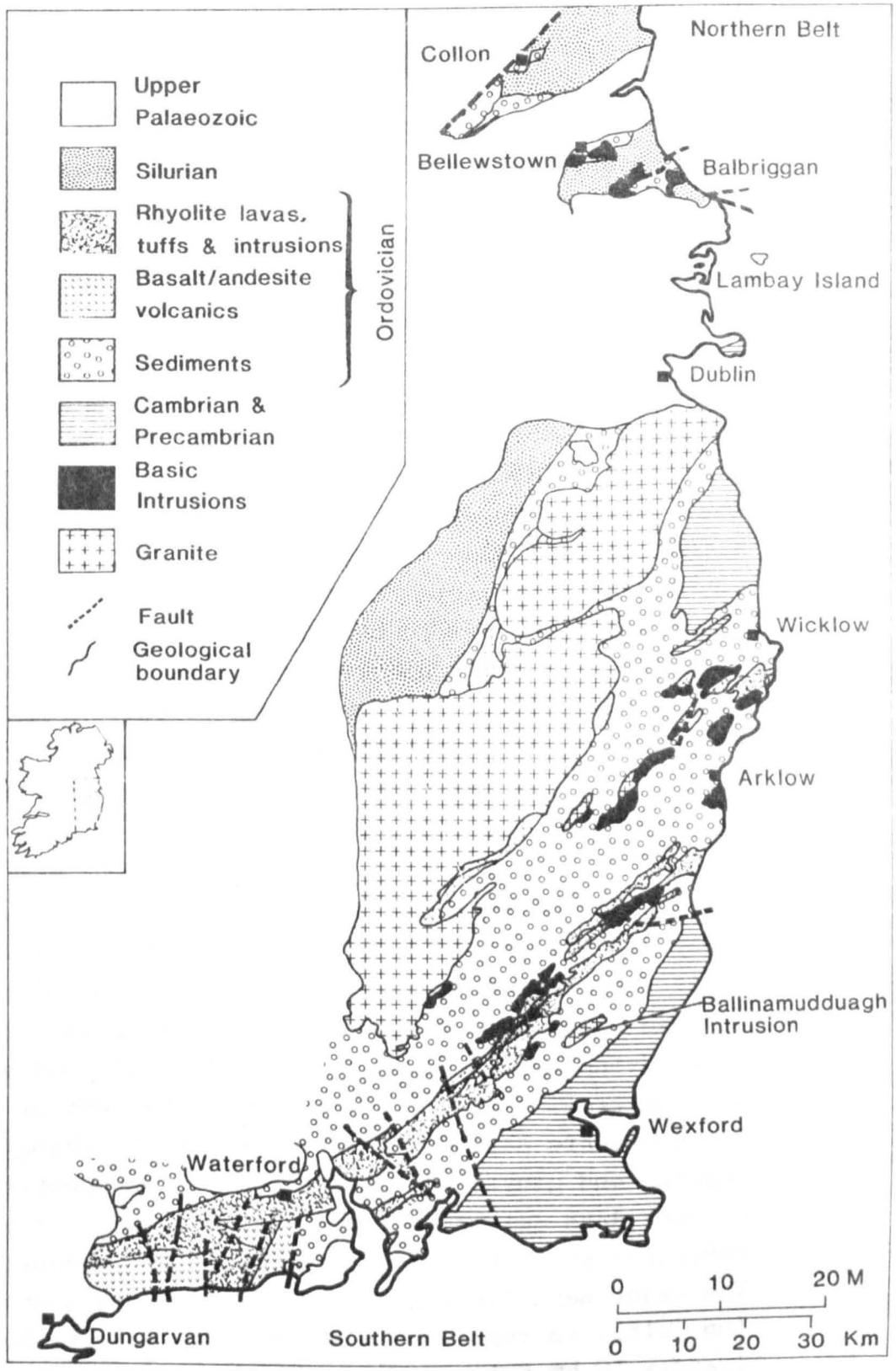

Waterford and large oval shaped bodies west of Waterford. Volcanism started in the Llandielo with major basalt/ andesite eruptions onto clastic marine sediments, with shield volcanoes being built up from the resulting lavas, hyloclastites and minor pyroclastics (Downes, 1974 unpublished Ph.D.). A quiescent period is marked by the overlying Middle to Upper Llandielo Tramore limestone, and the next volcanic episode (Caradoc/Ashgill) began with large volumes of acid pyroclastics (Stillman et al., 1974). Further volcanism was predominantly andesitic but terminated in a suite of rhyolites erupted from numerous small scattered vents (Stillman, 1971).

The distribution of rock types in the two sub areas is illustrated in Figure 4:2. Those in the north have a more restricted compositional range and are predominantly pyroxene and plagioclase phyric basalts and basaltic andesites, together with minor aphyric andesites and more rarely dacites. In the south there is a much greater variation in chemical composition, but the high abundance of rhyolites is particularly striking. The basic and intermediate lavas range from aphyric to plagioclase-pyroxene phyric.

4:1:2 The Leinster Batholith is emplaced into a sequence of Lower Palaeozoic sediments and calc alkaline rocks (Figure 4:1), it is the largest batholith in the British Isles and is made up of five separate dome-like units striking roughly north north east (Brindley, 1973). Brindley (op.cit.) has shown that the present erosion level lies close to the roof of the batholith. The domes are asymmetric with steep to overhanging eastern margins and gentle to moderately inclined western margins. Gravity data demonstrate that large volumes of granite are concealed at shallow depths (Locke, 1980 unpublished Ph.D.). The major negative gravity anomaly is interpreted by Locke, (op. cit.) to represent a steep sided granite body approximately 10 km thick with no extensive basic cumulates at depth.

The margins of the domes are generally irregular with numerous

Figure 4:2

FREQUENCY DISTRIBUTION OF ROCK TYPES IN THE NORTHERN AND SOUTHERN SUITES

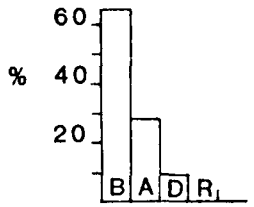

NORTHERN SUITE

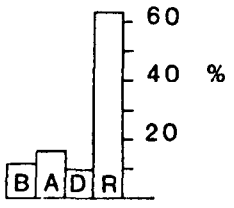

B Basalt
A Andesite
D Dacite
R Rhyolite

SOUTHERN SUITE

Division based on wt.% SiO_2

dyke-like bodies intruding the country rock, and large septa of country rock are found within the granite. These are interpreted as roof pendants by Brindley(1973). Small xenoliths have also been reported (Bruck and O'Connor, 1977) but they have not been studied in detail and little is known about their origins.

Most recent petrographic and geochemical work has been carried out in the north of the batholith where five major rock types are recognised by Bruck and O'Connor (1977), (Figure 4:3).

Type I Fine-grained, pale or dark grey quartz diorite/ granodiorite. The main feldspar is oligoclase with subordinate alkali feldspar, and although biotite is ubiquitous Brindley and Gupta (1974) report horneblende and pseudomorphed clinopyroxene. This rock-type occurs locally at the margins of Types IIa and IIb and as rare bands within them.

Type IIa Adamellite with characteristic large (up to 3 cm) microcline porphyroclasts form the bulk of the northern area. The groundmass is coarse (125 mm) and consists of quartz, plagioclase, microcline, biotite and muscovite.

Type IIb Medium to coarse grained equigranular adamellite with a similar mineralogy to IIa, but typically aphyric.

Type III and IV The type III and IV granitoids occur in the centre of the northern area and are interpreted as hydothermally altered equivalents of type IIb and IIa respectively (Bruck and O'Connor, 1977). Type III granitoids are porphyritic adamellites with muscovite porphyroclasts up to 3 cm in length plus minor tourmaline and topaz, whereas type IV rocks are distinguished by porphyroclasts of both microcline and muscovite. The muscovites locally overprint the microcline.

The Ballinamuddagh Granite intrudes the southern volcanic suite (Figure 4:1) and is approximately contemporaneous with the formation of the Leinster Batholith. The intrusion is

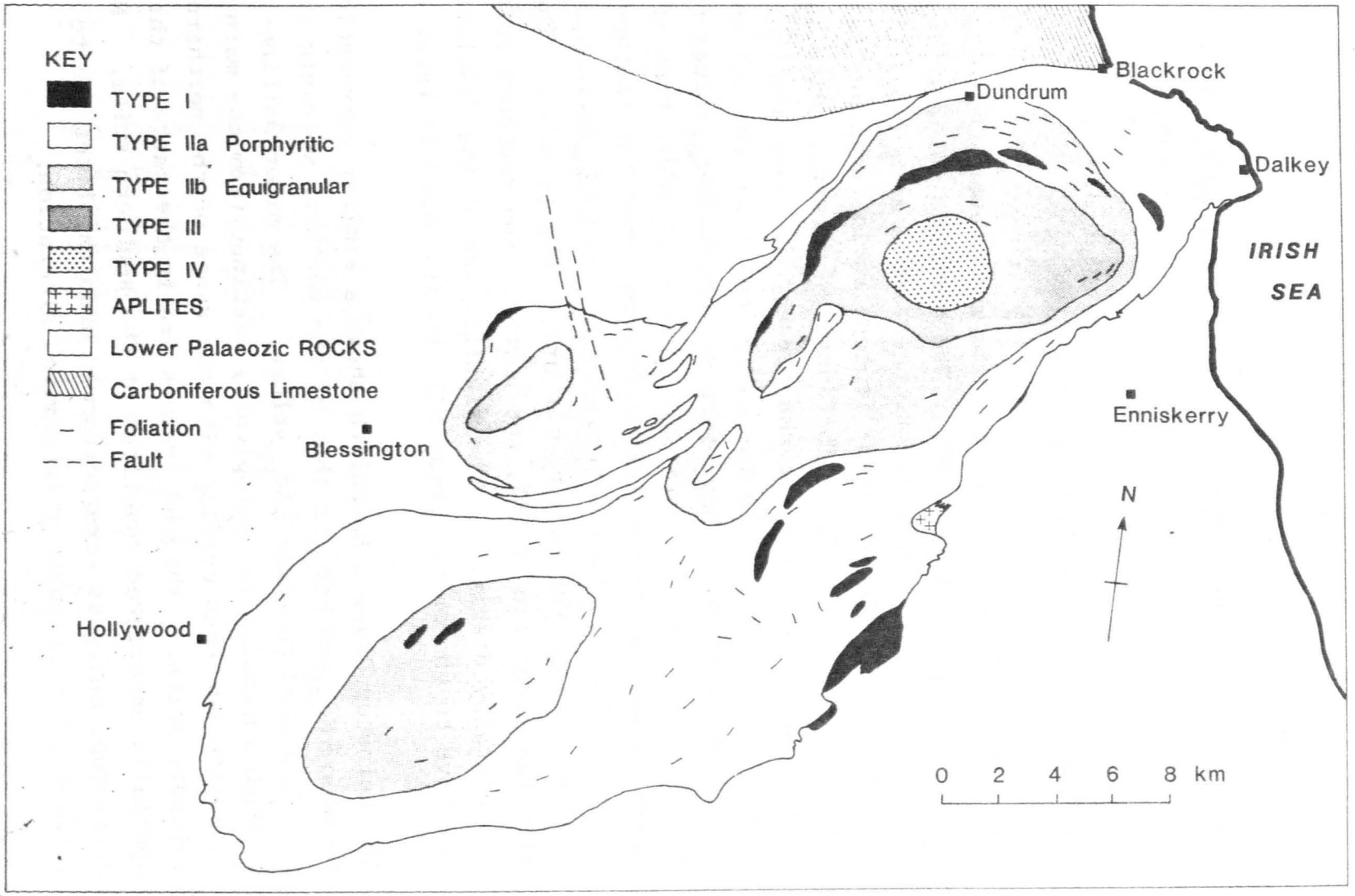

Figure 4:3 GEOLOGIAL MAP OF THE NORTHERN AND UPPER LIFFEY UNITS OF THE LEINSTER BATHOLITH

composed dominantly of diorite and granodiorite.

4:2 Isotope Data

Samples of Caradoc/Ashgill age were selected for Nd and Sr isotope analysis from both the northern and southern volcanic suites. The isotope results are presented in Tables 4:1 and4:2 Initial isotope ratios have been calculated at 425 Ma based on the time scale of Gale et al. (1980).

The initial Sr and Nd isotope data are presented in Figure 4:4, an εSr_{425} vs εNd_{425} diagram. The southern volcanic suite define a trend sub paralled to the mantle array, being more radiogenic in both Nd and Sr isotope ratios compared to Bulk Earth values at 425 Ma. The southern volcanic suite is isotopically equivalent to the present day Java arc (Whitford and Jezek, 1982). With the exception of LB7 the volcanic rocks of the northern suite have more radiogenic εSr_{425} values than the southern suite. Their εNd_{425} values straddle that of Bulk Earth at 425 Ma and are less radiogenic than the southern suite. The correlation between εSr_{425} and εNd_{425} defines a shallower slope than the mantle array (Figure 4:4). Therefore, with the exception of LB7, the northern and southern suite are isotopically distinct. The significance of the displacement relative to the mantle array will be discussed in later sections

The Leinster Granite Batholith shows a similar correlation between εNd_{425} and εSr_{425} to that of the northern volcanic suite but displaced to lower εNd_{425} values. The minor Ballina-muddagh intrusion is isotopically distinct from the main batholith but does overlap with the range of the northern volcanic suite. The εNd_{425} values are in the range of the spatially associated rhyolites of the southern suite. No Sr isotope analyses were performed upon rhyolites due to variable, but frequently extensive, alteration.

The igneous activity of south east Ireland can therefore be divided into 3 major groups, northern Ordovician volcanic

Table 4:2 Isotope results for the Leinster Batholith

Sample	Batholith Unit	Rock Type	Rb	Sr	Rb/Sr	$^{87}Sr/^{86}Sr$	Sm	Nd	Sm/Nd	$^{143}Nd/^{144}Nd$	εNd_{404}	εSr_{404}
Iso 1	I	Biotite Diorite	170.2	992.0	0.1716	0.70840 ± 2	11.6	92.00	0.1261	0.512261 ± 14 0.512240 ± 22	-1.4 ± 0.4	+18.9 ± 0.3
Iso 2	I	Biotite Diorite	127.1	365.0	0.3482	0.71262 ± 4	6.97	44.7	0.1559	0.512185 ± 18	-3.6 ± 0.4	+37.0 ± 0.5
Iso 3	I	Grandiorite	152.1	288.8	0.5267	0.71617 ± 3	6.478	42.0	0.1542	0.512159 ± 26	-4.0 ± 0.5	+45.2 ± 0.5
Iso 5	I	Adamellite	181.2	209.0	0.8670	0.72141 ± 4	4.288	24.07	0.1782	0.512171 ± 18	-5.1 ± 0.4	+38.9 ± 0.6
Iso 19	I	Aplite	443.1	5.763	76.89	2.17015 ± 8	0.0939	0.2344	0.4006	0.512497 ± 30	-5.1 ± 0.6	+100 ± 100
Iso 24	III	Grandiorite	176.1	201.5	0.8740	0.72171 ± 3	0.9333	4.289	0.2176	0.512290 ± 16	-3.5 ± 0.3	+41.6 ± 0.6
Iso 26	Ballyna-muddagh Intrusion	Diorite	84.53	576.5	0.1466	0.70762 ± 2	4.504	28.41	0.1585	0.512410 ± 18	-0.7 ± 0.4	+13.7 ± 0.3
Iso 27	- " -	Granodiorite	127.5	351.0	0.3633	0.71265 ± 4	1.917	10.43	0.1838	0.512387 ± 12	-0.5 ± 0.2	+33.9 ± 0.5

	La	Ce	Nd	Sm	Eu	Gd	Dy	Er	Yb
Iso 1	87.6	202	92	11.6	2.68	7.43	4.17	1.73	1.35
Iso 2	44.8	89.1	44.7	6.97	1.56	4.78	2.52	1.03	0.82

Unit I = Northern Unit
Unit III = Lugnaquillia Unit

Table 4:1 Isotope results for S.E.Ireland

Sample	Rock Type	Locality	La	Ce	Nd	Sm	Eu	Gd	Dy	Er	Yb	$(Ce/Yb)_N$	Sm/Nd	$^{143}Nd/^{144}Nd$	εNd_{425}	Rb	Sr	Rb/Sr	$^{87}Sr/^{86}Sr$	εSr_{425}
L37	andesite	Balbriggan	10.4	21.7	10.4	2.42	0.878	2.88	2.88	1.69	1.57	3.5	0.2327	0.512598 ±26	+2.2 ±0.5	52.3	223.1	0.2344	0.70820 ±4	+8.6 ±0.5
L29	dacite	Lambay Island	48.0	101.0	45.8	8.48	1.79	7.37	5.82	3.25	3.15	8.2	0.1854	0.512368 ±10	+1.1 ±0.2	119+	318+	0.3742	0.71360 ±3	+40.6 ±0.4
L33	basalt	Lambay Island	29.1	59.2	27.6	5.38	1.58	5.16	4.20	2.23	1.93	7.8	0.1949	0.512477 ±16	-0.7 ±0.3	30+	666+	0.0450	0.70634 ±4* 0.70594 ±3*	+13.7 ±0.4
L100	basalt	Lambay Island	36.9	79.7	35.7	6.80	1.93	6.20	4.87	2.67	2.43	8.4	0.1907	0.512407 ±14	-0.1 ±0.3	29+	423+	0.0686	0.70766 ±4* 0.70762 ±3	+31.8 ±0.4
L111	basalt	Lambay Island	29.4	62.6	29.7	6.01	1.72	5.67	5.11	2.97	2.85	5.6	0.2024	0.512359 ±12	-1.5 ±0.2	45+	481+	0.0936	0.70751 ±4	+24.0 ±0.5
L114	basalt	Lambay Island	46.6	103.5	46.0	8.37	2.38	7.07	5.94	3.26	3.01	8.8	0.1820	0.512402 ±10	+0.1 ±0.2	23+	1101+	0.0209	0.70622 ±3* 0.70607 ±3	+21.6 ±0.4
T18	andesite	County Waterford	15.5	37.6	24.0	6.14	2.10	7.85	9.10	5.49	5.08	1.9	0.2558	0.512697 ±16	+3.4 ±0.3	26.01	142.5	0.1825	0.70769 ±2	+4.4 ±0.3
T42	dacite	County Waterford	35.1	76.2	44.5	9.57	2.51	10.25	10.05	6.25	6.20	3.1	0.2151	0.512565 ± 8	+2.2 ±0.2	104.7	97.42	1.075	0.72355 ±3	+7.3 ±0.5
T63	andesite	County Waterford	7.18	17.6	11.7	2.88	0.901	3.05	3.56	2.48	2.68	1.7	0.2472	0.512531 ±12	+0.4 ±0.2	12.12	149.6	0.081	0.70631 ±4* 0.70624 ±3	+18.4 ±0.4
T192	basalt	County Waterford	7.89	19.5	12.2	3.04	1.03	3.36	3.90	2.46	2.36	2.1	0.2492	0.512595 ±10	+1.6 ±0.2	36.45	194.8	0.1871	0.70820 ±4	+10.4 ±0.5
T73	rhyolite	County Waterford	86.3	209.2	125.0	23.7	2.91	17.67	13.40	7.94	7.72	6.9	0.1896	0.512296 ±20	-1.9 ±0.4					
T74	rhyolite	County Waterford	52.9	112.0	53.1	8.73	1.08	6.84	6.66	4.57	5.15	5.5	0.1644	0.512377 ±18	+0.5 ±0.4					

+ Rb and Sr from Stillman and Williams,1978

* Unleached samples.

Figure 4:4 ϵNd vs ϵSr DIAGRAM FOR S.E.IRELAND IGNEOUS ROCKS

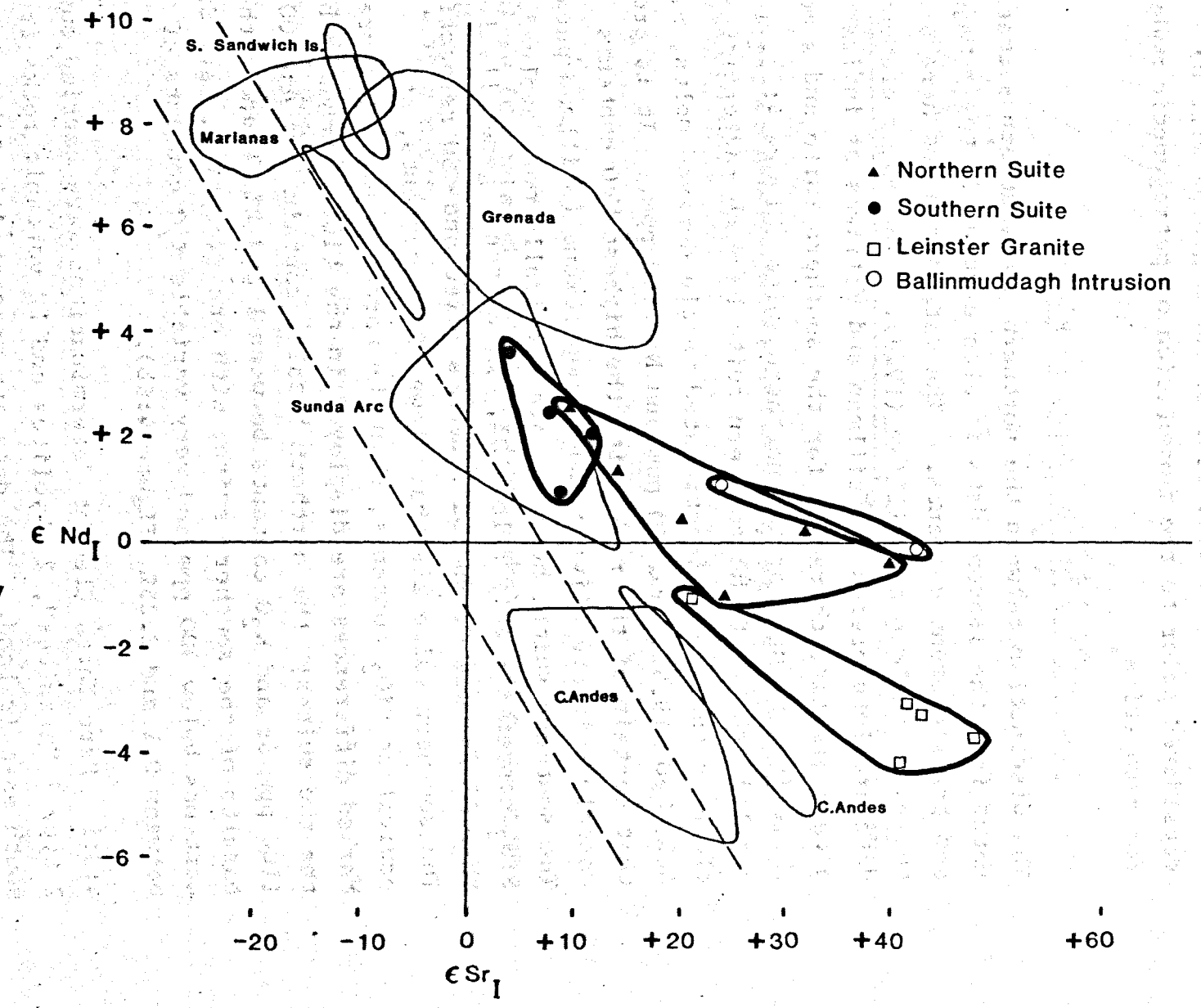

Data sources;

Depaolo and Wasserburg, 1977
Hawkesworth et al., 1979
James, 1982
Whitford and Jazek, 1982.

108

suite, southern Ordovician volcanic suite and the Leinster Granite Batholith. In the following sections the major and trace element characteristics of the 3 groups will be considered prior to the formulation of petrogenetic models for each suite.

4:3 Geochemistry of the Volcanic Rocks

The distinction between the northern and southern suites noted from the isotope data is also evident in their major and trace element contents. The data discussed here are those of Stillman and Williams(1978). The major element data are interpreted by Stillman and Williams as indicating a calc alkaline character for the southern suite and a more tholeiitic nature for the northern suite (Figure 4:5). The basaltic rocks of the northern suite have characteristics close to those of unfractionated mantle derived melts, $SiO_2 \leqslant$ 46%, $MgO \leqslant 19.9\%$, $Cr < 260$ ppm and $Ni \leqslant 100$ ppm. It is probable that certain of the rocks with the highest MgO contents contain cumulate olivine and clinopyroxene (Stillman pers com). The southern suite, however, are chemically more evolved, with SiO_2 contents rarely below 50%, MgO contents generally less than 8% and low Cr and Ni contents (<160 and <80 respectively). The southern suite also have lower P_2O_5 contents, at equivalent SiO_2 contents, than the northern suite (Figure 4:6a). Marked differences are displayed in the LILE abundances between the two suites; the northern basalts contain between 400 and 1100 ppm Sr and K_2O contents between 1 and 2%, whereas the basalts of the southern suite, with one exception, have Sr contents below 300 ppm and very variable K_2O contents of between 0.1 and 2.25% (Figure 4:6b).

4:3:1 Rare Earth Element determinations were carried out on 2 type I "granites", 2 rhyolites and 12 volcanic rocks from south east Ireland. The data are presented in Table 4:1,2 the REE patterns of the volcanic rocks in Figure 4:7a and b. With the exception of LB7 the rocks of the northern suite show variable but marked L.REE enrichment, $(Ce)_N = 68.4$ to 120 and $(Ce/Yb)_N$ ratios range from 5.6 to 8.8. There are also

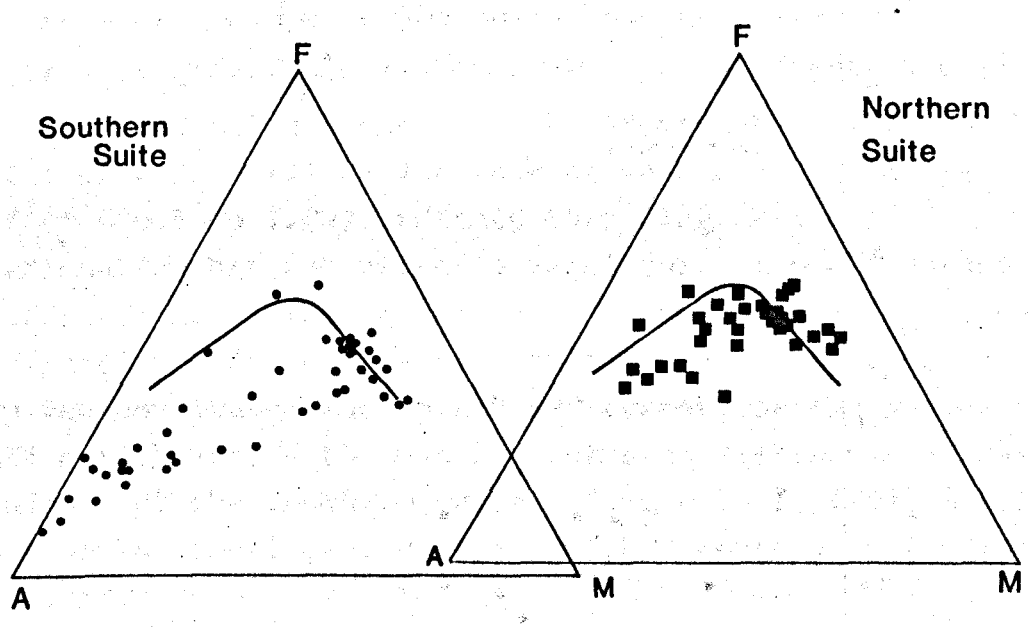

Figure 4:5 AFM DIAGRAM FOR THE SUB-ALKALINE ROCKS OF SOUTH-EAST IRELAND

Figure 4:5

Total Fe (Calculated as FeO), MgO and alkalis (Na_2O and K_2O) diagram showing typical iron enrichment trend defined by tholeiitic rocks.

Figure 4:6a P_2O_5-SiO_2 VARIATION DIAGRAM FOR THE VOLCANIC ROCKS OF S.E.IRELAND

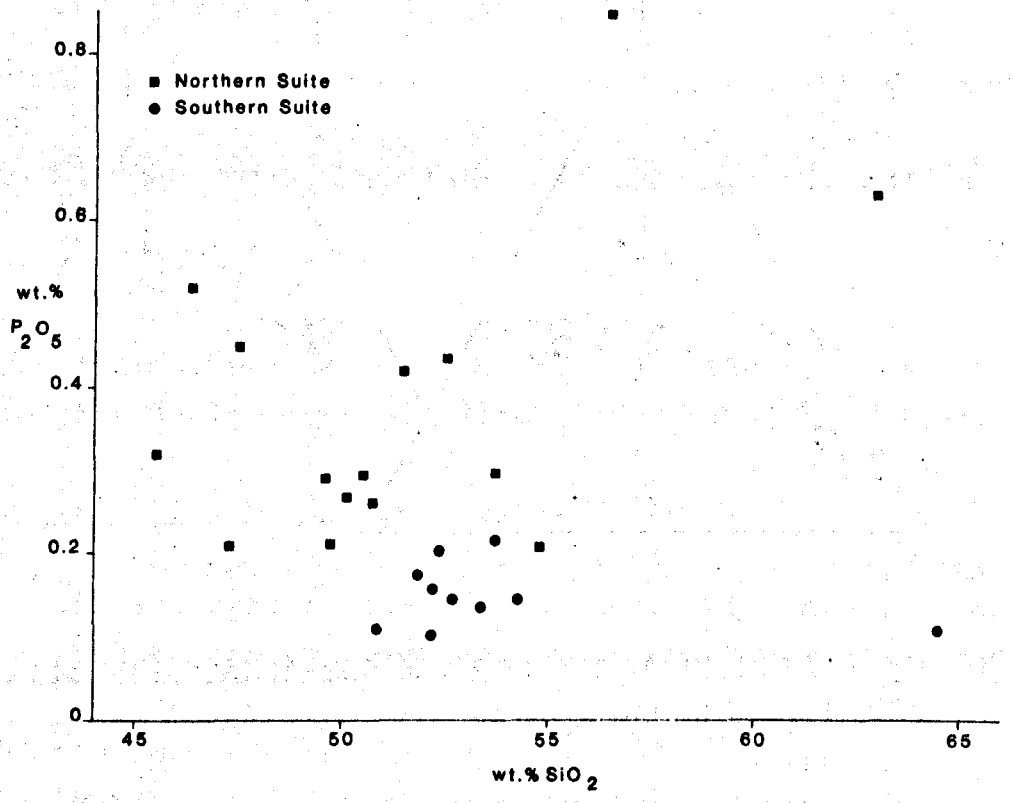

Figure 4:6b Sr-K_2O VARIATION DIAGRAM FOR THE BASALTIC ROCKS OF S.E.IRELAND

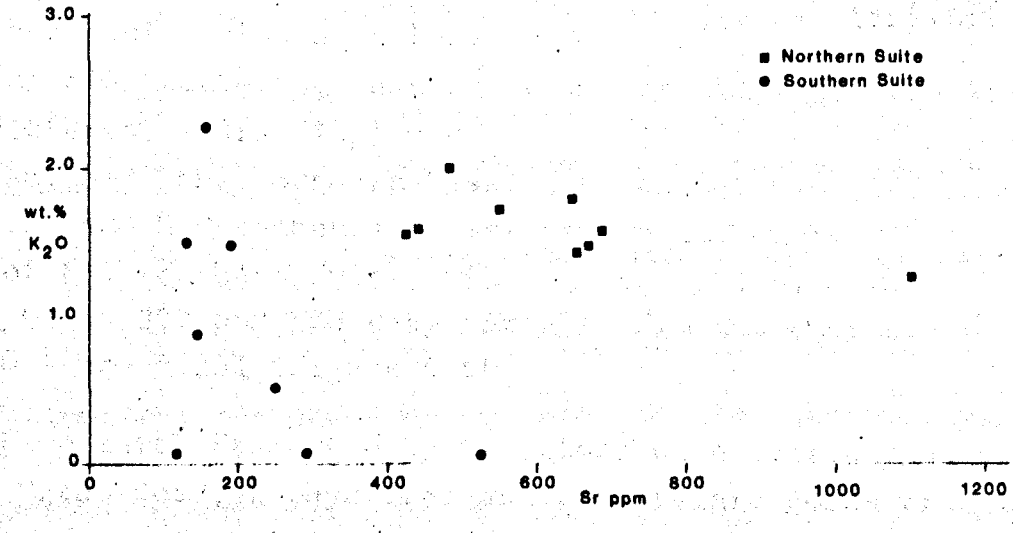

significant variations in the H.REE contents $(Yb)_N$ = 8.77 to 14.3. The H.REE are consistently fractionated with $(Dy/Yb)_N$ ratios of 1.2 to 1.4. The lack of marked Eu anomalies (Eu/Eu* = 0.9 to 1.04) indicate that plagioclase fractionation has not played a major role in the generation of these rocks. The MgO contents of the samples are given in Figure 4:7a and demonstrate that there is no simple relationship between fractionation and REE content or the degree of L.REE enrichment. LB7 has REE contents distinct from the remainder of the northern suite, $(Ce)_N$ = 25.1, $(Yb)_N$ = 7.16 and also has the lowest degree of L.REE enrichment $(Ce/Yb)_N$ = 3.5.

In marked contrast, the basalts of the southern suite have lower L.REE contents $(Ce)_N$ = 20.3 to 43.4, but similar H.REE contents, to those of the northern suite, $(Yb)_N$ = 10.7 to 23.1 (Figure 4:7b). The degree of L.REE enrichment is therefore significantly lower than in the basaltic rocks of the northern suite, $(Ce/Yb)_N$ = 1.66 to 2.1. The H.REE are variable fractionated, $(Dy/Yb)_N$ = 0.82 to 1.15 resulting in "U" shaped REE patterns in some samples, e.g. T63. A negative Eu anomaly (Eu/Eu* = 0.77) is present in the chemically most evolved sample, T42, which also has a higher $(Ce/Yb)_N$ ratio (3.1) than the remainder of the southern suite.

Simple Rayleigh fractionation modelling, using a fractionating assemblage typical of the phenocryst phases (i.e. 0.3 olivine, 0.35 clinopyroxene and 0.35 plagioclase) suggests that in excess of 50% fractional crystallisation is required to produce the REE variation within both the southern and northern suites. The major and trace element composition of L114, the most L.REE enriched sample of the northern suite, precludes significant fractional crystallisation in its genesis (MgO = 9.65%, CaO = 7.97%, SiO_2 = 46.3% and Sr = 1101 ppm). Similarly sample T18, contains the highest REE contents of the southern basalts, yet is chemically the least evolved, MgO = 8.27%. It is therefore apparent that the variations in the REE contents within each of the two distinct suites are not controlled by fractional crystallisation but by either heterogeneity or differing degrees of partial melting in the source regions.

Figure 4:7a REE PATTERNS OF VOLCANIC ROCKS FROM THE NORTHERN SUITE

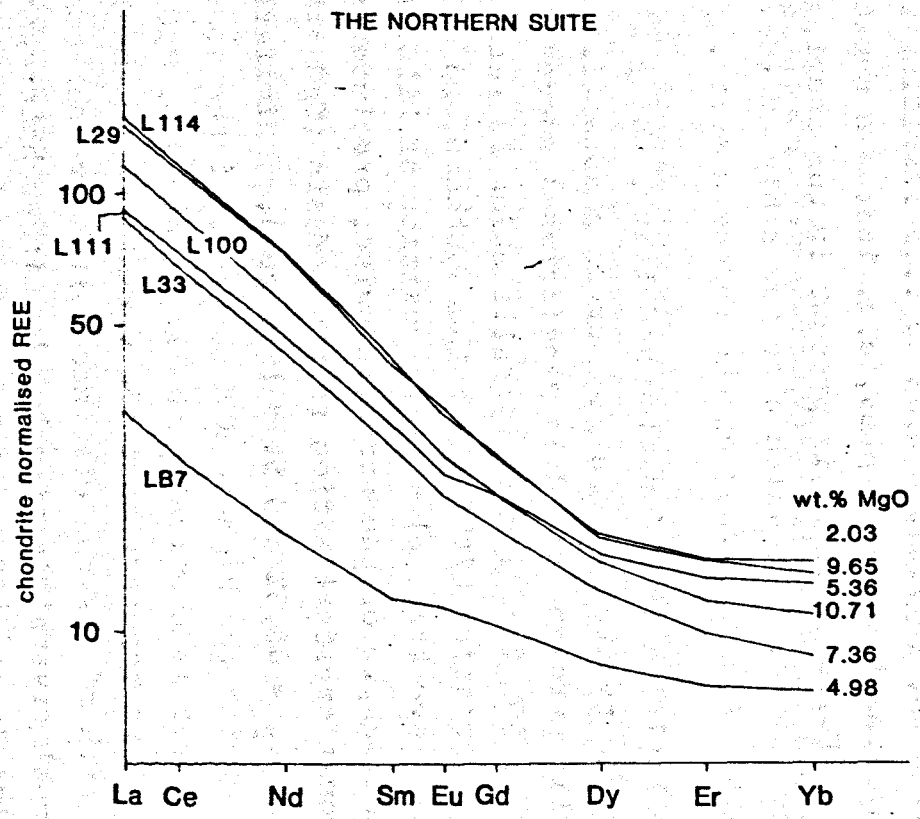

Figure 4:7b REE PATTERNS OF VOLCANIC ROCKS FROM THE SOUTHERN SUITE

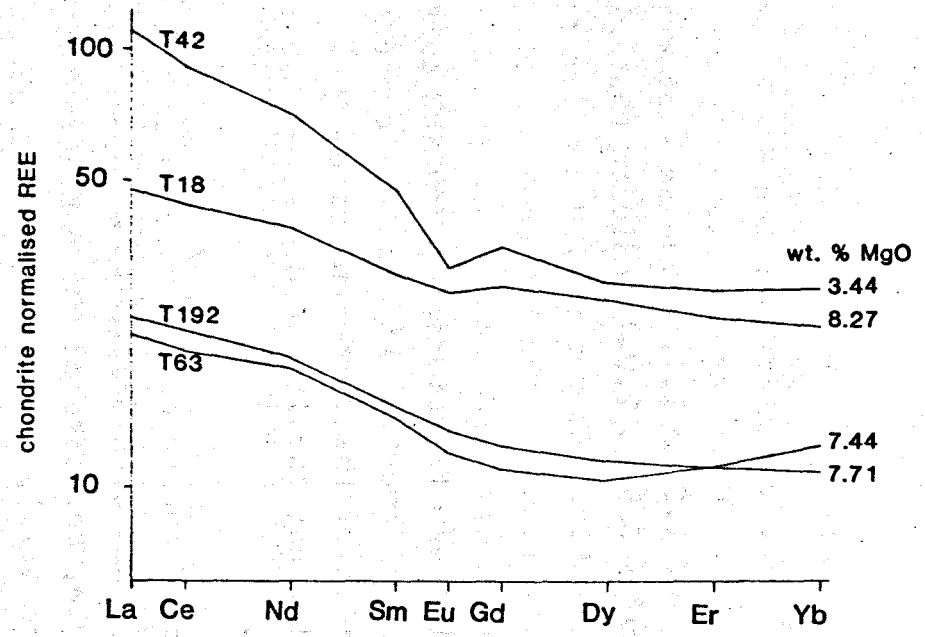

4:4 The Geochemical and Isotopic Characteristics of Subduction Related Volcanism

The aim of this section is to briefly outline the pertinent characteristics of subduction related volcanism and the dominant factors involved in their petrogenesis. For a more detailed discussion the reader is referred to chapters 3 and 8 in "Andesites" edited by Thorpe, (1982).

The geometry of subduction zones is such that any of the following three components may contribute material in the petrogenesis of subduction related volcanism:

i) Mantle wedge
ii) Subducted hydrothermally altered oceanic crust
    a) by dehydration
    b) by melting
iii) Subducted sediments

At continental margins the situation is further complicated by the possibility of contamination with crustal material en route to the surface.

Trace element patterns, normalised to MORB, of basaltic rocks from "typical" destructive plate boundaries are presented in Figure 4:8a. Such rocks consistently show enrichment in LILE greater than for Zr, Nb and L.REE. Often associated with this LILE enrichment are radiogenic $^{87}Sr/^{86}Sr$ ratios such that subduction related volcanic rocks plot to the right of the mantle array on an ε Nd vs εSr diagram, see Figure 4:4. This displacement and LILE enrichment is interpreted as due to a contribution from the hydrothermally altered subducted lithosphere in their petrogenesis (Hawkesworth et al., 1977).

Island arc tholeiites, e.g. South Sandwich Islands, tend to have relatively low abundances of L.REE Nb and Sr (Figure 4:8c). If partial melting of the subducted lithosphere were involved in their petrogenesis such trace elements would be relatively enriched. It is therefore argued that dehydration of the subducted lithosphere and not partial melting is responsible

Figure 4:8

MORB normalised trace element diagrams for basalts from "typical" tectonic settings.

a) MORB; shows flat patterns on this diagram, the exact values depending upon the degree of source depletion and the percentage melting. Transitional and alkalic MORB show trace element enrichment in all elements between Sr and Sm, and generally have peak enrichment at Ba/Nb.

b) Intra plate volcanism; Tholeiitic to alkalic within plate volcanism shows a progressive increase in the degree of trace element enrichment for all elements between Sr and Ti, again generally have peak enrichment at Ba/Nb.

c) Volcanic Arc volcanism; provides the most varied styles of trace element. Tholeiitic basalts are depleted (relative to MORB) in the least incompatible elements (i.e. Nb-Yb) indicating that their sources were probably very depleted. However, LILE show relative enrichment. Calc alkaline basalts (CAß) show a similar style of enrichment pattern, but with the least incompatible elements, especially La, being less depleted. High K. calc alkaline basalts and shoshonites show a more extreme form of CAB type enrichment, with L.REE and P enrichment relative to Nb, Zr and H.REE. They show the most marked LILE enrichment

MORB variations

Figure 4:9a

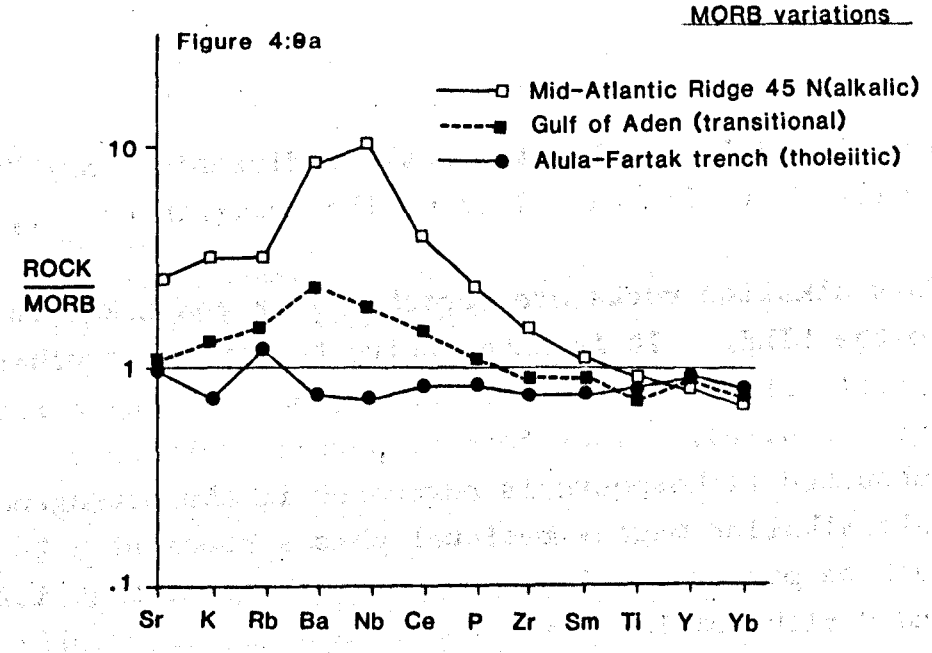

Figure 4:9b

Intra-plate Volcanism

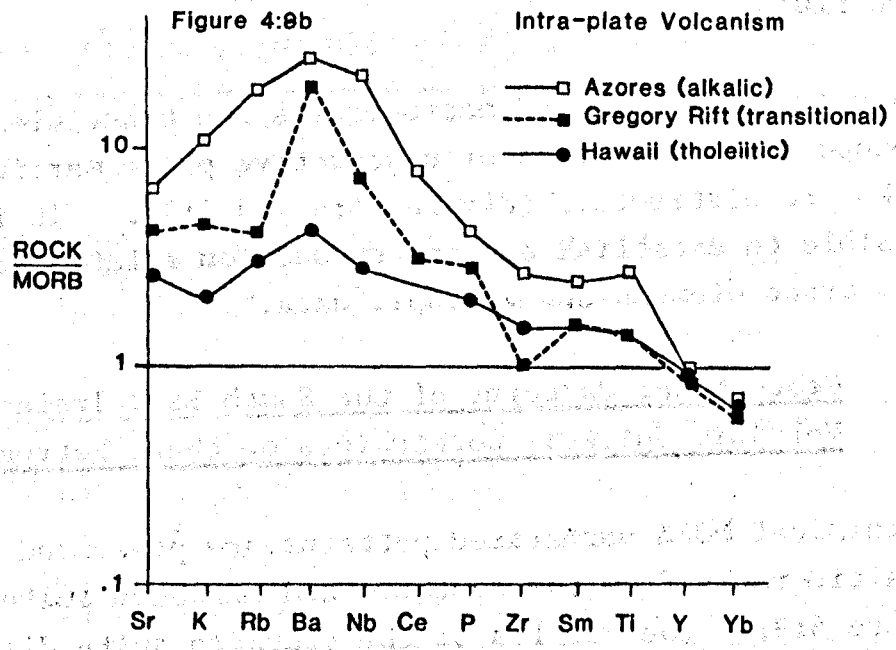

Figure 4:9c

Volcanic Arc Basalt variations

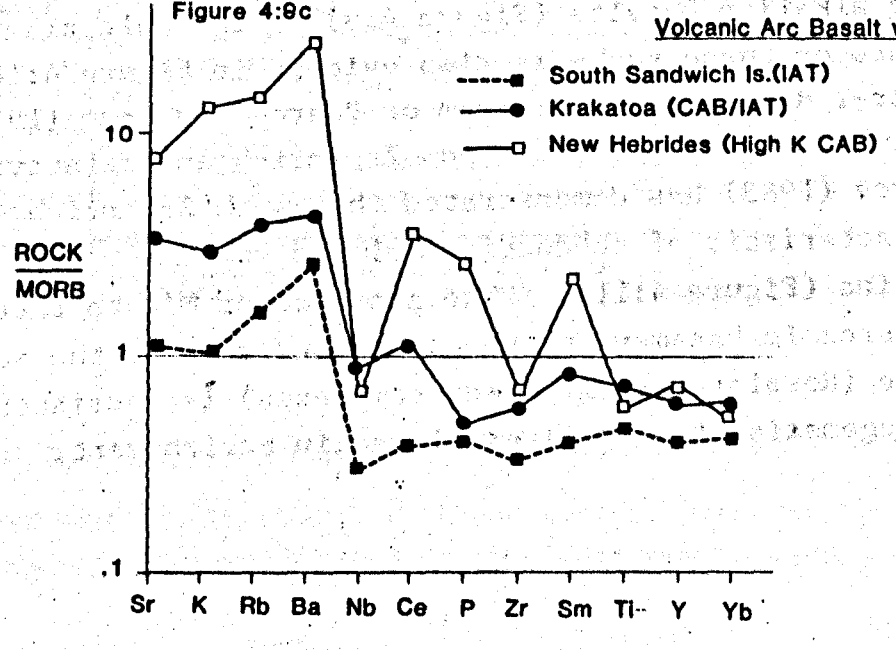

for the LILE enrichment and the radiogenic $^{87}Sr/^{86}Sr$ ratios in the South Sandwich Islands (Hawkesworth et al., 1977).

Calc alkaline rocks are enriched in P and L.REE in addition to the LILE. It is interesting to note that other incompatible elements, e.g. Nb and Zr, do not show enrichment (Figure 4:8a). Therefore if partial melting of the subducted lithosphere is advocated in the petrogenesis of calc alkaline magmas residual phases containing Zr and Nb must be present. A second possibility is that L.REE and P rich complexes are formed and preferentially released from the subducted lithosphere due to the presence of H_2O rich fluids.

Whatever their detailed petrogenesis the trace element and isotope characteristics of destructive plate margin volcanic rocks are distinctive (Figures 4:4 and 4:8). It is therefore possible to establish ancient subduction related volcanism from trace element and isotopic data.

4:5 Geochemical Patterns of the South East Ireland Volcanic Suites:- Constraints on their Petrogenesis I

Geochemical MORB normalised patterns are presented for basaltic rocks from the southern and northern suites in Figure 4:9. The basalts of the southern suite display LILE enrichment and Nb depletion similar to "typical" present day calc alkaline basalts (Figure 4:8). The calc alkaline nature of these rocks is also evident in Figure 4:10, the Ti-Zr-Y discriminant diagram of Pearce and Cann (1974). However, the sample also show Zr enrichment relative to MORB. Pearce (1983) has demonstrated that such Zr enrichment is characteristic of subduction related volcanism at continental margins (Figure 4:11). The presence of Mid to Late Proterozoic basement to the south and east of the southern suite (Rosslare and Anglesey complexes) is consistent with petrogenesis at a continental margin environment.

Figure 4:9a

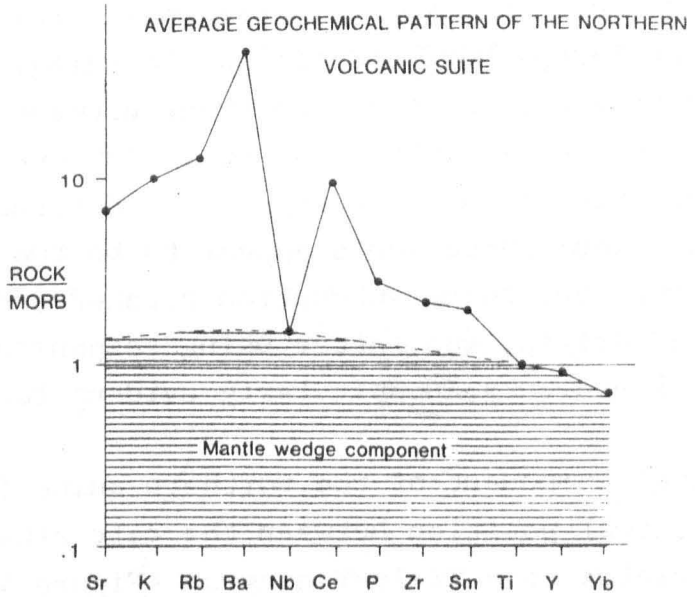

See text for explanation

Figure 4:9b AVERAGE GEOCHEMICAL PATTERN OF THE SOUTHERN VOLCANIC SUITE

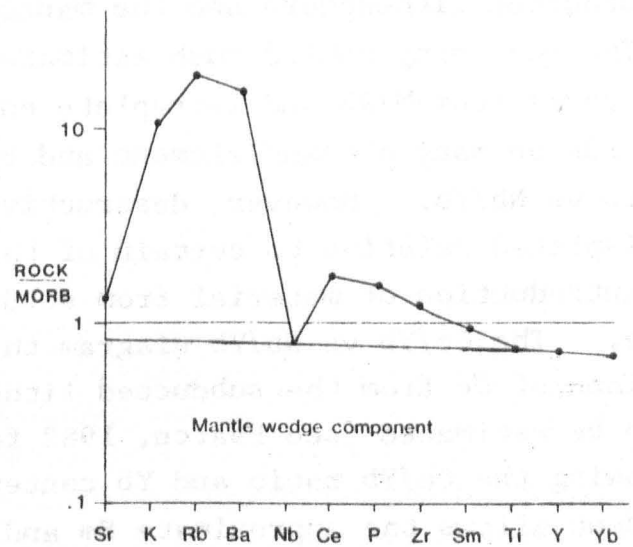

Basalts from the northern suite display relative enrichment in all elements except Ti, Y and Yb (Figure 4:9b). Although relative trace element enrichment in all these elements is characteristic of E-type MORB and similar to within plate basalts (Figure 4:8) the shape of the trace element patterns of the northern suite (with the greatest enrichment in LILE and relative depletion in Nb) are typical of destructive plate margin basalts. Thus there would appear to be two trace element components, one being subduction related and the second of "within plate" origin, the latter being responsible for some enrichment in all elements, (particularly evident for Zr and Nb).

The "within plate" component of the northern suite is evident from the transitional position between the calc alkaline and "within plate" fields on a Ti-Zr-Y diagram (Figure 4:10) and from the high Zr/Y ratios (Figure 4:11). The data therefore plot at the extreme limits of subduction related volcanism on both these diagrams.

It is possible to use the above normalised trace element diagrams to estimate proportions of different trace elements derived from the subducted lithosphere and the mantle wedge (Pearce, 1982). The reasoning behind such estimates is as follows; basaltic rocks from MORB and intraplate environments define coherent trends on many element/element and ratio/ratio diagrams, e.g. Ce/Yb vs Nb/Yb. However, destructive plate margin rocks are displaced relative to certain of these trends, presumably by the introduction of material from subducted lithosphere e.g. Ce. The Ce/Yb vs Nb/Yb diagram therefore allows the proportions of Ce from the subducted lithosphere and mantle wedge to be estimated (see Pearce, 1982 for a full explanation). Knowing the Ce/Yb ratio and Yb content of the mantle wedge component allows the approximate Sm and Nd contents of this component to be estimated. In addition since the Sr/Nd ratio within the mantle is between 18 and 22 an approximation of the Sr content derived from the mantle wedge can be determined. The estimated proportions of certain trace elements derived from the mantle wedge, for

Figure 4:10 Ti-Zr-Y DISCRIMINANT DIAGRAM FOR BASALTS

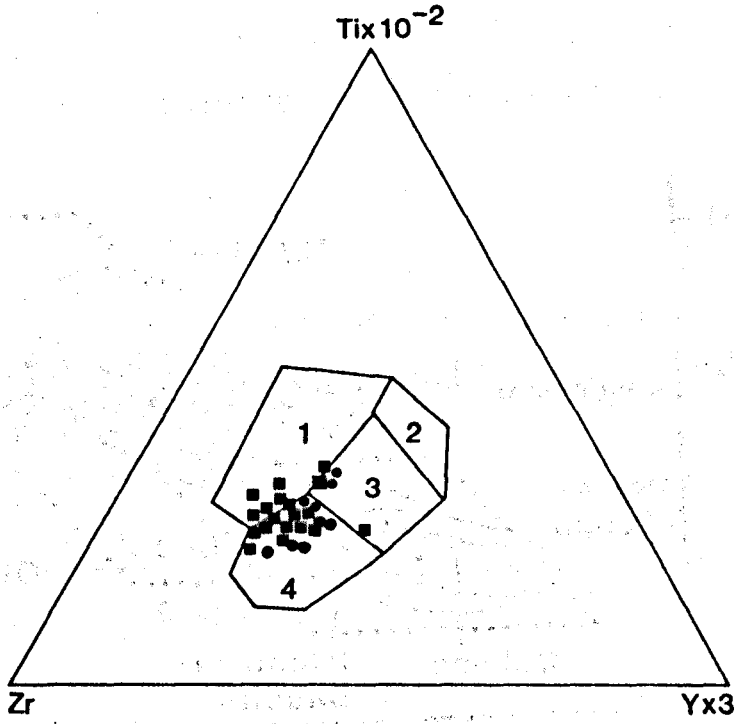

KEY

- • Southern Suite
- ■ Northern Suite
- 1 Within-plate Basalts
- 2-3 Low-K Tholeiites
- 3 Ocean Floor Basalts
- 3-4 Calc-alkaline Basalts

Figure 4:11 Zr vs Zr/Y DIAGRAM

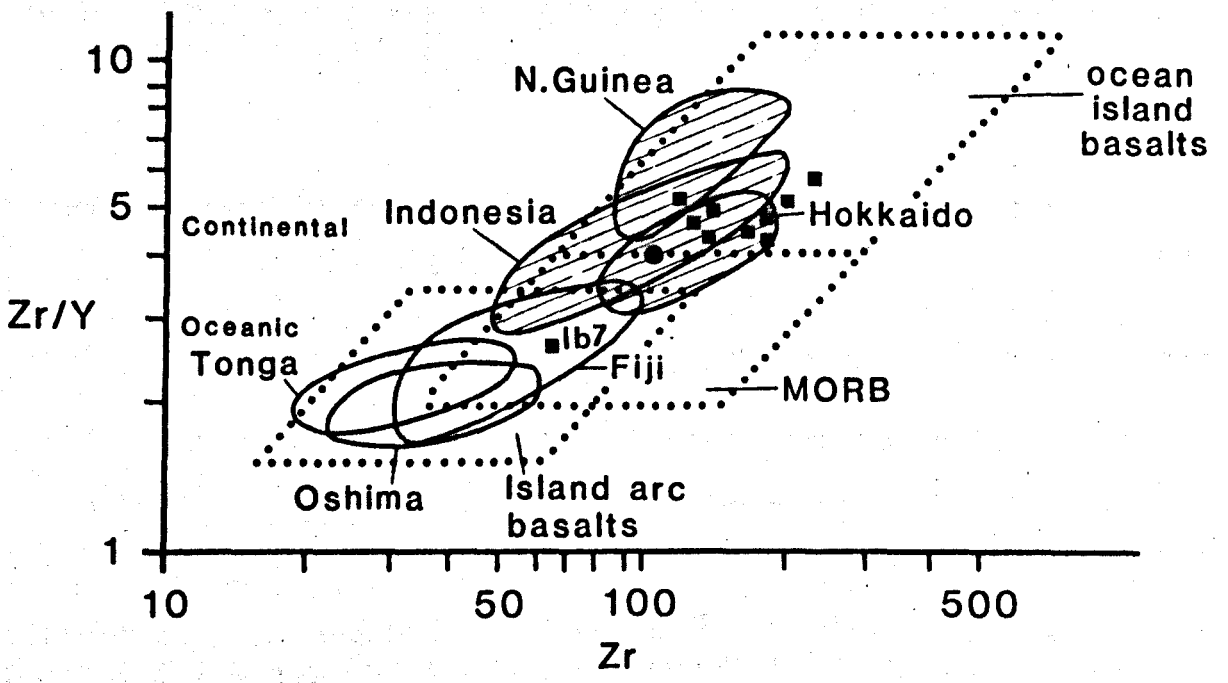

● Average Southern Suite

■ Northern Suite

both the northern and southern suite, are presented in Table 4:3 and displayed as hatched fields on Figures 4:9a and 4:9b.

Table 4:3

Percentage of elements derived from the mantle wedge and subducted slab

	Southern suite		Northern suite	
	a) % Mantle Wedge Component	b) % Subducted Slab Component	a) % Mantle Wedge Component	b) % Subducted Slab Component
Ce	40	60	16	84
Nd	46	54	23	77
Yb	100	--	100	--
K_2O	10	90	20	80
Sr	70	30	25	75
		Sr/Nd ratio = 9		Sr/Nd ratio = 19

Typical values are presented above, Table 4:3, notably the proportion of Ce derived from the subducted slab varies between 60 and 90% for the basaltic rocks of the northern suite.

The results show marked differences between the mantle wedge and subducted slab components of the two suites. The wedge component of the southern suite is L.REE depleted, $(Ce/Yb)_N$ ratio of 0.8 (i.e. similar to MORB), whereas in the case of the northern suite the wedge component is L.REE enriched with a $(Ce/Yb)_N$ ratio of 1.4. The Sr/Nd ratio within the estimated slab component is 19 for the northern suite and 9 for the southern suite. This low latter value is probably due to the relatively evolved nature of the southern volcanic suite and Sr depletion of the magmas during plagioclase fractionation. In many other respects, however, the slab component of the southern suite is typical of many calc

alkaline environments. The slab component of the northern suite shows marked LILE and L.REE enrichment atypical of island arc thoreiites.

It is concluded from the trace element data that the southern suite are compatible with a subduction related origin with significant fractional crystallisation in their petrogenesis. It is estimated that approximately 90% of the LILE and 50% of the Nd in these rocks are derived from a subducted slab component. The precursor mantle wedge was MORB like.

The northern suite, however, shows marked trace element enrichment compared to typical island arc tholeiites. Estimates show that in the region of 80% of the LILE and a similar percentage of the Nd are slab derived. The precursor mantle wedge was L.REE enriched.

4:6 Nd and Sr Isotope Data of the South East Ireland Volcanic Suites: Constraints on their Petrogenesis II

The Nd and Sr isotope data of the south east Ireland volcanic rocks were previously presented in Table 4:1 and as εSr_{425} vs εNd_{425} form in Figure 4:4. As in the case of the majority of subduction related volcanism all the data are displaced to more radiogenic εSr_{425} values than the mantle array at the time of formation. Before considering possible mantle processes that could produce radiogenic εSr values an evaluation of possible crust involvement is needed.

4:6:1 Crustal contamination has been advocated to explain the radiogenic Sr values found in some subduction regions (e.g. N.W. Argentine, (Francis et al., 1980), N. Chile and S.W. Bolivia (Deruelle et al., 1983, James, 1982)). The above mentioned areas of the central Andes are in a region of unusually thick crust 60 - 70 km (Cummings and Schiller, 1971). The intimate association of the northern volcanic suite with deep water pelagic sediments indicates that these rocks were not

erupted through, or in the vicinity of, abnormally thick continental crust. Precambrian crust is, however, exposed approximately 100 km to the south.

The process advocated for crustal contamination within the Andes is that of assimilation fractional crystallisation (A F C), whereby the bulk assimilation of relatively cold crustal material results in a temperature drop within the magma and hence causes crystallisation (Bowen, 1928, Taylor, 1980, DePaolo, 1981). A consequence of AFC is that chemically more evolved magmas will have suffered a greater degree of crustal contamination and are therefore, liable to have more radiogenic $^{87}Sr/^{86}Sr$ ratios. A positive correlation between $^{87}Sr/^{86}Sr$ and SiO_2 and Rb/Sr would be produced if LILE enriched upper crustal material were the assimilated material. Typical AFC relationships from Andean rocksare shown in Figures 4:12a and b. The volcanic rocks from south east Ireland do not show the equivalent coherent correlations on Figure 4:12a and b and it is therefore concluded that the relatively radiogenic εSr values of these rocks are not caused by simple contamination en route to the surface.

4:6:2 Northern volcanic suite. The isotopic data of the northern volcanic suite show an inverse correlation between εNd_{425} and εSr_{425} (Figure 4:4) which has a shallower slope than that of the mantle array. A general correlation is also found between εNd_{425}, Sm/Nd and the estimated % Nd derived from the "slab" component (Figure 4:13). These data therefore indicate that the "slab" component had unradiogenic Nd and radiogenic Sr isotope ratios and may be interpreted in one of two ways:

i) That the "slab" component was derived from subducted lithosphere during the Ordovician and that the radiogenic εSr and unradiogenic εNd values were due to the presence of subducted sediments.

Figure 4:12a $^{87}Sr/^{86}Sr_I$ vs SI 02 VARIATION DIAGRAM

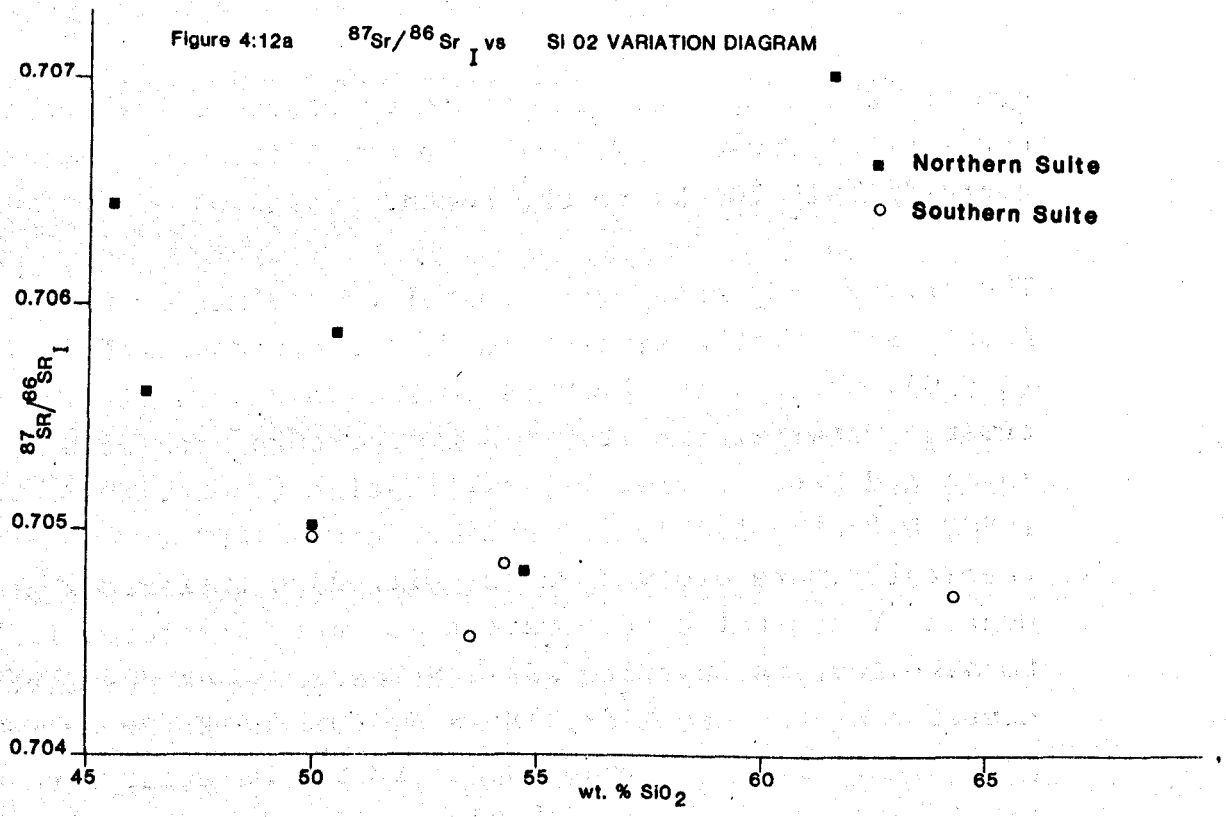

Figure 4:12b $^{87}Sr/^{86}Sr_I$ vs Rb/Sr DIAGRAM SHOWING A POSSIBLE AFC CURVE

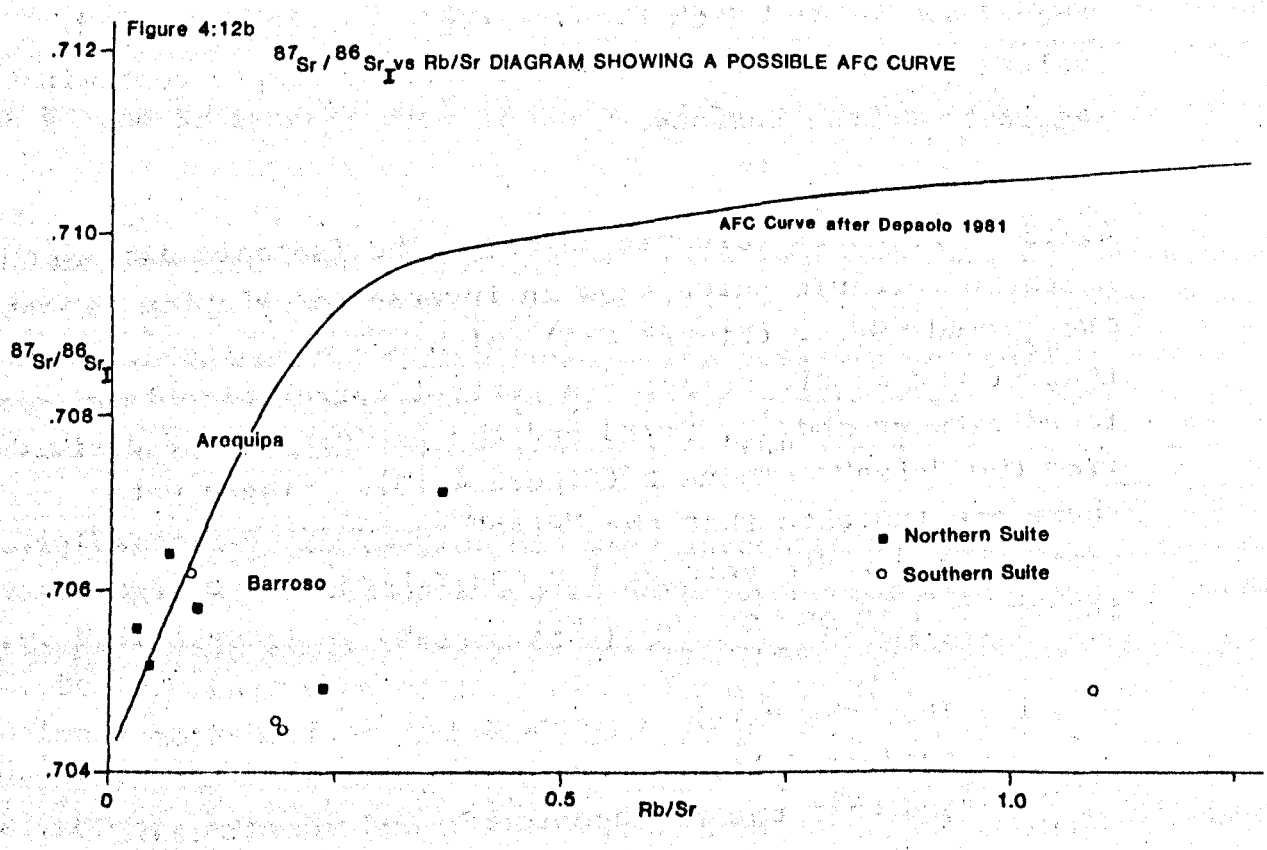

Data source: James ,1982

Figure 4:13

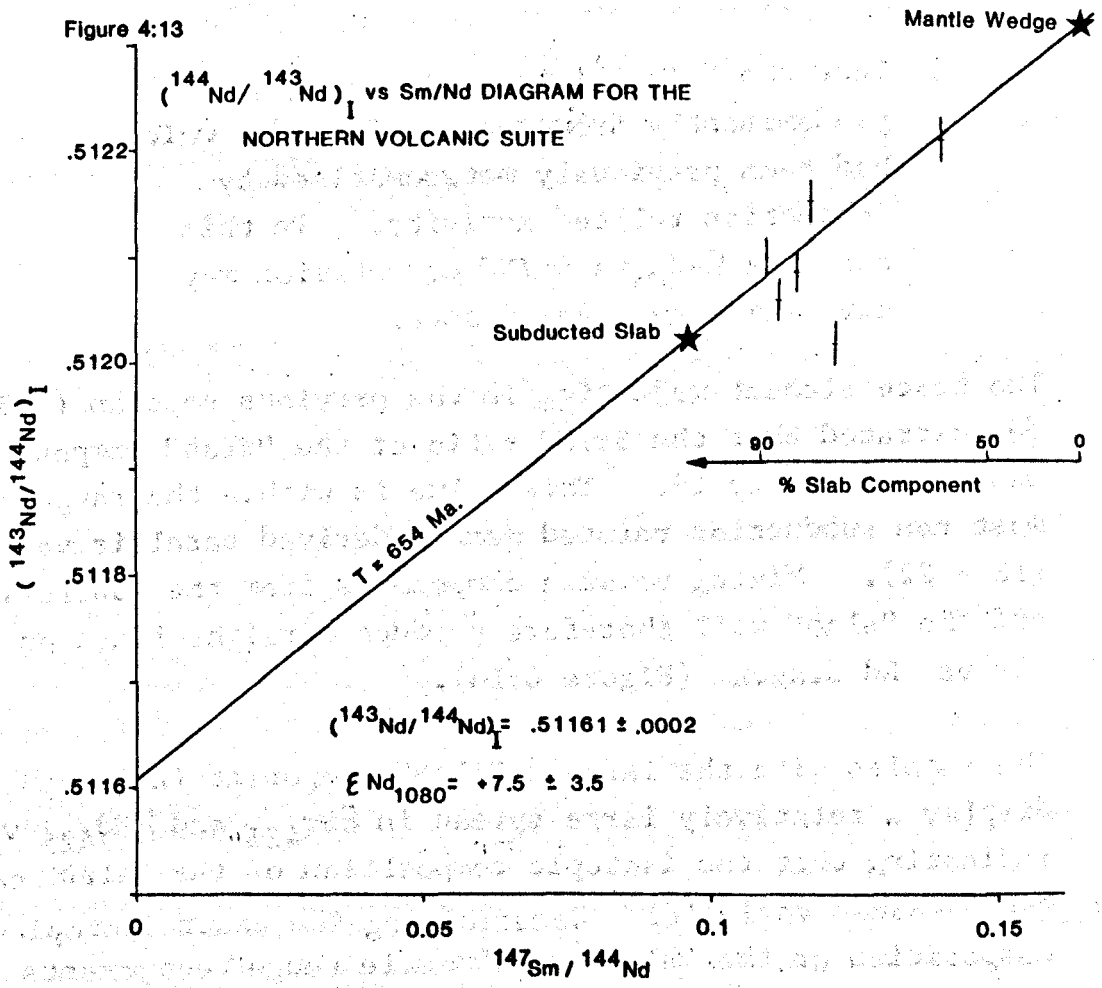
($^{144}Nd/^{143}Nd)_I$ vs Sm/Nd DIAGRAM FOR THE NORTHERN VOLCANIC SUITE
Mantle Wedge
Subducted Slab
90
50
0
% Slab Component
T = 654 Ma.
$(^{143}Nd/^{144}Nd)_I$ = .51161 ± .0002
εNd_{1080} = +7.5 ± 3.5
.5122
.5120
.5118
.5116
$(^{143}Nd/^{144}Nd)_I$
0
0.05
0.1
0.15
$^{147}Sm / ^{144}Nd$

ii) That the "slab" component was derived predominantly from the mantle wedge which had been previously metasomatised by subduction related activity. In this case the εNd_{425} vs Sm/Nd correlation may have some age significance.

The trace element modelling in the previous section (4:5) demonstrated that the Sr/Nd ratio of the "slab" component was approximately 19. This value is within the range of most non subduction related mantle derived basaltic volcanism (18 - 22). Mixing between components from the mantle wedge and the "slab" will therefore produce straight lines on an Sr vs Nd diagram (Figure 4:14).

The samples with the largest "slab" component (L111 and L29) display a relatively large spread in εSr_{425} and εNd_{425} values indicating that the isotopic composition of the "slab" component was somewhat variable. Constraining the exact isotopic composition of the "slab" and "mantle wedge" components can only be achieved if it is assumed that the "mantle wedge" component had εNd and εSr values within the mantle array. Due to the straight line mixing relationship the data from the northern suite can be projected until the centre of the mantle array is reached. εSr_{425} and εNd_{425} values of - 10 and + 3.7 respectively are obtained (Figure 4:14). Interestingly the εNd_{425} value of + 3.7 is close to the most radiogenic value measured in the southern volcanic suite, εNd_{425} = + 3.5.

The two mixing lines shown in Figure 4:14 were calculated assuming equal Sr and Nd concentrations within the two end members. The calculated isotopic values of the "slab" component are a) εSr_{425} = + 47, εNd_{425} = - 1.6, b) εSr_{425} = + 27, $\varepsilon Nd_{425} = -2{\cdot}4$ If, however, the Sr and Nd concentrations within the LILE and L.REE enriched "slab" component were greater than those of the mantle wedge component, as seems probable, then the isotopic composition of the "slab" component would be essentially the same as the samples with

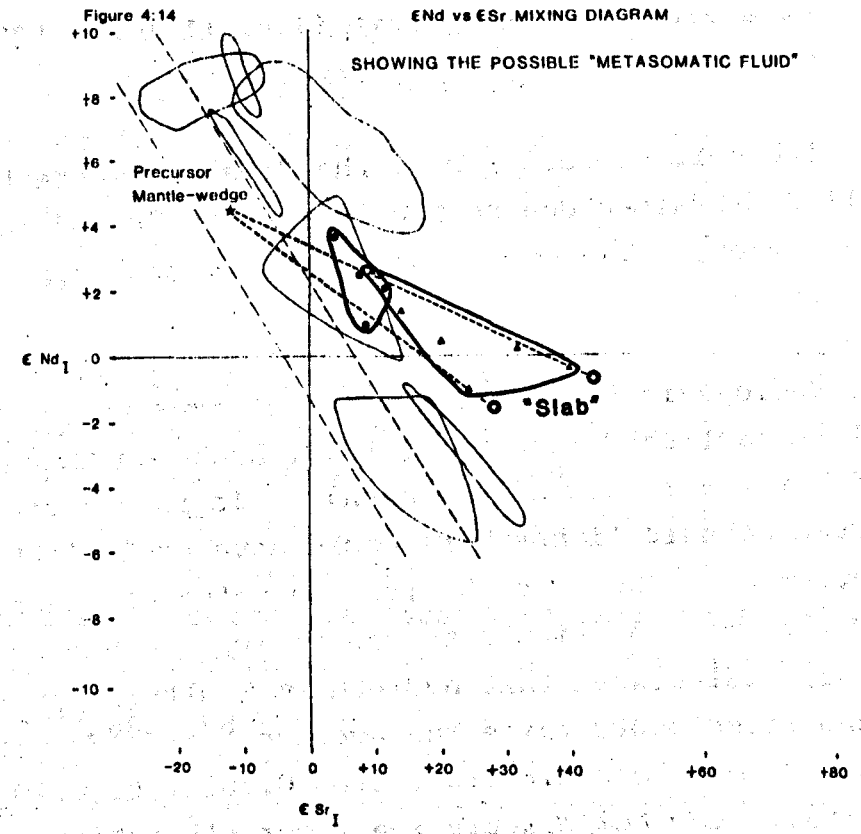

See text and Figure 4:4 for details of the shaded fields

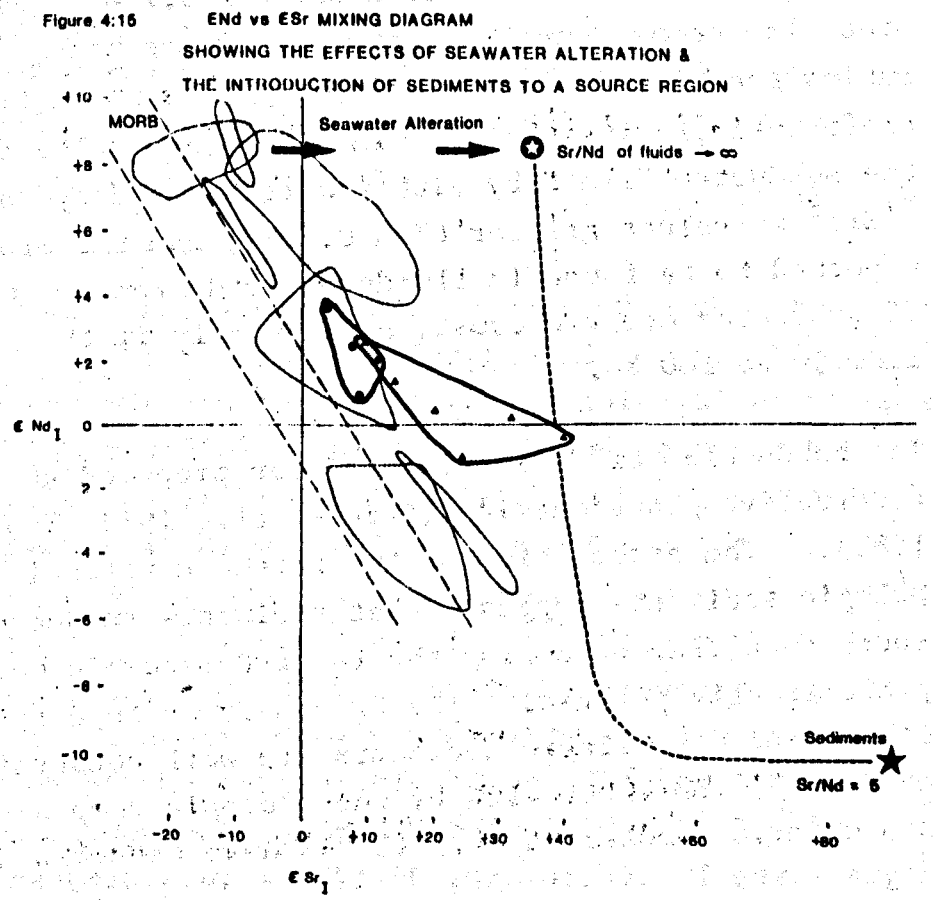

the greatest "slab" component (i.e. L111 and L29 having>80% of their Nd and Sr derived from the "slab").

The isotopic composition of the "slab" compenent is therefore well constrained due to the large % of Sr and Nd derived from the "slab". The origin of this component will now be discussed.

The radiogenic Nd isotope ratios of present day MORB are well established (see Hart, 1980, Hawkesworth and van Calsteren 1983, for a review of the data). It is expected that subducted oceanic lithosphere would have equivalent εNd values i.e.>+ 8. The exact Sr isotope value of oceanic crust is however, more difficult to constrain. Cohen and O'Nions (1982) calculated that hydrothermal alteration at a mid ocean ridge would raise the average $^{87}Sr/^{86}Sr$ value of the upper 3 km of oceanic crust from 0.70237 to 0.7043 (εSr -28 to -6). Low temperature sea floor alteration also has an effect on the $^{87}Sr/^{86}Sr$ values of MORB (Hart, 1974, Staudiguel et al., 1981). Staudiguel et al. (1981) report $^{87}Sr/^{86}Sr$ values from altered MORB in excess of 0.710. Smectites and other low temperature alteration products have $^{87}Sr/^{86}Sr$ ratios greater than 0.80. These phases would tend to be preferentially incorporated in fluids and melts derived from the subducted "slab" by either melting or dehydration. $^{87}Sr/^{86}Sr$ values greater than 0.7065, can therefore be expected to be found in fluids derived from the upper portion of subducted oceanic crust, particularly if the crust is old, i.e. 50 to 100 Ma.

The subduction of sediments has been proposed at several destructive plate margins (Fyfe et al., 1982, Thorpe et al., 1981). The association of the northern volcanic suite with pelagic sediments suggests that sediments subducted beneath south east Ireland during the Lower Palaeozoic would be predominantly pelagic. The Sr and Nd isotope systematics of present day pelagic sediments are well constrained (see chapter 7) and controlled by the isotopic composition of sea water. Hooker et al. (1981) have determined the εNd_I

values of Lower Ordovician sea water and these values will be used in subsequent mixing calculations ($\varepsilon Nd_{425} \div 5.0$). Continental derived sediments would have less radiogenic εNd_{425} values, -8 (see chapter 7). The $^{87}Sr/^{86}Sr$ ratio of Ordovician sea water was approximately 0.7080 (Veizer and Compston, 1974).

The Sr/Nd ratio of both pelagic and detrital sediments are low, <5, such that the mixing of sediments with a mantle derived component would produce a steep mixing curve on an εSr vs εNd diagram. The resultant mixture would have a Sr/Nd ratio lower than the calculated "slab" component. The melting of subducted lithosphere will produce magmas with relatively high Sr and Nd concentrations and high Sr/Nd ratios. However, although mixing with sediments may result in Sr/Nd ratios within the range required, large volumes, $>50\%$, of sediment would be needed to produce isotopic ratios within the range of the calculated "slab" component (Figure 4:15). It is possible to produce the calculated Sr/Nd and isotope ratios of the "slab" component by mxing hydrous fluids derived from the subducted lithosphere (Sr/Nd ratio tending to ∞) with sediments or melts of sediments. In this case, however, some Nd must be derived from the subducted lithosphere otherwise the εNd value of the mixture will be that of the sediments.

From the above discussion it can be concluded that subducted sediments could be responsible for the εSr_{425} vs εNd_{425} variations recorded in the northern volcanic suite but that due to our ignorance of subduction related processes insufficient constraints can be placed on the geochemical models to test this hypothesis rigorously.

If the trace element enrichment of the northern volcanic suite is, however, caused by an ancient subduction related event then the isotopic data can provide certain constraints on the timing of the metasomatic event. The relatively poor correlation between εNd_{425} and Sm/Nd yields an age of 654 ± 190 Ma (M.S.W.D. = 2.4) (Figure 4:13). Interestingly the

the initial ratio obtained, 0.511608, is equivalent to an εNd value of +7.5 at 1079 Ma (Age of the rocks 425 Ma plus 654 Ma). The depleted initial ratio indicates that derivation of melts from a subduced oceanic lithosphere and subsequent metasomatism of the overlying mantle wedge circa 1100 Ma is a possibility.

The Sr isotope systematics do not show a coherent relationship (Figure 4:12b). This is, however, not surprising since there is the possibility that LILE enriched fluids have been involved twice during the petrogenesis of the rocks, at 1100 and 425 Ma. Significantly, perhaps, the Sr model age of L111 (L111 is the sample with the least radiogenic εNd_{425} value, - 1.1) is approximately 1100 Ma.

It is concluded that the trace element and isotopic data of the northern volcanic suite provide evidence for either i) the subduction of sediments prior to the Upper Ordovician and the subsequent metasomatism of the mantle wedge by a mixture of an LILE enriched fluid with a high Sr/Nd ratio (derived by dehydration of the subducted slab) and melts from the sediments with low Sr/Nd ratios, or ii) an ancient LILE and L.REE enrichment of the upper mantle beneath south-east Ireland caused by a previous subduction related event, circa 1100 Ma.

Weight is added to the latter hypothesis by the probable Grenvillian age of the Rosslare complex (see chapter 7) indicating crust formation and hence stabalisation of the upper mantle circa 1100 Ma.

4:6:3 Southern volcanic suite. Figure 4:4 shows that the Nd and Sr isotope data of the southern volcanic suite are displaced to more radiogenic εSr_{425} values compared with the mantle array at 425 Ma. The εNd_{425} and εSr_{425} data are equivalent to present day subduction related volcanism of Java (Whitford and Jezek, 1982).

Due to the relatively evolved nature of the majority of the rocks of the southern suite, the Sr/Nd ratio of the "slab"

component cannot be determined from the trace element modelling. The most primitive rocks indicate that approximately 50% of their Nd is derived from the "slab". If the "slab" component is assumed to be the same as that for the northern volcanic suite then the mantle wedge component for the southern suite must be variable depleted, εNd + 9 to + 3 However, it is impossible to constrain either of the two components because no coherent relationships are shown between εSr_{425}, and εNd_{425}, Sr/Nd and the Sr/Nd ratio of the "slab" component is not known.

4:7 Geochemistry of the Acid Igneous Rocks

The second part of this chapter considers the petrogenesis of the Caledonian acid igneous rocks of south east Ireland. Such rocks occur in three forms; firstly as the Leinster Granite Batholith, secondly as voluminous intrusive and extrusive rhyolites of the southern volcanic suite and thirdly as small granitoid intrusions within the southern volcanic suite. The εNd and εSr isotope results of typical samples from each group are presented in Table 4:1. Due to the frequent occurance of hydrothermal alteration and low Sr contents, Sr isotope ratios were not determined on rhyolite samples. The εNd_I values of the rhyolites and grantoids (Figure 4:4) show limited overlap, with the rhyolites having more radiogenic values than the main Batholith. The εNd_I values of the Ballinamuddagh minor intrusion are, however, very similar to those of the rhyolites.

The geochemistry of the three rock groups are discussed below with the aim of assessing how, if at all, they are related and which factors in their petrogenesis produce the different εNd_I values in these spatially and temporally related acid igneous rocks.

4:7:1 Leinster Granite Batholith. Bruck and O'Connor, (1977) present major and trace element data for each of the

different granitoid types. Some of the data are illustrated in Figure 4:16 and demonstrate that the majority of the major elements (TiO_2, MgO, CaO and Fe^{tot}) show a negative correlation with differentiation. The exceptions are SiO_2, K_2O and Na_2O.

The chemical evolution within the Batholith corresponds to the intrusive history, i.e. the chemically most evolved rocks are intruded last. This relationship is not consistent with the progressive partial melting of a single source. Bruck and O'Connor, (1977) conclude that this chemical evolution within the "granites" represents, essentially, a single calc alkaline fractionation trend from the diorites of Type I to the Type IIa and then IIb adamellites. The aplites represent the final crystallisation products. The trace element data are consistent with this interpretation with Ba, Sr and Zr concentrations decreasing, whereas Rb increases, with differentiation (Figure 4:16).

The results of 2 REE determinations upon Type I granitoids are presented in Table 4:2, and along with unpublished REE data supplied by O'Connor as chondrite normalised REE patterns in Figure 4:17. The Type I diorites/granodiorites are extremely LREE enriched with $(Ce)_N$ = 233 to 74 and $(Ce/Yb)_N$ ratios between 38 and 26. The samples have low HREE abundances, $(Yb)_N$ 6.14 to 2.88, which are markedly fractionated $(Dy/Yb)_N$ ratios of 1.83 to 1.99. Interestingly these rocks do not have large negative Eu anomalies, Eu/Eu* $>$ 0.9. The chemically more involved adamellites of Types IIa and IIb show less L.REE enrichment and more pronounced negative Eu anomalies, $(Ce/Yb)_N$ ratios of 21 to 11.6 and Eu/Eu* = 0.8 to 0.6. The H.REE contents are lower than in the Type I granitoids ($Yb)_N$ = 2.29 to 2.41. The aplites have the lowest L.REE contents $(Ce)_N$ 8.4 = 4.9 and are the least L.REE enriched rocks within the Batholith, $(Ce/Yb)_N$ ratios of 5.3 to 3.0. The negative Eu anomalies are the most variable and pronounced of all the rock types, Eu/Eu* = 0.78 to 0.48.

Figure 4:16a

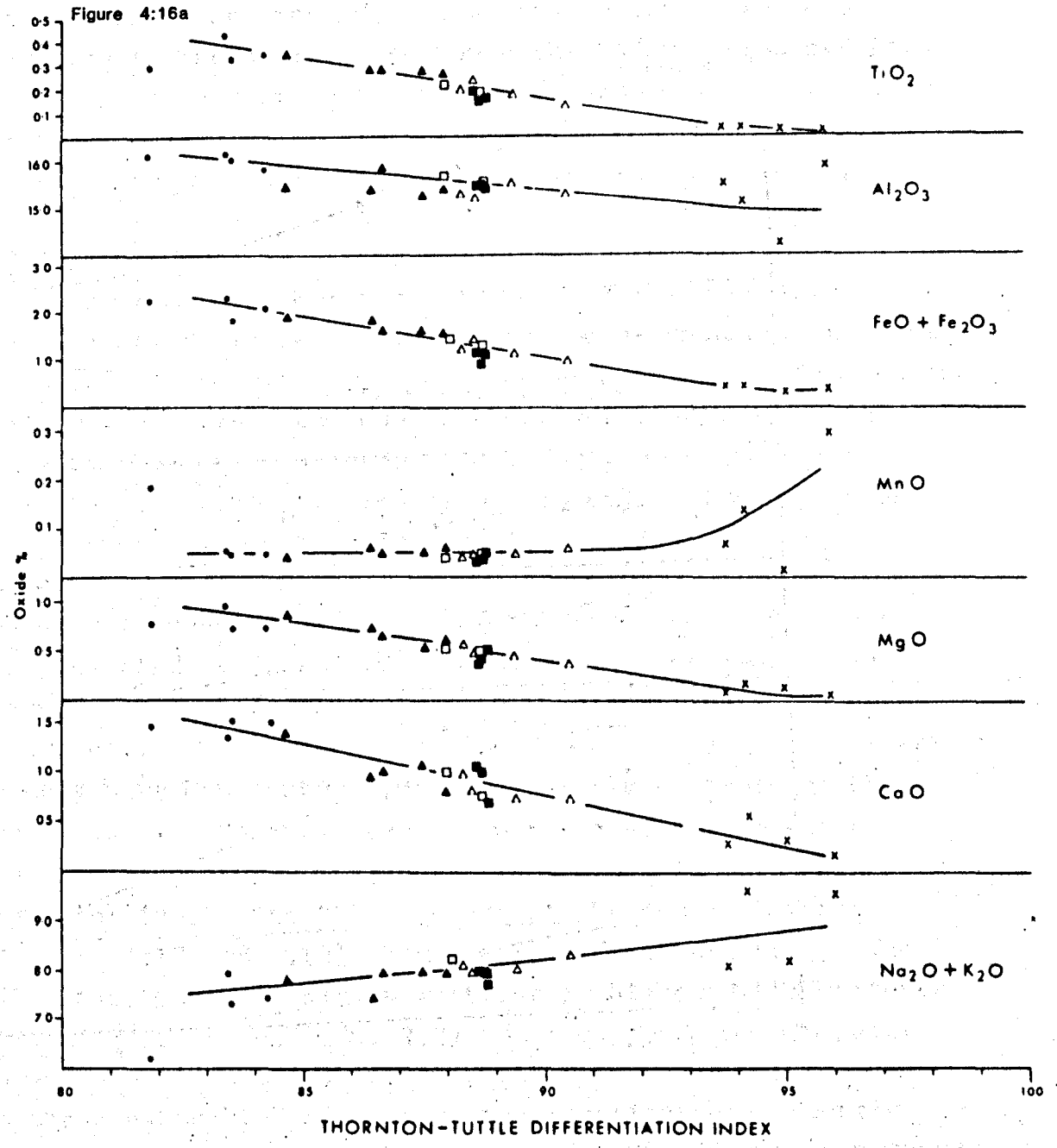
0·5
0·4
0·3
0·2
0·1
TiO_2
16·0
15·0
Al_2O_3
3·0
2·0
1·0
$FeO + Fe_2O_3$
0·3
0·2
0·1
MnO
1·0
0·5
MgO
1·5
1·0
0·5
CaO
9·0
8·0
7·0
$Na_2O + K_2O$
Oxide %
80
85
90
95
100
THORNTON-TUTTLE DIFFERENTIATION INDEX

Figure 4:16b

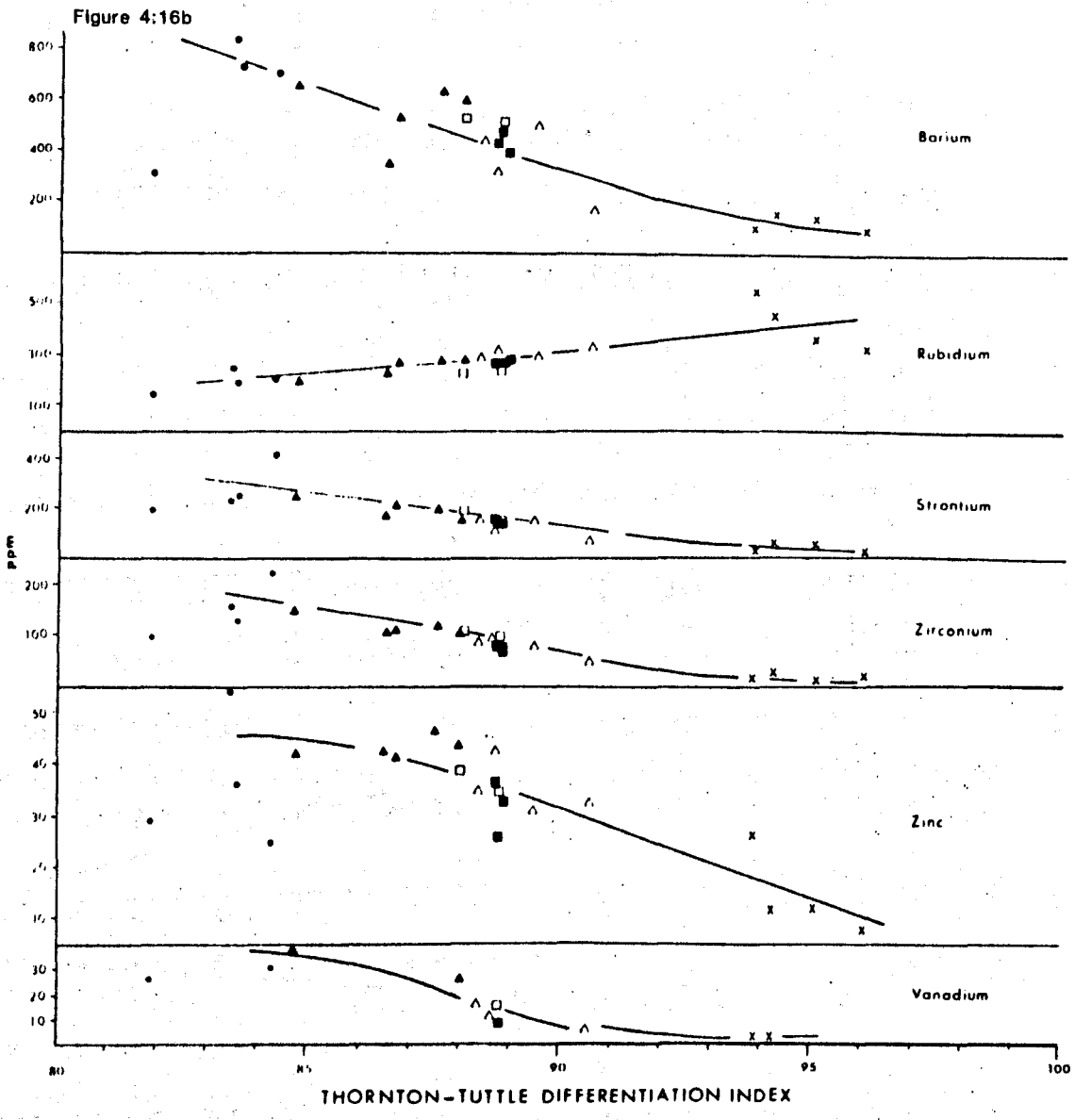
Barium
Rubidium
Strontium
Zirconium
Zinc
Vanadium
ppm
80
85
90
95
100
THORNTON-TUTTLE DIFFERENTIATION INDEX

4:7:2 Minor Granite Intrusions. Unfortunately, to date, no major and trace element studies have been completed on the minor granitoids of south east Ireland. The only geochemical data available are the Rb, Sr, Sm and Nd concentrations presented in Table 4:1. Although the Rb/Sr ratios and Rb and Sr concentrations of these diorites/granodiorites are within the range of equivalent rock types from the Leinster Batholith, their Sm and Nd concentrations are significantly lower.

4:7:3 Geochemistry of the rhyolites and comparison with the Leinster Granite Batholith. REE data for 2 rhyolites (T73 and and T74) are presented in Table 4:2 and as chondrite normalised patterns in Figure 4:18. The samples have high L.REE contents, $(Ce)_N$ = 129 to 242, but due to their relatively high H.REE contents $(Yb)_N$ = 23.4 to 35.1, have only moderate L.REE enrichment, $(Ce/Yb)_N$ ratios of 5.5 to 6.9. The rhyolites have pronounced negative Eu anomalies, Eu/Eu* = 0.43.

The average chemical analyses of the rhyolites and granitoids are presented in Table 4:4. MORB normalised geochemical patterns of Type I granitoids and rhyolites are compared in Figure 4:19. The Type I granitoids were chosen for comparison as they have MgO contents most comparable to those of the rhyolites. Both rock types show relative Sr depletion compared with other LILE, but this feature is more marked in the rhyolites. The REE patterns of the two rock types (Figures 4:17 and 4:18) show similar L.REE contents. The rhyolites, however, have significantly higher H.REE contents ($(Yb)_N$ = 29.2 compared to 2.2) and more pronounced negative Eu anomalies (Eu/Eu* of 0.42 compared to 0.9) In addition to the greater H.REE contents, the rhyolites also contain higher concentrations of Zr, Nb and Y (425, 20 and 76 compared to 164, 7 and 3). The extremely low concentrations of P_2O_5 and TiO_2 in the rhyolites are very apparent in Figure 4:19 and indicative of significant apatite and iron oxide fractionation in the petrogenesis of the rocks.

Table 4:4

Average Chemical Analyses of the Acid Igneous Rocks of S.E. Ireland

		Granitoids		
	Rhyolites	Type I	II b	Aplites
SiO_2	74.67	70.4	72.53	73.98
TiO_2	0.19	0.36	0.17	0.02
Al_2O_3	13.11	15.98	15.29	15.17
Fe_2O_3	2.70 *	0.57	0.42	0.27
FeO		1.51	0.77	0.14
MnO	0.04	0.05	0.05	0.13
MgO	1.19	0.79	0.45	0.11
CaO	0.10	1.46	0.84	0.37
Na_2O	3.83	3.73	3.77	4.96
K_2O	4.12	3.9	4.38	3.98
P_2O_5	0.02	0.10	0.18	0.16
Cr	188	10	<10	<10
Ba	796	752	548	131
Rb	134	210	245	426
Sr	80	291	196	39
Zr	425	164	114	21
Nb	20	7	7	10
Y	76	3	2	2
Ce	161	63.7	24.1	5.75
Sm	16.2	4.0	2.1	0.62
Yb	6.43	0.49	0.41	0.041

* All Fe reported as Fe_2O_3

Major and trace element data for the rhyolites from Stillman and Williams, 1978, for the granitoids from Bruck and O'Connor, 1977.

Figure 4:17 REE PATTERNS OF GRANITOIDS FROM THE LEINSTER BATHOLITH

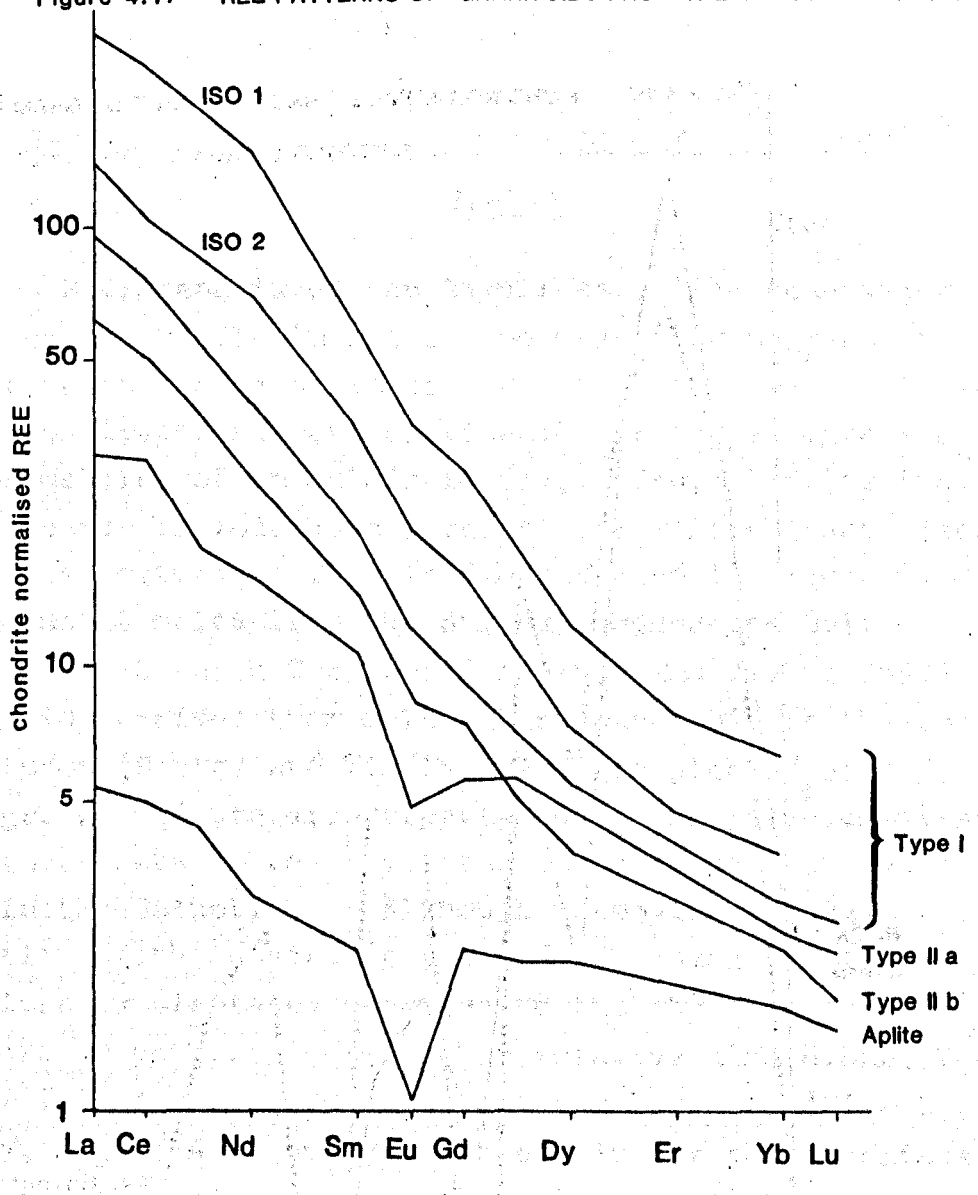

Figure 4:18 REE PATTERNS OF RHYOLITES FROM THE SOUTHERN SUITE

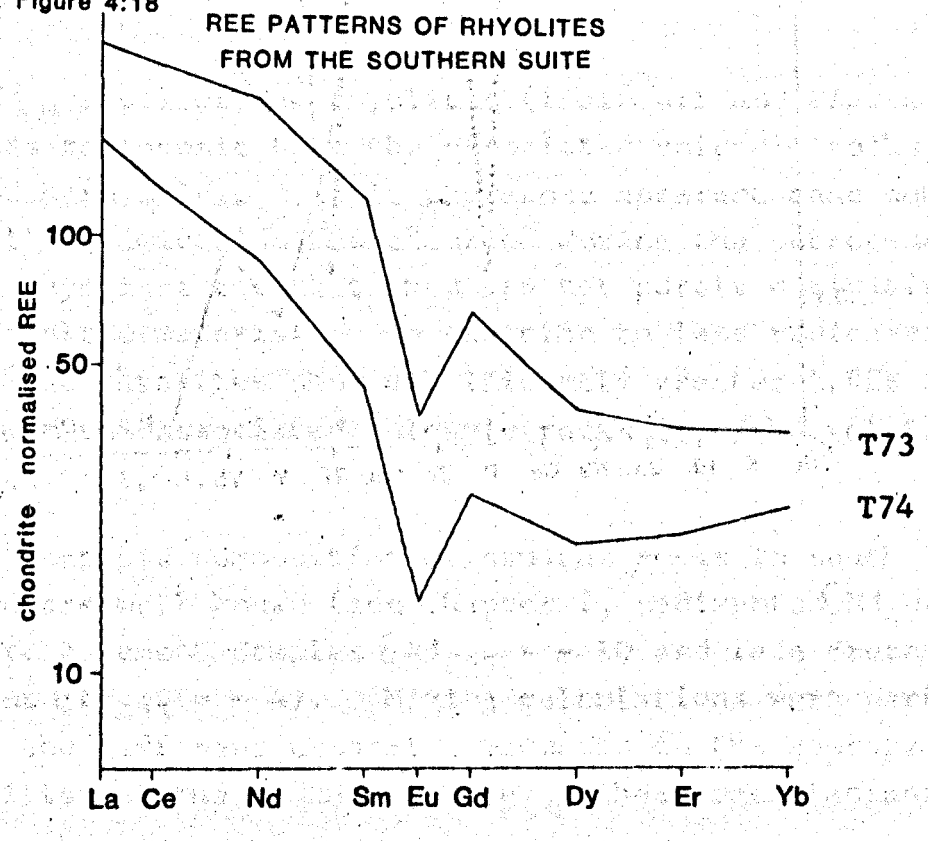

Figure 4:19 MORB NORMALISED TRACE ELEMENT DIAGRAM FOR RHYOLITES & GRANITES FROM S.E. IRELAND

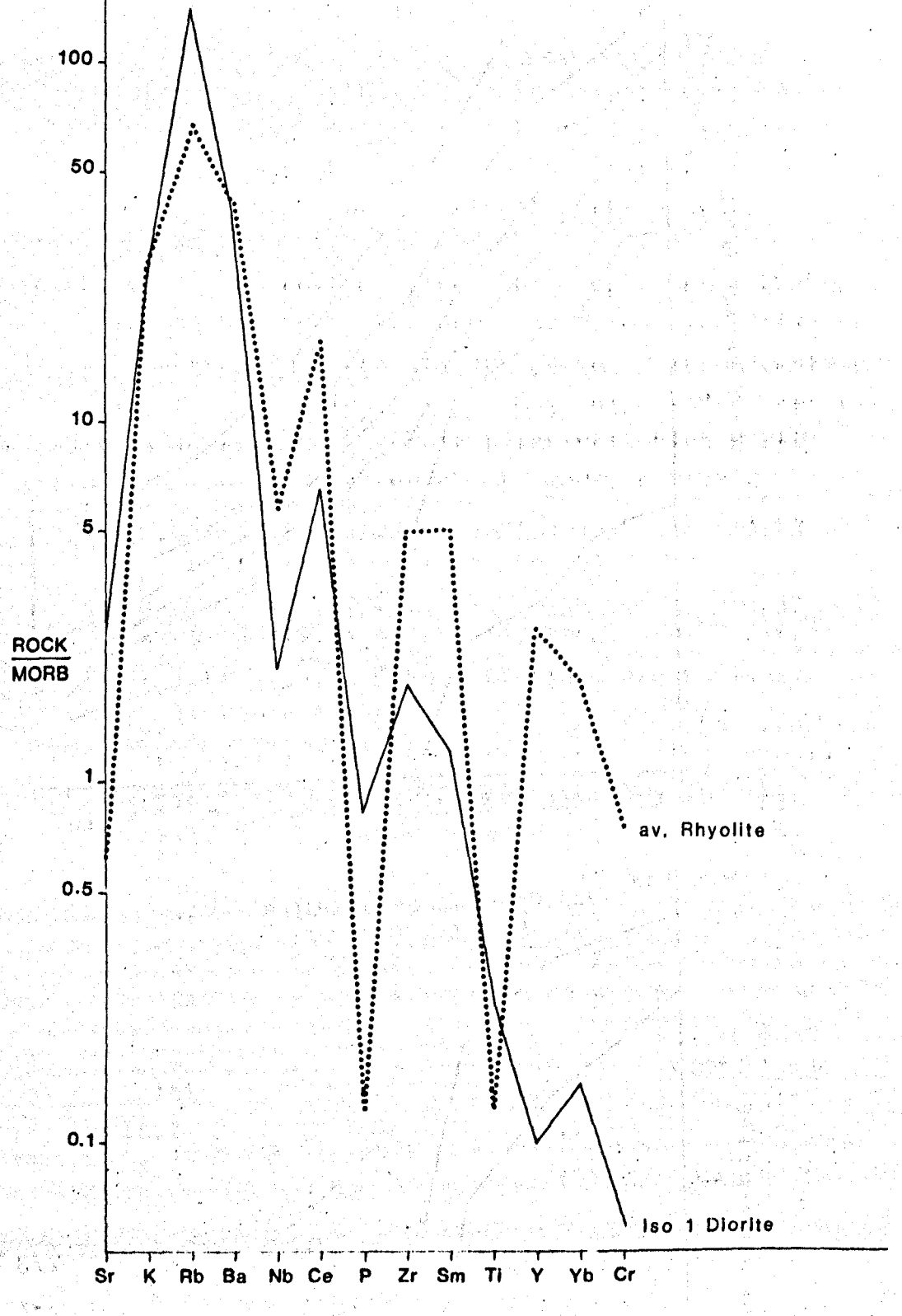

4:8 Petrogenesis of the Acid Igneous Rocks of South East Ireland

4:8:1 Petrogenesis of the Rhyolites. The generation of rhyolites can result in one of two ways, low degrees of partial melting of a basic source region followed by large amounts of fractional crystallisation, or large degrees of partial melting of an acidic source. Crustal melts from acidic source regions have a relatively well characterised chemical signature. This is demonstrated in Figure 4:20 where crustal melts from the St. Malo Migmatite Belt (Brown 1982) Cornish Granites (Atherton and Pearce 1980) and liquids derived from melting greywacke within the Loch Doon Pluton (Pearce and Tindle 1983) are plotted on a Sr vs Zr diagram. Figure 4:20 clearly shows the large chemical differences between the rhyolites and all the rock types of the Leinster Batholith. Although occupying a large proportion of the diagram the field of crustal melts is significantly displaced relative to the rhyolite data. Therefore in conjunction with the relative high H.REE, Y and Nb, low TiO_2 and P_2O_5 contents and the large negative Eu anomaly, Figure 4:20 suggests an origin for the rhyolites controlled by extensive fractional crystallisation from a basic magma.

The εNd_{425} values of the rhyolites (Table 4:1 and Figure 4:4) are less radiogenic than the associated volcanic rocks of the southern suite. It is therefore apparent that some crustal contamination has occurred during the petrogenesis of the rhyolites and that they are not purely derivatives from basaltic material. In addition to less radiogenic εNd_{425} values the rhyolites show significantly greater L.REE enrichment than the associated volcanic rocks ($(Ce/Yb)_N$ of 6.2 compared to 1.9).

The Nd isotopic composition of crustal rocks in south east Ireland are well known (see Chapter 7, sediments $\varepsilon Nd_{425} = -7$, Rosslare Basement Complex $\varepsilon Nd_{425} = -10$ and late Precambrian basement $\varepsilon Nd_{425} = -4$). Mixing calculations were performed adding the different crustal components to the average basaltic composition of the southern suite. These calculations

Figure 4:20 Sr – Zr VARIATION DIAGRAM FOR THE ACID IGNEOUS ROCKS OF S.E. IRELAND

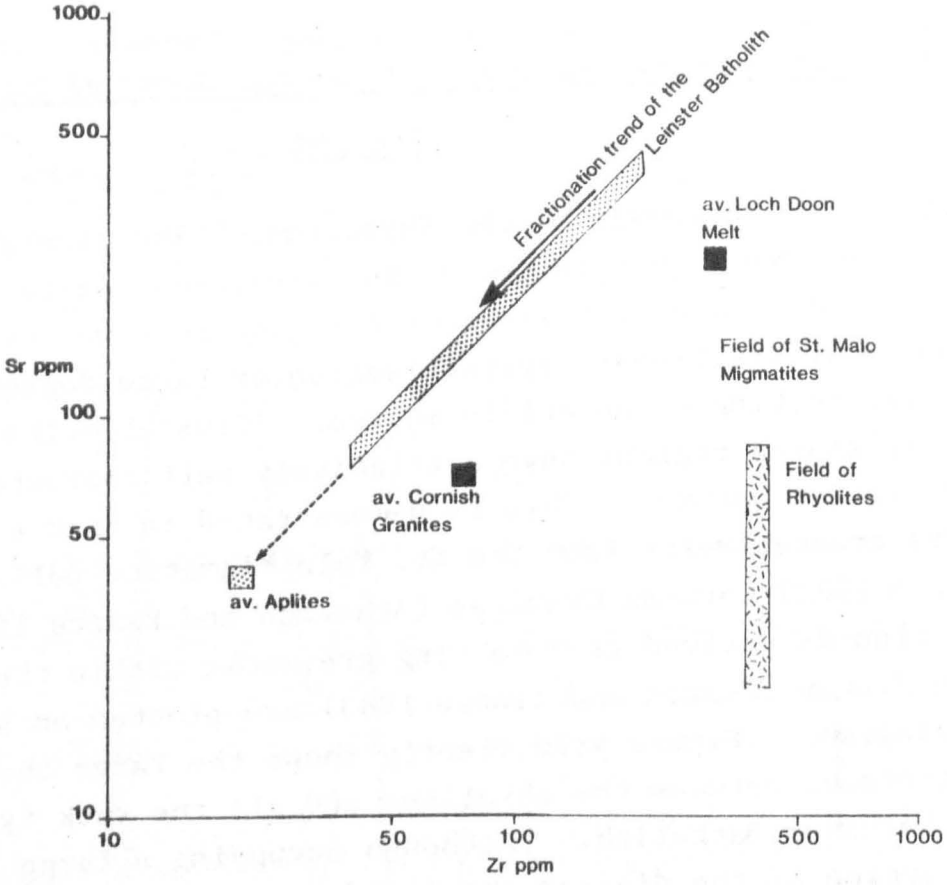

Data sources; Alderton et al.,1980
Brown,1982
Tindle,1982

Figure 4:21 REE PATTERNS OF UPPER CRUSTAL MELTS

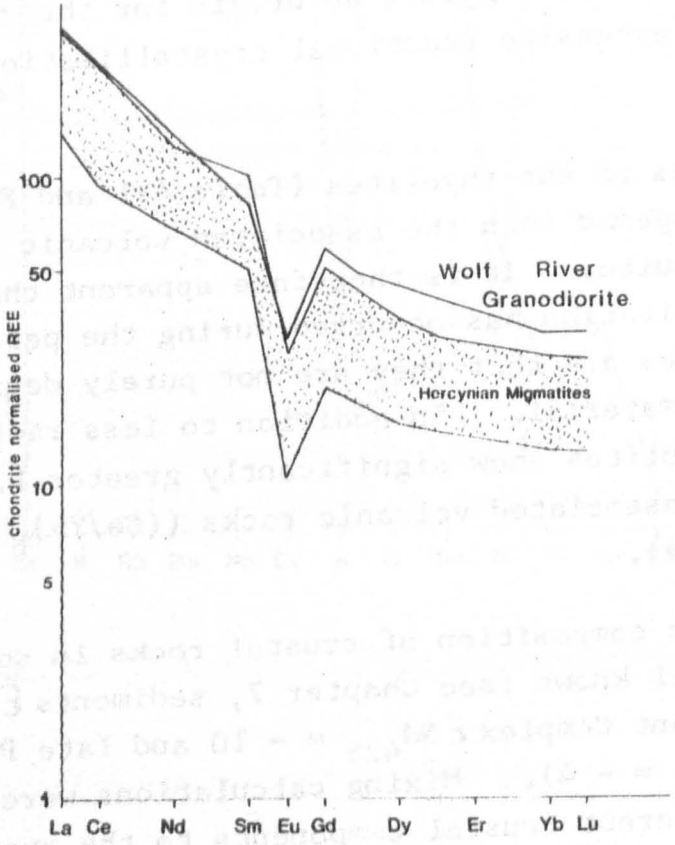

Data sources: Anderson and Cullers, 1978.
Brown,1982

demonstrate that crustal material with a very fractionated REE pattern and low H.REE contents is required as a contaminant to produce the rhyolites. The addition of sediments or upper crustal melts (Figure 4:21) does not result in a significant increase in the $(Ce/Yb)_N$ ratio of the basalt. The model most consistent with the data is one in which a crustal melt with $(Ce/Yb)_N$ ratio of approximately 80 is derived by 30% partial melting of a garnet bearing assemblage within the lower crust (Figure 4:22a) and 7 to 22% contamination of the basalt occurs (7% if crust has εNd of -1 and 22% if crust has εNd of - 4). Addition of the melt will result in cooling of the basalt and hence fractional crystallisation will occur. Rayleigh fractionation modelling indicates that in excess of 70% fractional crystallisation of a dominantly plagioclase and clinopyroxene assemblage is required, subsequent to contamination, to produce the trace element contents (particularly the marked negative Eu anomaly and low Sr contents) found in rhyolites.

4:8:2 Petrogenesis of the Ballinamuddagh minor granite intrusions. The Ballinamuddagh Granite intrudes the Ordovician volcanic rocks of the southern suite. Unfortunately no major and trace element data are yet available to help constrain petrogenetic models.

The Nd and Sr contents of the diorite from the intrusion are significantly lower than for similar rocks of the Leinster Batholith. The more radiogenic εNd_{404} values (+0.8 to -0.5), which straddle the Bulk Earth value, are also distinct from those of the Batholith suggesting a different petrogenetic history. The similarity of the εNd_{404} values with those of the rhyolites from the southern suite might suggest an analogous origin.

4:8:3 Petrogenesis of the Leinster Granite Batholith.

A) Evidence for assimilation and fractional crystallisation. The systematic variation of several major and trace elements within the granitoid rocks of the Batholith (Figure 4:16)

Figure 4:22

Calculated lower crustal melts compared with the least evolved magma of the Leinster Granite Batholith and typical rock types from calc alkaline batholiths.

Data sources; Frey et al., 1978
Fourcade and Allegre, 1981

Source of lower crustal melts; Garnet granulite xenoliths from Partan Craig: 30% plagioclase, 55% quartz and kyanite, 15% garnet.

Melting proportions 35 : 40 : 25

Melt A 30% partial melt
Melt B 50% partial melt

Figure 4:22a

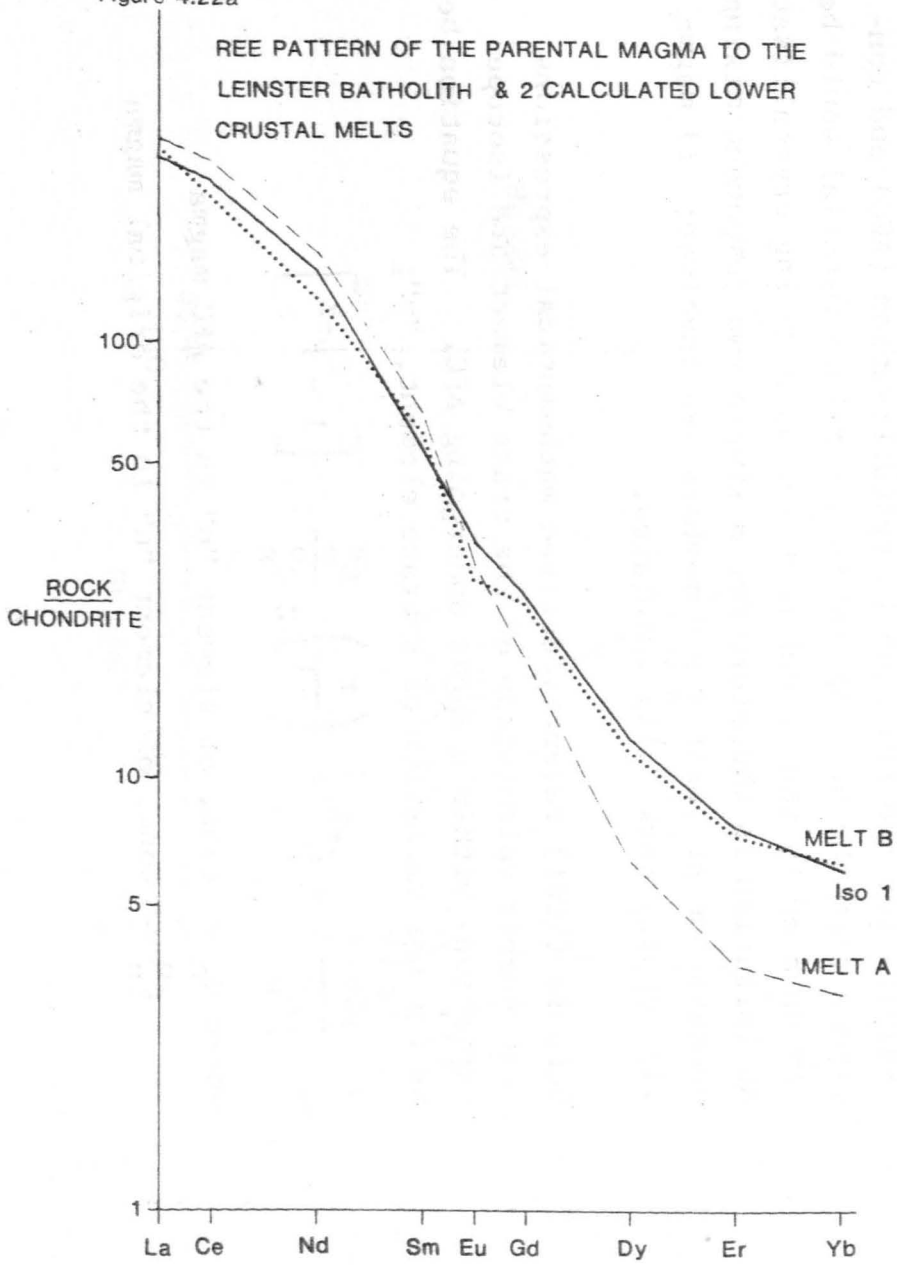

Figure 4:22b REE PATTERNS FOR CALC-ALKALINE BATHOLITHS

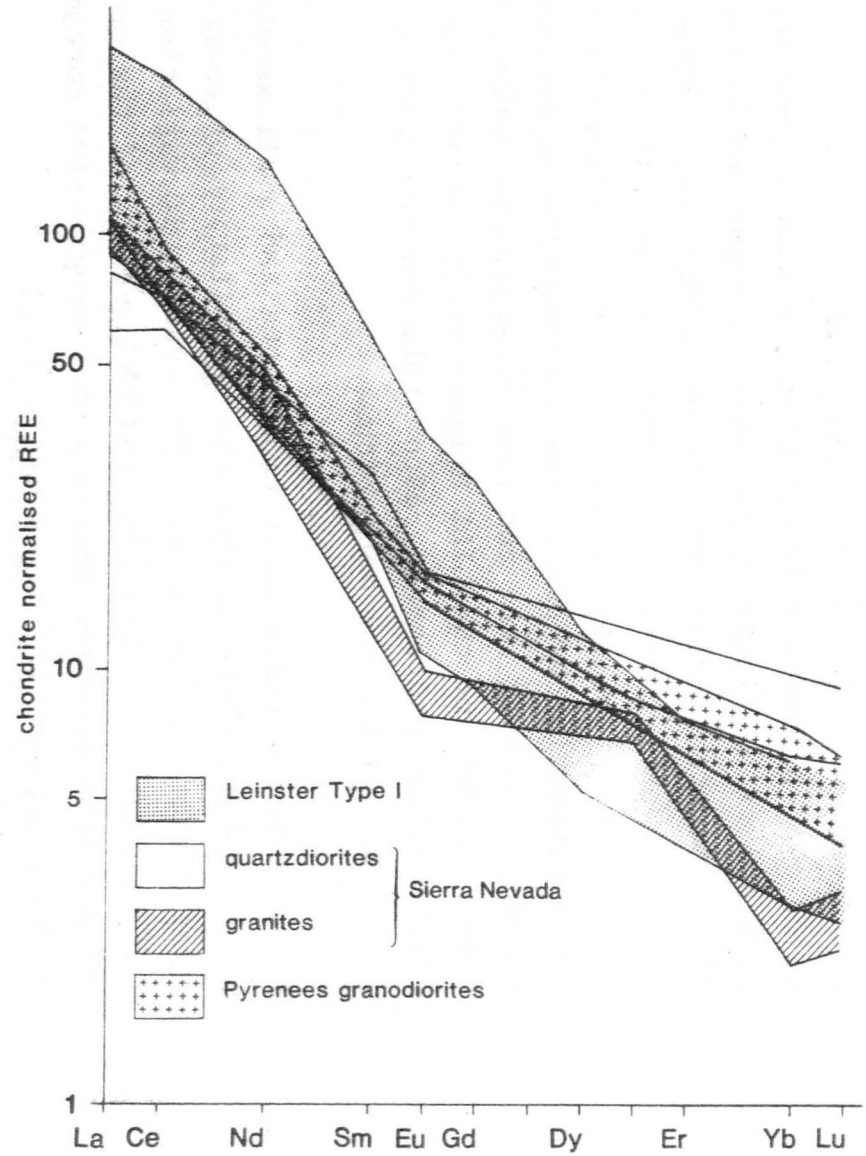

indicates that fractional crystallisation was involved in their petrogenesis. The petrography of the granitoids show that the major phases involved in possible fractional crystallisation were quartz plagioclaze, potassic feldspar and biotite with minor amounts of clinopyroxene and amphibole. Potassic feldspar frequently occurs in a porphyroclastic form. The origin of the porphyroclasts is uncertain, being either by sub-solidus re-equilibration or due to the introduction of metasomatic fluids. However, the coherent relationship between Sr and Zr (Figure 4:20) and the LILE (Figure 4:23) implies that a single fractionation process is responsible for the trace element variations within the batholith.

The presence of large walls rock septa and small xenoliths within the batholith indicate that the assimilation of country rock metasediments has occured. The systematic variation with differentiation of the εSr_{404} and εNd_{404} values of the granitoids (Figure 4:4) strongly suggests that progressive contamination of the fractionating magma has occured.

Bowen (1928) first considered the effects of combined assimilation and fractional crystallisation (AFC) and concluded that the heat needed to assimilate material would be compensated by the latent heat released during crystallisation. Assimilation is therefore not a simple two component mixing process but at least 3 end members are involved; i) magma ii) country rock iii) cumulates.

DePaolo (1981) recently derived mathematical expressions that enable calculation of the trace element and isotope variations within a magma undergoing AFC. The equation below is for the variation of a trace element, "n";

$$\frac{Cn}{C_n^o} = F^{-Z} + \left(\frac{r}{r-1}\right) Z \frac{C_n^a}{C_n^o} \left[1 - F^{-Z}\right]$$

where C_n = conc. of element "n" in the AFC magma

C_n^o = conc. of element "n" in the original magma

Figure 4:23a Ba-Sr VARIATION DIAGRAM

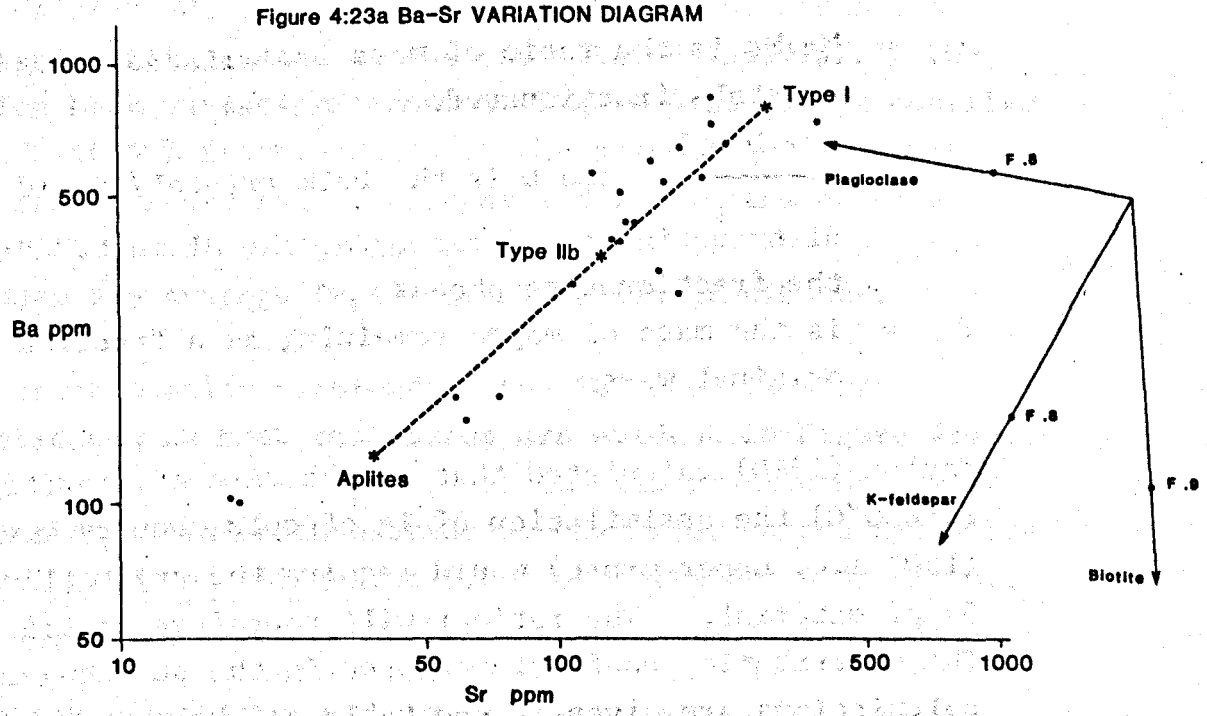

Figure 4:23b Ba- Rb VARIATION DIAGRAM

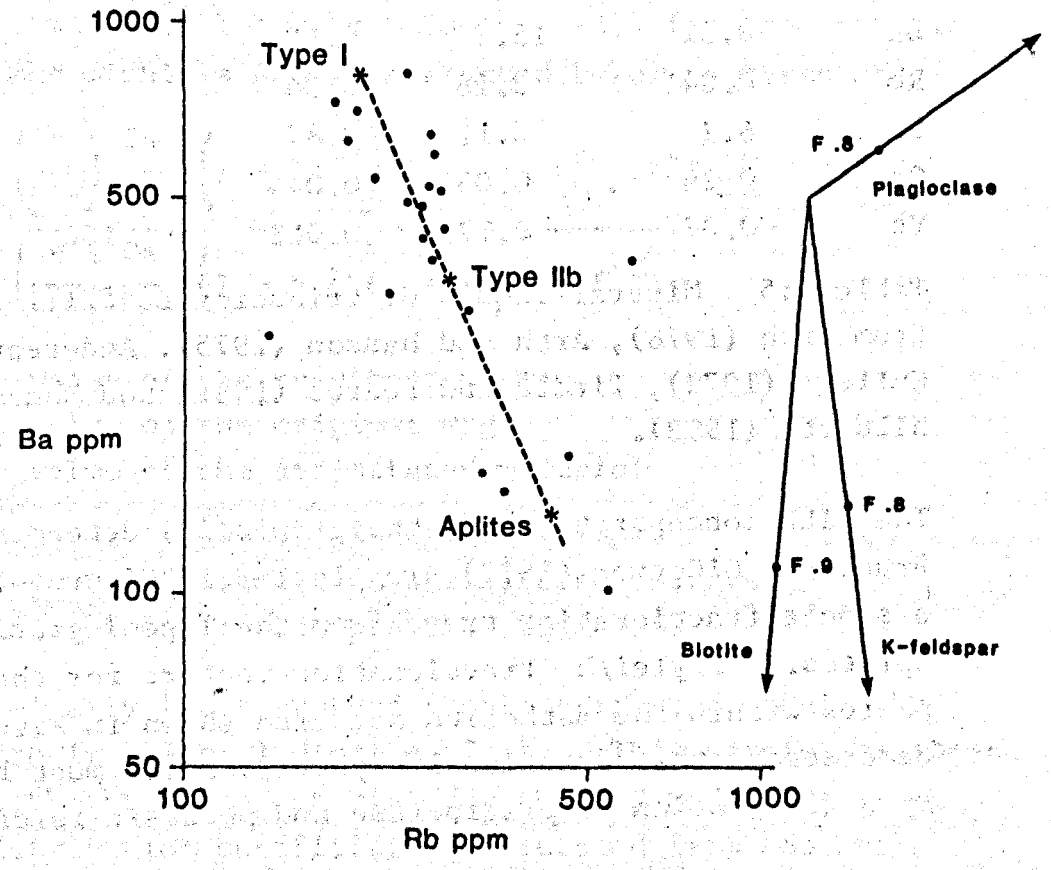

C_n^a = conc. of element "n" in the assimilated material

r = Ma/Mc is the ratio of mass assimilated to mass of crystals fractionated.

$Z = \frac{r + D - 1}{r - 1}$ and D is the bulk crystal/liquid distribution coefficient for the element "n" in the fractionating phases

F = is the mass of magma remaining as a fraction of the original mass.

Taylor (1980) calculated that in the case of granitic magmas ($\simeq 850^{o}C$) the assimilation of 1g of cold country rock (150^{o} i.e. upper crust) would require the crystallisation of 5g of material. The ratio r will therefore be 1:5 i.e. 0.2. The distribution coefficients used in the subsequent calculations are given in the table 4:5 below.

	plagioclase	biotite	K.feldspar	allanite	zircon
Ba	0.31	15.3	6.12		
Rb	0.041	3.26	0.34		
Sr	6.2	0.12	3.87		
Ce	0.24	0.037	0.044	5000	100
Yb	0.077	0.179	0.012	100	1000

Table 4:5 Mineral-liquid distribution coefficients taken from Arth (1976), Arth and Hanson (1975), Anderson and Cullers (1978), Tindle and Pearce (1981) and Mahood and Hildreth (1983).

The LILE concentrations of the granitoids determined by Bruck and O'Connor (1977) are plotted in Figure 4:23 and show a single fractionation trend from the Type I granitoids to the aplites. Rayleigh fractionation vectors for the major phases within the Batholith are also shown in Figure 4:23 and demonstrate that fractional crystallisation must be dominated by a combination of plagioclase and potassic feldspar. In

all subsequent AFC modelling the trace element and isotopic compositions of EIR 5 (a typical shale from south east Ireland) will be used as the assimilated material. The entire LILE variations shown in Figure 4:23 can be modelled by AFC if 60% fractionation of the assemblage 40% quartz, 35% plagioclase, 18% K.feldspar and 7% biotite occurs. Only 40% fractionation is needed to explain the variation between the average Type I and Type IIa granitoids.

The fractionation recorded by the REE data is more complicated in that two trends are evident in Figure 4:24. Trend A encompasses Type I, IIa and IIb granitoids and is modelled by 40% fractionation of the major phases calculated in the LILE modelling plus 0.09% allanite and 0.4% zircon. Trend B, resulting in the formation of the aplites, records extreme L.REE depletion and requires a further 30% fraction of 0.13% allanite and 0.31% zircon. The calculated Eu anomalies in the evolved magmas are equal to those of the aplites.

The equation formulated by DePaolo (1981) for the isotopic variations within a AFC is presented below in terms of

$$m = \frac{\left(\frac{r}{r-1}\right)\frac{Ca}{Z}\left(1 - F^{-Z}\right)\varepsilon_a + C_m^o \cdot F^{-Z}\varepsilon_m^o}{\left(\frac{r}{r-1}\right)\frac{Ca}{Z}\left(1 - F^{-Z}\right) + C_m^o \cdot F^{-Z}}$$

m = value of the resultant magma
m^o = value of the original magma
a = value of the assimilated material
Cm^o = conc. of element in original magma
Ca = conc. of element in assimilated material
Z, F and r are as in the previous equation.

The chemically least evolved sample collected within the Batholith is a Type I diorite, Isol. This sample has been used as the starting material for the AFC modelling along with distribution coefficients calculated from the trace

Figure 4:24 Ce-Yb VARIATION DIAGRAM

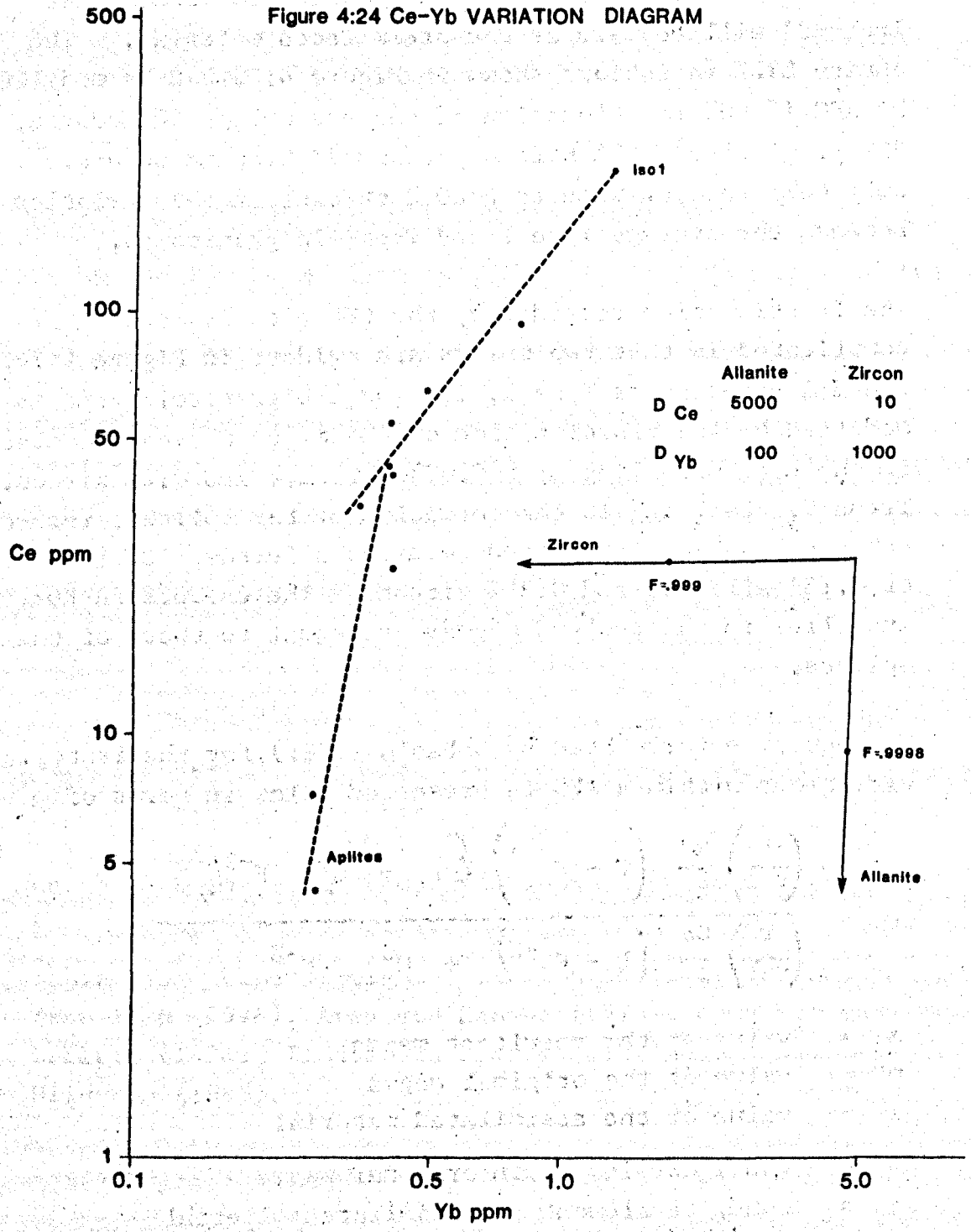

element modelling. The fractionation paths shown in Figure 4:25 demonstrate the influence of varying the D_{Nd} value while keeping D_{Sr} constant. The curves demonstrate that approximately 50% fractionation is required to account for the data with a D_{Nd} value varying between 4 and 6. The slightly greater degree of fractionation compared to the trace element calculations was expected due to the more primitive nature of the starting magma, Iso I, in the isotope calculations, i.e. higher Sr content.

It is therefore concluded that the trace element and isotopic variations within the Leinster Batholith are controlled by the fractional crystallisation of a primary quartz-diorite magma, induced, to some extent, by the assimilation of cold country rock sediments.

The aplite sample Iso 19 is not plotted on the εNd vs εSr diagrams (Figure 4:4 and 4:25) due to the large uncertainty in the initial $^{87}Sr/^{86}Sr$ ratio. This uncertainty is brought about due to the extremely high Rb/Sr ratio, 76.9, in conjunction with the lack of precision in the age determination of the Batholith 404 $\pm$ 24 Ma. If the age used to calculate the initial $^{87}Sr/^{86}Sr$ ratio is in error by 1 Myr then the ratio will be in error by 0.003. The significance of the calculated initial ratio of 0.716 is therefore, dubious.

If the origin of the aplites was as late stage "sweatouts" or partial melts from the granitoids, then the aplites will have εNd_{404} values within the range of rocks from the Batholith (εNd_{404} 1.3 to - 4.5). The less radiogenic εNd_{404} value of Iso 19 (- 5.0) clearly indicates that this is not the case, but that the aplites possibly originated by a continuation of the AFC process.

B) Petrogenesis of Parental Magma to the Leinster Granite Batholith.

If the AFC scheme outlined in the previous section is correct

Figure 4:25 An εSr vs εNd diagram showing the effects of varying D_{Nd} on a magma undergoing assimilation fractional crystallisation (AFC)

(The data plotted are those from the Leinster Granite Batholith) Due to the large error in the $^{87}Sr/^{86}Sr_I$ ratio of the aplite sample only the εNd_I value is plotted.

EIR5, a shale from S.E. Ireland was used in the calculations as the assimilated material (Nd = 31.8 ppm Sr = 155 ppm, $\varepsilon Nd_{404} = -7.9$, $\varepsilon Sr_{404} = +155$). As a result of the straight line relationship shown by the granitoids on the LILE variation diagrams (Figure 2:23) a constant D_{Sr} of 2.88 is used in the isotope AFC calculations. The residual liquid trajectories are marked with F, the fraction of magma remaining. The effect of varying D_{Nd} is clearly shown by the series of curves, which represent between 0.02% and 0.2% allanite fractionation.

Figure 4:25 DIAGRAM SHOWING THE EFFECT OF ASSIMILATION -FRACTIONAL CRYSTALLISATION

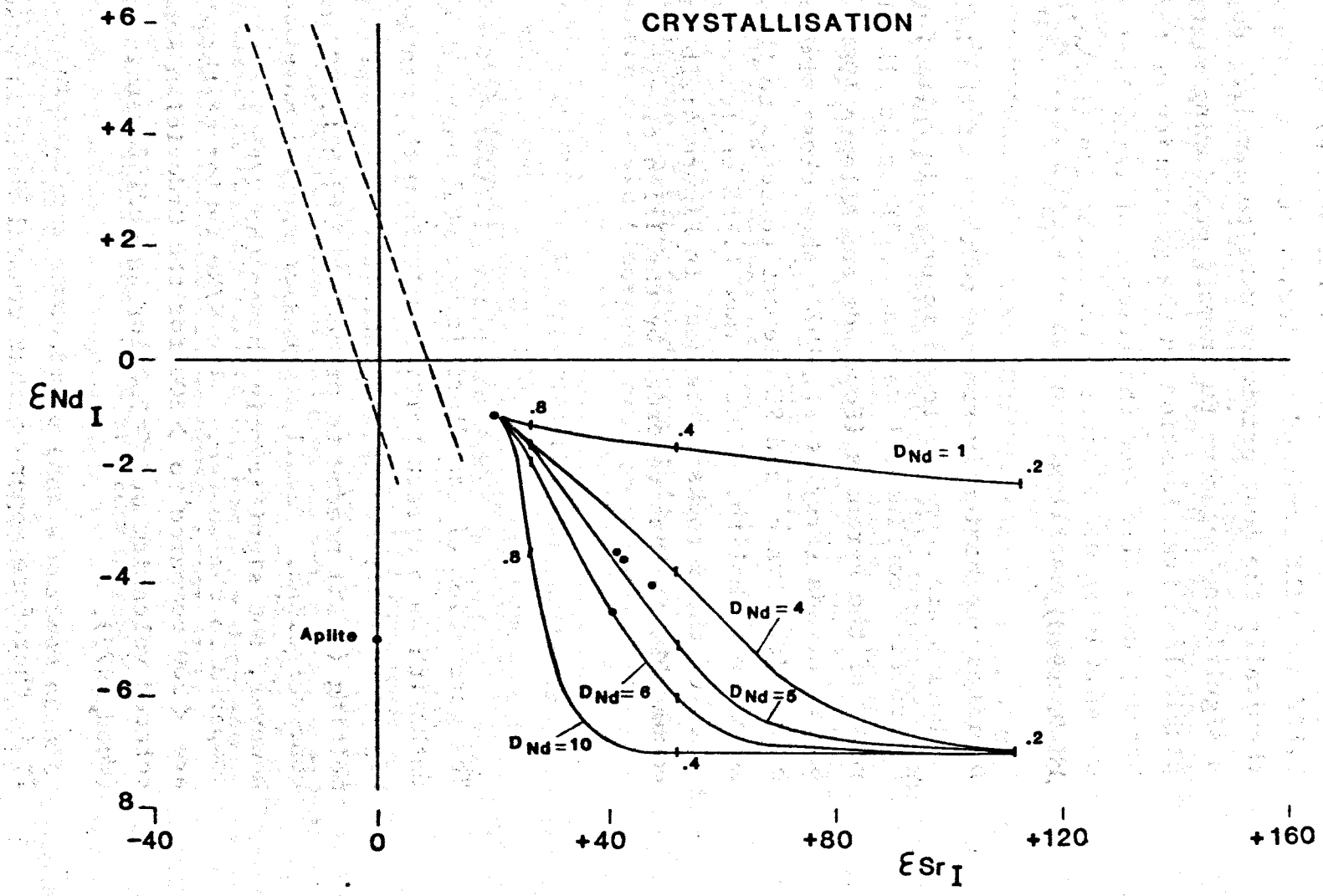

then the parental magma to the Leinster Granite Batholith is L.REE and LILE enriched diorite. It is notable that Iso 1, chemically the most primitive diorite sampled, does not have a significant negative Eu anomaly precluding significant plagioclase fractionation in the generation of the magma. Gravity data also show the absence of large basic/ultrabasic cummulates at depth beneath the Batholith (Locke, unpublished Ph.D. 1980).

Diorites geochemically similar to those of the Leinster Batholith are commonly found in orogenic belts formed at destructive continental margins. The calc alkaline plutonic rocks of the Pyrenees (Fourcade and Allegre, 1981) and the Sierra Nevada (Frey et al., 1978) show close similarities in both major, trace and RE element contents to those of the Leinster Batholith. The marked L.REE enrichment, $(Ce/Yb)_N > 15$, of these rocks is evident in Figure 4:22b and is comparable to that recorded by the Irish diorites (Figure 4:17).

The generation of the dioritic parental magma of the Leinster Batholith as a direct partial melt from the mantle is considered highly unlikely due to the extremely small degree of partial melting ($< 1\%$) needed to produce the high L.REE and LILE concentrations. Small degrees of partial melting would, however, not significantly change the K/Rb ratio of the melt compared to the source. The K/Rb ratios of the diorites are < 200 compared to > 300 for the Ordovician subduction related volcanism and $\simeq 300$ for an undifferentiated mantle (Wood, 1979).

It is therefore apparent that crustal material must provide an important component in the generation of the calc alkaline Leinster Batholith. Fourcade and Allegre (1981) come to the same conclusion for the plutonic rocks of the Pyrenees. The nature and origin of the crustal component can be constrained

from the combined trace element and isotope data. The following points are of significance;

i) Iso 1 has a $(Ce/Yb)_N$ ratio of 38, $(Yb)_N$ = 6.1, εNd_{425} = -1.3, εSr_{425} = +21 and no significant Eu anomaly.

ii) The average values of the basalts of the southern volcanic suite are $(Ce/Yb)_N$ = 1.9, $(Yb)_N$ = 15, εNd_{425} = +2.2, εSr_{425} = +8 and no significant Eu anomaly.

iii) Upper crustal melts have $(Ce/Yb)_N$ ratios of 8, $(Yb)_N$ =30 negative Eu anomalies Eu/Eu* = 0.35 (see Figure 4:21)

iv) Lower crustal melts have high $(Ce/Yb)_N$ ratios of > 20 $(Yb)_N$ = 1-5 and little or no Eu anomaly. The exact values depend upon the amount of garnet and plagioclase within the residue (see Figure 4:22).

v) The εNd and εSr values of crustal melts depend on the age and metamorphic conditions of the crust. There is no evidence of LILE depletion within the crust of southern Britain (Thorpe et al., in press).

From the above points it is apparent that the Leinster Batholith must contain a large lower crustal component to produce the high $(Ce/Yb)_N$ ratio and H.REE depletion. The age of the lower crust in south east Ireland is not well constrained but is likely to be one of i) Mid Proterozoic e.g. Rosslare Complex (εNd_{400} = -10, εSr_{400} = +400) ii) Late Precambrian e.g. Anglesey Complex (εNd_{400} =-5, εSr_{400} = +175) iii) Caledonian, formed by underplating during the Caledonian subduction event (εNd_{400} = +3.4 to -2, εSr_{400} = 0 to +40, depending upon the exact age of the crust, Cambrian to Silurian).
(See chapter 7 for the isotope data of crustal rocks).

Mass balance calculations demonstrate that a maximum of 30% mantle derived material can be involved in the petrogenesis of the Batholith if the crustal component is melt A shown in Figure 4:22a. Melt A is, however, of an extreme composition, REE pattern equivalent to that of Iso 1 can be produced purely from the lower crust (Figure 4:22a). If the mantle component

mixed with melt A has an εNd value of + 3.5 (most radiogenic found within the southern suite) then the crustal component has a εNd_{400} value of - 3.3. This crustal component would have a T_{CHUR} age of 720 Ma. Even if a more depleted mantle source is considered, (i.e. using the depleted mantle model of DePaolo 1981b $\varepsilon Nd + 7$) the curstal component would only have a maximum T_{CHUR} age of 900 Ma i.e. $\varepsilon Nd_{400} = - 5$. The above modelling therefore indicates that the Leinster Batholith is predominantly produced from relatively juvenile crust similar, or younger, than the Anglesey Complex ($\varepsilon Nd_{400} = - 5$). The maximum mantle component is 30% but a purely crustal origin is not ruled out. In the latter case the εNd_{400} value of the crust would be - 1.3 and would have a T_{CHUR} age of 525 Ma The maximum T_{CHUR} age of the crustal component is 720 Ma. It can therefore be concluded that upper crustal sediments and Mid Proterozoic basement (Rosslare Complex) are not involved in the petrogenesis of the Leinster Batholith.

The model invoked to explain the petrogenesis of the parental magma to the Leinster Batholith is one in which subduction related volcanism, during the Late Precambrian and Lower Palaeozoic, causes a gradual thickening of the crust. The period of igneous activity is in the order of 200 Ma, comparable to the evolution of the Andes. The thickened crust will make it more difficult for volcanism to reach the surface. In addition to heat supplied by possible trapped igneous rocks, the isotherms will rise due to radioactive decay within the thickened crust (England, 1978). The Leinster Granite Batholith forms by regional melting of a relatively juvenile lower crust possibly caused by the introduction of a mantle derived magma.

Chapter 5

Metamorphic Age of the North East Ox Mountains

5:1 Introduction

Plate tectonic reconstructions of northern Europe and America indicate that the Grenvillian and Caledonian orogenic belts intersect in north west Britain. However, the possible presence of significant Grenvillian aged basement is obscured by Caledonian sedimentation and the effects of Caledonian metamorphic over-printing. van Breeman et al. (1978), demonstrated the existence of Grenvillian aged gneissose rocks in the Annagh Gneiss Complex of north west Ireland (Figure 5:1). The relationship between the rock types of the Ox Mountains inlier and their relationship to the remainder of the orthotectonic Caledonides has been the subject of considerable recent debate, particularly as to whether the inlier comprises mainly pre-Caledonian basement (Andrews et al., 1978) or Dalradian rocks (Long and Max, 1977). Detailed mapping has shown that the granulite facies metamorphism is restricted to the north east Ox (Figure 5:1) and this region is considered by all recent authors to represent pre-Caledonian basement (Phillips et al., 1975, Sanders, 1979, Yardley et al., 1979). The interpretation of the main Ox Mountains sequence of metasediments remains enigmatic.

The aim of this study is to constrain the formation age of the pre-Caledonian rocks of the north east Ox and to date the granulite facies metamorphism from a Nd isotope study of garnet-pyroxenite bodies found within the north east Ox.

5:2 General Geology

The Ox Mountains inlier of north west Ireland comprises five major rock units (Figure 5:1);

i) Granulite facies metasediments of the north east Ox Mountains are predominantly psammitic paragneisses with subordinate semipelites and rare marbles containing minor garnet pyroxenites and serpentinites (Lemon, 1971). On the basis of coexisting kyanite and microperthite, Phillips et al.

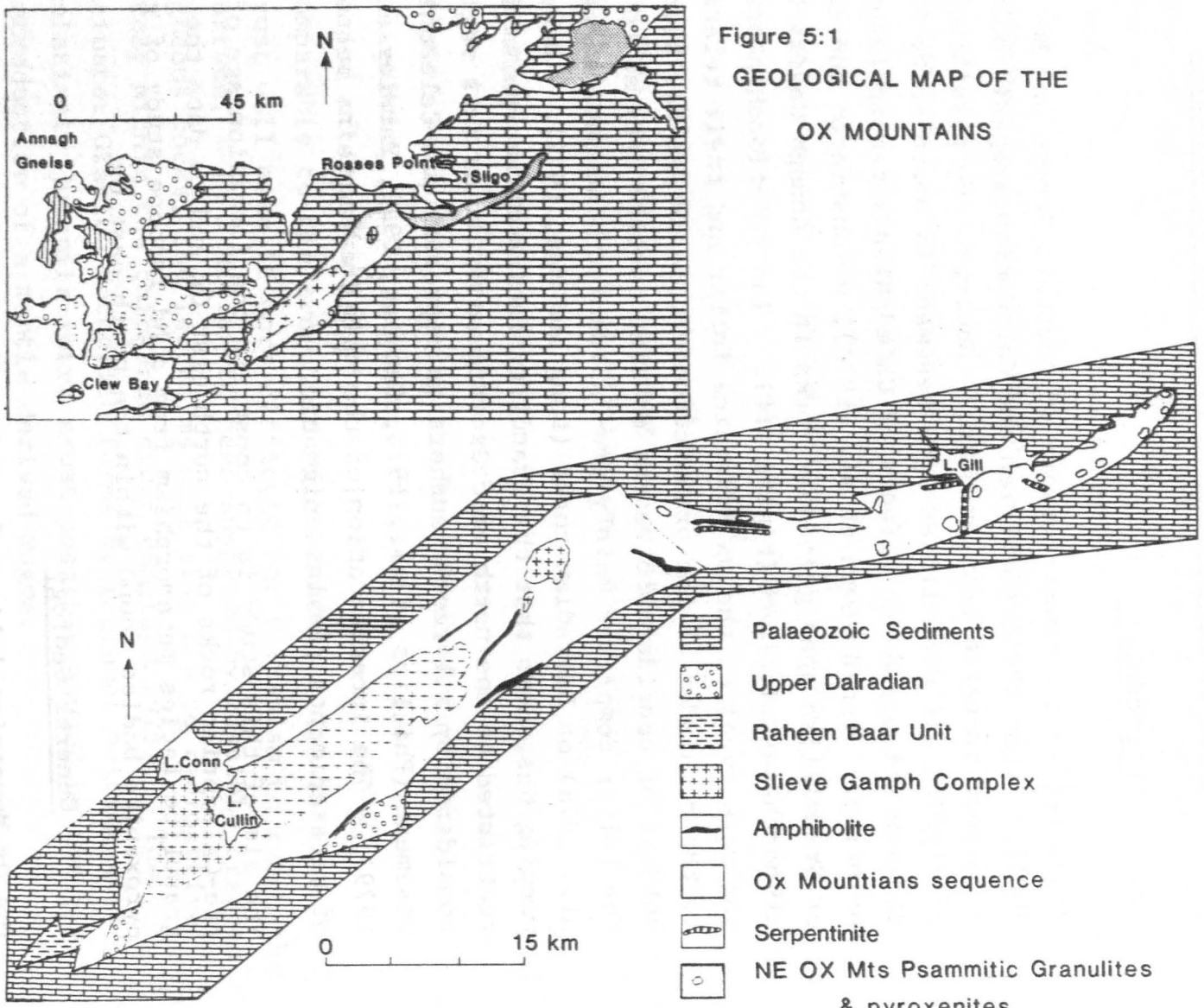

Figure 5:1

GEOLOGICAL MAP OF THE

OX MOUNTAINS

(1975) estimated that the minimum P-T conditions of the granulite facies metamorphism at 10 kb and 800°C. Similar granulite facies rocks occur at the Rosses Point and Lough Derg inliers (Lemon, 1952, Church, 1969) (Figure 5:1).

ii) The Ox Mountain sequence of metasediments comprises the central and south-western part of the inlier (Phillips et al., 1975, Long and Max, 1977, Yardley et al., 1979). Metamorphism reaches amphibolite facies with staurolite or staurolite and kyanite developed in pelites of appropriate composition. The sediments record polyphase deformation.

iii) The Slieve Gamph igneous complex is a syn-kinematic granitoid body approximately 25 km long and 5 km wide that intrudes the Ox Mountain sequence of metasediments, cross-cutting F_3 folds (Currall and Taylor, 1965, Pankhurst et al., 1977). The igneous complex is made up of multiple intrusions of tonalite, granodiorite, adamellite and pegmatite. The complex has suffered 2 phases of deformation.

iv) In the south west of the inlier the Raheen Barr succession of metasediments also record polyphase deformation and regional metamorphism up to garnet grade.

v) Two areas of very low grade proximal turbidite metasediments occur near the south east side of the inlier. A tectonic contact separates these Upper Dalradian rocks from the remainder of the complex.

5:3 Samples

Garnet pyroxenite samples from the Lough Gill area (Figure 5:1) were supplied by I. Sanders. Rocks from this region were analysed because the retrogression of granulite facies rocks to an epidote amphibolite facies assemblage, common elsewhere, is rare in the Lough Gill area. From a detailed microprobe study of the garnet-pyroxenites Sanders et al. (1982) report maximum P-T conditions of 11 ± 2 kb and 850 ± 50°C followed by cooling

from the sillimanite to the kyanite stability field. Energy dispersive microprobe analyses at the Open University have shown that inclusions within the garnets of these rocks are sulphides, oxides, sphene and rutile. These phases are unlikely to be L.REE enriched and the garnets are therefore liable to have a high Sm/Nd ratio favourable for dating.

Several garnet-pyroxenite outcrops show mineralogical banding on a 10 to 20 cm scale. Eight 1 inch diameter drill core samples were taken from one such outcrop (79-3) with the aim of providing a whole rock isochron suite. All the remaining samples were 2 kg or greater.

Representative major and trace element analyses of the garnet-pyroxenites are given in Table 5.1 and demonstrate their tholeiitic nature. The samples are trace element enriched compared to "typical" MORB but to variable degrees. Significant trace element variations are shown between the drill core samples suggesting heterogeneity on a 10 centimetre scale. The variations do not show any simple correlation with the mineralogical banding.

Mineral separates were taken from Ox 27 a plagioclase-garnet-pyroxenite due to the relatively large abundance of plagioclase >15%.

A single granulite facies metasediment Ox 79 from the north east Ox was analysed to place some constraints on the depositional age of the north east Ox metasediments.

5:4 Nd Isotope Data

The results of the Nd isotope analyses are presented in Table 5.2 and plotted in Figure 5:2. The garnet-pyroxenite whole rock samples have a narrow range in Sm/Nd ratios, 0.235 to 0.272 with a large range in $^{143}Nd/^{144}Nd$ ratios, 0.51200 to 0.51273. The mineral separates show a significantly greater

Table 5:1 Major and Trace Element analyses of Ox Mountains Garnet-Pyroxenites

	4/79-3/2	4/79-3/5	4/79-9	4/79-13	4/79-14	OX 27
SiO_2	49.6	48.2	43.7	47.6	51.2	52.7
TiO_2	0.55	0.64	1.0	1.49	1.3	1.52
Al_2O_3	9.7	10.4	12.2	13.6	13.6	15.4
Fe_2O_3	7.2	7.7	8.7	13.8	11.6	12.4
MnO	0.15	0.16	0.20	0.21	0.15	0.21
MgO	12.5	11.2	11.2	9.3	6.5	6.5
CaO	17.7	17.7	15.8	12.4	10.6	11.5
Na_2O	0.9	0.3	0.4	1.5	0.84	3.6
K_2O	0.38	0.43	0.44	0.71	0.57	0.85
Cr	152	197	404	211	240	146
Ni	29	44	58	92	132	49
V	142	139	166	307	214	293
Rb	2.2	2.2	5.7	24.1	5.2	15.9
Sr	163.3	151.5	146.4	97.7	90.3	99.4
Ba	32	50	118	220	212	297
Zr	162	154	120	169	119	117
Y	25	28	32	45	27	31
Nb	13	11	22	24	15	13
Ce	32	34	121	69	31	40

Major element analyses by Steve Daly (Dublin).
Trace element analyses at Nottingham.

Table 5:2 Nd isotope results for the Ox Mountains

Sample		Sm	Nd	Sm/Nd	$^{143}Nd/^{144}Nd$	T^{Nd}_{CHUR} Ma
Ox 27	whole-rock	8.749	32.14	0.2722	0.512727 ± 18	
Ox 27	garnet	1.53	1.638	0.9341	0.514321 ± 34	
Ox 27	clinopyroxene	6.833	26.61	0.2568	0.512662 ± 16	
Ox 27	plagioclase	0.2566	1.6900	0.1518	0.512460 ± 22	
4/79-3-2	drill-core	2.879	12.276	0.2345	0.512141 ± 20	1385
4/79-3-3	drill-core	4.321	18.101	0.2387	0.512382 ± 20	750
		4.503	18.880	0.2385		
4/79-3-5	drill-core	3.438	14.016	0.2453	0.512130 ± 22	1610
4/79-3-8	drill-core	2.022	8.475	0.2386	0.511997 ± 26	1865
		2.063	8.734	0.2382		
Ox 79	sediment	3.513	19.84	0.1771	0.511955 ± 12	1165

Figure 5:2 Nd ISOCHRON DIAGRAM FOR THE OX MOUNTAINS GARNET-PYROXENITES

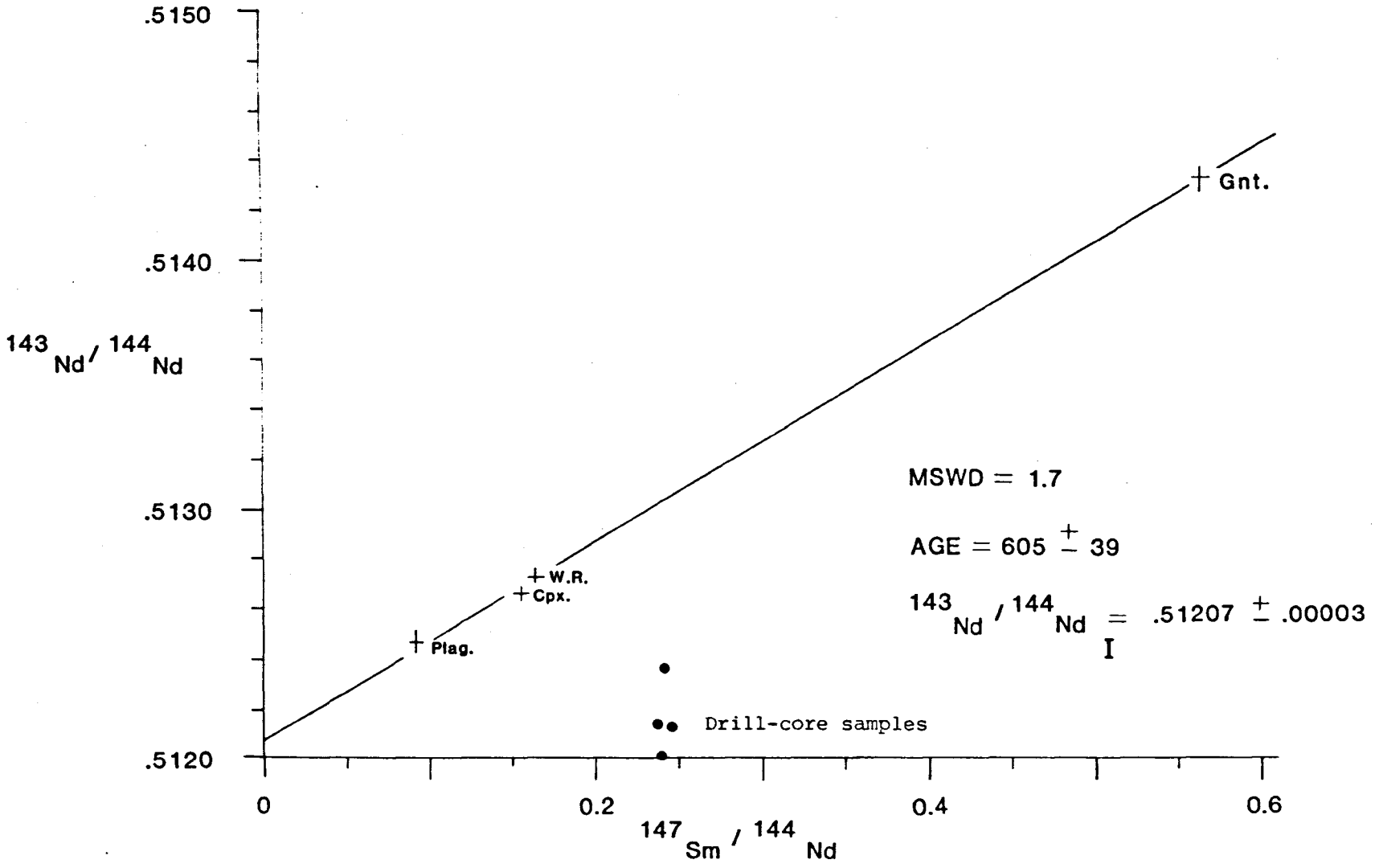

range in both Sm/Nd and $^{143}Nd/^{144}Nd$ ratios, 0.152 to 0.934 and 0.51246 to 0.51432 respectively.

The metasediment Ox 79 has the lowest whole rock Sm/Nd ratio 0.177, and the least radiogenic $^{143}Nd/^{144}Nd$ ratio, 0.51196.

5:5 Discussion

5:5:1 North East Ox Metasediment. The Sm/Nd ratio of Ox 79 (0.177) lies within the range of typical sediments (see Chapter 7) being more L.REE enriched compared to the average crustal value of 0.19 (McCulloch and Wasserberg, 1978). The T_{CHUR} Nd model age of Ox 79 is 1170 $\pm$ 20 Ma and represents the average model age of the sediments' source region. Therefore although the Nd model age has no direct age significance, it does rule out derivation from a predominantly Archean source region. O'Nions et al. (1983) have shown that Precambrian and Lower Palaeozoic sediments formed in northern Britain contain a significant Archean component such that their Nd model ages are greater than their formation ages (see also Chapter7). However, the T_{CHUR} ages of the Dalradian (2500 to 1500 Ma), Torridonian (2100 to 1500), Moinian (circa 1450 Ma) and Lower Palaeozoic sediments (1450 to 600 Ma) are well constrained (O'Nions et al., 1983, van Breemen and Hawkesworth, 1980, and Chapter 7). It should therefore be possible to use the Nd model age of a sediment as a crude geological tracer in northern Britain. The 1170 $\pm$ 20 Ma model age of the north east Ox Mountain metasediment is most comparable with those of the Lower Palaeozoic sediments. The Ox Mountains inlier is, however, uncomformably overlain by Upper Dalradian sediments and must be of Precambrian age. It is therefore concluded that the north east Ox Mountains inlier most likely formed in Late Precambrian times, probably as Lower Dalradian sediments significantly post 1000 Ma.

5:5:2 Garnet-Pyroxenites. The 4 drill core samples do not provide an isochron relationship (Figure 5:2). The data therefore indicate that 10 cm scale Nd isotope disequilibrium exists over a $2m^2$ sized outcrop in these granulite facies rocks.

It is concluded that the 1 inch diameter core samples are not sufficiently large to be used for whole rock Nd isotope age determinations.

The Nd isotope data for the mineral separates show an isochronous relationship equivalent to an age of 605 $\pm$ 37 Ma (Figure 5:3). The scatter in the data (M.S.W.D. = 1.7) is just outside analytical error. The initial $^{143}Nd/^{144}Nd$ ratio of 0.51207 $\pm$ 0.00003 is equivalent to an εNd_I value of + 4.1 $\pm$ 0.5.

The L.REE enriched nature of the garnet pyroxenite Ox 27 (Sm/Nd = 0.27) along with the depleted initial ratio (εNd_I = + 4.1 $\pm$ 0.5) indicates that the rock was derived from a depleted mantle source. The T_{DM} model age of Ox 27 provides a maximum possible mantle derivation age for the rock (900 $\pm$ 30 Ma) (see Chapter 1 for explanation). However, the trace element enriched nature of this tholeiitic rock argues for derivation from a source region less depleted than that of MORB, probably more equivalent to that of present day intra plate volcanism. The 900 $\pm$ 30 Ma depleted mantle derivation age is therefore probably an over estimate.

The mineral isochron records the closure of the Sm/Nd system of the rock at some stage during its cooling history subsequent to the peak of granulite facies metamorphism. The slope on the isochron diagram is predominantly controlled by the garnet analysis. The relationship of the cooling age to the peak of granulite facies metamorphism therefore depends upon the period of time needed for the garnet to reach its blocking temperature.

From their study of Scourian basic granulites, Humphries and Cliff (1982) established that a 170 Myr gap existed between the peak of granulite facies metamorphism and the closure of the Sm/Nd mineral system. The inferred cooling rate for the Scourian is extremely slow, 1 to 2^{o}C/Myr. However, in Ireland relatively rapid uplift of the Ox Mountains, Lough Derg and

Central Tyrone inliers is inferred by the presence of granulite facies detritus in Middle and Upper Dalradian sediments (Phillips et al., 1976). The rocks were therefore unroofed prior to 550 Ma i.e. within approximately 50 Myr of the closure of the Sm-Nd mineral system. Humphries and Cliff (1982) calculated that the blocking temperature for Scourian garnets ($Alm_{1.6}$ $Pyr_{0.9}$ $Gross_{0.5}$) were in the order of 600°C. Assuming an equivalent blocking temperature and constant cooling rate, a cooling rate of 12°C/Myr is inferred for the north east Ox Mountains. This value is in the order of that found subsequent to regional metamorphism. (Hart, 1981).

Dodson (1976) derived an expression which enables theoretical blocking temperatures for a mineral to be calculated. The blocking temperature is dependant upon the diffusion coefficient and cooling rate. Experimentally determined diffusion coefficients are only available for Sm in grossular and pyrope at temperatures between 1100 and 1500°C (Harrison and Wood, 1980). For these data to be applied to the Nd isotope systematics three assumptions must be made;

i) the diffusion of Nd and Sm are comparable.
ii) extrapolation of the experimental data to a geological situation using the Arrhenius equation is valid
iii) the difference in diffusion coefficients between pure pyrope and grossular encompass the value of the dated garnet ($Alm_{1.3}$ $Pyr_{1.0}$ $Gross_{0.7}$)

The calculated closure temperatures for the Ox Mountains garnet pyroxenite are given in Table 5:3

Table 5:3 Calculated Garnet Closure Temperatures

Mineral	T^+	T^*
Pyrope	550°C	480°C
Grossular	750°C	700°C

$^+$ cooling rate 12°C Myr^{-1} * cooling rate 5°C Myr^{-1}. Humphries and Cliff(1982)

The calculated garnet closure temperatures in this work are 50 to 70°C higher than those of Humphries and Cliff (1982) due to; i) the coarser grain size of the Ox Mountain garnet-pyroxenite compared to the Scourian granulites (5 mm cfd. 2.5 mm) and
ii) a higher estimated cooling rate.

The blocking temperature for the garnet from the Ox garnet-pyroxenites is most likely to be 650°C i.e. 200°C below the peak of granulite facies metamorphism. If the entire cooling history of Ox 27 is constant, then the peak of metamorphism occurred less than 20 Myr prior to the Sm-Nd closure temperature i.e. circa 625 Ma.

5:6 Conclusion

It is concluded that the mineral isochron of the plagioclase-garnet-pyroxenite Ox 27 records the closure of the Sm-Nd system circa 650°C, at 605 Ma, probably 20 M. subsequent to the peak of granulite facies metamorphism. The T_{DM} model age of Ox 27 indicates a maximum mantle derivation age of 900 Ma but does not rule out the original intrusion of the tholeiitic magma into the north east Ox Mountains metasediments during the peak of granulite facies metamorphism at circa 625 Ma.

The Nd model age of the north east Ox Mountains metasediment Ox 79 is most comparable with the Lower Palaeozoic metasediments of northern Britain. However, the sediments are Precambrian and it is therefore probable that they were deposited during the Late Precambrian, significantly post 1000 Ma. It is therefore apparent that the north east Ox Mountains sequence of metasediments were formed, buried to approximately 30 km (10kb), metamorphosed and subsequently uplifted within a short time span, probably less than 100 Ma. These data therefore provide evidence for orogenesis occuring in northern Britain during the late Precambrian and suggest that subduction related processes associated with a well established Iapetus Ocean were occuring.

Chapter 6

Lower Crustal Xenoliths from Northern Britain

6:1 Introduction

Mantle and crustal xenoliths are found in Carboniferous volcanic rocks at several localities in the Britihs Isles (Figure 6:1). This chapter presents REE and isotopic results on lower crustal xenoliths from County Westmeath (Ireland), Partan Craig (North Berwick) and Hawks Nib (South Bute), and compares the age and nature of the lower crust in these areas with the granulite facies rocks of the Lewisian. The data are discussed in the context of models for the tectonic evolution of northern Britain and of lower crustal involvement in the genesis of the Caledonian granites.

6:2 Rock Types

The presence of tectonised peridotite xenoliths within the lavas and tuff rings at the above localities is evidence for rapid transport of material through the crust. The crustal lithologies range from gabbroic to granitic and trondhjemitic gneisses, but the majority are undeformed sediments of Carboniferous and Devonian age.

Samples from Central Ireland were supplied by P. Strogen and M.D. Max. B.G.J. Upton and P. Aspen provided the xenoliths from the Midland Valley. Petrological descriptions of the analysed samples are given in Appendix A. The more significant points of the different rock-types are outlined below.

6:2:1 Partan Craig. The granulite facies xenoliths from Partan Craig occur in Carboniferous vent agglomerates and can be divided into 3 petrographic groups (Graham and Upton, 1978, Upton et al., 1982):-

a) Pyroxene Granulites; The pyroxene granulites are composed predominantly of plagioclase with variable amounts of quartz

Figure 6:1

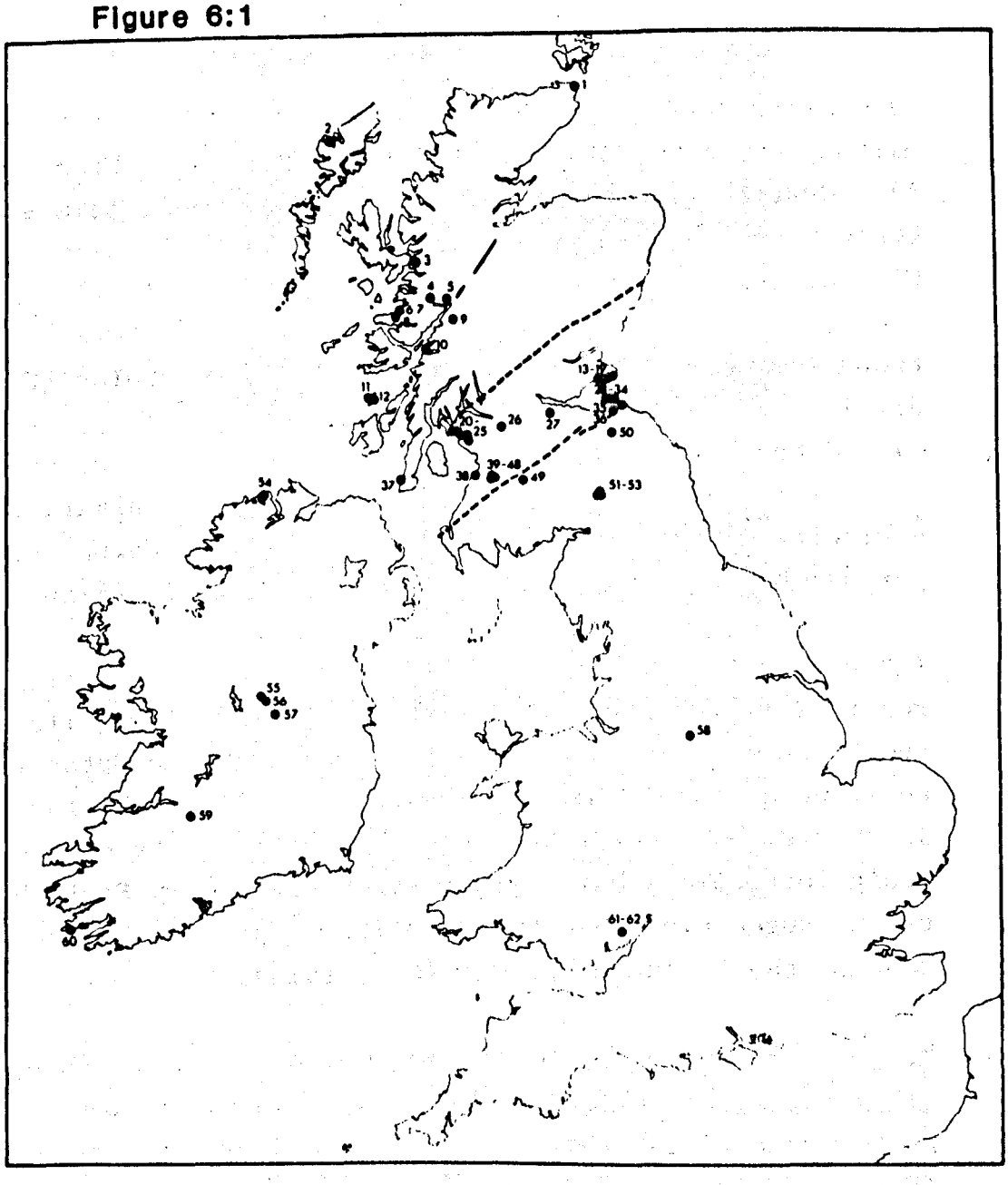

Sketch map indicating principal localities of inclusion-bearing alkali basalts in the British Isles.
1, Duncansby Ness; 2, Loch Roag; 3, Eilean Donan; 4, Streap Comlaidh; 5, Stob a'Ghrianain; 6, Eilean Shona; 7, Riska; 8, Camas an Lighe; 9, Coire na Ba; 10, Ardmucknish; 11, Kilchatten; 12, Riasg Buidhe; 13, Kellie Law; 14, Ruddon's Point; 15, Elie Ness–Lady's Tower, Ardross; 17, Wadeslea; 18, Coalyard Hill; 19, Newark; 20, Hawk's Nib; 21, Great Cumbrae; 22, Black Rocks, Fairlie; 23, Hunterston; 24, Holmbyre; 25, Baidland Hill; 26, Barrhead; 27, Bathgate Hills; 28, Weak Law; 29, Fidra–Briggs o'Fidra; 30, Partan Craig; 31, Car Rocks; 32, Seacliff; 33, Beggar's Cap; 34, Kidlaw; 35, Dunbar; 36, Chesters; 37, Macrihanish; 38, Heads of Ayr; 39, River Doon; 40, Meikleholm Glen; 41, Carskeoch; 42, Patna Hill; 43, Carnochan; 44, Kirklafinn; 45, Keirs Hill; 46, Green Hill; 47, Ashentree Glen; 48, Dunaskin Glen; 49, Sanquhar; 50, Earnscleugh; 51, Black Rock–Rough Gill; 52, Cooms Fell (Strait Hill); 53, Hog Fell; 54, Inishowen; 55, Dungolman River; 56, Clare Castle; 57, Croghan; 58, Calton Hill; 59, Upper Lavas, Limerick; 60, Black Ball Head; 61, Great House; 62, Glen Court. (N.B. No's 39–48 incl. are representative localities within the Patna–Dalmellington area).

and clinopyroxene. They have an equigranular texture but display distinct mineralogical banding (Figure 6:2a).

b) Quartzo feldspathic Granulites; As their name suggests these xenoliths are predominantly composed of quartz and plagioclase with subordinate amounts of alkali feldspar and biotite. Mineralogically the rocks are therefore trondhjemites. The texture is again equigranular (Figure 6:2b).

c) Garnet Granulites; The typical assemblage of the garnet granulites is garnet + plagioclase + quartz $\pm$ alkali feldspar $\pm$ biotite $\pm$ kyanite with accessory rutile. Garnet occurs as porphyroblasts in a weakly foliated groundmass (Figure 6:2c).

Interestingly similar garnetiferous gneissose xenoliths are reported in several parts of the Midland Valley (Wilson, 1918 and Upton et al., 1982). This led Graham and Upton (1978) to infer a similar basement beneath the entire Midland Valley. It should, however, be noted that the proximity of the Partan Craig locality to the Southern Upland Boundary Fault has led to the suggestion that the xenoliths represent basement from beneath the Southern Uplands (Max, 1976).

Microprobe studies on the Partan Craig xenoliths suggest that all three lithologies have undergone granulite facies metamorphism with P-T conditions exceeding 11 kb and 850°C (Graham and Upton, 1978).

6:2:2 County Westmeath. Garnet granulites petrographically similar to those of the Midland Valley are found in the Carboniferous vent agglomerates of County Westmeath. The samples are taken from 2 localities approximately 6 miles apart. When compared with the Midland Valley garnet granulites the only significant petrological difference is the presence of sillimanite instead of kyanite (Figure 6:3). This indicates that the Irish xenoliths last equilibrated at relatively higher T - lower P conditions than the granulites from the Midland Valley.

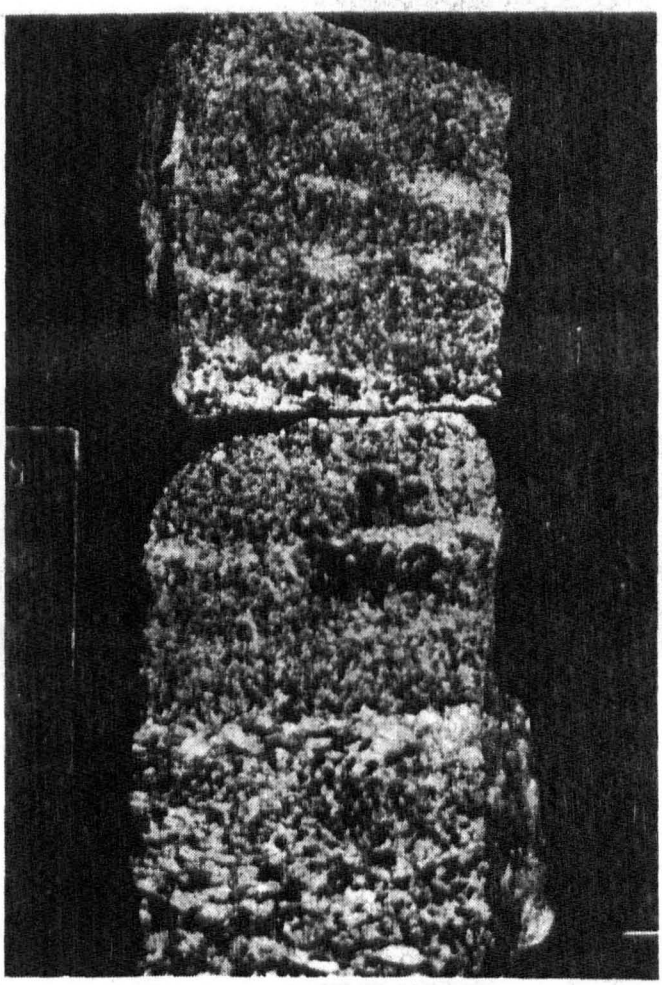

Figure 6:2a Pyroxene granulite PC 342; Partan Craig

Figure 6:2b Quartzo feldspathic granulite PC 368; Partan Craig

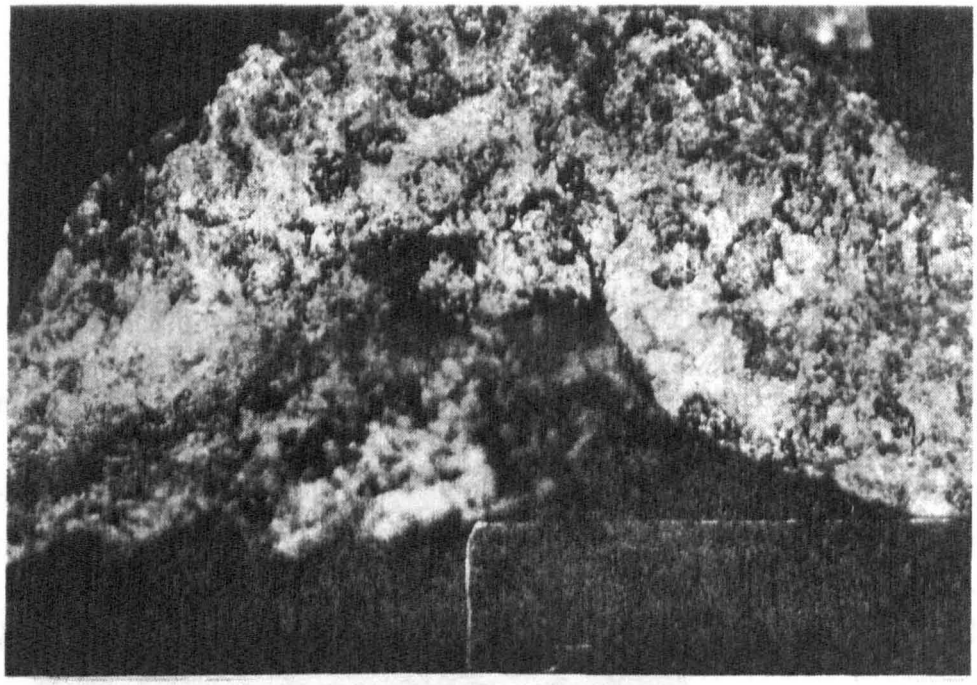

Figure 6:2c Garnet granulite PC 374; Partan Craig

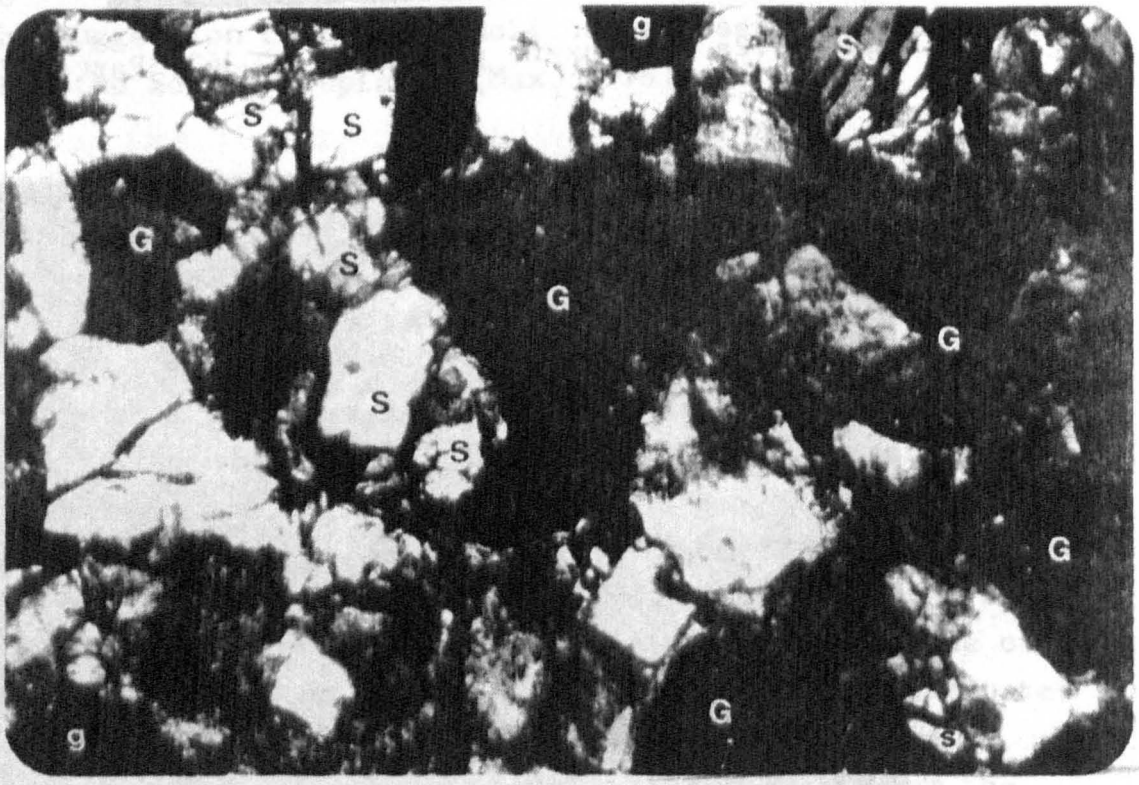

Figure 6:3 Photomicrograph of agarnet granulite from Clare Castle,Co. Westmeath

Field of view = 12 mm. Rutile,dark brown ,quartz , altered orthoclase, G-garnet, S- sillimanite.

6:2:3 Hawks Nib. The basic granulites of Hawks Nib occur in a Carboniferous lava flow and show a large petrological range from dunite, basic granulite (orthopyroxene + clinopyroxene + plagioclase) to olivine gabbro. The rocks have an equigranular texture. The high Al_2O_3 contents recorded by both augites (8 to 11 wt. %) and orthopyroxenes indicate formation at relatively high pressures (5 to 10 Kb) (Upton pers. com.).

6:3 Rb-Sr and REE variations

In the following sections REE and Rb-Sr data will be presented for representative xenoliths from each of the 3 localities and used in conjunction with available major and trace element data to constrain possible precursors to the granulite xenoliths and to compare their chemistry with typical rocks from the Lewisian lower crustal terrain. To date major and trace element data are only available on the Partan Craig xenoliths (Graham and Upton, 1978, Upton pers. com.) (see Tables 6:1, 6:3 and 6:4). REE data for 12 xenoliths are presented in Table 6:2 and as chondrite normalised patterns in Figures 6:4 and 6:5. Rb-Sr data are given in Table 6:5 along with the Nd and Sr isotope data.

6:3:1 Garnet Granulites. The garnet granulites from Partan Craig have moderate to high L.REE contents, $(Ce)_N$ of 60 to 140, flat H.REE, $(Yb)_N$ of 6.2 to 10.1, and show marked L.REE enrichment, $(Ce/Yb)_N$ ratio of 9.7 to 15.9 (Figure 6:4a). The three samples analysed have negative Eu anomalies Eu/Eu* = 0.9. These results are slightly different from those reported by van Breeman and Hawkesworth (1980) on a similar garnet granulite which had higher H.REE contents, $(Yb)_N$ of 12 and a positive Eu anomaly, Eu/Eu* of 1.2.

The REE patterns of the petrologically similar garnet granulites from central Ireland show equivalent L.REE enrichment, $(Ce/Yb)_N$ ratios of 7.2 to 11.4, but have higher average REE abundances, $(Ce)_N$ of 180 and $(Yb)_N$ of 19.7 (Figure 6:5a). Although variable, the negative Eu anomalies are more pronounced

Figures 6:4 and 6:5

REE patterns for the lower crustal granulite xenoliths from the Midland Valley of Scotland

4a) Garnet Granulites from Central Ireland

4b) Pyroxene (342) and Quartzo feldspathic (369, 378) granulite xenoliths from Partan Craig

4c) REE patterns from Lewisian tonalites and trondhjemites (Weaver and Tarnley, 1980, 1981) (solid line granulite facies, dashed line amphibolite facies). Also shown is the field of melts extracted from Quartz Diorites within the Loch Doon Pluton (Tindle, 1982).

5a) Garnet Granulites from Partan Craig; note lower H.REE contents and less pronounced Eu anomaly compared to Figure 4a.

5b) Basic Granulites from Hawk's Nib.

Figure 6:4a

CENTRAL IRELAND :-GARNET GRANULITES

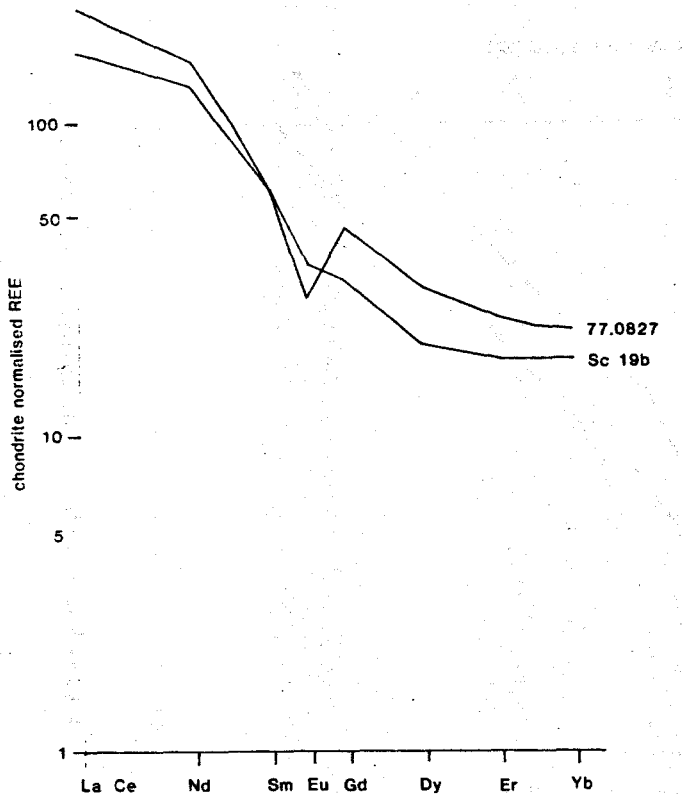

Figure 6:4b PARTAN CRAIG :- PYROXENE & QUARTZOFELDSPATHIC GRANULITES

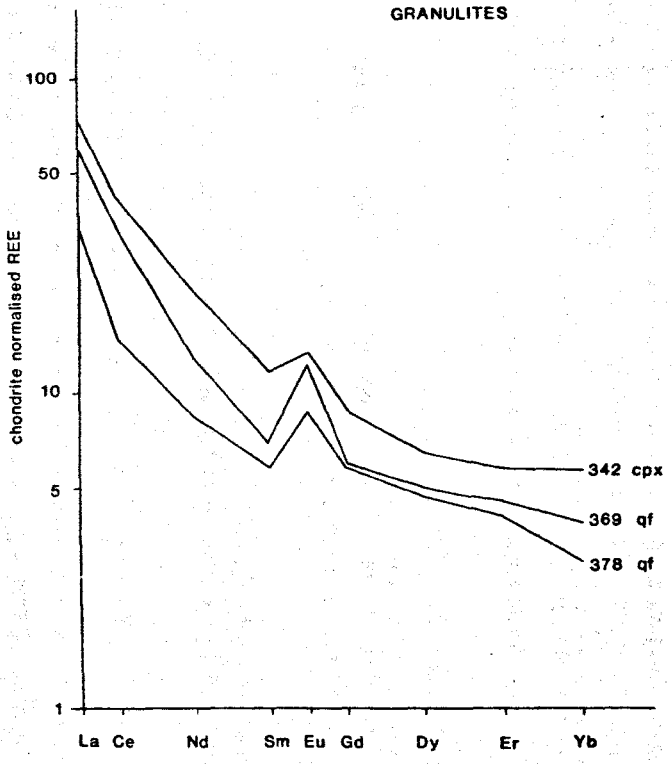

Figure 6:4c

REE PATTERNS OF TONALITES & TRONDHJEMITES

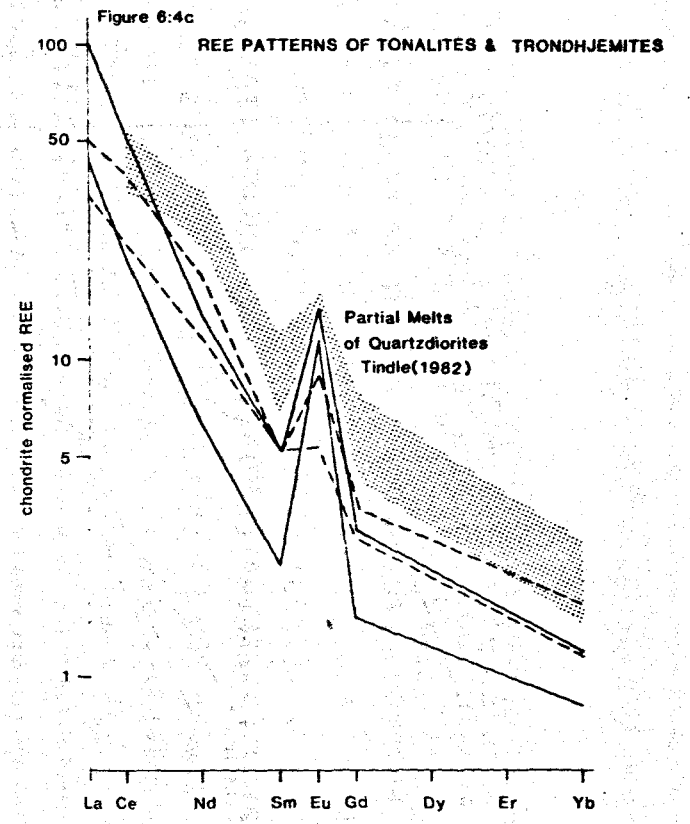

Figure 6:5a PARTAN CRAIG :- GARNET GRANULITES

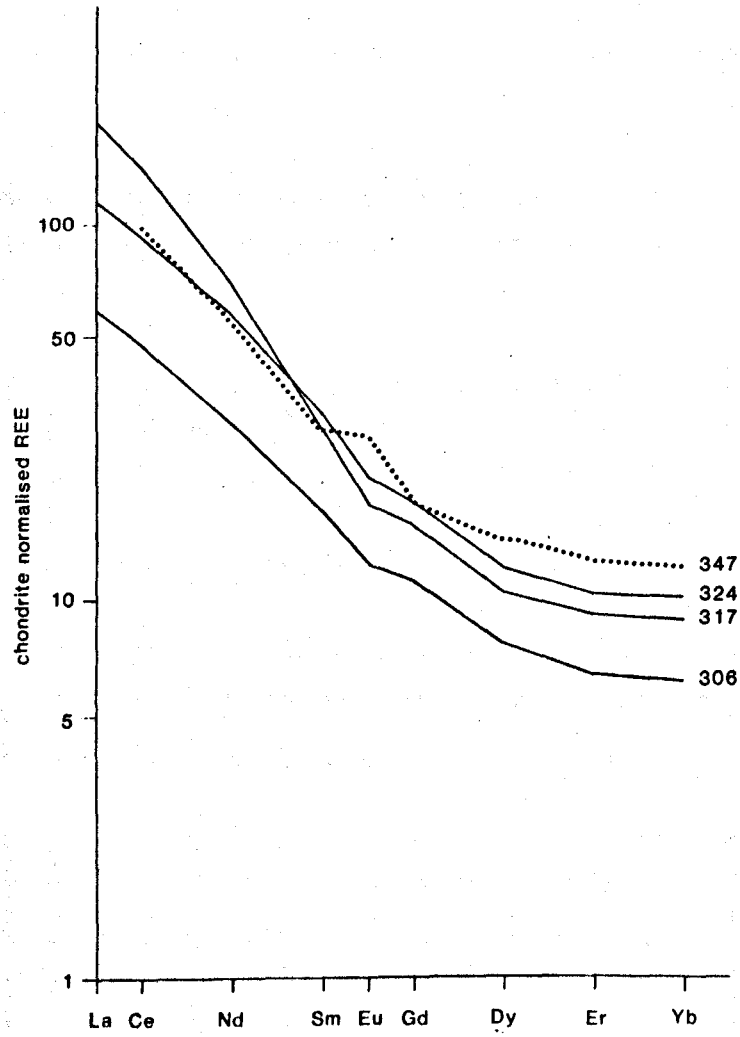

Figure 6:5b HAWKS NIB :- BASIC GRANULITES

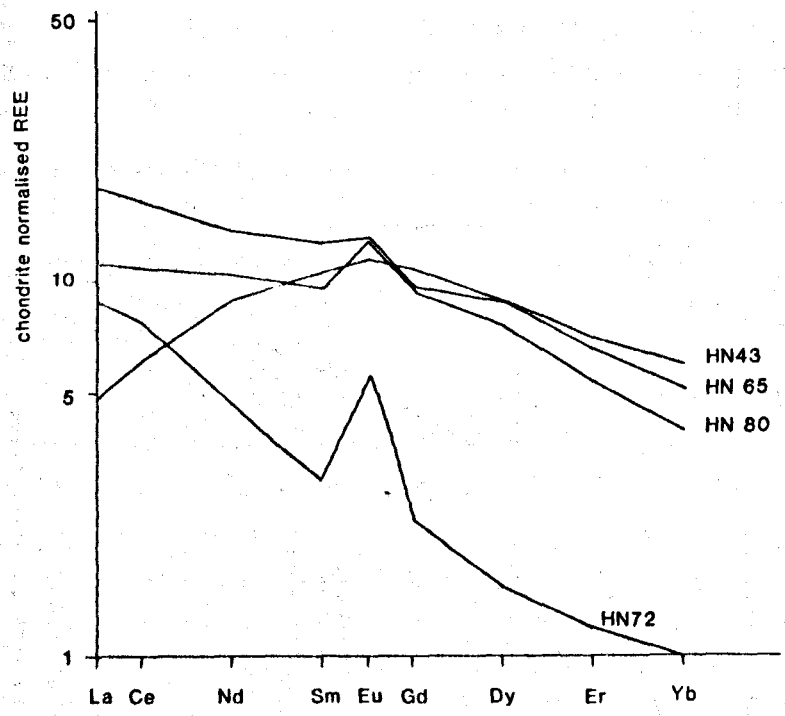

than the Scottish samples, Eu/Eu* of 0.52 to 0.8.

6:3:2 Quartzo feldspathic and Pyroxene Granulites from Partan Craig. Two quartzo feldspathic and one pyroxene granulite xenolith from Partan Craig were analysed for REE (Figure 6:4b). The patterns show significant L.REE enrichment, $(Ce/Yb)_N$ ratios between 5 and 8.6, and marked positive Eu anomalies, Eu/Eu* of 1.3 to 1.9. The samples have low, but varied, H.REE contents, $(Yb)_N$ of 2.9 to 5.6, and moderate L.REE contents, $(Ce)_N$ of 14.5 to 41.

6:3:3 Basic Granulites from Hawks Nib. The basic granulites from Hawks Nib have low absolute REE contents but display variable REE patterns from L.REE enriched, HN72, $(Ce/Yb)_N$ ratio of 7.2, to the convex upwards patterns of HN43, $(Ce/Yb)_N$ ratio of 1.2 (Figure 6:5b). Two features are common to all four samples, fractionated H.REE $(Dy/Yb)_N$ ratios of 1.5 to 1.9, and a positive Eu anomaly Eu/Eu* of 1.1 to 2.1.

6:3:4 Discussion :- Possible Precursors to the Granulite Xenoliths.

a) Partan Craig Garnet Granulite Xenoliths: Due to the presence of an aluminous phase, kyanite, Graham and Upton (1978) postulated that the garnet granulites of Partan Craig represent metapelites. The average chemical analysis for these xenoliths is given in Table 6:1 along with data for Lewisian and Moinian metasediments. With the exception of CaO (high in the xenoliths due to secondary calcite) the data are comparable. The similarity in these data does not, however, provide conclusive proof of a sedimentary origin in that Archean tonalites and present day granitoids display similar chemical characteristics (Table 6:1). Tarney (1976) and Winchester et al. (1980) used a Ti vs SiO_2 diagram to distinguish between metasedimentary and meta-igneous rocks. The latter authors also proposed the Ni vs Zr/Ti diagram as an effective discriminant. The garnet granulites from Partan Craig plot within the sedimentary field on both diagrams

(Figure 6:6). However, the most convincing evidence that the garnet granulites are of a sedimentary origin is provided by their REE patterns. Although the L.REE nature and contents of sedimentary rocks are comparable to tonalitic gneisses and granitoids, the relatively unfractionated H.REE so diagnostic of sediments are rare in these latter rocks. These aspects of the REE patterns are well displayed in Figure 6:7, a diagram of L.REE fractionation $(La/Nd)_N$ vs H.REE fractionation $(Dy/Yb)_N$. The diagram effectively discriminates between sedimentary and igneous rocks. There is limited overlap between diorites from recent calc alkaline batholiths and the field of sediments. However, the 2 may be distinguished by major elements or by the fact that diorites frequently do not have the well developed negative Eu anomalies characteristic of Proterozoic to recent sediments. The garnet granulites from Partan Craig plot within the sedimentary field on Figure 6:7 and it is therefore concluded that the majority of the Partan Craig garnet granulite xenoliths are metasediments.

Interestingly the LILE data of the garnet granulites show no evidence of the K and Rb depletion indicative of Lewisian granulites facies gneisses (Table 6:1). The Rb/Sr and K/Rb ratios of the xenoliths are more comparable to the Lewisian amphibolite facies gneisses. It should be noted that the Rb/Sr ratios of the xenoliths are lower than typical pelites (Rb/Sr = 1.0 see Chapter 7) but lie within the range of more immature sediments e.g. greywackes, Rb/Sr, 0.05 to 1.0 (Tindle unpublished Ph.D. 1982).

b) Central Ireland Garnet Granulite Xenoliths: Only REE and Rb-Sr data are available for the Irish xenoliths but these data suggest that the xenoliths are not of sedimentary origin due to the following;

i) High H.REE contents $(Yb)_N > 17$ compared to < 16 in sediments

ii) Marked negative Eu anomalies Eu/Eu* $\leqslant 0.8$ compared to $\geqslant 0.8$ in sediments

iii) Little fractionation of the L.REE $(La/Nd)_N \leqslant 1.4$ compared to $\geqslant 1.8$ in sediments (see Figure 6:7).

Figure 6:6 Zr/Ti vs Ni DISCRIMANANT DIAGRAM
for rocks of intermediate composition

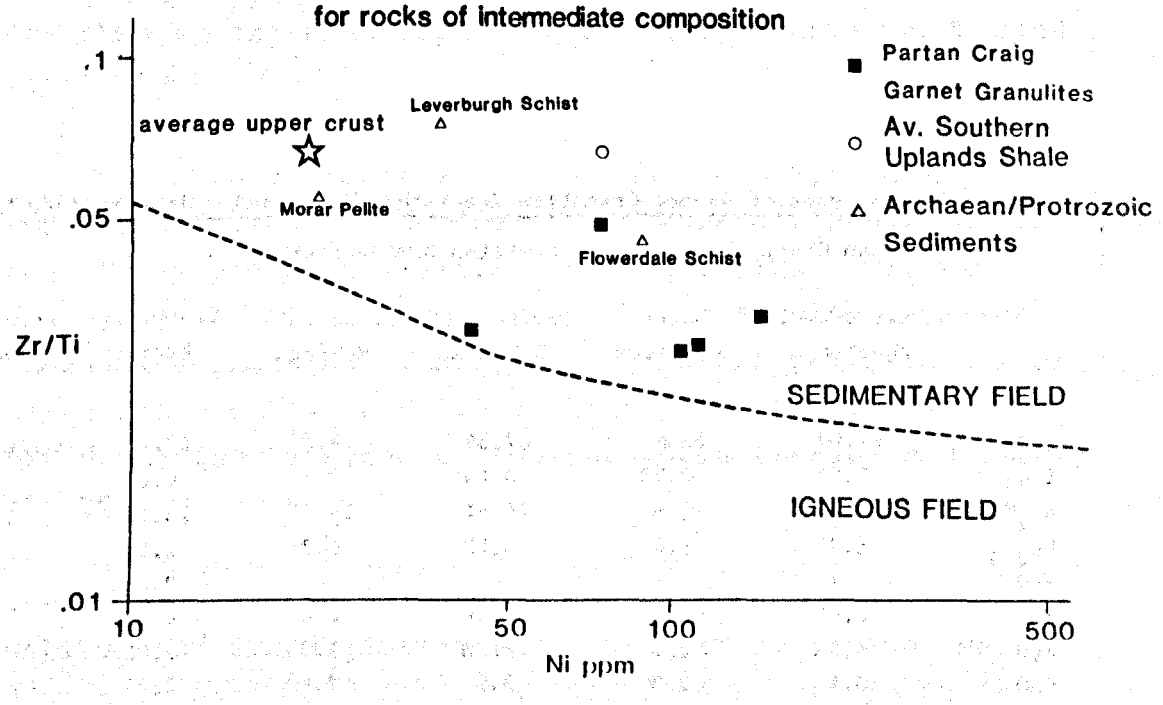

Data sources : Winchester et al., 1980, 1981,
Lambert et al., 1981, Tindle, 1982.

Figure 6:7 DIAGRAM OF L.REE FRACTIONATION vs H.REE FRACTIONATION

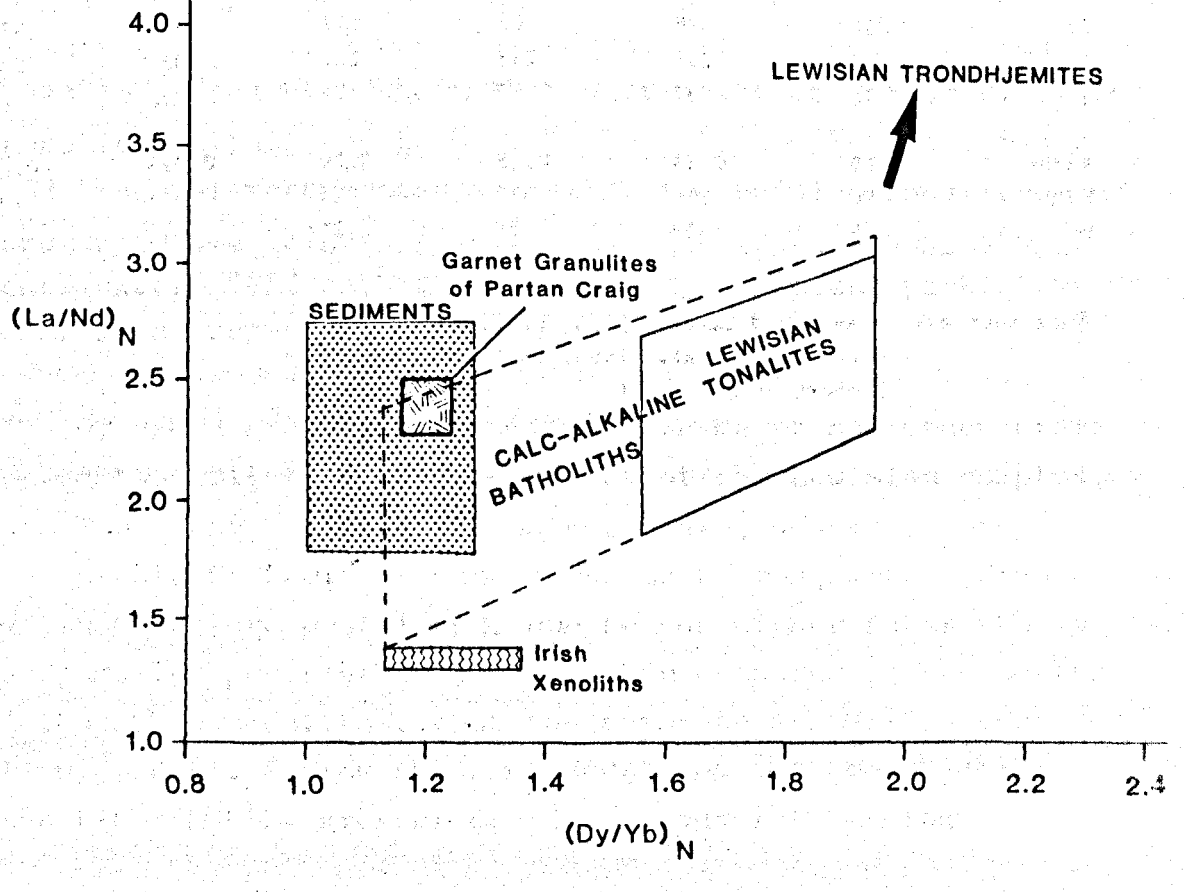

Data sources : Taylor and McLennan, 1981
Weaver and Tarney, 1980, 1981.

Table 6:1

Comparative Analyses of Garnet Granulite Xenoliths, Moine and Intermediate Lewisian Gneisses

	Partan Craig	Lewisian Semipelites				
	Garnet Granulite Xenoliths	Morar Pelites	Leverburgh Schists	Flowerdale Schists	Granulite Facies	Amphibolite Facies
SiO_2	62.07	62.8	67.36	64.57	62.40	63.48
TiO_2	1.03	0.93	0.64	0.81	0.69	0.49
Al_2O_3	14.18	16.9	14.61	14.03	16.15	16.75
Fe_2O_3	5.77	6.4	6.12	6.86	2.58	4.44
FeO	-	-	-	-	2.44	-
MnO	0.09	0.1	0.06	0.05	0.07	0.05
MgO	4.93	2.0	2.86	5.3	2.81	1.65
CaO	4.1	2.3	3.2	2.68	2.79	3.62
Na_2O	2.23	2.8	2.52	2.29	4.19	4.82
K_2O	2.35	3.8	2.75	2.95	1.32	2.35
P_2O_5	0.13	0.29	0.13	0.18	0.22	0.32
Ni	95	22	36	88	37	12
Ba	1289	990	1100	562	11	82
Rb	50	109	59	109	464	648
Sr	261	328	405	147	751	885
Zr	199	298	288	221	203	296
Y	23	37	19	24	12	8
Rb/Sr	0.19	0.33	0.15	0.74	0.023	0.167
K/Rb	390	290	387	225	1043	238
n	5	39	21	21		

Data sources: Weaver and Tarney, 1980, 1981,
Winchester et al., 1980, 1981,
Lambert et al., 1981.

It is not possible to constrain further their petrogenesis other than to say that amphibole and garnet have not played a significant role.

c) Partan Craig Quartzo feldspathic and Pyroxene Granulite Xenoliths. The quartzo feldspathic xenoliths from Partan Craig are highly siliceous rocks, $SiO_2 > 70\%$, with major and trace element contents comparable with Lewisian trondhjemite gneisses, Table 6:3. The REE patterns are also similar (Figure 6:4b and 6:4c) although with less extreme H.REE depletion recorded by the xenoliths (Weaver and Tarney, 1980, 1981).

Several authors have discussed the petrogenesis of the Archean tonalites and trondhjemites and generally agree that garnet and/or amphibole have played a significant role in their petrogenesis either as fractionating phases or as residual phases during partial melting (Arth et al., 1978, Weaver and Tarney, 1980, 1981). The absence of garnet and amphibole rich cumulate rocks among Archean terrains argues against significant garent and amphibole fractionation. Interestingly Tindle (1982 unpublished Ph.D) and Tindle and Pearce (1983 in press) have shown that melts extracted from dioritic autoliths within the Loch Doon plutonic complex have major and trace element contents similar to Lewisian tonalites and trondhjemites (Figure 6:4c). It is therefore suggested that the quartzo feldspathic xenoliths may represent partial melts extracted from a basic source rock.

The pyroxene granulite xenoliths have major and trace element contents similar to basic gneisses of the Lewisian complex, see Table 6:4. Their REE patterns are, however, more comparable to Lewisian tonalites and trondhjemites (Figure 6:4c). It is therefore postulated, due to the higher total REE contents and smaller positive Eu anomaly when compared to the quartzo feldspathic xenoliths, that the pyroxene granulites represent liquids derived from the same source as the trondhjemitic xenoliths but by greater degrees of partial melting.

Table 6:2 REE and Isotope results for the Lower Crustal Xenoliths

Sample	Rock Type	La	Ce	Nd	Sm	Eu	Gd	Dy	Er	Yb	$(Ce/Yb)_N$	Sm/Nd	$^{143}Nd/^{144}Nd$	εNd_{400}	Rb	Sr	Rb/Sr	$^{87}Sr/^{86}Sr$	εSr_{400}
PC 303	Garnet Granulite			23.58+	3.86+							0.1637	0.511990 ±10	-7.6 ±0.2	44[1]	212	0.207	0.71428 ±2	+94.4
PC 306	Garnet Granulite	22.4	43.3	18.0	3.31	0.94	3.19	2.62	1.45	1.36	8.1	0.1839	0.512103 ±16	-6.1 ± 0.3	21[1]	253	0.083	0.71065 ±2	+71.9
PC 317	Garnet Granulite	55.6	107.0	43.91+ 44.1	5.585+ 5.60	1.59	5.06	3.52	2.07	2.01	13.5	0.1272	0.511770 ±10 0.511792 ±20	-10.7 ±0.4	82[1]	371	0.221	0.71664 ±3	124.6
PC 324	Garnet Granulite	52.6	89.7	37.0	6.36	1.64	5.33	4.14	2.30	2.22	10.2	0.1716	0.511877 ±16	-10.1 ±0.3	33[1]	261	0.126	0.71239 ±4	+86.6
PC 347*	Garnet Granulite		83.7	29.89+ 33.9	5.202+ 5.75	2.08	5.10	4.90	2.81	2.59	8.1	0.1740 0.1700	0.511962 ±14 0.511952 ±12	-8.8 ±0.3	70[1]	210	0.333	0.72220 ±4	+177.3
PC 369	Trondhjemite Granulite	19.9	28.6	8.10	1.41	0.942	1.63	1.69	0.998	0.844	8.6	0.1741	0.512486 ±14	+1.7 ±0.3	13[1]	375	0.035	0.70627 ±4	+21.0
PC 378	Trondhjemite Granulite	10.7	12.6	5.31	1.14	0.664	1.59	1.61	0.92	0.634	5.1	0.2147	0.512610 ±20	+2.9 ±0.4	13[1]	418	0.031	0.70632 ±3	+22.6
PC 342	Pyroxene Granulite	23.4	35.5	13.2	2.36	1.02	2.41	2.22	1.28	1.23	7.2	0.1788	0.512443 ±24	+0.7 ±0.5	12[1]	309	0.039	0.70628 ±4	+28.4
PC 355	Pyroxene Granulite			10.80+	2.050+							0.1897	0.512461 ±22	+0.7 ±0.5	13[1]	705	0.018	0.70449 ±4	+3.4
HN 43	Basic Granulite	1.63	5.29	5.66	2.19	0.892	2.98	3.00	1.46	1.11	1.2	0.3867	0.512944 ±30 0.512912 ±22	+3.9 ±0.4	1.02	311.5	0.00327	0.70328 ±3	-14.0
HN 65	Basic Granulite	5.95	14.5	8.75	2.58	1.02	2.63	3.05	1.57	1.31	2.8	0.2957	0.512751 ±14	+3.1 ±0.3	19.29	423.8	0.04552	0.70424 ±4	-10.2
HN 72	Olivine Gabbro	2.83	6.65	2.98	0.618	0.429	0.65	0.531	0.271	0.224	7.3	0.2072	0.512566 ±18	+2.3 ±0.4	3.85 3.82	499.1 493.9	0.00772 0.00774	0.70375 ±2	-8.4
HN 80	Basic Granulite	3.72	9.44	6.62	1.92	1.01	2.56	2.60	1.18	0.876	2.7	0.2903	0.512688 ±22 0.512688 ±30	+2.0 ±0.4	6.26	590.2	0.01060	0.70393 ±4	-6.5
HN 83	Olivine Gabbro			6.945+	2.269							0.3267	0.512860 ±14	+4.2 ±0.3	13.08	548.2	0.02386	0.70459 ±4	-0.4
77.0827	Garnet Granulite	53.9	84.3	82.0	12.73	2.13	13.0	10.1	5.35	4.82	4.5	0.1552	0.512033 ±14	-6.6 ±0.3	75.90	153.1	0.4956	0.72130 ±2	+126.5
Sc 19a	Garnet Granulie			190.78+	21.348+							0.1119	0.511896 ±18	-7.9 ±0.4	100.3	269.4	0.3723	0.71463 ±	+60.7
Sc 19b	Garnet Granulite	75.7	175.4	100.45	12.96	2.68	8.42	6.63	3.87	3.85	11.6	0.1290	0.511862 ±24	-9.1 ±0.5	137.3	338.6	0.4055	0.71559 ±4	+161.0
Sc 20	Garnet Granulite			245.49+	27.83+							0.1290	0.511916 ±10	-7.6 ±0.2	99.74	319.0	0.31267	0.71460 ±4	+74.1
Sc 27	Garnet Granulite			30.12+	5.062+							0.1681	0.512125 ±18	-5.2 ±0.4	6.09	448.1	0.01358	0.70965 ±3 0.70965 ±2	+74.0

* REE analysis from van Breeman and Hawkesworth(1980)

\+ Sm,Nd determined seperately

1 Rb,Sr determined by XRF at Edinburgh.Graham and Upton(1978)

Table 6:3

Comparative analyses of Quartzofeldspathic Xenoliths and Lewisian Trondhjemites

	Partan Craig Quartzo feldspathic Xenoliths	Lewisian Trondhjemites	
		Granulite Facies	Amphibolite Facies
SiO_2	70.00	70.50	70.23
TiO_2	0.31	0.23	0.23
Al_2O_3	13.80	15.41	15.70
Fe_2O_3	1.84	1.45	1.91
FeO		0.53	
MnO	0.05	0.02	0.02
MgO	1.17	0.70	0.72
CaO	5.77	2.33	2.46
Na_2O	4.12	5.11	4.87
K_2O	0.68	1.25	2.46
P_2O_5	0.11	0.13	0.09
Ni	36	13	12
Rb	14	10	82
Sr	337	464	613
Ba	600	1680	892
Zr	81	145	170
Y	11	< 5	< 2
Rb/Sr	0.0415	0.022	0.14
K/Rb	412	1230	252
n	4	5	3

Data sources: Weaver and Tarney 1980, 1981.

Table 6:4

Comparative analyses of Pyroxene Granulites and Lewisian Basic Gneisses

	Partan Craig Pyroxene Granulite Xenoliths	Lewisian Basic Gneisses	
		Granulite Facies	Amphibolite Facies
SiO_2	50.81	48.74	53.2
TiO_2	0.92	0.87	0.81
Al_2O_3	17.92	17.09	18.40
Fe_2O_3	5.93	4.27	9.68
FeO		6.25	
MnO	0.09	0.18	0.11
MgO	3.24	6.98	3.59
CaO	11.52	11.14	4.94
Na_2O	3.87	2.31	5.02
K_2O	0.57	0.91	2.10
P_2O_5	0.35	0.07	0.21
Ni	49	95	17
Rb	13	9	83
Sr	387	183	676
Ba	541	260	684
Zr	105	51	618
Y	17	21	24
Rb/Sr	0.034	0.050	0.120
K/Rb	363	821	210

Data sources: Weaver and Tarney, 1980, 1981.

In marked contrast to the garnet granulites from Partan Craig these latter 2 xenolith types show evidence of low Rb contents (Table 6:3). Although the K/Rb ratios are comparable to present day mantle derived volcanism (300 to 440) the low Rb/Sr ratios, 0.04, are in the same order of magnitude as Lewisian granulite facies rocks (Table 6:3). However, the calculated partial melts derived from quartz diorites within the Loch Doon complex (Tindle opt. cit.) have equal or lower Rb/Sr ratios than the xenoliths (0.012 to 0.064). It is therefore concluded, due to their underpleted K/Rb ratios, that the low Rb/Sr ratios of the xenoliths are a primary feature and not caused by K and Rb depletion as in the case of the Lewisian granulite facies rocks.

d) Hawks Nib Basic Granulites: The mineralogy of the basic granulites (plagioclase + clinopyroxene $\pm$ orthopyroxene $\pm$ olivine) suggests basaltic/gabbroic precursors. The low Rb/Sr ratios, 0.003 to 0.04, are consistent with this interpretation. The REE data can most easily be interpreted in terms of a cumulate origin. For example HN72, a plagioclase rich xenolith, has the lowest total REE contents and a marked positive Eu anomaly ($Eu/Eu^* = 2.1$) indicative of a placioclase rich cumulate rock. Rayleigh fractionation calculation show that the rock could be produced by the fractional crystallisation of 85% plagioclase and 15% clinopyroxene from a L.REE enriched magma comparable to HN65, $(Ce/Yb)_N$ ratio of 3.0. (Distribution coefficients for a basaltic liquid after Arth, 197[illegible])

The consistent H.REE fractionation recorded in all the xenoliths, $(Dy/Yb)_N$ ratios of 1.4 to 1.9, suggests that the xenoliths are cogenetic. The presence of a positive Eu anomaly in all the basic xenoliths may possibly be a primary feature of the magmas from which they formed but more likely represents the result of cumulate processes.

6:3:5 Interim Summary. The geochemical data suggest that the garnet granulites from Partan Craig originated as sediments but that the remaining xenolith types studied are much more varied and probably formed as a wide variety of igneous rocks.

6:4 Isotope Results

19 crustal xenoliths were analysed for both Nd and Sr isotope ratios (Table 6:5). All the samples from Partan Craig and Central Ireland were leached with 1M HCl to remove possible secondary calcite. The data presented in Table 6:5 demonstrate that the leaching had no significant effect on either $^{87}Sr/^{86}Sr$ or $^{143}Nd/^{144}Nd$ ratios (the freshest possible samples being analysed).

The present day $^{143}Nd/^{144}Nd$ ratios range from 0.51178 to 0.51293. Each petrographic group shows distinct Nd isotope ratios. The basic granulite from Hawks Nib have the most radiogenic ratios, 0.51257 to 0.51293, and the garnet granulites the lowest ratios, 0.51178 to 0.51213, while the quartzo feldspathic and pyroxene granulites of Partan Craig have intermediate values, 0.51244 to 0.51261. A similar distinction is found in the Sr isotope data. The garnet granulites have the most radiogenic $^{87}Sr/^{86}Sr$ ratios, 0.70965 to 0.72220 and the basic granulites the least radiogenic ratios, 0.70328 to 0.70459. The quartzo feldspathic and pyroxene granulites of Partan Craig again have intermediate values, 0.70449 to 0.70632.

6:4:1 Discussion of the Isotope Data

a) Garnet Granulites; Partan Craig

The Sr isotope data for the Partan Craig garnet granulites show a positive correlation on a Rb-Sr isochron diagram, Figure 6:8. Isochron calculations reveal that four of the five points lie on a line equivalent to an age of 1101 $\pm$ 63 Ma. The scatter in the data, although outside analytical error (M.S.W.D. = 8) is surprisingly small considering that the xenoliths represent a suite of randomly sampled lower crustal rocks. The initial ratio of 0.7068 $\pm$ 0.0002 is equivalent to an εSr_{1100} value of + 48. This implies, that if the data represent an isochron, the rocks had a relatively short crustal residence prior to the formation

Figure 6:8

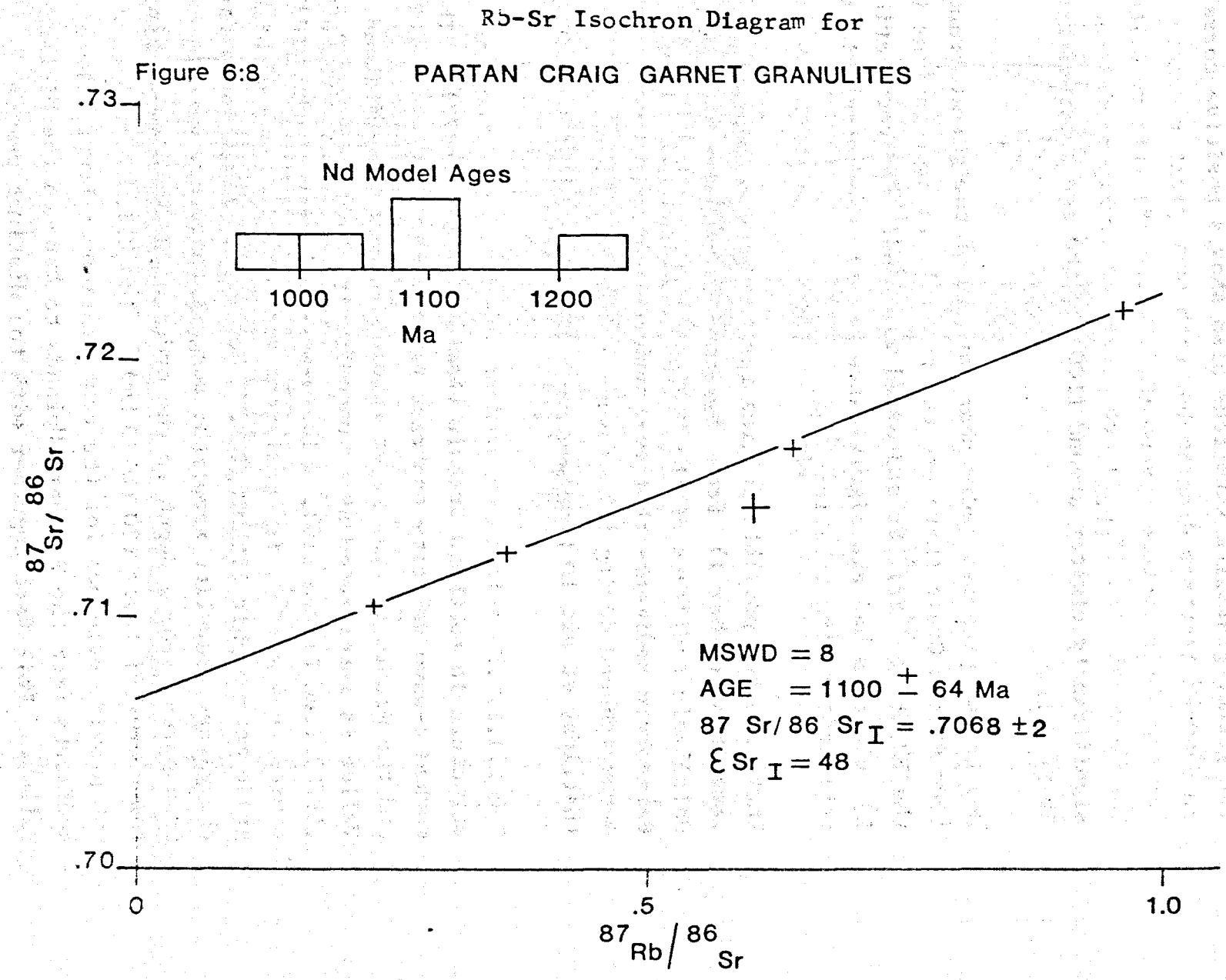
Rb-Sr Isochron Diagram for
PARTAN CRAIG GARNET GRANULITES
Nd Model Ages
1000
1100
1200
Ma
.73
.72
.71
.70
$^{87}Sr/^{86}Sr$
0
.5
1.0
$^{87}Rb/^{86}Sr$
MSWD = 8
AGE = 1100 ± 64 Ma
87 Sr/86 Sr_I = .7068 ±2
εSr_I = 48

of the isochron (less than 200 Ma).

The garnet granulite xenoliths also show a positive correlation on a Sm-Nd isochron diagram but with much greater scatter than for the Rb-Sr isotope system (M.S.W.D. = 18) (Figure 6:10b). The Nd model ages (T_{CHUR}) are presented in Figure 6:8 and significantly cluster around 1100 Ma, the age obtained from the Rb-Sr data.

Due to the proposed sedimentary origin of the garnet granulites from Partan Craig there are two possible interpretations for the Rb/Sr vs $^{87}Sr/^{86}Sr$ and Sm/Nd vs $^{143}Nd/^{144}Nd$ correlations, i) the data has age significance or ii) the correlations represent mixing relationships.

There are two possible origins for the metasedimentary xenoliths, either i) from Precambrian basement beneath the Palaeozoic sediments of the Midland Valley or ii) Lower Palaeozoic sediments that were underthrust and metamorphosed during the closure of the Iapteus Ocean (Halliday et al. in prep).

The L.I.S.P.B. seismic experiment has determined the crustal structure in northern Britain (Bamford et al., 1977). The marked p-wave velocity contrast between the Palaeozoic sediments and the middle crustal layer recorded beneath the Midland Valley is interpreted as an uncomformity by Graham and Upton (1978) (see Figure 6:9). The p-wave velocity of the middle crust, 6.4 kms $^{-1}$, is consistent with the presence of high grade metamorphic lithologies. However, P-T estimates for the garnet granulite xenoliths suggest that they were transported from a depth in the order of 30 km i.e. within the lower crustal layer (20 to 30 km). The L.I.S.P.B. data does not provide evidence for the continuation of Lower Palaeozoic sediments from the Southern Uplands to beneath the Midland Valley. This fact together with the distinct p-wave velocities of the middle crustal layers beneath the two regions, argues against an origin for the xenoliths as underplated Lower Palaeozoic sediments from the Southern Uplands.

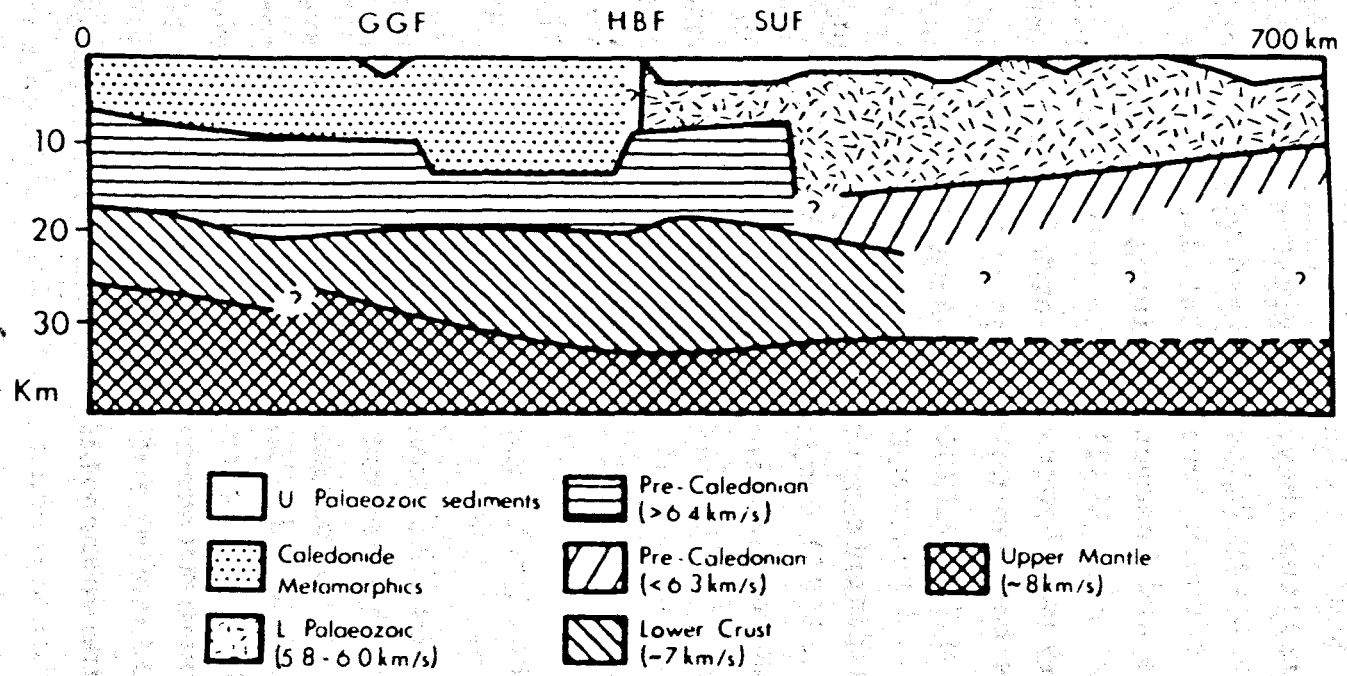

Figure 6:9

An interpretation of the crustal structure of Scotland from the LISP3 seismic data after Bamford et al., 1978

G.G.F. Great Glen Fault H.B.F. Highland Boundary Fault S.U.F. Southern Uplands Fault

To assess the possibility of a mixing origin for the Rb-Sr and Sm-Nd isotope systematics of the metasedimentary xenoliths during the Caledonian Orogeny crustal rocks are plotted on Rb/Sr vs $^{87}Sr/^{86}Sr_{450}$ and Sm/Nd vs $^{143}Nd/^{144}Nd_{450}$ diagrams (Figures 6:10a and b). Significantly although the Southern Uplands sediments have $^{143}Nd/^{144}Nd_{450}$ ratios equivalent to the xenoliths they have greater Sm/Nd ratios (Figure 6:10b). The Lower Palaeozoic sediments lie on a possible mixing line between juvenile Caledonian crust and Precambrian sediments and basement defining a 1500 Ma errorchron (O'Nions et al., 1983). The garnet granulites record a significantly shallower slope and do not lie on possible mixing lines between Caledonian and Precambrian crust. Similarly the Rb-Sr systematics of the Lower Palaeozoic sediments and the xenoliths are distinct (Figure 6:10b) The Southern Upland sediments record a Rb-Sr errorchron of circa 700 Ma (Halliday et al., 1980) compared to 1100 Ma for the garnet granulites. The Sm-Nd and Rb-Sr isotope systematics of the Southern Upland sediments therefore record the mixing of Precambrian and Caledonian crust which results in markedly different Sm-Nd and Rb-Sr ages. The consistent 1100 Ma ages obtained from the Partan Craig garnet granulite xenoliths suggest that the age has geological significance.

The 1100 Ma Rb-Sr whole-rock errorchron may be interpreted as representing one of three events i) sediment formation, ii) diagenesis, iii) regional metamorphism. The clay fraction within a sediment, which contains a large proportion of the rocks' Sr and Rb, will recrystallise during diagenesis and particularly regional metamorphism. The presence of significant H_2O and CO_2 during metamorphism will cause extensive redistribution of the LILE. Whole-rock Rb-Sr ages obtained from sediments are therefore considered most likely to represent post depositional re-equilibration during regional metamorphism. Significantly Kroner et al. (1978) conclude that the whole-rock age obtained on Damaran metasediments is markedly younger than their depositional age and that the isochron records the first regional metamorphic event. From the above discussion it is concluded that the

Rb-Sr whole-rock errorchron of the garnet granulites records post depositional re-equilibration during regional metamorphism. The relatively low initial ratio of the rocks 0.7068 indicates a short crustal residence time prior to metamorphism (< 200 Ma) and that the sediments most probably represent detritus eroded from a dominantly juvenile terrain circa 1200 Ma. The data do not however, rule out rapid formation, burial and metamorphism of the sediments circa 1100 Ma.

b) Garnet Granulites; Central Ireland

The Sm-Nd and Rb-Sr isotope systematics of the garnet granulites of Central Ireland display similar characteristics to those of the petrographically similar xenoliths from the Midland Valley (Figure 6:10a and b). The Nd and Sr model ages of the Irish xenoliths plotted in Figure 6:11 are younger than those of the Scottish xenoliths. Nd model ages are circa 900 Ma whereas the Sr model ages display a greater scatter and a tendancy to younger model ages circa 850 Ma (see Chapter 7 for discussion of the significance of Sr model ages). However, if the Irish xenoliths were derived from a more depleted mantle source than the Scottish xenoliths then the Nd model ages of the 2 suites are comparable (Nd T_{DM} = 1150 to 1250 Ma Sr T_{DM} = 850 to 1050 Ma). The Nd and Sr isotope data are plotted in Figures 6:10a and b where the slightly younger T_{CHUR} model ages of the Irish xenoliths are evident. These data again show no evidence for a mixing origin between Archean and Caledonian components.

It is concluded from the above discussion that the garnet granulite xenoliths from Central Ireland most probably represent igneous rocks derived from a mantle source between 900 and 1200 Ma. The exact timing depends upon the degree of LILE and L.REE depletion of the mantle source region.

c) Basic Granulites; Hawks Nib

The basic granulites from Hawks Nib record the largest range in Sm/Nd ratio of all the xenoliths suites, 0.207 to 0.387, and are hence suitable for an age determination. The Nd

Figure 6:10a $^{87}Sr / ^{86}Sr$ vs Rb/Sr MIXING DIAGRAM AT 450 Ma

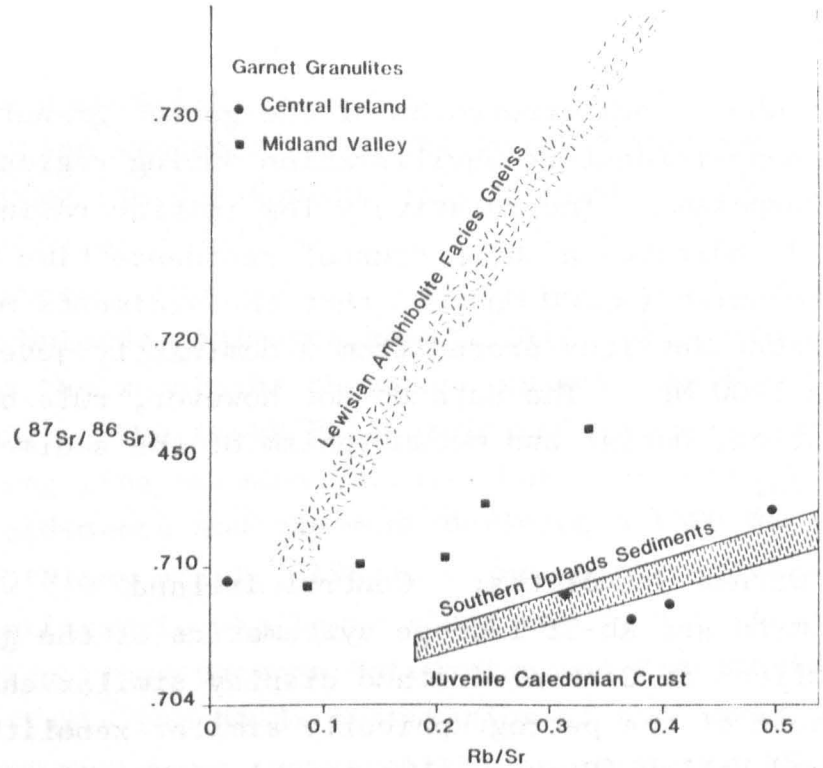

Data from; Haliday et al., 1980

Figure 6:10b $^{143}Nd / ^{144}Nd$ vs Sm/Nd MIXING DIAGRAM AT 450 Ma

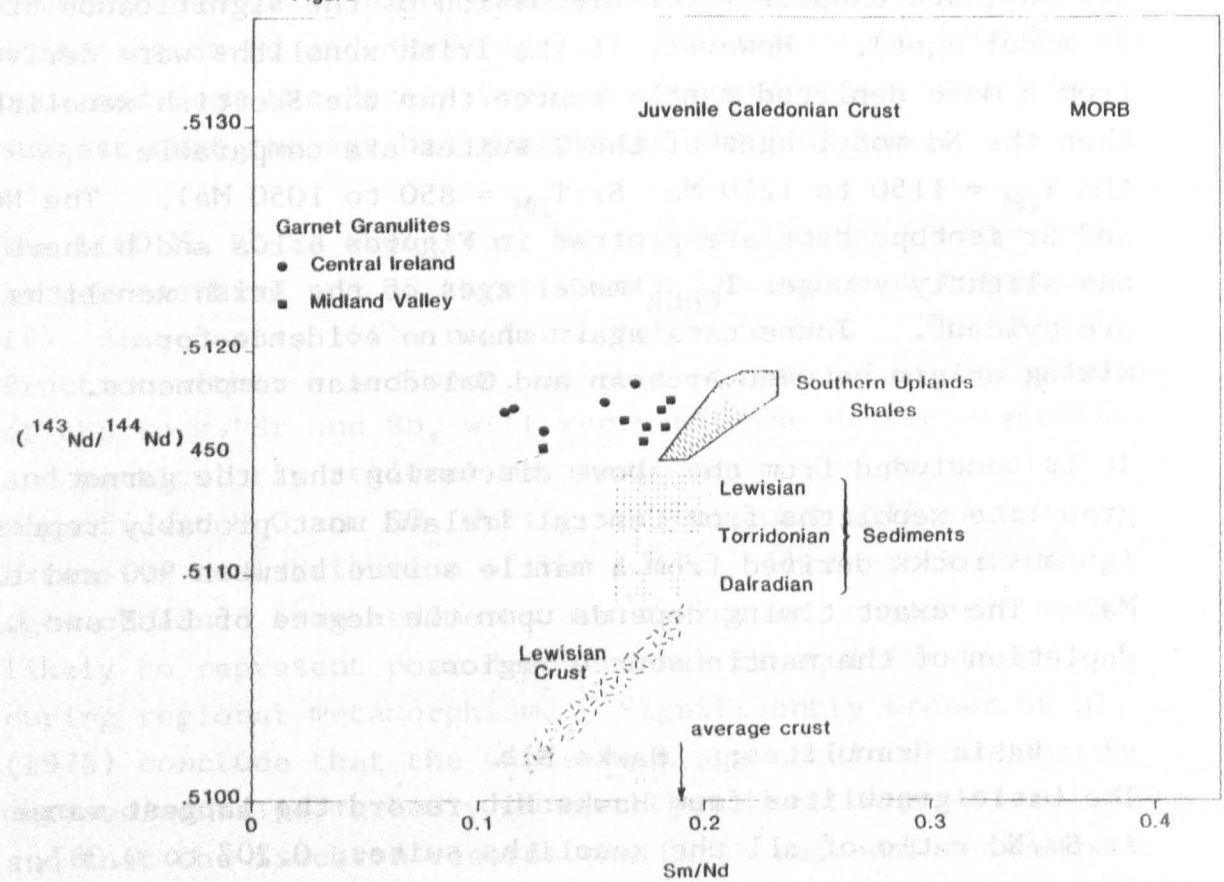

Data from; O'Nions et al., 1983, van Breeman and Hawkesworth, 1980, Hamilton et al., 1979.

Figure 6:11

CENTRAL IRELAND
LOWER CRUSTAL XENOLITHS

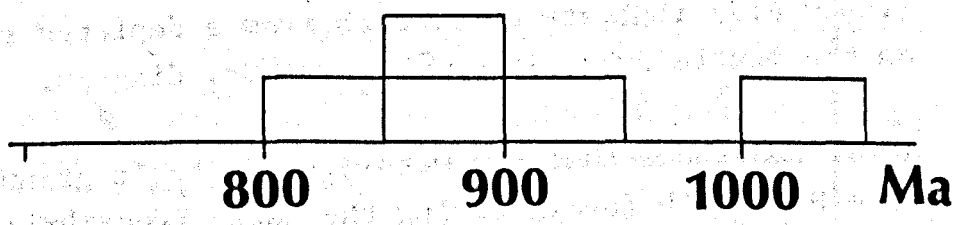

Nd Model Age

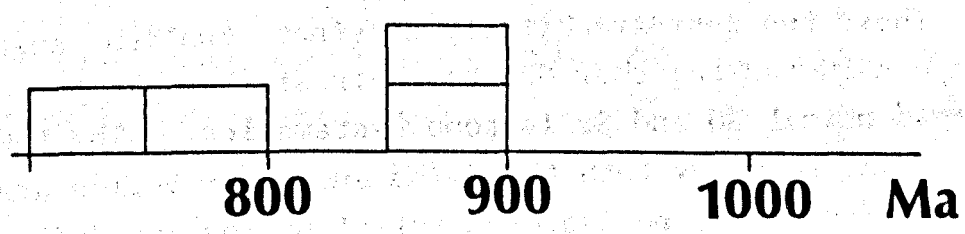

Sr Model Age

isotope data are presented on a Sm-Nd isochron diagram Figure 6:12. The data define a isochron with an age of 574 $\pm$ 137 Ma (M.S.W.D. = 3.8) and an initial ratio of 0.51209 $\pm$ .00008 equivalent to an εNd_I value of + 3.7. Although showing a positive correlation between $^{87}Sr/^{86}Sr$ and $^{87}Rb/^{86}Sr$ the Rb-Sr isotope data has a very limited spread and hence no age significance can be established. The present day $^{87}Sr/^{86}Sr$ ratios of the xenoliths are all lower than the Bulk Earth value. The εNd_I and εSr_I values of the basic granulites (Table 6:5) indicate derivation from a depleted source and plot on the mantle array in an εNd_I vs εSr_I diagram.

It is concluded that the meta-igneous basic granulite xenoliths from Hawks Nib formed during the Late Precambrian originating from a depleted mantle source. The significance of the Late Precambrian age will be discussed in a later section.

d) Quartzo feldspathic and pyroxene granulites - Partan Craig These two petrographically distinct xenolith suites are considered together due to their similar REE patterns and identical Nd and Sr isotope systematics. The low and narrow range shown by both the Sm/Nd and Rb/Sr ratios are not condusive to dating and no isochron relationships are defined. The Rb/Sr ratios of the xenoliths straddle the Bulk Earth value (0.019 to 0.039) as do their present day Sr isotope ratios, $\varepsilon Sr = -3$ to +23. All the present day Nd isotope ratios are less radiogenic than the Bulk Earth value $\varepsilon Nd = -0.2$ to -3.5.

Nd model ages provide a constraint on the formation age of the xenoliths. T_{CHUR} ages are found to be younger than the eruption age of the Carboniferous volcanic rocks which contain the xenoliths. A chondritic mantle reservoir is therefore inapplicable as a source for these samples. However, T_{DM} ages are between 760 and 900 Ma (Table 6:5) and provide a maximum possible mantle extraction age for the igneous precursors to the xenoliths. The fact that the data plot close to those of the Hawks Nib xenoliths on a $^{147}Sm/^{144}Nd$ vs $^{143}Nd/^{144}Nd$ diagram (Figure 6:12) may indicate a similar origin and hence derivation from a depleted mantle source with an

Figure 6:12

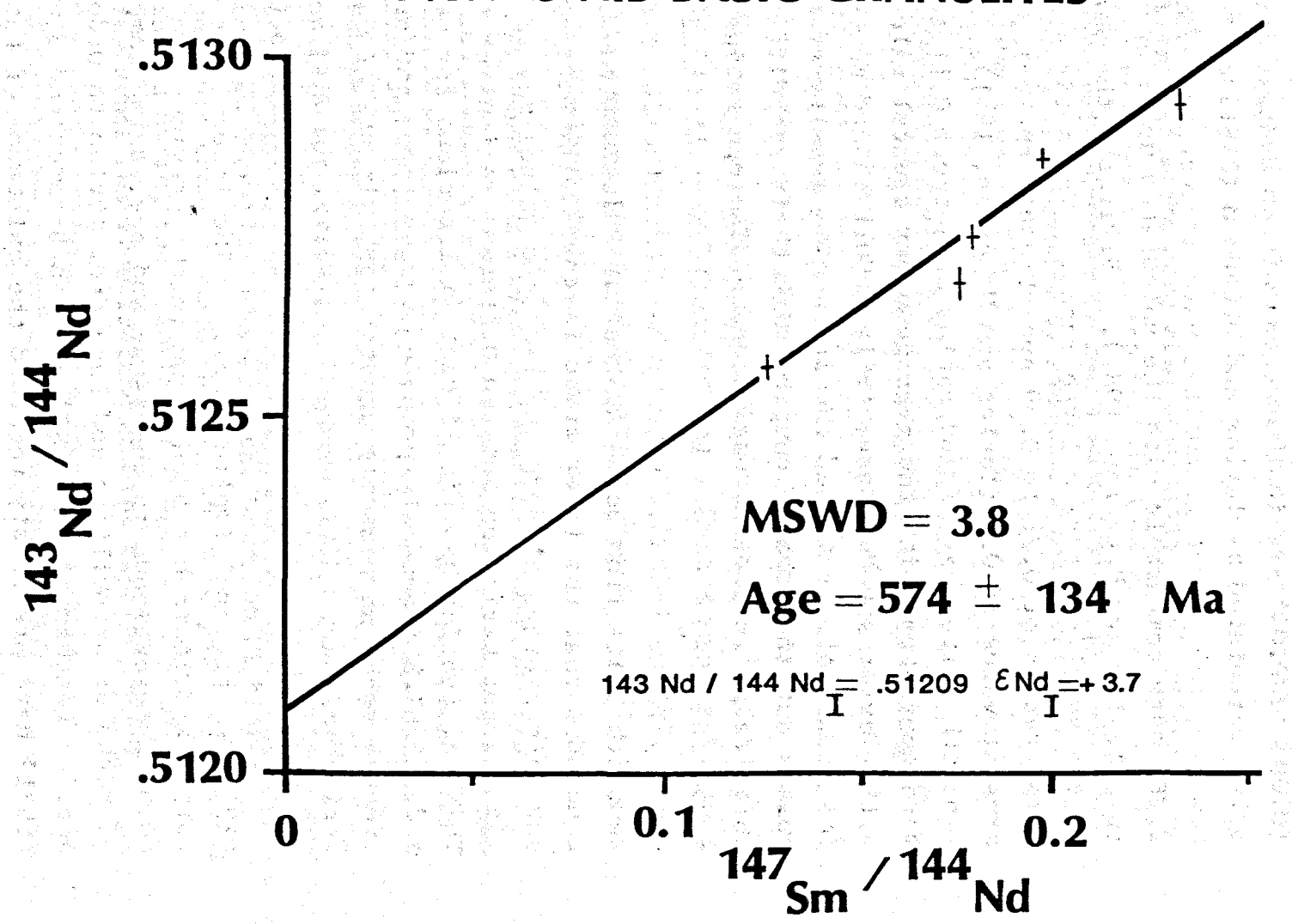
HAWKS NIB BASIC GRANULITES
.5130
.5125
.5120
143Nd / 144Nd
0
0.1
0.2
147Sm / 144Nd
MSWD = 3.8
Age = 574 ± 134 Ma
143 Nd / 144 Nd I = .51209 εNd I = +3.7

εNd_I value of +4 during the Late precambrian. The quartzo feldspathic and pyroxene granulite xenoliths are therefore genetically unrelated to the garnet granulites from the Partan Craig locality and probably formed approximately 500 Myr later.

An interesting aspect of the above data is that the Rb/Sr ratios of the basic pyroxene and quartzo feldspathic xenolith suites (0.003 to 0.04) are in the region of the average lower crustal value calculated by Taylor and McLennan (1981) of 0.02. However, the garnet granulites have an average Rb/Sr ratio of 0.26, more comparable with the calculated upper crustal average (0.3 Taylor and McLennan, 1981). Similarly the Sm/Nd ratios of the xenoliths show a large range. The basic granulites have Sm/Nd ratios of 0.21 to 0.39 and straddle the calculated lower crustal value of 0.3 (Taylor and McLennan, 1981). The remaining xenolith suites have Sm/Nd ratios of between 0.11 to 0.22 and are more consistent with the average upper crustal values, 0.17 to 0.19 (Taylor and McLennan, 1981, McCullach and Wasserburg, 1978). The result of the marked chemical heterogeneity of the xenolith suites outlined above, coupled with their age differences, is a large range in present day Nd and Sr isotope ratios, εSr_0 - 20 to + 250 and εNd_0 + 6 to - 16. McCulloch et al (1982) report equally large isotopic variations within the lower crustal xenolith suite from South Australia. It must therefore be concluded that the lower crust is chemically heterogeneous and that average element and isotopic values may show significant variation between different regions of the world. This observation has significant implications for petrogenetic models which frequently propose average lower and/or upper crustal rocks as possible crustal contaminants of mantle derived magmas.

6:4:2 Regional Implications. The lower crust beneath northern Britain has been shown in the previous sections to be heterogeneous in chemistry and age, being composed of rocks or Grenvillian and Late Precambrian to Ordovician age. Longman et al. (1980) and van Breemen and Bluck (1981) have previously recorded the existence of Late Precambrian subduction related volcanic activity in Southern Scotland. They dated granite

boulders from Ordovician conglomerates (believed to be derived from an area of positive relief in the region of the Midland Valley) between 570 and 470 Ma. Late Precambrian volcanic rocks are also recorded within the Dalradian sequence of Scotland and Ireland (Graham, 1976) and within the north-east Ox Mountains (see Chapter 5). There is therefore evidence of widespread igneous activity in northern Britain during the Late Precambrian suggesting that the northern margin of the Iapetus Ocean was active at this time.

Grenvillian aged rocks have also been recorded at several localities throughout northern Britain (see Figure 6:1). In the Annagh Gneiss Complex of north west Ireland post Lewisian metasediments are intruded by abundant syn-tectonic granite sheets (1070 $\pm$ 30 Ma) which are cut by post-tectonic granite masses (1000 $\pm$ 30 Ma) (van Breemen et al., 1978). The Ardgour granite gneisses of north-west Scotland have been dated by Brooks et al. (1976) as 1024 $\pm$ 46 Ma (recalculated using ^{Rb} = 1.42×10^{-11} yr^{-1}). A similar Rb-Sr whole-rock isochron has been obtained for Moinian rocks from the Morar Pelite, 1002 $\pm$ 96 Ma (Brooks et al., 1977). However, other isotopic studies on the Morar Division rocks have yielded U/Pb and Rb/Sr ages in the region of 700 to 800 Ma. The interpretation of the Morar Pelite therefore remains enigmatic. A K-Ar Grenvillian age has been obtained from the Rockall Bank, 987 $\pm$ 5 Ma (Miller et al., 1973).

From their study of the U/Pb systematics of zircons from Caledonian Granites, Pidgeon and his co-workers have established the presence of Proterozoic crust beneath a large proportion of central and northern Scotland. An old inherited Pb component is dated between 900 and 2000 Ma (see Pidgeon and Aftalion 1978 for review). Clayburn (1981 Unpublished Ph. D.) concluded from a combined Sr-Nd-Pb isotopic study of Caledonian Granitic rocks from the Grampian Highlands that the lower crust beneath the region is composed of juvenile crust formed during the Grenvillian Orogeny. The garnet granulite xenoliths from Ireland and the Midland Valley

similarly provide evidence for juvenile Grenvillian lower crust (significantly parts of the Grenvillian Orogenic belt have been shown to be composed of predominantly juvenile crust (Krogh and Hurley 1968)). It is therefore apparent that the Grenvillian Orogenic event may have played a significant role in the tectonic evolution of northern Britain.

The L.I.S.P.B. seismic experiment has provided data on the structure of the Scottish Lithosphere (Figure 6:9). Interestingly the middle and lower crustal layers which extend from beneath Cape Wrath to the Midland Valley are seismically homogeneous. The p-wave velocities of the middle crustal layer are comparable to those of Lewisian granulite facies gneisses which led Bamford et al. (1977) to propose a Lewisian age for the middle and lower crust. However, the xenoliths from the Midland Valley palpably demonstrate that no Lewisian crust exists in this region. If the seismically homogeneous nature of the lower and middle crust does in fact indicate that they represent a single structural unit of uniform age then it would appear that the lower and middle crust beneath all of Scotland is of Grenvillian and Caledonian age. It was shown above that such an interpretation is not inconsistent with available data from the present day upper crust.

The presence of Grenvillian aged lower and middle crust would have significant implication for the generation of the Caledonian granites of Scotland. Nd and Sr isotope data for the "newer" post-tectonic and "older" pre-tectonic Caledonian granites are plotted on an εNd vs εSr diagram at 400 Ma (Figure 6:13). These data are predominantly those of Hamilton et al. (1980). The εSr_{400} and εNd_{400} values of the Caledonian granites clearly demonstrate that they are not solely derived from a depleted mantle source as is the case for the Hawks Nib granulites. The correlation between εSr_{400} and εNd_{400} shown by the post-tectonic granites, particularly well developed in the case of Foyers and Strontian, indicates possible mixing between a mantle derived magma and crustal material. The

Figure 6:13 εNd vs εSr diagram showing the isotopic variations of the lower crustal xenolith suites of northern Britain in relation to those of pre- and post-tectonic Caledonian granites. Hatched field is that of ORS lavas; Thirwall, 1982.

Mixing line A is between a mantle derived magma and oulk assimilated average garnet granulite.

Mixing line B is between a mantle derived magma and a 30% partial melt of average garnet granulite (55% quartz and kyanite, 30% plagioclase and 15% garnet. Melting proportions 40:35:25, Partion coefficients from Arth, 1976).

Figure 6:13

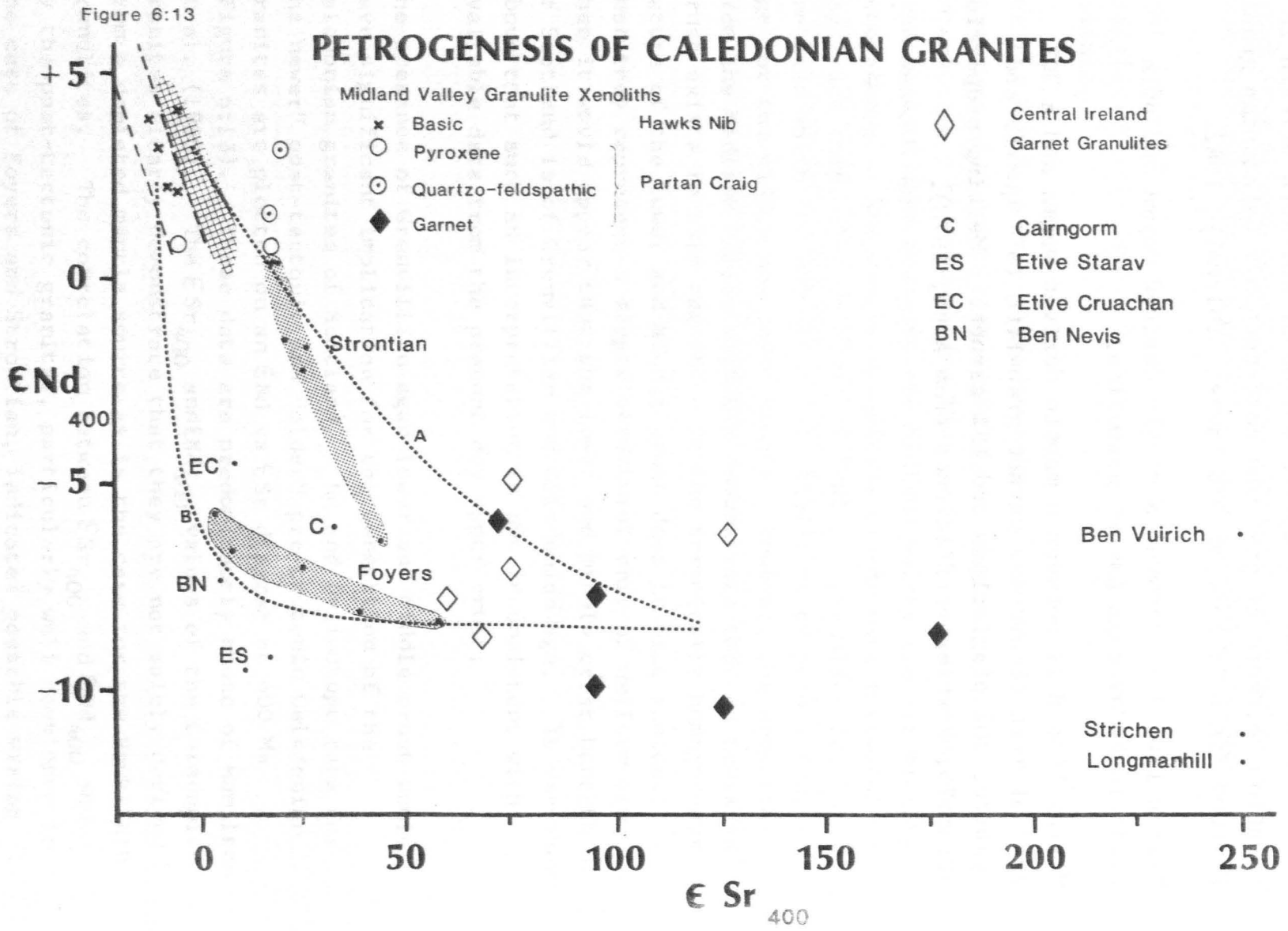
PETROGENESIS OF CALEDONIAN GRANITES
Midland Valley Granulite Xenoliths
Basic
Pyroxene
Quartzo-feldspathic
Garnet
Hawks Nib
Partan Craig
Central Ireland
Garnet Granulites
C Cairngorm
ES Etive Starav
EC Etive Cruachan
BN Ben Nevis
Strontian
Foyers
A
B
C
EC
BN
ES
Ben Vuirich
Strichen
Longmanhill
+5
0
−5
−10
εNd 400
0
50
100
150
200
250
ε Sr 400

unradiogenic Nd isotope ratios of Lewisian gneisses ($\varepsilon Nd_{400} < -25$ Hamilton et al., 1981) demonstrate that Archean lower crust is not involved in the petrogenesis of the Caledonian Granites (Hamilton et al., 1980). Figure 6:13 shows that the Grenvillian aged garnet granulites represent a possible crustal end member in a mantle-crust mixing origin for the "newer" granites. Two mixing lines are shown in Figure 6:13 between mantle derived components (Hawks Nib basic granulites and Midland Valley O.R.S lavas (Thirlwall, 1982)) and a) bulk assimilated lower crust b) a lower crustal melt (see Figure 6:13 for details). These two extreme possibilities encompass the majority of the range in εSr_{400} and εNd_{400} recorded by the post-tectonic Caledonian Granites.

The "older" pre-tectonic granites (Ben Vuirich, Strichen and Longmanhill) were emplaced circa 510 Ma. They have high initial Sr isotope ratios, $>.710$, and are considered to represent crustal melts (Pankhurst and Pidgeon, 1976). Partial melting of crustal rocks does not appear to greatly change the Nd isotope systematics of the melt compared to that of the source, such that the $^{143}Nd/^{144}Nd$ ratios of the two components will evolve similarly with time. Significantly the present day $^{143}Nd/^{144}Nd$ ratios of the "older" granites and Grenvillian xenoliths are similar. However, partial melts generally have greater Rb/Sr ratios than their source rocks. Crustal melts therefore evolve with time to significantly more radiogenic $^{87}Sr/^{86}Sr$ ratios than their source rocks. The εSr_I values of the pre-tectonic granites, 145 to 190, and εSr_{500} values of the Grenvillian granulites 30 to 160, overlap. The Nd and Sr isotope systematics of the "older" pre-tectonic Caledonian granites are therefore compatible with an origin by crustal anatexis of Grenvillian lower crust. The Caledonian granites therefore provide indirect evidence of Grenvillian aged crust beneath a large proportion of Scotland.

6:4:3 Crustal Evolution; Implications from the lower crustal xenoliths of northern Britain.

a) Crustal Evolution of northern Britain. The crustal evolution of northern Britain is dominated by three major periods of crustal growth. Scourian crust formed circa 2.9 Ga. The P-T estimates of the granulite facies gneisses indicate the crust was at least 30 km thick. The presence of metasediments within the granulite facies terrain indicates that large tectonic displacements were involved in the orogenic event. There was only minor addition to the crust during the Laxfordian orogeny but extensive crustal reworking. Significant crustal growth occured during the Grenvillian orogeny with again large tectonic displacements transporting sediments into the lower crust. The oldest rocks associated with the development of the Iapetus Ocean are found in southern Britain and are circa 700 Ma (Stanner Hanter Complex (Patchett et al., 1980) Malvern Complex (Beckinsale et al., 1981)). There is evidence for intermittent crustal accretion in northern Britain prior to 600 Ma (Ox Mountains), during the Late Precambrian (lower crustal xenoliths and calc alkaline volcanism) and until the closure of the Iapetus Ocean at the end of the Silurian. The Caledonian orogeny also resulted in extensive reworking of the existing crust.

b) Crustal evolution with time. Granulite facies gneisses with markedly fractionated REE patterns and positive Eu anomalies similar to the pyroxene and quartzo feldspathic xenolith suites are abundant in Archean and early Proterozoic terrains but have not previously been reported in recent metamorphic terrains (Weaver and Tarney, 1980, 1981 and Arth et al., 1978). A significant reason for this apparent time dependance may be due to sampling bias in that few young high grade metamorphic terrains are exposed.

Significantly, however, sediments (which represent close approximations to an average upper crustal composition) show a marked change in their REE patterns circa 2.4 Ga. Prior to this time sediments had no significant Eu anomaly, but over a

period of 400 Ma they developed greater L.REE enrichment, $(Ce/Yb)_N$ 4 to 7.5, and a negative Eu anomaly (Taylor and McLennan, 1981). Taylor and McLennan (opt. cit.) interpret these variations as due to a large increase in the total volume of crust between 3 and 2.5 Ga which enabled intracustal processes (crustal melting and fractional crystallisation) to play an important role in the formation of the upper crust. Weaver and Tarney (1981) demonstrated that partial melting of Archean tonalites would produce melts with RE and trace element contents similar to present day calc alkaline granodiorites i.e. average upper crust. Pride and Muecke (1982) report Lewisian pegmatites, derived by partial melting of the associated tonalites, with REE patterns equivalent to those calculated by Weaver and Tarney (1981).

It was argued in section 6:3:4 that Archean tonalites and trondhjemites and the pyroxene and quartzo feldspathic xenolith suites were produced by the partial melting of basaltic rocks (eclogite or amphibolite) and that their positive Eu anomalies are a primary feature. It is therefore implied that the generation of granodioritic upper crust is probably a three stage process involving the generation of oceanic crust, subduction related volcanism to form theLILE enriched lower crust and finally melting of the lower crust.

The presence of tonalitic/trondhjemitic granulite facies xenoliths of Late Precambrian age at Partan Craig therefore argues against a significant change in crustal forming processes since the stabilisation of large volumes of crust circa 3.0 Ga. It is suggested that detailed study of Palaeozoic high grade terrains would find further evidence for a tonalitic/trondhjemitic lower crust and provide useful information as to the nature of intra-crustal melting processes.

6:5 Conclusions

1) The garnet granulite xenoliths from Partan Craig are metasediments derived from juvenile crust during the Grenvillian Orogeny circa 1200 Ma. The 1100 Ma Rb-Sr whole rock isochron records re-equilibration during regional metamorphism.

2) The quartzo feldspathic and pyroxene granulites from Partan Craig are chemically similar to rocks from Archean gabbro-tonalite - trondhjemite suites. They are derived by partial melting of an amphibolitic/eclogitic source presumably at the base of the lower crust. These xenoliths are of Late Precambrian age derived from an isotopically depleted source and are hence genetically unrelated to the garnet granulites.

3) The basic granulites from Hawks Nib are metagabbroic rocks derived from an isotopically depleted source (εNd + 3.7, εSr - 10) in the Late Precambrian, circa 575 Ma.

4) The garnet granulite xenoliths from Central Ireland are not metasediments being probably of a meta-igneous origin They formed during the Grenvillian Orogeny circa 900 - 1000 Ma.

5) The lower crust beneath the Midland Valley of Scotland is therefore a mixture of Caledonian and Grenvillian aged rocks. The L.I.S.P.B. seismic experiment indicates that the lower and middle crust beneath the Midland Valley of Scotland extends at least as far north as Cape Wrath. The seismically homogeneous nature of these crustal layers suggests they are a possible single structural units of one age. However, the significant variations in the chemical compositions of Caledonian Granites suggests this simple model is not correct and that the seismic data simply record changes in metamorphic grade. There is no evidence of Archean lower crust.

6) The isotopic systematics of the Grenvillian lower crustal rocks are such that they provide a possible source for the pre-tectonic Caledonian granites. Mixing calculations demonstrate that Grenvillian crust is the most likely crustal component involved in the petrogenesis of the post-tectonic Caledonion Granites.

Chapter 7

Implications for the Crustal Evolution of Southern Britain from Nd and Sr Isotope Studies of Crustal Rocks

7:1 Introduction

This chapter presents Nd and Sr isotope results on selected samples of basement granites and gneisses and sediments of Precambrian to Jurassic age from southern Britain and Ireland. They are used to constrain models for the crustal evolution of this area, to assess the relative contributions from new and pre-existing crust in the Caledonian orogeny, and to evaluate the petrogenesis of granitoids of various ages.

The central rationale is that the major fractionation in the Sm/Nd ratio of a crustal rock occurs during derivation from the mantle and that subsequent crustal processes have minimal effect (McCulloch and Wasserburg, 1978). It is therefore possible to obtain some constraints as to the mantle derivation age of crustal rocks from their present day $^{143}Nd/^{144}Nd$ and Sm/Nd ratios. Significantly the majority of crustal rocks have Sm/Nd ratios that lie within the relatively narrow range of 0.17 to 0.21.

However, for the Rb-Sr isotope system the picture is more complicated because there are at least three common intra-crustal processes which can significantly change Rb/Sr ratios;

i) Weathering:- Martin and Meybeck (1979) demonstrate that the weathering cycle results in a significant increase in the Rb/Sr ratio of sediments compared to their source rocks.

ii) Crustal melting:- Crustal melts have higher Rb/Sr ratios than their source rocks due to the presence of plagioclase in the residue.

Figure 7:1 LOCATION MAP FOR SEDIMENTARY SAMPLES

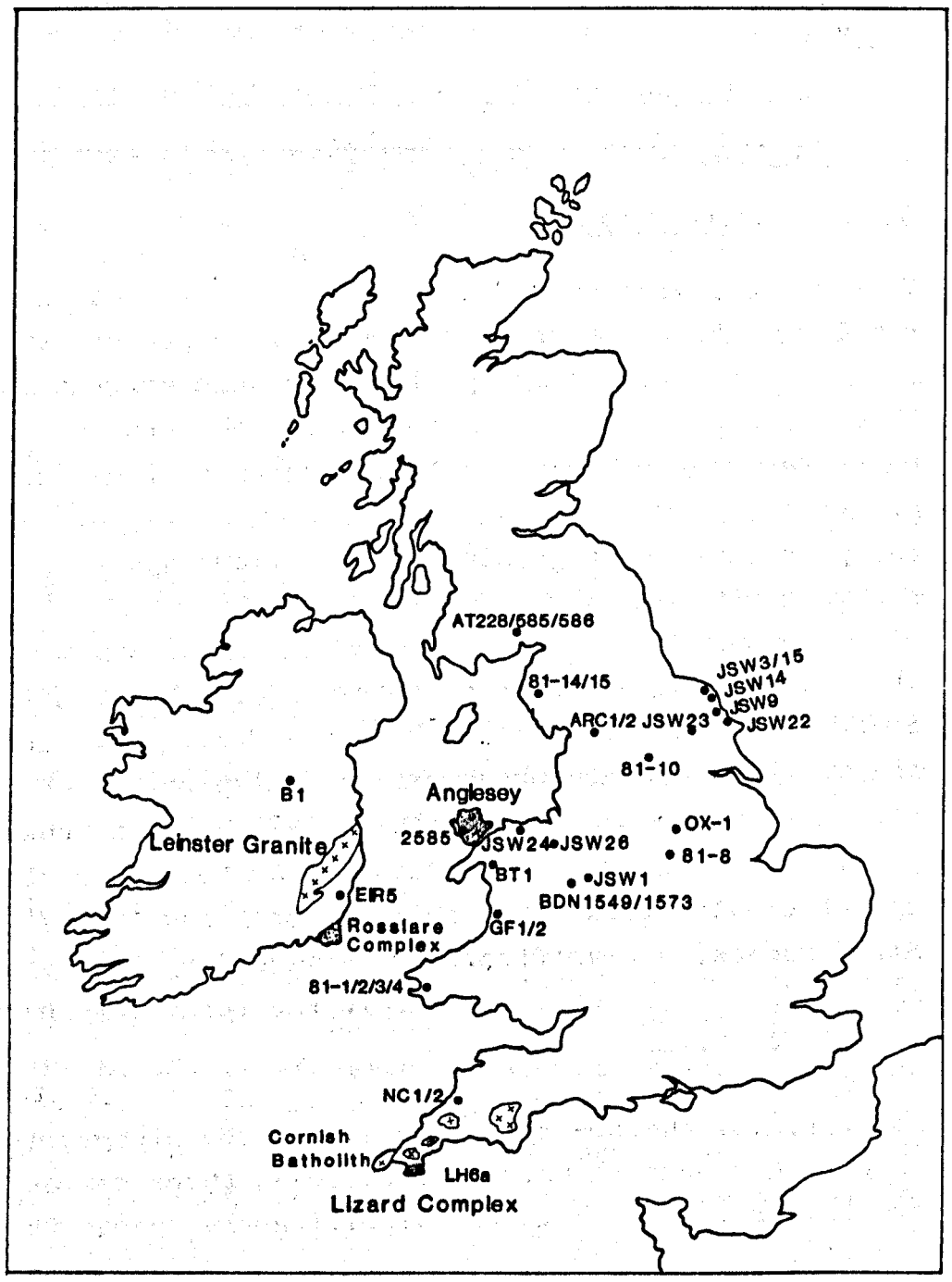

iii) Metamorphism:- Granulite facies metamorphism causes LILE depletion, particularly K and Rb, which results in low Rb/Sr and high K/Rb ratios (e.g. Lewisian granulite facies gneisses (Weaver and Tarney, 1980)).

Except in cases where the latter process is significant, it is usually possible to detect the presence of a large component of "ancient" crust in sedimentary and metamorphic rocks from their high initial $^{87}Sr/^{86}Sr$ ratios. However, their Sr model ages are unlikely to provide direct age information.

This particular study concentrates upon the Late Precambrian and Palaeozoic sediments of southern Britain. The sedimentary rocks probably originate from a wide variety of source regions ranging from Archean basement (Lewisian Complex) to contemporaneous mantle derived material. One aim is to assess the relative importance of the different crustal components and to establish possible spatial and temporal variations recorded in the sediments. One important factor to be considered is the scale of mixing between the different source regions which will be controlled to a great extent by the existing drainage patterns.

7:2 Factors Effecting the $^{143}Nd/^{144}Nd$ and $^{87}Sr/^{86}Sr$ ratios in Seawater

The majority of the sediments analysed in this study are of marine origin and, due to the presence of variable amounts of authigenic material in the sediments, it is necessary to consider the Nd and Sr isotope composition of seawater.

Geochemically Sr and Nd behave differently in present day seawater. Sr is relatively abundant, $\simeq$ 8 mgl^{-1}, and has a relatively long residence time, 10^6 yrs, compared with the mixing time of oceanic waters (10^3 yrs Brass, 1976). Nd, however, is much less abundant, 2.7 ngl^{-1}, and has a short residence time, probably less than 300 yrs (Goldberg, 1965,

Piepgras and Wasserburg, 1980). Despite the variability of the $^{87}Sr/^{86}Sr$ ratios of continental runoff (typically 0.704 to 0.725, see Brass, 1976 for review) the long residence time of Sr in the oceans results in a uniform present day $^{87}Sr/^{86}Sr$ ratio of 0.7091. In contrast Nd isotope ratios show inter- and intra-ocean variations (Atlantic Ocean 0.5119 to 0.5122, Indian Ocean 0.5120 to 0.5123 and Pacific Ocean 0.5124 to 0.5126) (O'Nions et al., 1978, Piepgras et al., 1979, Piepgras and Wasserburg, 1980).

Nd and Sr may enter oceanic waters due to; i) hydrothermal interaction with oceanic crust and ii) continental runoff, both as particulate matter and in solution. The concentration of Sr in solution in river water (0.06 mgl^{-1}) is lower by a factor of 100 compared to seawater, whereas the Nd concentrations in solution in river water is significantly greater (40 compared to 2.7 ngl^{-1}) (Martin and Maybeck, 1979). However, it should be noted that a large proportion of the REE in solution in river water flocculate out in esturine environments and hence do not reach the ocean, (Hoyle et al., in press, Martin et al., 1976).

Alberade et al. (1981) report $^{87}Sr/^{86}Sr$ ratios of hydothermal waters from the East Pacific Rise of 0.703 which indicates almost complete Sr exchange between seawater and oceanic crust. Estimates of the flux of water through MOR indicate that approximately half the amount of Sr that enters the oceans from the continents may exchange with oceanic crust (see Wolery and Sleep, 1976 and Brass, 1976). The Nd isotope ratios of metalliferous sediments precipitated from hydrothermal waters are in equilibrium with seawater and hence the Nd has undergone little, if any, exchange with oceanic crust.

It is therefore apparent that the $^{143}Nd/^{144}Nd$ ratio of seawater primarily reflects the composition of crustal runoff whereas the $^{87}Sr/^{86}Sr$ ratio of seawater is buffered by the interaction with oceanic crust. Authigenic minerals (e.g. clays and carbonates) within a sediment frequently contain a high

proportion of the rocks' Sr but only a small proportion of the Nd. The presence of any authigenic component within present day sediments will therefore lower their $^{87}Sr/^{86}Sr$ ratio except in those sediments derived from juvenile crust.

The variation of the $^{87}Sr/^{86}Sr$ ratio of seawater during the Palaeozoic is well documented from the study of marine carbonates (Peterman et al., 1970, Veizer and Compston, 1974). The data show a minimum value of 0.707 circa 200 Ma with a maximum value of 0.709 both at the present day and during the Late Precambrian (see Figure 7:7). To date there are only published Nd isotope measurements for Lower Ordovician seawater. Hooker et al, (1981) obtained εNd_I values of between - 4.1 and - 6.8 for metalliferous sediments from the Southern Uplands (Figure 7:6). A. Gledhill has kindly supplied unpublished data for Jurassic carbonates which are also plotted in Figure 7:6.

7:3 Samples

The sediment, granite and basement sample localities are plotted on Figure 7:1 which also shows the age provinces of the basement rocks of southern Britain. The approximate ages of the rocks are given in Table 7:1, based on the time scale of Gale et al, (1980).

In order to study possible geographic and temporal variations within the sedimentary column samples were taken from the same stratigraphic period throughout southern Britain (e.g. Carboniferous) and at several horizons within a confined area (the Lower Palaeozoic in Pembrokeshire). Jurassic sediments from a relatively restricted geographic area (Yorkshire to the Midlands) but from several palaeo-environments were also selected to assess the influence of the depositional environment upon their Nd and Sr isotope systematics (JSW 3 and 9 :- non marine, JSW 22, 23 and Ox 1 :- marine and JSW 14 and 15 :- organic rich marine).

Wherever possible fine grained sediments, shales and clays, were samples as they are more likely to be isotopically homogeneous and more representative of the local sedimentary column than immature sediments.

Precambrian basement gneisses and schists were analysed from Anglesey, Rosslare and Rushton in addition to Precambrian sediments from North Wales. Granitoid rocks from Anglesey and the Hercynian Batholith of south west England were also studied.

7:4 Isotope Data

Nd and Sr isotope results of the basement and sedimentary rocks are presented in Table 7:1 and 7:2 and in histogram form in Figures 7:2 and 7:3. There is no distinction between the measured $^{87}Sr/^{86}Sr$ and $^{143}Nd/^{144}Nd$ ratios of the basement and sedimentary rocks. However, the granitic rocks generally have more radiogenic $^{143}Nd/^{144}Nd$ ratios than the sediments. With the exception of the Cornish granites, (Rb/Sr = 5.0 to 5.8 and $^{87}Sr/^{86}Sr$ = 0.7672 to 0.7854) the granitoid rocks have lower Rb/Sr ratios and less radiogenic $^{87}Sr/^{86}Sr$ ratios than the sedimentary and basement rocks (Figure 7:3 and 7:5). The Sm/Nd ratios are presented in histogram form in Figure 7:4 and show a gaussian distribution about 0.19, the average crustal value (McCulloch and Wasserburg, 1978).

7:5 Discussion

The Nd and Sr isotope data are presented in Figure 7:6 and 7:7 as εNd_I and εSr_I values versus time. The solid lines shown in these diagrams are isotopic evolution lines equivalent to an Sm/Nd ratio of 0.19 (average crust) and an Rb/Sr ratio of 1.15 (average value of basement and sedimentary rocks in this study) respectively. The evolution lines are marked with T_{CHUR}/T_{BE} ages. Nd model ages assuming derivation from a

Table 7:1 Isotope data for Crustal Rocks from Southern Britain

Sample	Locality	Rock Type	Stratigraphic Age	Age Ma	Rb[1]	Sr	Rb/Sr	$^{87}Sr/^{86}Sr$	εSr_I	Sm	Nd	Sm/Nd	$^{143}Nd/^{144}Nd$	εNd_I	T^{Nd}_{CHUR}	T^{Nd}_{DM}	T^{Sr}_{BE}
BDN 1549	Rushton	Schist	Precambrian	667	132[3]	64	2.132	0.77956	+236.0	8.218	47.81	0.1719	0.511841 ±10	-7.6	1315	1550	860
BDN 1573	Rushton	Schist	Precambrian	667	145[3]	502	0.297	0.72817	+236.0	7.232	36.10	0.2003	0.511934 ±24	-7.3	1425	1670	1880
2601+	Anglesey	Coedana Granite	Precambrian	603	138	208	0.6635	0.72542	+69.8	2.14	11.92	0.1795	0.512109 ±12	-3.6	920	1270	790
2609+	Anglesey	Coedana Granite	Precambrian	603	142	268	0.5299	0.72156	+62.3	3.788	19.34	0.1959	0.512149 ±10	-3.6	955	1330	820
AS 16+	Anglesey	Gneiss	Precambrian	595	104	75	1.3867	0.73962	+21.2	6.090	30.995	0.1965	0.512198 ±16	-2.7	860	1265	625
2622+	Anglesey	Gneiss	Precambrian	562	87	84	1.0357	0.73233	+60.2	5.820	29.428	0.1978	0.512171 ±18	-3.6	925	1310	670
R7734	Rosslare	Gneiss	Precambrian	600*	185	91	2.0330	0.76762±4	+185.0	6.574	33.035	0.1990	0.511920 ±16	-7.6	1440	1675	760
R7744	Rosslare	Gneiss	Precambrian	600*	137	114	1.2038	0.76030±4	+375.3	5.891	29.58	0.1992	0.511960 ±10	-7.2	1360	1620	1150
2585	Anglesey	Arkose	Precambrian	550						11.688	66.638	0.1754	0.512237 ±16	-1.5	680	1085	
BT1	Bryn Teg	Shale	Precambrian	550	54.1	55.1	0.9819	0.72681±4	+6.6	3.31	16.934	0.1955	0.512144 ±12	-4.2	960	1330	565
ARC 1	Ingleton	Shale	Cambro/Ordo	493	78.6	157.1	0.5003	0.71760±2	+47.2	4.899	24.613	0.1990	0.512248 ±20	-2.8	780	1210	670
ARC 2	Ingleton	Shale	Cambro/Ordo	493	70.1	144.7	0.4845	0.71824±2	+60.8	8.529	43.178	0.1975	0.512259 ±22	-2.6	750	1185	725
JSW 1	Wrekin	Shale	Tremadoc	490	168[2]	93	1.8065	0.74374±4	+42.8	8.848	56.88	0.1556	0.512138 ±24	-3.4	750	1100	535
JSW 24	Bethesda	Shale	Tremadoc	490	122[2]	144	0.8472	0.73153±2	+145.8	2.617	13.17	0.1987	0.512120 ±16	-5.3	1035	1370	800
81/14	Lake District	Slate	Ordovician	475	181.2	137.1	1.3217	0.73620±3	+86.9	9.800	55.01	0.1782	0.512038 ±16	-5.2	930	1350	590
81/2	Pembroke	Shale	L.Arenig	475	64.0	79.0	0.8101	0.72433±4	+61.2	13.92	68.47	0.2033	0.512128 ±18	-5.5	1060	1415	610
81/3	Pembroke	Shale	Arenig/Llanv	460	41.5	55.6	0.7464	0.72449±3	+87.6	4.79	24.28	0.1973	0.512188 ±12	-4.3	890	1285	670
81/1	Pembroke	Shale	Llande/Carad	450	83.2	24.6	3.3821	0.76784±4	+8.3	11.716	61.492	0.1905	0.512046 ±16	-6.9	1110	1430	455
EIR 5	C.Wicklow	Shale	M.Ordovician	450	156.1	155.1	1.0065	0.72733±3	+49.1	6.433	31.794	0.2023	0.512039 ±26	-7.2	1230	1535	565
AT 228	S.Uplands	Greywacke	M.Ordovician	450	64[2]	252.6	0.2534	0.71283±4	+56.4	7.8[a]	40.8	0.1918	0.511974 ±20	-8.3	1250	1530	885
AT 585	S.Uplands	Slate	M.Ordovician	450	101[2]	100	1.01	0.73015±3	+102.6	5.8[a]	29.6	0.1960	0.511911 ±28	-9.7	1420	1660	630
AT 586	S.Uplands	Slate	M.Ordovician	450	148[2]	135	1.0963	0.73173±3	+102.1	6.5[a]	32.1	0.2025	0.511915 ±24	-9.9	1490	1715	615
GF 1	Glanfred	Shale	M.Silurian	415	124.1	123.2	1.0073	0.72685±3	+76.5	11.62	79.77	0.1457	0.512059 ±16	-5.6	815	1140	550
GF 2	Glanfred	Shale	M.Silurian	415	109.3	73.5	1.4871	0.73510±3	+76.7	2.40	9.452	0.2539	0.512150 ±18	-7.3	1725	1950	510
JSW 26	Llanollen	Shale	Wenlock	415	156[2]	157	0.9936	0.73198±4	+152.7	7.485	40.47	0.1850	0.512017 ±22	-7.7	1120	1425	690

Sample	Locality	Rock Type	Stratigraphic Age	Age Ma	Rb[1]	Sr	Rb/Sr	$^{87}Sr/^{86}Sr$	ε_{Sr_I}	Sm	Nd	Sm/Nd	$^{143}Nd/^{144}Nd$	ε_{Nd_I}	T^{Nd}_{CHUR}	T^{Nd}_{DM}	T^{Sr}_{BE}
81/15	Lake District	Shale	Wenlock	415	138.2	84.6	1.6336	0.74511±2	+182.8	5.16	28.22	0.1830	0.512024 ±22	-7.5	1095	1400	610
LH 6a	Lizard	Slate	? pre-375							8.752	49.866	0.1755	0.512032 ±16	-7.3	1025	1340	
B1	C.Eire	Shale	L.Carb	330	77.3	103.0	0.7503	0.71956±4	+71.5	7.264	32.74	0.2219	0.511981 ±12	-10.2	1600	1820	500
NC 1	N.Cornwall	Shale	L.Carb	330	38.8	59.8	0.6488	0.72292±3	+138.9	4.439	23.278	0.1907	0.512026 ±14 0.512034 ±18	-8.4	1135	1450	1015
NC 2	N.Cornwall	Shale	L.Carb	330	161.4	79.7	2.0251	0.74130±3	+133.3	2.826	15.43	0.1832	0.512009 ±10	-8.7	1120	1425	445
81/4	Pembroke	Shale	Coal Meas.	300	95.2	55.7	1.7092	0.74168±2	+229.5	9.789	65.05	0.1505	0.511927 ±24	-9.9	1030	1310	535
81/10	S.Yorks	Shale	Coal Meas.	300	110.6	84.7	1.3058	0.73396±4	+191.0	5.405	30.89	0.1750	0.511916 ±24	-10.7	1215	1480	560
81/8	Leic.	Shale	Permian	270	165.4	53.0	3.1208	0.78919±4	+707.8	15.496	79.23	0.1956	0.511924 ±20	-11.3	1385	1640	660
JSW 14	N.Yorks	Shale	U.Lias	185	181[2]	141	1.2837	0.72730±4	+185.0	5.132	26.04	0.1971	0.511921 ±14	-12.2	1415	1515	440
JSW 15	N.Yorks	Shale	U.Lias	185	148[2]	475	0.3116	0.71175±5	+69.5	4.347	22.558	0.1927	0.519962 ±20	-11.4	1310	1580	610
JSW 3	N.Yorks	Shale	M.Jurassic	170	126[2]	208	0.6058	0.71562±3	+97.7	6.116	32.601	0.1876	0.511816 ±20	-14.4	1595	1785	460
JSW 9	N.Yorks	Shale	M.Jurassic	170	144[2]	130	1.1077	0.72458±3	+175.0	2.597	13.56	0.1915	0.511953 ±16	-11.7	1330	1595	450
OX/1	Bucks	Clay	Oxford Clay	155									0.511941 ±20	-12.0	1305	1565	
JSW 22	N.Yorks	Clay	Kimmeridge	150	161[2]	293	0.5495	0.71317±4	+74.7	9.854	51.99	0.1895	0.511920 ±14	-12.5	1395	1640	400
JSW 23	N.Yorks	Clay	Kimmeridge	150	120[2]	339	0.3540	0.71144±2	+67.2	8.533	45.10	1.892	0.511843 ±20	-14.0	1540	1745	505

*Age of Rosslare Complex unknown

Rb/Sr determined by XRF [1] Nottingham [2] Open University

[a] REE by INAA (Tindle pers com)

[+] Rb/Sr data from Beckinsale and Thorpe 1979

[3] Rb/Sr data from Beckinsale (pers com)

Table 7:2 Isotope data for the S.W.England Batholith

Sample	Rb	Sr	Rb/Sr	$^{87}Sr/^{86}Sr$	εSr_{270}	Sm	Nd	Sm/Nd	$^{143}Nd/^{144}Nd$	εNd_{270}
C202	453.9	80.34	5.650	0.78544 ±4	+252	6.878 6.896	37.457 37.67	0.1836 0.1830	0.512181 ±18	-6.0
C205	429.7	73.7	5.830	0.77734 ±4	+109	7.395 7.404	39.76 39.87	0.1860 0.1857	0.512184 ±22 0.512206 ±34	-5.8
Pe 33+	488	96	5.083	0.76724 ±4	+86	7.4	33.5	0.2209	0.512175 ±26	-6.9
Pe 36+	212	96	2.208	0.76724 ±5	+542	6.9	32.9	0.2097	0.512160 ±10	-7.0
Pe 69+						6.5	30.8	0.2110	0.512160 ±18	-7.0
P 1	667.1	21.6	30.884	1.08360 ±10	+332	5.614	34.17	0.1643	0.512217 ±10	-4.9
D 1	493.2	97.99	5.033	0.76707 ±10	+91	6.56	34.60	0.1896	0.512184 ±18	-6.1

+Samples supplied by Julian Pearce ,Sm,Nd by INAA

FIGURE 7:2 $^{143}Nd/^{144}Nd$ HISTOGRAM FOR CRUSTAL ROCKS

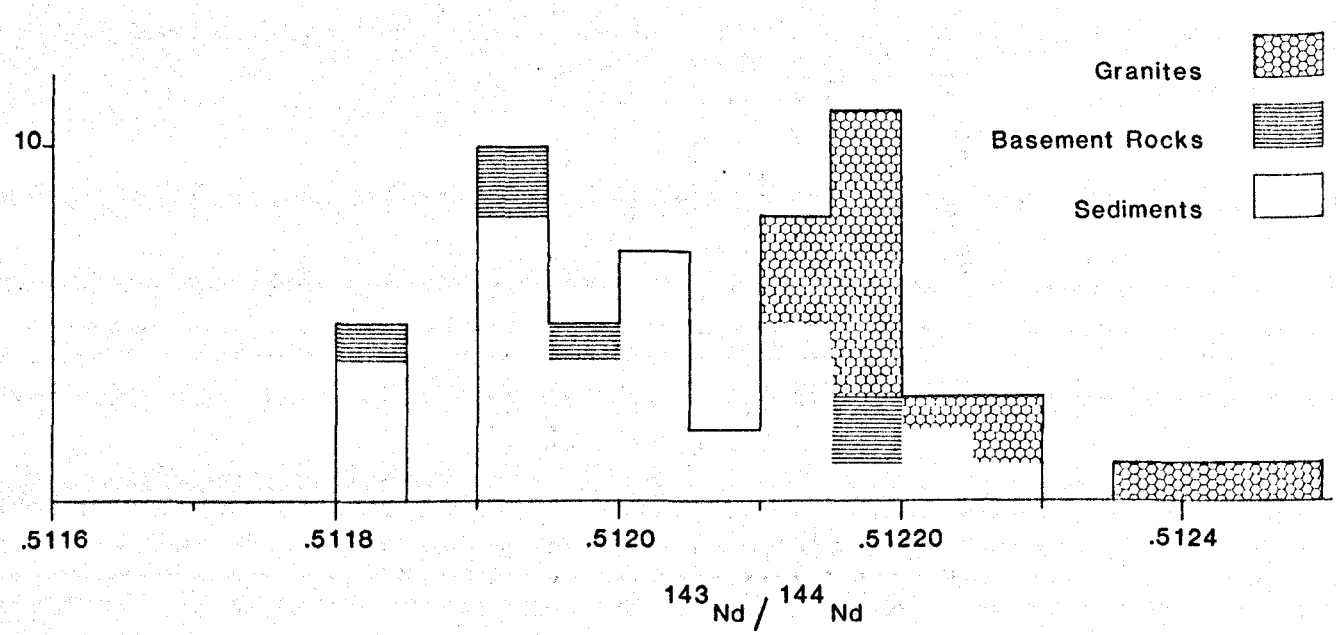

FIGURE 7:3 $^{87}Sr/^{86}Sr$ HISTOGRAM FOR CRUSTAL ROCKS

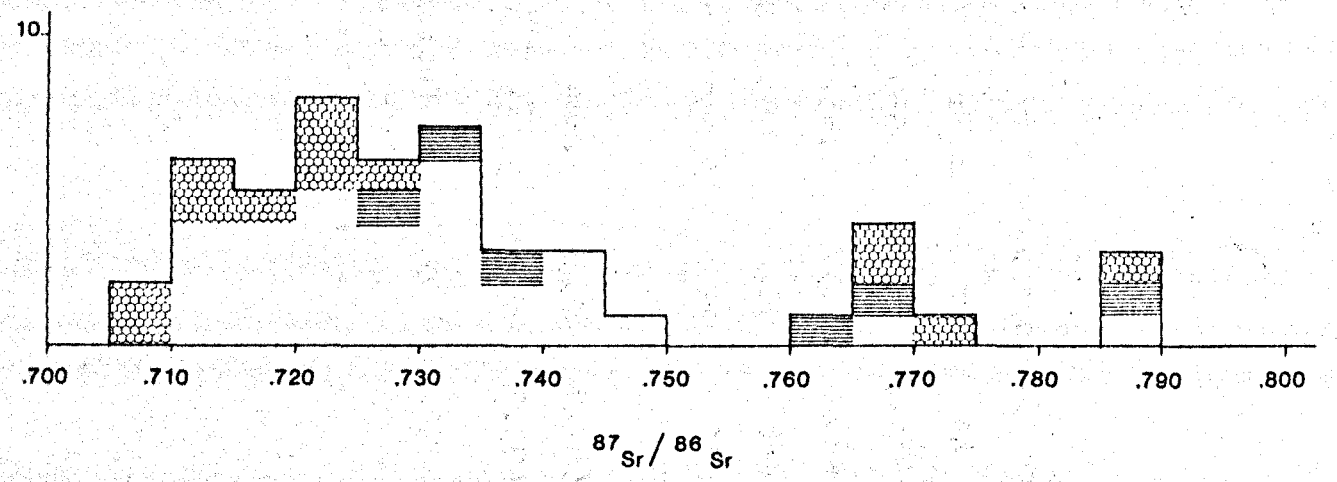

FIGURE 7:4 Sm/Nd HISTOGRAM FOR CRUSTAL ROCKS

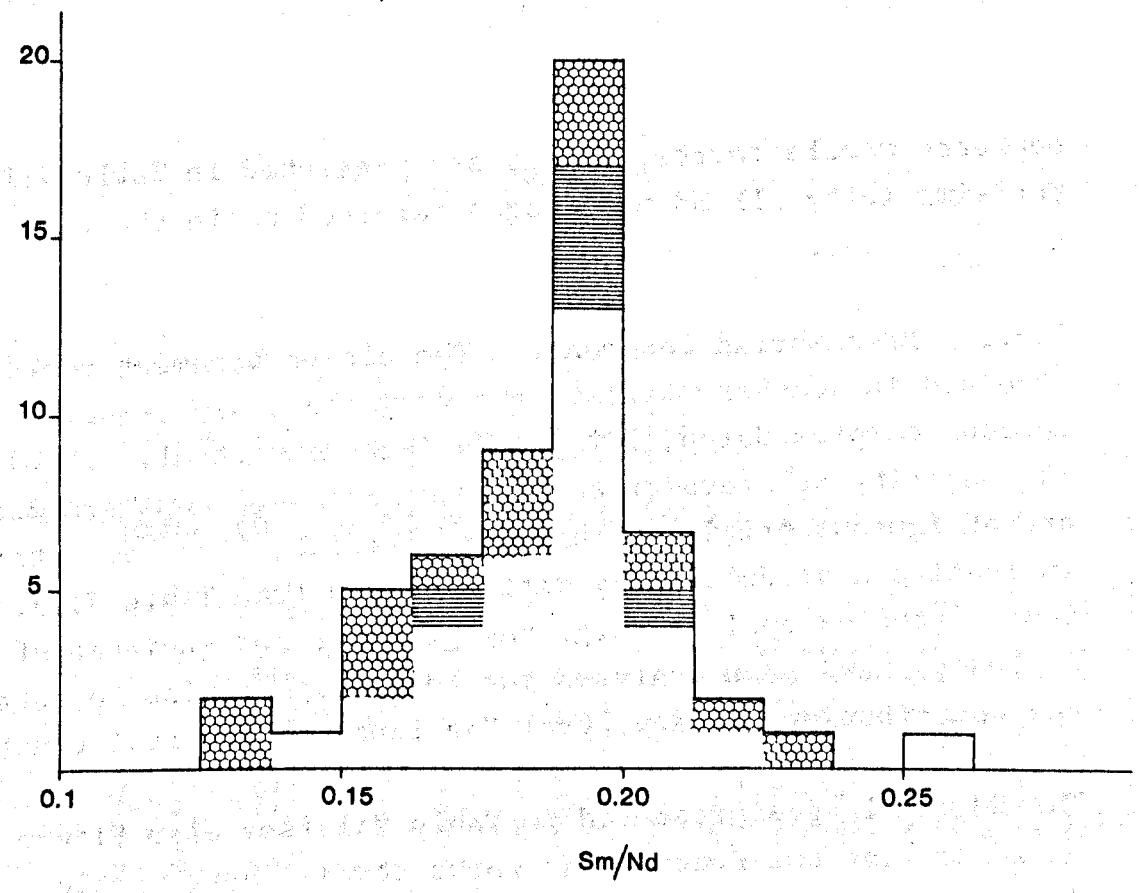

See Figure 7:2 for legend

FIGURE 7:5 Rb/Sr HISTOGRAM FOR CRUSTAL ROCKS

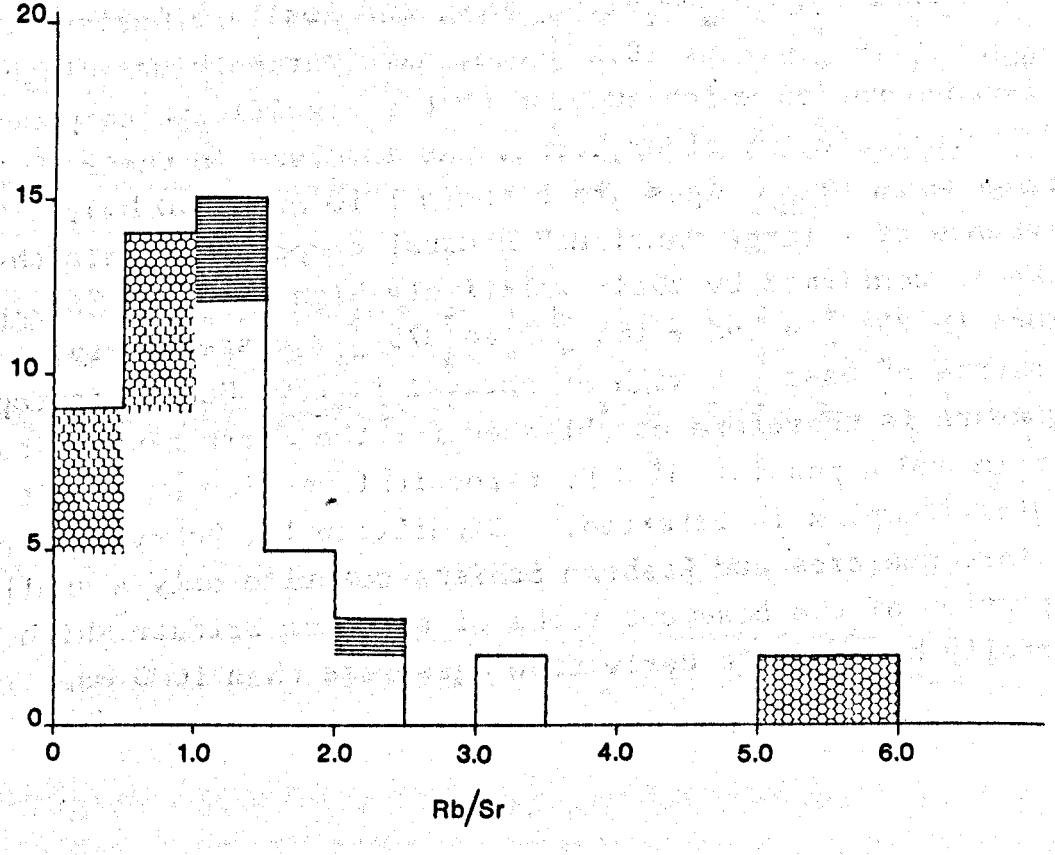

depleted mantle source, T_{MORB}, are presented in Table 7:1. For simplicity all Nd model ages referred to in the text will be T_{CHUR} ages.

7:5:1 Precambrian Basement. The oldest basement rocks recorded in southern Britain are from the Stanner-Hanter igneous complex Salop, 702 $\pm$ 8 Ma (Patchett et al., 1980). The majority of Precambrian basement rocks of southern Britain are of igneous origin and have low initial $^{87}Sr/^{86}Sr$ ratios indicating a predominantly mantle origin (see Table 7:2). Some of the exceptions (e.g. the granites and gneisses of Anglesey) have been analysed for Nd isotope ratios to establish the contribution, if any, from "ancient" continental crust.

The Nd model ages presented in Table 7:1 (see also Figure 7:6) indicate that the Precambrian rocks studied have mantle derivation ages over 200 Ma greater than their geological ages. It should be noted that the Rosslare Complex has not yet been successfully dated and that the εNd_I and εSr_I values presented in Table 7:1 are calculated at 600 Ma purely to facilitate direct comparison with the Anglesey Complex (see Chapter III). The Rushton Schists, $\varepsilon Nd_I = -7.4 \pm 0.4$, and Rosslare Gneisses, $\varepsilon Nd_{600} = -7.4 \pm 0.2$ to -8.2 ± 0.3, have markedly unradiogenic Nd isotope ratios which suggest that a significant component of Mid Proterozoic, or older, crust was involved in their petrogenesis (T_{CHUR} ages are between 1310 and 1440 Ma). The existence of a large "ancient" crustal component within these rocks is confirmed by their relatively high εSr_I and εSr_{600} values ($+ 236 \pm 4$ and $+ 185 \pm 2$ to 375 ± 2 respectively). The existence of basement with an ancient (>1300 Ma) Nd isotopic signature is therefore established for the first time in southern Britain and a possible Mid Proterozoic formation age for the Rosslare Complex is inferred. Significantly, however, the Rosslare gneisses and Rushton Schists comprise only a small proportion of the basement rocks of southern Britain which generally have mantle derivation ages less than 1000 Ma.

TABLE 7:3 ISOTOPIC AGE DATA FOR LATE PRECAMBRIAN - LOWER PALAEOZOIC IGNEOUS ROCKS FROM ENGLAND AND WALES

Rock Unit	Age *(Ma)	Method	$(^{87}Sr/^{86}Sr)i$	Comment	Reference
Stanner - Hunter Complex	702 ± 8	Rb-Sr whole rock	0.7053 ± 3	Magmatic age	Patchett et al. (1980)
Malvernian Complex	681 ± 53	Rb-Sr whole rock	0.7049 ± 5	Magmatic age	Beckinsale et al. (1981)
	670 ± 10	U-Pb monazite			Patchett (unpub)
	Ca.600	U-Pb zircon			
Johnston Complex	643^{+5}_{-28}	U-Pb zircon		Lower intercept of intersection with concordia. Magmatic age cannot be 720 Ma	Patchett & Jocelyn (1979)
St Davids granophyre	587^{+25}_{-14}	U-Pb zircon			Patchett & Jocelyn (1979)
		(Rb-Sr whole rock	0.7037 - 0.7053)		
Coedana granite	603 ± 34	Rb-Sr whole rock	0.7086 ± 9	Magmatic age	Beckinsale & Thorpe (1979)
					Patchett (unpub)
Mona Complex metamorphism (1)	595 ± 12	Rb-Sr whole rock	0.7061 ± 3	Metamorphic age	Beckinsale & Thorpe (1979)
Mona Complex igneous event (2)	562 ± 31	Rb-Sr whole rock	0.7081 ± 8	Magmatic age	Beckinsale & Thorpe
Eastern Uriconian volcanic rocks	558 ± 16	Rb-Sr whole rock	0.7044 ± 16	Probable magmatic age	Patchett et al. (1980)
Rushton schist	536 ± 8	Rb-Sr biotite		Mineral cooling age	Patchett et al. (1980)
Ercall granophyre	533 ± 1	Rb-Sr whole rock	0.7057 ± 16	Magmatic age	Patchett et al. (1980) plus 2 additional analyses
Charnwood S diorites	540 ± 57	Rb-Sr whole rock	0.7058 ± 8	Magmatic age	Cribb (1975)
S Leicestershire diorites	(535 ± 22)	Rb-Sr whole rock	0.7053-0.7061	A clear discrepancy	Cribb (1975)
	452 ± 8 / 6	U-Pb zircon		The U-Pb age is an upper intersection agreeing with the U-Pb age for the Mountsorrel granite and is most likely to be correct. Range of initial $^{87}Sr/^{86}Sr$ ratios calculated using U-Pb age.	Pidgeon & Aftalion (1978)
Mountsorrel granite	(423 ± 17)	Rb-Sr whole rock	0.7060-0.7066		
Sarn complex	522 ± 19	Rb-Sr whole rock	0.7098 ± 3	Probable magmatic age	
Parwyd metamorphic rocks	581 ± 9	Rb-Sr whole rock	0.7066 ± 2	Metamorphic age (preliminary result for 3 points; MSWD 0.9)	
TWT Hill granite	498 ± 7	Rb-Sr whole rock	0.7095 ± 11	Magmatic age	
Charnwood N diorites	(304 ± 90)	Rb-Sr whole rock		Discrepant result, doubtful significance	Cribb(1975)
Ingletonian sediments	493 ± 17	Rb-Sr whole rock	0.7062 ± 13	Diagenesis and/or low grade metamorphism. Errors x 2.53 to reduce MSWD to 1	

* Calculated using decay constants recommended by Steiger and Jager (1974). Crib $^{87}Sr/^{86}Sr$ ratios quoted relative to 0.7080 for the Eimer and Amend standard

Figure 7:6 ε_{Nd} vs Time for crustal rocks of Southern Britain

Sedimentary rocks

Sedimentary rocks from the Southern Uplands

A Anglesey RS Rushton Schists RC Rosslare Complex

The faint solid lines marked with ages, e.g. T = 700 Ma, represent Nd isotope evolution lines for a rock having the average sedimentary Sm/Nd ratio determined from this work (also equivalent to the average upper crustal Sm/Nd ratio determined by previous workers, e.g. McCulloch and Wasserburg, 1978). With the exception of the Rosslare Complex and Rushton Schists the basement rocks of Southern Britain have late Precambrian Nd model ages. The most significant aspect of the diagram is that sediments younger than the Ordovician (< 425 Ma) have progressively older Nd model ages. Sediments from the Southern Uplands provide the key to the interpretation of the sedimentary data in that they represent a mixture between juvenile Caledonian crust and Archean/Proterozoic detritus (O'Nions et al., 1983) and hence, have Nd model ages that span almost the entire range of those from Southern Britain. Note that Nd model ages for seawater reflect the Nd isotope composition of the sediments forming at the same time. (Data from Hooker et al., 1981, Piepgras et al., 1979 and A Gledhill, pers. comm.)

The Nd isotope compositions of the Leinster and Cornwall Granite Btholiths indicate derivation from crustal sources with late Precamrbian Nd model ages.

Figure 7:6 εNd_I vs TIME FOR CRUSTAL ROCKS OF SOUTHERN BRITAIN

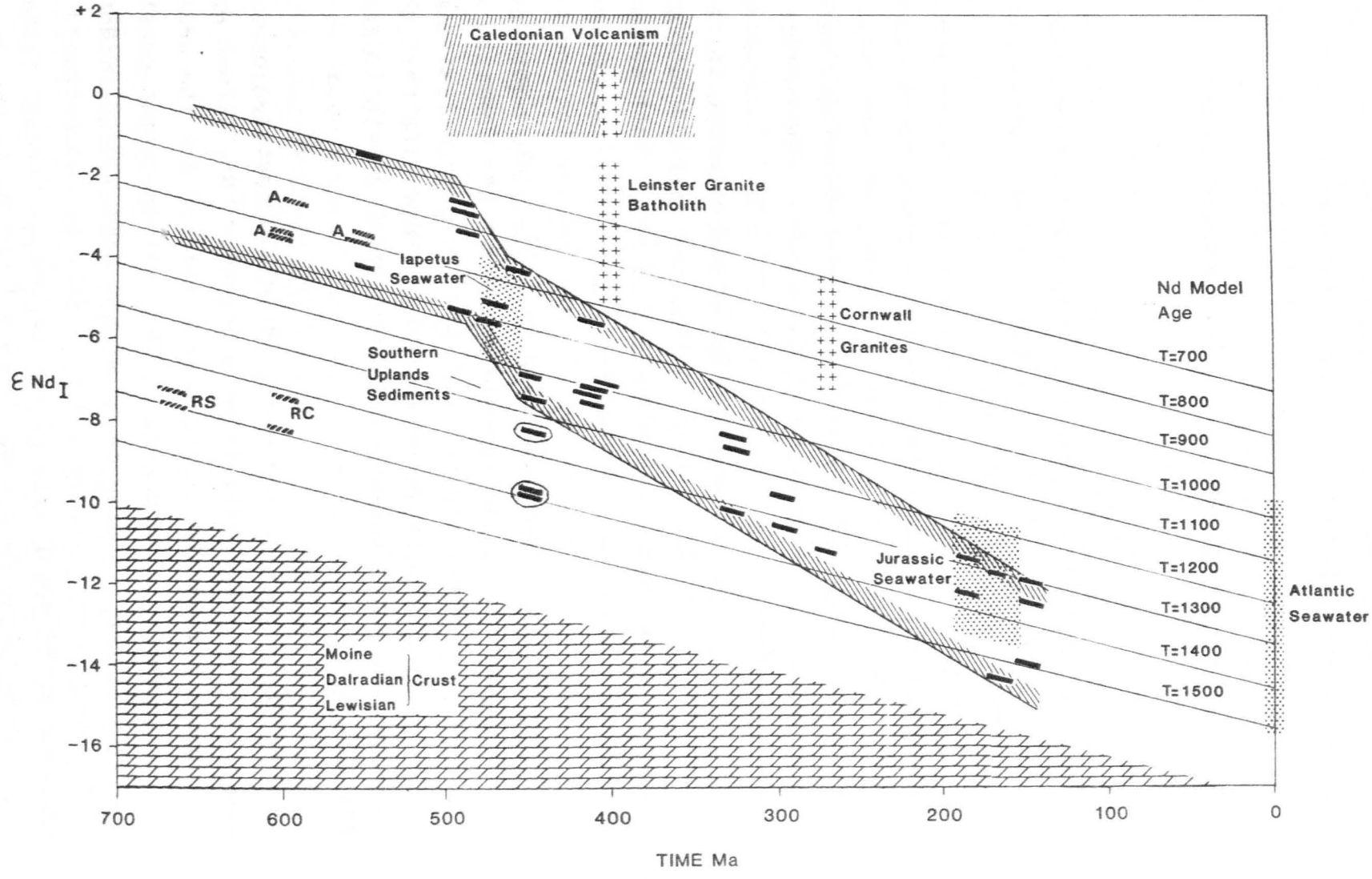

7:5:2 Late Precambrian and Palaeozoic Sediments. Sediments of Late Precambrian age (BT1 and 2585) have Nd model ages between 700 and 950 Ma suggesting that their dominant source regions were of Late Precambrian age and that a Mid Proterozoic component is much less important in these rocks compared to, for example, the Rushton Schists.

During the Late Precambrian and the majority of the Lower Palaeozoic there was apparently widespread intermittent igneous activity associated with the closure of the Iapetus Ocean (Caledonian Orogeny see Thorpe et al., in press). An interesting aspect of this situation is that juvenile crust will have radiogenic Nd isotope ratios and hence young model ages (600 - 400 Ma) such that the addition of significant new crust ($>$20% see Figure 7:9) would result in a detectable lowering of the Nd model ages of the sedimentary pile. Obviously a major period of crustal addition (e.g. formation of large granitoid batholiths) would not become immediately apparent in the sedimentary pile, but depending upon the erosion rate of the crust would be evident within circa 50 Ma. When compared with Precambrian basement and sediments, the Cambrian and Lower Ordovician sediments show no evidence for the introduction of radiogenic crustal material (Figure 7:6). This would suggest that the volume of crust generated during the Cambrian was insignificant when compared with that of the pre-existing crust, i.e. less than 20% by volume, further suggesting that the Cambrian was not a period of major crustal growth in southern Britain.

Interestingly younger sediments (Middle Ordovician onwards) actually show progressively more negative εNd_I values with time, the opposite relationship to that predicted for the addition of juvenile crust. The change in εNd_I values cannot purely be accounted for by the reworking of the same crustal material which is becoming progressively older. This is demonstrated by the increase in Nd model ages of the sediments from an average of 860 ± 80 Ma prior to 475 Ma to 1410 ± 100 Ma in the Upper

Jurassic (see Figure 7:6). The maximum Nd model age recorded by the Jurassic sediments is 1590 $\pm$ 40 Ma. These data therefore record the progressive addition of "ancient" crustal material to the sedimentary column of southern Britain for a period of 300 Ma. There are two possible source regions for this "ancient" crustal component; i) the Precambrian basement of southern Britain which has a large Proterozoic compenent, i.e. Rushton Schists and Rosslare Complexes, ii) the mixed Archean and Proterozoic terrains of northern Europe and America. However, the Precambrian rocks of southern Britain are considered an unlikely source because of; a) their small volume, b) the Rosslare Gneisses and Rushton Schists were unconformably overlain by sediments for a significant proportion of the Lower Palaeozoic, and c) the maximum Nd model age recorded by the Jurassic sediments is significantly greater than those of the Rushton and Rosslare rocks. Thus the mixed Archean and Proterozoic terrains of northern Europe and America are the more likely source areas for the "ancient" crustal component and this is supported by the southerly transport directions of the majority of Carboniferous and younger sediments (Benison and Wright, 1970).

The Nd isotope systematics of the Lower Palaeozoic sediments therefore record the introduction of an "ancient" crustal component beginning circa 450 Ma. Interestingly McKerrow and Cocks (1976) propose from palaeontological evidence that the Iapetus Ocean was circa 2000 Km wide at 450 Ma. The data presented above suggest that this distance is too great or that a mixed Archean/Proterozoic landmass (that is no longer evident) existed in the region of southern Britain during the Ordovician/ Silurian.

The Nd isotopic composition of Lower Palaeozoic sediments from the Southern Uplands are reported in Table 7:1 and by O'Nions et al. (1983) (see Figure 7:6). These rocks represent continental detritus formed on the northern margin of the Iapetus Ocean and the large range in εNd_I values (-4 $\pm$ 0.3 to - 10.4 $\pm$ 0.3) indicate the mixing of variable amounts of juvenile Caledonian

crust with detritus from the mixed Proterozoic/Archean terrain of Scotland. The εNd_I values of Lower Ordovician metalliferous sediments from the Southern Uplands (- 4.1 $\pm$ 0.3 to - 6.6 $\pm$ 0.3) represent the isotopic composition of Iapetus seawater. The seawater composition therefore has a more radiogenic isotopic composition than the average crustal runoff recorded by the Southern Uplands shales (εNd_{470} = -6.8 $\pm$ 1.8) and indicates that a significant juvenile crustal component was added to the ocean waters elsewhere, possibly from southern Britain.

The εNd_I values of Jurassic carbonates and fossils (i.e. seawater composition (εNd_I - 10.5 to - 13.4, A.Gledhill pers. com.) encompass almost the entire range of the Jurassic sediments of southern Britain indicating that the Nd is derived from a similar crustal source. Moreover the Nd model ages of the Jurassic sediments and seawater are within the range of Atlantic seawater (O'Nions et al., 1978, Piepgrass et al., 1979). Thöni et al. (1983) report Nd isotope data for present day (British) off shore and river sediments that are also within the range of Atlantic seawater. It can therefore be concluded that the Nd model age of the sedimentary material formed in southern Britain since the Jurassic has probably been relatively constant. Another significant aspect of the Nd model ages of the Jurassic to recent sediments is that they are similar to the average value of the world's major rivers (Thoni et al., 1983). An Nd model age of between 1200 and 1300 Ma for the average present day crustal runoff considerably constrains possible crustal evolution models. For example models proposing the formation of the majority of present day crust during the Archean and subsequently reworking it, would result in an average Nd model age for the crust greater than 2.0 Ga and are hence untenable. The available Nd isotope data for crustal rocks are most compatible with models in which crust is first stabalised circa 3.6 Ga and subsequently grows by episodic or continuous linear accretion (Depaolo, 1980, Jacobsen and Wasserburg, 1979). To date published Nd isotope data do not conflict with an

approximate constant crustal growth rate. Further studies, particularly of Mid and Late Proterozoic sediments may enable possible variations in crustal growth rates to be evaluated.

7:6 The Efficiency of Nd Mixing within the Sedimentary Column

A preliminary study was undertaken on the homogeneity of Nd isotope ratios within the sedimentary column on a local and regional scale. Pairs of samples from four localities (see Table 7:1) display a maximum variation in εNd of $\pm$ 1.0 indicating there is very little Nd isotope heterogeneity on a local scale. Similarly the Lower to Upper Jurassic sedimentary rocks collected from several depositional environments within Yorkshire and the North Midlands only show a variation in εNd_I of $\pm$ 1.6 (see Table 7:2) suggesting that the deposition environment has no significant control on the Nd isotope systematics of these fine grained sediments. The Carboniferous shales sampled from all over southern Britain also show small variation in εNd_I, $\pm$ 1.0, (see Table 7:1) and therefore in marked contrast to the situation in northern Britain, where O'Nions et al. (1983) report εNd_I variations for Dalradian and Lower Palaeozoic sediments of $\pm$ 5 and $\pm$ 4.5 respectively, the sediments in southern Britain are relatively homogeneous within a single stratigraphic unit. This suggests that the Palaeozoic sediments in southern Britain were deposited in a more mature sedimentary environment compared with northern Britain.

7:7 Rb-Sr Isotope Systematics of the Crustal Rocks of Southern Britain

As with the εNd_I data, the εSr_I data for the Precambrian basement rocks of southern Britain cluster into two groups, with the Rushton Schists and Rosslare Gneisses having significantly more radiogenic εSr_I values, 185 $\pm$ 2 to 375 $\pm$ 2, compared with less than 75 for the remainder of the Precambrian basement. These data suggest that the Rushton and Rosslare rocks contain large "ancient" crustal components.

In section 7:1 some effects of intra-crustal processes on the Rb-Sr systematics of crustal rocks were considered and it was suggested that the Sr model ages of crustal rocks with polyphase histories are unlikely to have meaningful age significance. Figure 7:8 demonstrates that the Sr model ages, T_{BE}, of the crustal rocks in this study are generally lower than their Nd model ages due to a combination of fractional crystallisation, weathering and intra-crustal melting. The Sr model ages of the Rushton and Rosslare samples therefore cannot be used to assess the age of their precursors.

The Palaeozoic sediments show a general increase in their εSr_I values with time (Figure 7:7). However, Sr model ages remain relatively constant and therefore suggest that no "ancient" crustal component has been introduced to the sedimentary column as is indicated by the increase in the Nd model ages. There are three possible factors that could explain this decoupling between the Rb-Sr and Sm-Nd isotope systematics;

i) the introduction of basaltic material:- The Sr content of basalts (> 200 ppm) are greater than of sediments (< 100 ppm) whereas the reverse if true for Nd (< 15 ppm compared to $\simeq$ 35 ppm). Thus the effect of adding basaltic material to a sedimentary pile would be to lower the Sr model age to a greater degree than the Nd model age (see Figure 7:8).

ii) the introduction of old LILE depleted crust:- Adding LILE and L.REE enriched crust to a Palaeozoic sedimentary pile would result in lower εNd_I and higher εSr_I values. If, however, old LILE depleted crust (e.g. Lewisian granulite facies gneisses) were the source of the detritus than both εNd_I and εSr_I values of the sedimentary pile would be lowered.

iii) Authigenic material:- As discussed in section 7:2 authigenic material contains relatively high Sr and low Nd contents and due to the unradiogenic $^{87}Sr/^{86}Sr$ ratios of seawater (see Figure 7:7) the εSr_I values of a Palaeozoic sediment with a large authigenic component would be lowered (Figure 7:8).

Figure 7:7 εSr vs Time for crustal rocks of southern Britain

Sedimentary rocks

Precambrian basement gneisses and granites

A Anglesey R.S. Rushton Schists R.C. Rosslare Complex

The faint solid lines marked with ages, eg T = 500 Ma, represent Sr isotope evolution lines for a rock having the average Rb/Sr ratio determined in this work, 1.15. Interestingly the Sr model ages of samples are generally significantly less than their Nd model ages (see section 7:7 for a discussion of the effects of crustal processes on Rb/Sr ratios).

Note that with the exception of the Rosslare Complex and Rushton Schists, sediments and basement rocks have Sr model ages less than 800 Ma.

The Sr isotope evolution path for seawater is extrapolated curve from the data of Peterman et al. 1970 and Veizer and Compston, 1974.

Figure 7:7 εSr_I vs TIME FOR CRUSTAL ROCKS OF SOUTHERN BRITAIN

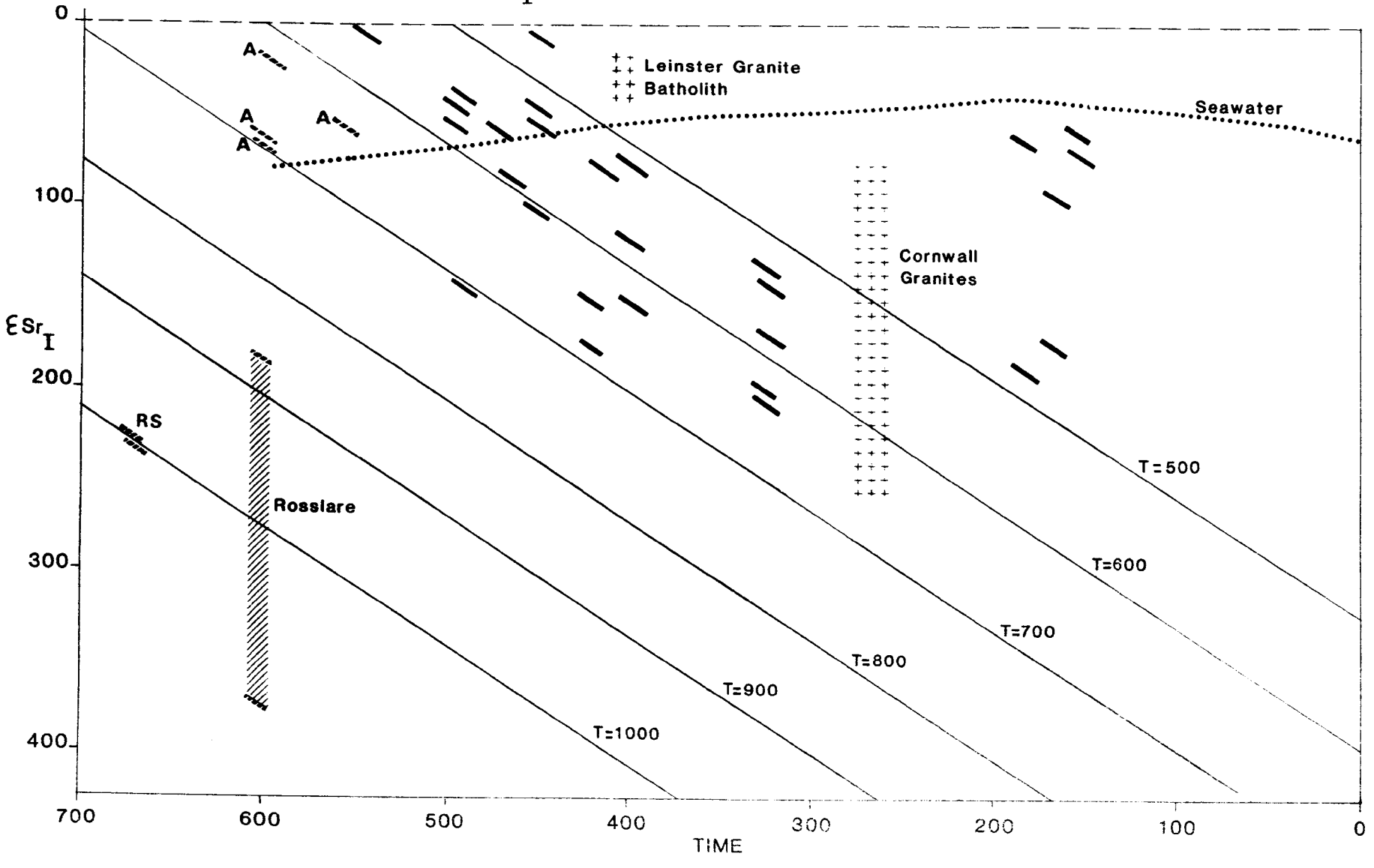

Due to the large increase in the Nd model ages of sediments during the Palaeozoic, with little resultant change in their Sr model ages, it is considered that the latter two processes were probably important in generating their εSr_I values. Notably of all the Palaeozoic sediments, the Jurassic samples have the lower Rb/Sr ratios and the greatest disparity between their Nd and Sr model ages (Figure 7:8). These samples have high Sr contents, 200 to 475 ppm, compared to an average of 100 ppm for the remaining Palaeozoic shales (max = 160 ppm) and have εSr_I values that approach those of Jurassic seawater. It is therefore probably that the Jurassic sediments contain a large Sr rich authigenic component which causes their low εSr_I values and Rb/Sr ratios.

7:8 Crustal Formation during the Caledonian Orogeny

One of the aims of this combined Nd and Sr isotope study was to calculate the amount of juvenile crust added to southern Britain during the Caledonian Orogeny. It was shown in Figures 7:6 and 7:9 that during the Cambro-Ordovician period the addition of new crust was not detectable (i.e. less than 20% added) and that sediments formed subsequent to the closure of the Iapetus Ocean record the introduction of an "ancient" L.REE enriched, possibly LILE depleted, crustal component. It is not possible to precisely constrain the volume or isotopic composition of this "ancient" crustal component and hence it is impossible to assess the amount of juvenile crust formed during the Caledonian Orogeny from the sedimentary record. If a Nd model age of 2.2 Ga is assumed for the "ancient" crustal component, approximately 40% of the present day crust of southern Britain is derived from this source.

7:9 Petrogenesis of Granitoids in Southern Britain

Having constrained the Nd and Sr isotope systematics of the major crustal rocks of southern Britain, a preliminary study was made of the petrogenesis of some granitoids in terms of three components; Late Precambrian basement (T_{CHUR} = 900 $\pm$ 50 Ma, T_{BE} 700 $\pm$ 100 Ma), sediments (T_{CHUR} = 1000 to 1600 Ma,

Table 7:3

Sample	Sample Type	Locality	Stratigraphic Age	εNd_{175}	T_{CHUR} Ma
JSW 3	Freshwater Shale		M. Jurassic	-14.3 ± 0.4	1590 ± 30
JSW 9	" "		M. Jurassic	-11.7 ± 0.3	1330 ± 40
JSW 22	Marine Clay		U. Jurassic	-12.3 ± 0.3	1390 ± 40
JSW 23	" "		U. Jurassic	-13.8 ± 0.2	1540 ± 30
Ox 1	" "		U. Jurassic	-11.8 ± 0.3	1310 ± 40
JSW 14	Alum Shale		L. Jurassic	-12.3 ± 0.3	1410 ± 40
JSW 15	Bituminous Shale		L. Jurassic	-11.5 ± 0.4	1310 ± 30

Figure 7:8 $\frac{Nd}{Sr}$ Model Age vs Rb/Sr

This diagram demonstrates the general disparity between the Nd and Sr model ages of crustal rocks.

Chemical weathering of a rock results in detritus with a higher Rb/Sr ratio (preferential dissolution of Sr) but with an equivalent Sm/Nd ratio. Partial melting produces the same result in the melts only to a more extreme degree (e.g. Cornish Granites). Residues after melt extraction therefore have similar Sm/Nd, but lower Rb/Sr ratios. LILE depletion during granulite facies metamorphism has an equivalent effect.

The introduction of an authigenic component into a sedimentary rock has a marked effect on the Sr isotope systematics, but little on Nd isotopt systematics; the authigenic component will have a high Sr concentration and relatively low $^{87}Sr/^{86}Sr$, whereas the Nd concentration is low and the $^{143}Nd/^{144}Nd$ ratio is probably similar to that of the sediment (seesection 7:2).

One other factor may effect the Sr and Nd isotope systematics of crustal rocks, the introduction of mantle derived material; due to its higher Sr/Nd ratio compared to the crust, Sr model ages will be lowered to a greater degree than Nd model ages.

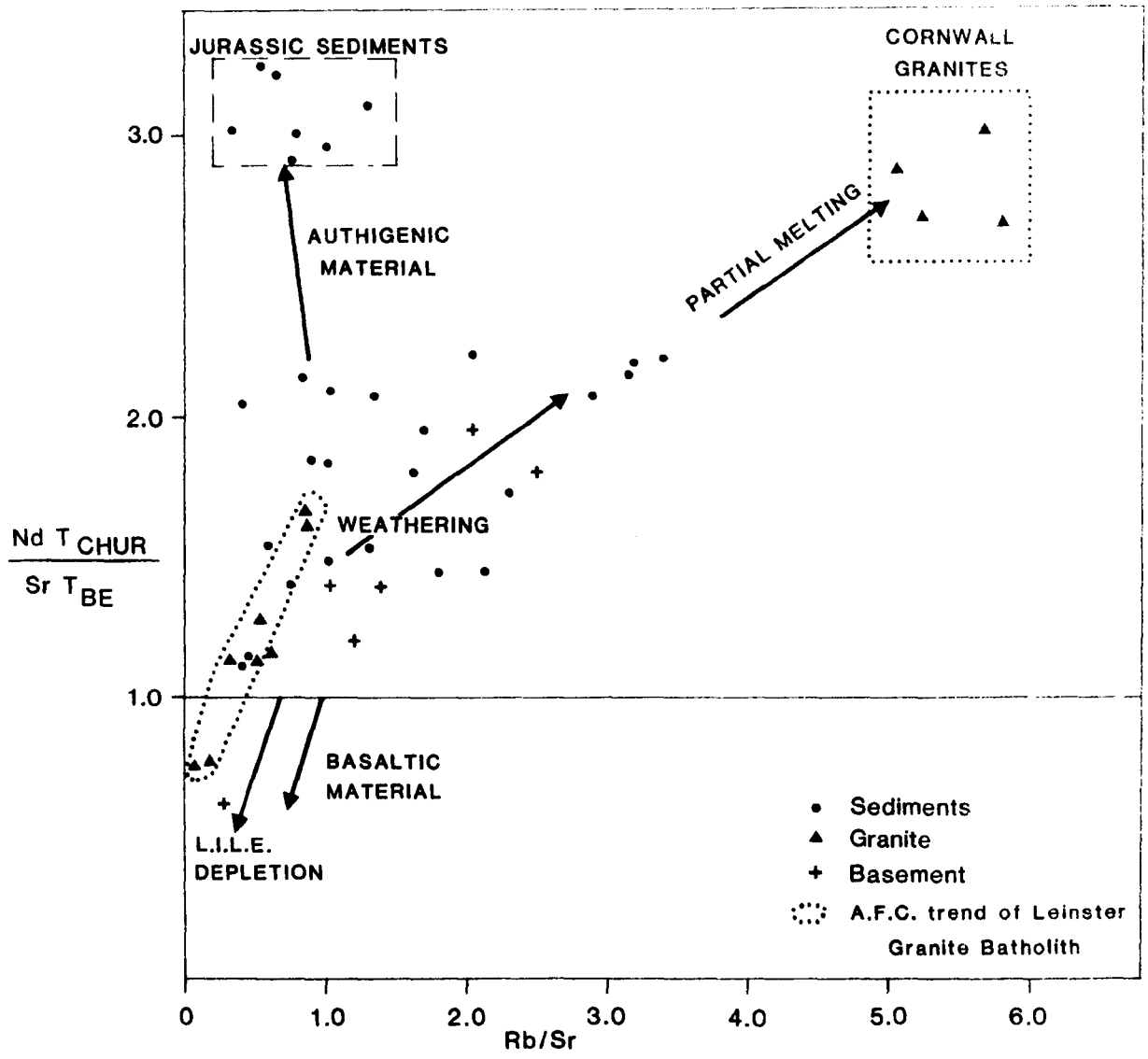

Figure 7:8 Nd T_{CHUR}/ Sr T_{BE} vs Rb/Sr DIAGRAM

SHOWING THE EFFECTS OF CRUSTAL PROCESSES

Figure 7:9 εNd vs Time diagram

See Figure 7:6 for explanation

The hatch regions are crustal evolution paths showing the effect on εNd of adding:

a) varying degrees of juvenile crustal material ($\varepsilon Nd_I = 0$)

b) 40% "ancient" continental crust with a Nd model age of 2.2 Ga .

Figure 7:9

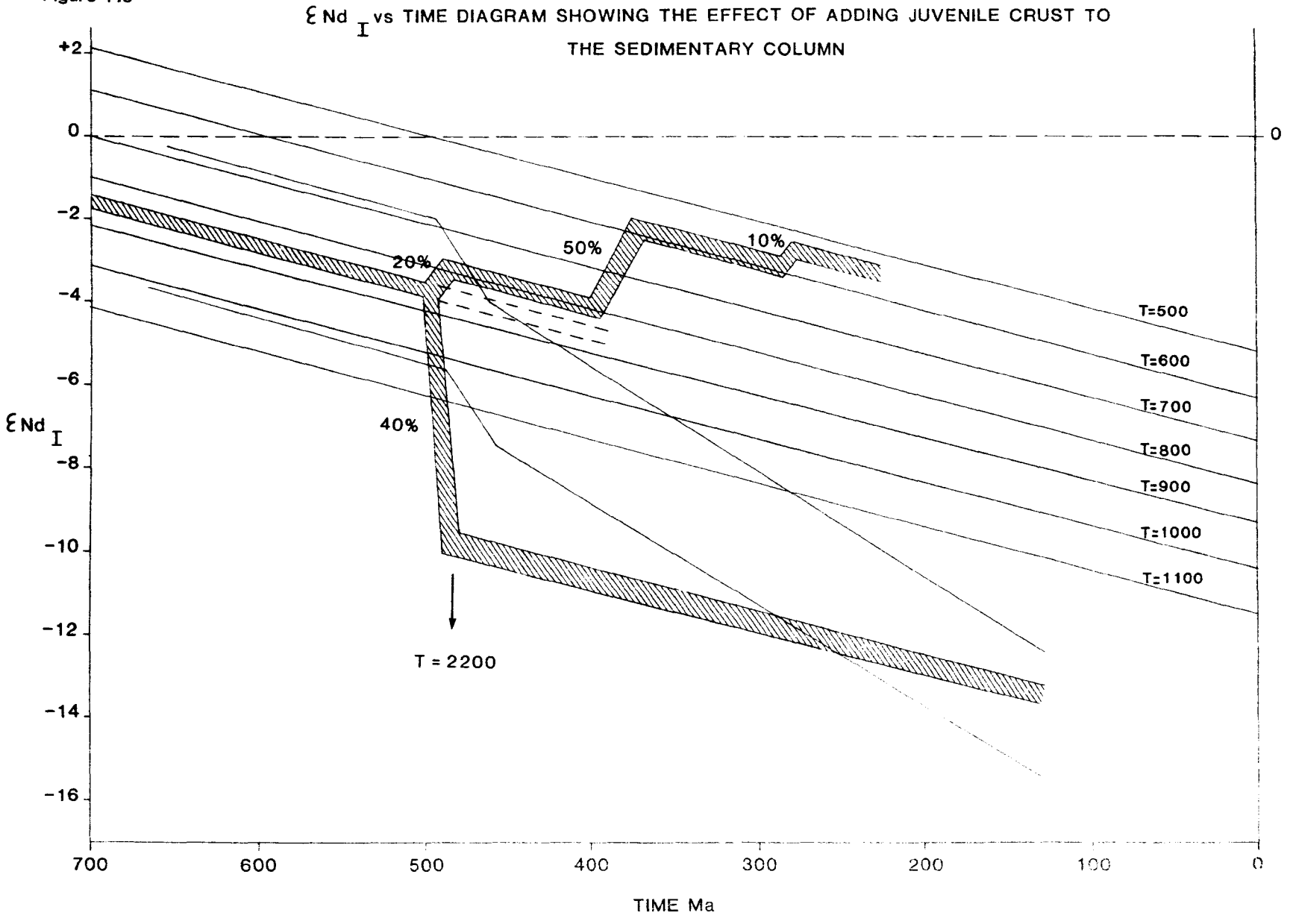
εNd I vs TIME DIAGRAM SHOWING THE EFFECT OF ADDING JUVENILE CRUST TO THE SEDIMENTARY COLUMN
+2
0
-2
-4
-6
-8
-10
-12
-14
-16
εNd I
20%
50%
10%
40%
T = 2200
T=500
T=600
T=700
T=800
T=900
T=1000
T=1100
700
600
500
400
300
200
100
0
TIME Ma

T_{BE} = 500 $\pm$ 100 Ma) and Mantle (T_{CHUR} T_{BE} formation age).

The Sm-Nd and Rb-Sr isotope systematics of the Cornish Granites are presented in Table 7:2. Similar data for the Leinster Granite Batholith is presented in Table 4:1 (Chapter 4) and for Anglesey granitoids in Table 7:1.

The Precambrian Anglesey granitoids have εNd_I and εSr_I values equivalent to those of the Precambrian basement rocks (see Figure 7:6 and 7:7). The εNd_I and εSr_I values of the Cornish Granites, which are crustal melts, are within the range of he εNd_{270} and εSr_{270} values of the Late Precambrian basement rocks (Figure 7:6 and 7:7) suggesting that the granites represent crustal melts solely from Late Precambrian basement rocks.

Figures 7:6 and 7:7 clearly show that the Leinster Batholith contains large components from both the mantle and crust. It is not possible purely from the isotope data to constrain the nature of the crustal component. However, in conjunction with the trace element data, it was concluded in Chapter 4 that partial melts from basement rocks were involved in the petrogenesis of the primary magma to the Batholith and that assimilation of sediments occurred during fractional crystallisation within the upper crust.

This preliminary study suggests that it may be possible, in the case of southern Britain, to distinguish between predominantly mantle, basement or sedimentary derived granites purely from their Sm-Nd or Rb-Sr isotope systematics.

Chapter 8

The Isotopic Evolution of the British Lithosphere

The evolution of the British Lithosphere has been investigated by detailed Nd and Sr isotope studies on selected suites of upper mantle, and both lower and upper crustal material. The primary aims were to elucidate the age structure of the crust and upper mantle south of the Highland Boundary Fault, and to constrain models for crustal evolution by studying the changing Sr and Nd isotope systematics of late Precambrian to recent sediments. The Lizard Peridotites provide direct samples of the upper mantle, and the associated igneous rocks, together with those from the Mona Complex Anglesey, are unambiguous examples of mantle derived magmas. Lower crustal rocks are available as xenoliths from the Midland Valley of Scotland and Central Ireland, and in the granulites of the N. E. Ox Mountains. Granitic rocks have been analysed from S. E. Ireland and S.W. England to evaluate the degree of crustal recycling involved in their petrogenesis.

An Sm-Nd mineral isochron age of 375 $\pm$ 34 Ma on an olivine gabbro is thought to represent the formation age of the Lizard Complex. Furthermore, the spinel lherzolites, which comprise the majority of the complex, record Nd depletion ages of 830 - 420 Ma, only slightly older than the formation age. The plagioclase and pargasite peridotites, which show mineralogical evidence of melt infiltration, have Nd isotope systematics indicative of L.REE depletion followed by recent L.REE enrichment (i.e. $<$200 Ma prior to the formation of the complex). The early, L.REE enriched, dyke suite of the complex, has similar Sm-Nd isotope systematics to the plagioclase and pargasite lherzolites, whereas the late, L.REE depleted, dykes record late to mid Proterozoic depletion ages of 1.0 to 1.7 Ga. The magmatic evolution of the Lizard Complex has been compared with that of the initial rifting of the Red Sea, since in both areas the emplacement of MORB-like magmas appear to be preceded by that of trace element enriched tholeiites during the initial rifting of the sub-continental mantle.

Metabasalts from Anglesey yield an isochron age of 595 $\pm$ 86 Ma. As at the Lizard Complex, there is evidence of both an early trace element depletion event (prior to 1200 Ma) followed by subsequent enrichment. However, at Anglsey the enrichment event must have occurred at, or just prior to, magma genesis because there is little variation in initial εNd values.

The mantle beneath southern Britain records evidence of mid to late Proterozoic depletion events resulting in initial ε Nd values, + 4 to + 12, generally within the range of MORB i.e. + 7 to + 13. Trace element enrichment events are apparently restricted to the latest Proterozoic.

Lower crustal xenolith suites from the Midland Valley of Scotland and Central Ireland record two distinct crustal accretion events. Garnet granulites from both regions yield Sm-Nd whole-rock errorchrons of between 1000 and 1100 Ma and have Nd model ages within this range. The basic to trondhjemitic granulites from various parts of the Midland Valley record late Precambrian formation ages. Basement Schists and gneisses from south of the Iapetus Suture generally have Nd model ages of less than 1000 Ma. However, the Rushton schists and Rosslare Complex represent the first recorded basement rocks of the region with an old (1300 - 1400 Ma) isotopic signature. Thus Nd isotope analyses indicate that they were formed in the mid to latest Proterozoic comparable to the age of trace element enrichment depletion events within the upper mantle. There is no direct evidence for crustal rocks older than 1500 Ma in these parts of the British Isles.

Similarly granitoids from throughout Britain have been used to infer the nature of basement rocks below sedimentary cover. For example the post-tectonic Caledonian granites of the Scottish Highlands have Nd, Sr and Pb isotope systematics indicating a major Grenvillian aged crustal component in their petrogenesis,

but provide no evidence of Archaean aged crust beneath the Highlands. Furthermore, the largely crustally derived Cornish and Leinster Granite Batholiths suggest the presence of late Precambrian basement beneath these regions (see Figure 7:6).

Late Precambrian to lower Ordovician sediments from southern Britain have present day ε_{Nd} values between - 7.4 and - 11.7 and Nd model ages of 680 to 1060 Ma. It is argued that they were therefore derived from late Precambrian basement, and that basement material similar to that of the Rushton schists and Rosslare Complex is volumetrically insignificant. The addition of mantle derived material during the Caledonian Orogeny (with radiogenic Nd isotope ratios) might be expected to result in sediments with progressively younger Nd model ages. However, sediments younger than the Ordovician have progressively older Nd model ages (1100 - 1600 Ma) suggesting that they reflect an increasing contribution from "ancient" crustal provinces. This relatively sudden, and subsequently continual, addition of an "ancient" crustal component to the sedimentary column, presumable resulted from the closure of the Iapetus Ocean, which enabled detritus from the mixed Archaean/Proterozoic terrains of northern Europe and America to reach southern Britain. Jurassic to present day sediments and coastal waters, have relatively constant Nd model ages (1300 - 1500 Ma), suggesting that steady state may have been reached since the Jurassic. To account for the increase in average Nd model ages from 850 to 1400 Ma between the Ordovician and the Jurassic, 40% of the sedimentary pile would have to be introduced from source areas with Nd model ages of 2.2 Ga. Interestingly at any one time the Nd within the sedimentary column is well mixed on both a local and regional scale, but subsequent to the closure of the Iapetus Ocean a period of around 300 Ma was needed for the sediments to reach a constant Nd model age. It is concluded, that since the late Proterozoic, sediment and magmatic recycling have been the dominant processes responsible for the Nd and Sr isotope composition of the British upper crust.

This study has shown that detailed studies of particularly lower

crustal granulites and sediments of varying ages can usefully constrain models for the isotope evolution of a segment of continental crust. Further detailed studies of older Archaean to early Proterozoic sediments are now required to determine temporal and spatial variations in the crustal growth rate and to evaluate the significance of sediment recycling into the mantle.

PAGE MISSING IN ORIGINAL

PAGE MISSING IN ORIGINAL

APPENDIX

A:1 SAMPLES

A1:1 Lizard Complex

P1	Fine grained, 0.1 mm, subophitic dolerite.	S. of Porthoustock
P2	Coarse grained, 0.5 mm, ophitic dolerite. Plagioclase laths show local alteration.	S. of Porthoustock
P4	Coarse grained, 0.4 mm, ophitic dolerite. Locally clinopyroxene is chloritised and plagioclase sausseritised	S. of Porthoustock
P5	Fine grained, 0.1 mm, dolerite containing plagioclase xenocrysts	S. of Porthoustock
P7	Granular, 0.4 mm, plagiogranite with extensively sausseritised plagioclase and accessory sphene and zircon	Porthoustock
P11a	Medium grained, 0.2 mm, ophitic dolerite	Porthoustock
P11b	Coarse grained, 0.4 mm, phitic dolerite. Clinopyroxene is locally amphibolitised and plagioclase xenocrysts are resorbed and extensively sausseritised.	Porthoustock
CV1	Porphyroclastic spinel lherzolite	2 km S. of Coverack
CV2	Coarse grained, 0.5 mm, subophitic dolerite	Coverack
CV5	Coarse grained, 5-10 mm olivine gabbro Pockilitic subhedral plagioclase encloses rounded olivines. Clinopyroxene is interstitial	Coverack
CV10	Porphyroclastic spinel lherzolite	0.5 km S. of Coverack

LZ01	Porphyroclastic plagioclase lherzolite containing plagioclase rich veins	1 km S. of Coverack
AT 133	Foliated pargasite peridotite	Goonhilly Downs
2553+	Porphyroclastic spinel lherzolite	Gwenter Goonhilly Downs
2554+	Porphyroclastic spinel lherzolite	Gwenter Goonhilly Downs
2555+	Foliated pargasite harzburgite	Kernewas Goonhilly Downs
2559+	Foliated plagioclase lherzolites	Kernewas Goonhilly Downs
2560+	Foliated plagioclase lherzolites	Kernewas Goonhilly Downs
MV 1	Foliated dioritic gneiss (Man of War Gneiss)	Lizard Head
KS 1A	Granular granite gneiss with biotite (Kennack Gneiss)	Kennack Sands
KS 1C	Foliated biotite amphibotite (Kennack Gneiss)	Kennack Sands
15/11A/4*	Metabasalt	Mélange
18/9B/10*	Metabasalt	Mélange
28/6C/3*	Metabasalt	Mélange
18/4C/1*	Foliated granite gneiss clasts from a conglomerate within the melange	Mélange
28/6B/2A5*	Foliated granite gneiss clasts from a vonglomerate within the melange	Mélange

\+ Samples supplied by Fred Frey, originally collected by D.H. Green

* Samples supplied by Rob Barnes

A:1:2

MONA COMPLEX

MB 2*	Gwna Group metabasalt
MB 4*	Gwna Group metabasalt
MB 5*	New Harbour Group metabasalt
MB 6*	Gwna Group metabasalt
MB 8*	Gwna Group metabasalt
MB 10*	Gwna Group metabasalt
MB 13*	New Harbour Group metabasalt
MB 19*	New Harbour Group metabasalt
PBG *	Gwna Group metabasalt
2585*	New Harbour Grpup metasediment
2601+	Coedana Granite
2609+	Coedana Granite
AS 16+	Mona Gneiss (Holland Arms)
A80 2622	Mona Gneiss (Holland Arms)

* Samples supplied by Richard Thorpe

\+ Samples from the isochron suites of Beckinsale and Thorpe, 1979.

A:1:3 S.E. Ireland

A) Volcanic rocks

L.B7:	Andesite pillow lava	Balbriggan, Co. Dublin
L.22:	Andesite Sill	Lambay Island, Co. Dublin
L.29:	Dacite Sill	Lambay Island, Co. Dublin
L.33:	Basalt lava	Lambay Island, Co. Dublin
L.100:	Basalt sill	Lambay Island, Co. Dublin
L.114:	Basalt lava	Lambay Island, Co. Dublin
T.18:	Diorite intrusion	Kilmurrin Cove, Co. Dublin
T.42:	Dacite intrusion	Annstown, Co. Waterford
T.63:	Andesite sill	Bonmahon, Co. Waterford
T.73:	Rhyolite	Co. Waterford
T.74:	Rhyolite	Co. Waterford

B) Leinster Granite

Iso.1:	Biotite diorite	Northern Unit, Inchanore Brook
Iso.2:	Biotite diorite	Northern Unit, Inchanore Brook
Iso.3:	Granodiorite	Northern Unit, Inchanore Brook
Iso.5:	Adamellite	Northern Unit, Inchanore Brook
Iso.19:	Aplite	Northern Unit, Dalkey
Iso.24:	Granodiorite	Lugnaquillia Unit, Turlough Hill
Iso.26:	Diorite	Ballynamuddagh minor intrusion
Iso.27:	Diorite/granodiorite	Ballynamuddagh minor intrusion

Samples supplied by ; volcanics Chris Stillman (Stillman and Williams,1979), granitoids Padrig Kennan.

Al:4 N.E. Ox Mountains
All samples from S. of Lough Gill

Ox 27: Plagioclase garnet pyroxenite

Ox 79: Coarse psammitic gneiss :- quartz-plagioclase orthoclase - garnet.

4/79 - 3/2: garnet pyroxenite + plagioclase and rutile; low garnet/pyroxene ratio

4/79 - 3/3: garnet pyroxenite + plagioclase; high garnet/pyroxene ratio

4/79 - 3/5: garnet pyroxenite + plagioclase, biotite and rutile; high garnet/Pyroxene ratio

4/79 - 3/8: garnet pyroxenite + plagioclase; low garnet/pyroxene ratio.

Samples supplied by Ian Sanders and Steve Daly.

A 1:5 Lower Crustal Xenoliths

A) Midland Valley of Scotland

303:	Garnet granulite:-	Garnet - plagioclase - quartz - biotite (rutile + zircon)	Partan Craig North Berwick
306:	Garnet granulite:-	Garnet - plagioclase - quartz (rutile + zircon)	"
317:	Garnet granulite:-	Garnet - plagioclase - quartz - orthoclase - trace biotite (rutile + zircon)	"
324:	Garnet granulite:-	Garnet - plagioclase - quartz - biotite (magnetite + rutile + zircon)	"
342:	Pyroxene granulite:-	Plagioclase - clinopyroxene quartz	"
347:	Garnet granulite:-	Garnet - plagioclase - quartz - biotite (magnetite + rutile + zircon)	"
355:	Pyroxene granulite:-	Plagioclase - clinopyroxene - quartz	"
369:	Quartzo feldspathic granulite:-	Quartz - plagioclase - orthoclose (biotite)	"
378:	Quartzo feldspathic granulite:-	Quartz - plagioclase - orthoclose - biotite	"

All Partan Craig samples contain secondary calcite, garnets have kelyphitic rims, clinopyroxenes are rimmed by chlorite and calcite. The feldspars show variable saussuritisation.

B) Central Ireland

77.0827: *	Garnet granulite:- Orthoclase microperthite - garnet - sillimanite - quartz (rutile, zircon - trace biotite)	Clare Castle Co. Westmeath
Sc 19a: +	Garnet granulite:- Plagioclase - orthoclase microperthite - sillimanite - garnet (rutile - trace biotite).	"
Sc 19b: +	Garnet granulite:- Orthoclase microperthite - garnet - sillimanite (rutile)	"
Sc 20: +	Garnet granulite:- Orthoclase microperthite - garnet - sillimanite - quartz (rutile)	"
Sc 27 +	Garnet granulite:- Plagioclase - garnet - orthopyroxene - quartz (biotite)	Dungolman River Co. Westmeath

* Samples supplied by Mike Max

+ Samples supplied by Peter Strogen

HN43: Basic granulite:- Labradorite (An_{56-51}), dull brown aluminous augite (c. En_{41} Fs_{19} Wo_{40} with $\simeq$8 wt % Al_2O_3) and an opaque spinel. — Hawk's Nib, Isle of Bute, Strathclyde

HN65: Basic granulite:- Plagioclase - augite - opaque spinel showing an 'equilibrium' granoblastic texture — "

HN72: Olivine gabbro:- Olivine wholly serpentinised. Cloudy augite poikilitically encloses olivine. Plagioclase is abundant and shows a granoblastic texture with 120° grain-boundaries (also clouded). — "

HN80: Basic granulite:- Labradorite (An_{58-54}), aluminous augite (En_{41} Fs_{17} Wo_{42} with >11 wt % Al_2O_3) and aluminous Ti-magnetite. — "

HN83: Olivine gabbro:- Coarse grained, olivine wholly pseudomorphed by yellow-brown "serpentine". Augite large and twinned. Majority of the rock is unzoned plagioclase with accessory opaque oxides/spinels. — "

All the Midland Valley samples supplied by Brian Upton and Peda Aspen.

A:1:6 **SEDIMENTS**

81/1	Mid Ordovician shale	Pembrokeshire
81/2	L. Arenig shale	Pembrokeshire
81/3	Arenig/Llanvirn shale	Pembrokeshire
81/4	Mid Coal Measures carbonaceous shale	Pembrokeshire
81/8	Permian marl	Leicestershire
81/10	Mid Coal Measures carbonaceous shale	N. Yorkshire
81/14	Skiddaw Slate	Lake District
81/15	L. Silurian shale	Lake District
JSW1*	Tremadoc Shineton Shale	Salop
JSW3*	M. Jurassic freshwater shale	Whitby
JSW9*	M. Jurassic freshwater shale	Burniston
JSW14*	U. Lias alum shale	Ravenscar
JSW15*	U. Lias shale	Whitby
JSW22*	Kimmeridge Clay	Whitby
JSW23*	Kimmeridge Clay	Pickering
JSW24*	Tremadoc Shale	N. Wales
JSW26*	Wenlock Shale	N. Wales
AT 228+	M. Ordovician greywacke	Southern Uplands
AT 585+	M. Ordovician slate	Southern Uplands
AT 586+	M. Ordovician slate	Southern Uplands
NC 1	L. Carboniferous carbonaceous shale	Cornwall
NC 2	L. Carboniferous carbonaceous shale	Cornwall
GF 1^{A}	Lower Palaeozoic Aberystwyth Grit	Dyfed
GF 2^{A}	Lower Palaeozoic Aberystwyth Grit	Dyfed
EIR 5	M. Ordovician shale	Wicklow S.E. Eire

ARC 1^{A}	Ingletonian shale	N. Yorkshire
ARC 2^{A}	Ingletonian shale	N. Yorkshire
BT 1^{A}	Late Precambrian arkose	N. Wales
OX 1	Oxford Clay	Bedfordshire

* Samples supplied by John Watson

\+ Samples supplied by Andy Tindle

A Samples supplied by Steve Richardson

A:1:7 S.W. ENGLAND GRANITES

Sample	Intrusion	Location
D1	Dartmoor	Dartmoor prison
C202	Bodmin	Corbilly Tor Quarry
C205	St. Austell	Tregarden Quarry Luxulyan
Pe 33+	Carnmenellis	Pendarves Mine
Pe 36+	Carnmenellis	Pendarves Mine
Pe 69+	Carnmenellis	Holman Quarry
P1	Lands End	Porthleden

+ Samples supplied by Julian Pearce

Appendix 2 Sample Preparation and Analytical Procedures

A:2:1 Sample Preparation

Wherever possible,>2 kg samples were collected. Samples were split into 2 to 4 cm cubes using a hydraulic splitter and then crushed into pieces <0.5 cm cubed in a jaw crusher. The sample was quartered and about 50 grams of rock were powdered to less than 200 mesh using an agate Tema mill.

XRF Analysis

The major element analyses were carried out on the Link Systems ED XRF at the Open University. Trace element analyses were performed at Nottingham University on an automated wavelength XRF.

A:2:2 General Chemistry

All the chemical separations described below are carried out in laminar flow cupboards within a laboratory under a positive pressure generated by filtered air. Sample dissolutions are carried out in teflon bombs and beakers. The standard cleaning procedure for teflon ware is i) thoroughly rinsing until visible clean, ii) soak in HNO_3 (80°C) for 24 hours, iii) 24 hours in quartz distilled H_2O at 80°C.

The reagents are purified as below:
H_2O :- Tap water is fed to a high efficiency pyrex still which in turn feed into a 2 stage quartz still.
HCl, Hf, HNO_3:- Analar chemicals are doubly distrilled in quartz stills and then purified in sub-boiling teflon stills.

Over the past three years the following blanks have been determined; 0.9, 0.8, 0.4, 0.17, 0.4, 0.46, 0.7 ng. The HF blank has been reduced from 0.33 to 0.01 ng. The air blank is 0.1 ng (1 week). The most significant component in the total blank is believed to be the result of contamination from previous samples; beaker, 0.2 - 0.6 ng, and bomb blanks, 0.2-9 ng, are found to be very variable. In order to overcome the problem of contamination, the chemistry of samples with low Nd concentrations, e.g. mineral separates and peridotites, is carried out on separate sets of columns, stringent precautions are taken in cleaning teflon ware; beakers are kept apart from those in general use and cleaned twice in frequently charged reagents, while bombs are cleaned and then filled with 6 MHCL and placed in an over at 180°C for 24 hours before use. Following such a procedure a bomb blank of 0.07 ng was obtained and it is expected that the total blank is probably less than 0.2 ng. The $^{143}Nd/^{144}Nd$ ratio of the blank is predicted to be 0.51192 i.e. the composition of local Jurassic sediments.

As a result of the low Nd concentrations of the spinel lherzolites from the Lizard complex the blank may cause a significant lowering of the measured $^{143}Nd/^{144}Nd$ ratio of the sample. Consideration of sample 2554 (with the lowest Nd content) shows how significant the blank could be; sample wt. 1.177 g Nd = 0.0354 ppm $^{143}Nd/^{144}Nd$ = 0.514143

A) A 2 ng blank accounts for 4.8% of Nd and the actual

$^{143}Nd/^{144}Nd$ of 2554 would be 0.514255.

B) A 0.2 ng blank accounts for 0.5% of Nd and actual $^{143}Nd/^{144}Nd$ of 2554 would be 0.514154.

In the latter and probably most realistic situation the effect of the bland is within typical precision i.e. $\pm$ 20 It is concluded that when dealing with very low Nd concentrations, 0.1 ppm, extreme care must be taken to ensure a blank of at most 0.2 ng.

A:2:3 Rb, Sr, Sm and Nd Chemistry

Approximately 150mg of rock powder is weighed into a teflon bomb. Sample dissolution is achieved as follows; i) add 5 ml 40% HF and 2 ml concentrated HNO_3 ii) the bomb is closed, placed in a monel jacket in an oven at 180°C over night iii) dried in a teflon oven with air circulation at 80°C iv) add 5 ml HNO_3 and when the sample is almost dry v) add 6 ml 6M HCl. At this stage the sample is entirely in solution. Rarely, e.g. when chromite or garnet are present, the entire procedure may need to be repeated. The solution is evaporated and dissolved in 1 to 2 ml 2.5 M HCl and any residue is centrifuged off and the clear solution loaded onto preconditioned cation exchange columns containing 10 ml Bio-Rad AG 50 W X8 200-400 mesh resin. The sample is washed in with 2 x 1 ml 2.5 M HCl and eluted with a further 43 ml. Rb is contained in the 22 to 30 ml fraction. Sr is collected in a further 10 ml 2.5M HCl .

If Sm and Nd are required the column is washed with 1 ml H_2O and eluted with a further 21 ml of 3 M HNO_3. The subsequent 20 ml 3 M HNO_3 contains the Sm and Nd. The solution is evaporated to driness and then dissolved in circa 1 ml solution I:- (75% MeOH, 10% 8M HoAc, 10% 5M HNO_3, 5% H_2O) and loaded on to preconditioned anion exchange column containing 3 ml Bio-Rad AG1 x 8 200-400 mesh resin and washed in with 2 x 1 ml solution I. The columns are kept at 25°C by the circulation of thermostatically regulated water. 13 ml of solution I is eluted and Sm is collected in the subsequent 19 ml. The temperature is increased to 35°C and the columns are eluted with 15 ml solution II (75% MeOH, 10% 8M HoAc, 5% 5M HNO_3, 10% H_2O). The following 29 ml contains the Nd.

TABLE A:2:1

BCR 1 SPIKE Sm/Nd

Sm	Nd	Sm/Nd
6.535	29.1	0.22457
6.48	28.74	0.22547
6.47	28.79	0.2247
6.47	28.80	0.22465
6.45	28.88	0.22334
6.53	29.15	0.2240
6.56	29.18	0.2241
6.55	29.21	0.22424
6.54	29.15	0.22439
6.539	29.15	0.22432
6.514	29.02	0.22445
6.55	29.2	0.22432
6.51	29.03	0.22442

BCR 1	$^{143}Nd/^{144}Nd \pm 2\sigma$
11/80	0.512612 ± 18
12/80	0.512622 ± 18
1/81	0.512634 ± 8
3/81	0.512617 ± 30
5/81	0.512632 ± 8
8/81	0.512602 ± 12
11/81	0.512613 ± 16
12/81	0.512595 ± 14
3/82	0.512634 ± 8
5/82	0.512637 ± 16
3/83	0.512640 ± 20
10/83	0.512602 ± 12
11/83	0.512623 ± 22

BCR 1

La	Ce	Nd	Sm	Eu	Gd	Dy	Er	Yb
25.8	56.44	30.474	6.408	1.976	7.284	6.734	3.828	3.506
		30.528			7.323	6.659	3.825	3.151
24.1	56.5	29.2	6.38	1.94	7.18	6.51	3.73	3.37
		29.2			7.18	6.47	3.71	3.37
		29.1	6.48					
		29.3						
25.4	55.3	29.2	6.47	1.91	7.22			
		29.3			7.22			
25.0	54.8	29.4	6.43	1.90	7.22			
		29.2			7.21			
24.4	55.5	27.7	6.23	1.93	-	6.51	3.85	3.47
						6.46	3.82	3.46
	56.4	28.6	6.25	-		8.21	4.73	4.31
					-	8.06	4.67	4.30
25.3	56.7	29.5	6.48	1.98	7.31			
					7.32			
		29.5	6.51	1.91	7.21	6.47	3.68	3.33
		29.0			7.21	6.37	3.65	3.34
26.6	56.5	29.1	6.47	1.96	7.27	6.64	3.85	3.52
		29.3			7.26	6.65	3.77	3.53
27.6	68.7	30.8	6.84	2.02	7.65	6.75	3.91	3.55
		30.8			7.66	6.70	3.83	3.55
	50.3	29.92	6.6	2.0				
	58.42	30.44	7.16	-	6.06	7.31	3.73	
	57.82	30.44	6.75	1.98	-	6.66	3.85	
	56.2	30.22	6.69	1.91	6.99	6.57	3.70	3.44
Mean								
25.40	57.1	29.64	6.57	1.95	7.14	6.80	3.90	3.56

A third, "clean up", column is used to separate Ba from the Sm and Nd fractions. The sample is dissolved in 1 ml 90% HoAc - 10% 5M HNO_3 and loaded onto preconditioned anion exchange columns containing 1 ml Bio-Rad AG 1 x 8 200-400 mesh resin. The sample is washed in with 2 x 1 ml and eluted with 10 mls. Nd and Sm are stripped from the columns with 5 ml 0.05 M HNO_3. The solutions are evaporated to driness and stored in quartz/teflon microbeakers.

A:2:4 Spiking

The sample is weighed out on a 0.01 mg balance and 1-2 drops of spike are added and weighed. Dissolution and chemical separations are performed as above. The spikes used in the laboratory are;

98% ^{87}Rb
99.78% ^{84}Sr
96.66% ^{149}Sm
84.10% ^{145}Nd

REE

92.97% ^{139}La
92.11% ^{142}Ce
89.67% ^{145}Nd
98.08% ^{149}Sm
96.83% ^{151}Eu
91.61% ^{155}Gd
90.41% ^{161}Dy
91.54% ^{167}Er
95.07% ^{171}Yb

Duplicate analyses performed on BCR-1 over the past 3 years show that Nd and Sm concentration are determined to within 1% but that the Sm/Nd ratio is found to be within 0.2%. (See Table A:2:1)

The Sm, Nd, Rb and Sr concentrations of mineral separates and samples being analysed as part of an isochron study are obtained by aliquoting. Samples are weighed and dissolved as described in Section A:2 :3 and 20 to 30 ml of 2 M HCL solution are obtained. The solution is transferred to a zeroed beaker and the weight recorded. A second beaker is zeroed and one or mor drops of spike are added. The beaker is zeroed again and circa 20% of the solution is added and the weight recorded. Chemical separations proceed as in section A:2:3.

A:2:5 REE Chemistry

Dissolutions and spiking for REE separations are as described in sections A:2:3 and A:2:4. 1 to 2 ml of solution is loaded onto a preconditioned cation exchange column and washed in with 2 x 1 ml 2.5 M HCl. A further 35 ml 2.5 M HCl are eluted and the REE stripped from the columns in 10 ml 6 M HCl and evaporated. Ba is separated by the use of the "clean up" column. It is now standard prcedure to load the entire sample onto a triple filament (Ta side, Re centre) and obtain La, Ce, Nd, Sm, Eu, Gd, Dy, Er, Yb concentrations from a sample analysis. However, in the past the REE were separated into 3 groups:- HREE (Dy, Er, Yb), "lights" (Nd, Sm, Eu, Gd) and La, Ce. For this procedure the sample is dissolved in 1 ml of Solution III (90% MeOH, 10% 5 M HNO_3) and loaded onto preconditioned anion columns containing 3 ml AG 1 x 8 200-400 mesh resin. The sample is washed in with 2 x 1 ml and 3 ml are eluted. The H.REE fraction is collected in the following 8 ml. The "lights" fraction is collected in 15 ml of Solution IV (90% MeOH, 10% 0.01 M HNO_3) and the La, Ce fraction by stripping the column with 3 ml 1.5 M HNO_3.

A:2:6 Mass Spectrometry

Samples are loaded onto filaments made of Re and or Ta ribbon welded onto pins mounted in glass beads. The type of filament used for an analysis is element dependant; Sr and Sm are dissolved in 1 ml H_2O and loaded on single Ta filament with 1 ml 1 M H_3PO_4. Rb is loaded in H_2O on the side filaments of a triple Ta filament. Nd is also loaded in H_2O on Ta side filaments of a triple filament, Re centre and Ta sides. La-Ce and "Lights" fractions are loaded as for Sr whereas the H.REE fraction is loaded as for Nd.

The filaments are placed, in batches of 6, in a turret in a Vacuum Generators Isomass 54E thermal ionisation mass spectrometer equiped with a Solartron 7060 DVM incorporating a real time clock. Rb, Sr, Sm and Nd isotope analyses are run authomatically by software predominantly developed by P. van Calsteren and D. Wright, on a HP 9845T computer. All elements are analysed at $<10^{-7}$ atmospheres with an accelerating potential of 8 kv.

Sr Isotopic Abundances

Sr beams are managed to give an intensity of >15 p A using a 10Ω feed back resistor at a filament current of circa 2.5 A. The measuring cycle is 88, 87, 86, 86.5, 85, 84. The 85 peak is eliminated when the Rb contribution of peak 87 is less than 0.01% and 84 after the first set. All peaks are counted for four periods of 1.28 seconds. The intensities are calculated using a double interpolation algorithm (Dodson, 1978) corrected for zero, dynamic memory and Rb interference if necessary. The $^{87}Sr/^{86}Sr$ ratio is corrected for mass fractionation assuming that the fractionation is linearly correlated with mass and is normalised to an $^{86}Sr/^{84}Sr$ ratio of 0.1194. Ratios are stored in sets of 10, the mean and the error are calculated and ratios are rejected that do not satisfy Chauvenet's criterion (Pugh and Winslow, 1967). If the total error for the set is still > 100 ppm, the whole set is rejected and if this error is >500 ppm the set is ignored. Chauvenet's criterion is tested again for all stored ratios, including the rejected ones, but not the ignored sets to form a running mean. The run is terminated when at least 100 ratios are accumulated and the error is <20 ppm. The NBS 987 Sr standard gives 0.71017 $\pm$ 4 which is indistinguishable from the certified value.

Sr concentrations are obtained as above but the 84 peak is not eliminated. From the fractionation corrected ratios the 88 Sr and 86 Sr abundances are calculated by the computer using the standard isotope dilution relationship

$$\text{Sr ppm} = \text{Conc Sp 84} \times \frac{100 \text{ At.wt.Sr} \times \text{Spwt.}}{\%\,{}^{84}\text{N} \times \text{Sa wt.}} \left[\frac{({}^{88}Sr/{}^{84}Sr)_M - ({}^{88}Sr/{}^{84}Sr)_{sp.}}{({}^{88}Sr/{}^{84}Sr)_N - ({}^{88}Sr/{}^{84}Sr)_M} \right]$$

Sp. = Spike Sa. = Sample M. = Measured N = Natural

Errors are propagated automatically by the computer assuming a constant weighing error of 0.00002 g. Concentrations, ratios and errors are calculated after every set and the run is terminated when at least 50 ratios are collected and the error is less than 100 ppm.

Rb Concentrations

Rb analyses are performed rapidly to minimise mass fractionation with centre and side filament currents at 2.2A and 0.3A respectively. Termination conditions are equivalent to those of Sr.

Nd Isotopic Abundances

A stable Nd beam is produced with centre and side filament currents at 3.9 and 2.0A respectively. The beam is managed to produce an intensity of $\simeq$ 7 pA. The measuring cycle is 146, 144, 143, 142.5, 142, 145, 147. The 145 peak is only included in the cycle in spiked samples and the 147 peak is eliminated when the Sm interference on 144 is $< 0.01\%$. The $^{143}Nd/^{144}Nd$ ratio is corrected for mass fractionation assuming $^{146}Nd/^{144}Nd = 0.7219$. An isotopic analysis is terminated when at least 200 ratios are accumulated and the error is <20 ppm. BCR-1 gives a $^{143}Nd/^{144}Nd$ ratio of 0.512620 ± 20 which is within the "accepted" range.

Nd concentrations are obtained as above but the 145 peak is not eliminated. Run termination conditions are the same as for Sr and Rb

Sm Concentrations

Sm beams are managed to give an intensity of $\simeq$3 p A with a filament current of 2.6 A. Termination conditions are as for Sr.

REE Concentrations

Dy, Er and Yb concentrations are determined in a single semiautomatic analysis. Yb, Dy and Er beams are obtained with a centre filament current of 3.9 A and side filament currents of 1.8, 2.2 and 2.4 A respectively.

Eu, Sm, Nd and Gd beams are obtained with a filament current of 1.3, 2.5, 2.7, and 2.9A respectively.

Ce and La beams are obtained at filament currents of 2.4 and 2.6 A respectively. The computer automatically corrects for Sm, Nd and Ce interferences where applicable.

No mass fractionation is taken into account in the REE determinations and errors are therefore liable to be in the region of 2% for each element and nearer 5% for La and Ce due to the interferences.

REE concentrations are reported normalised to the chondritic values of Nakamura (1974).

A:2:7 Electron Microprobe Analysis

All mineral chemistry data were collected at the Open University on a wavelength dispersive Cambridge Instruments Microscan 9 electron probe microanalyser ("microprobe"). The "microprobe" is fully computerised and enables spectrometer angles, count times, crystal selection, speciment movement and ZAF corrections to be controlled automatically. Rountine silicate analyses were performed at an accelerating potential of 20 KV, a speciment current of 30.5 nA, and a typical spot size of 10 to 15 μ . The instrument was calibrated using mineral standards (jadite (Na, Al), forsterite (Mg), wollastonite (Si, Ca), sythetic potassium chloride (K), rutile (Ti), fayalite (Fe), and metals (Cr, Mn, Ni)). The calibration is performed daily and the consistency of the data is checked by analysing internal standards (ABG, a basaltic glass; ABX, a chromite; (see Table A:2:2).

Energy dispersive (ED) Link Systems detector is also attached to the Microscan 9 and was used occasionally to set up the analytical points, particularly the small chromites included in silicates.

	ABG Basaltic glass mean of 73 analyses		ABX Chromite mean of 35 analyses	
		2σ		2σ
SiO_2	51.49	0.47	-	
TiO_2	1.32	0.05	0.14	0.03
Cr_2O_3	-	-	46.58	0.43
Al_2O_3	15.05	0.19	22.67	0.24
FeO	9.07	0.14	15.13	0.20
MnO	0.18	0.03	0.31	0.04
MgO	7.95	0.15	15.17	0.18
CaO	11.14	0.16	-	
Na_2O	2.75	0.08	-	
K_2O	0.07	0.01	-	
NiO	-		0.15	0.03
Total	99.02		100.15	

Table A:2:2 Secondary standard data obtained over the period of this work. Analyses by A. Tindle, P. Browning and myself.

A:3:1 Major and Trace Element data for the Igneous Rocks of the LIZARD COMPLEX

	Dolerite P1	Dolerite P2	Dolerite P4	Dolerite P5	Plagio-granite P7	Dolerite P11a	Dplerite P11b	Dolerite CV2
SiO_2	48.13	49.78	49.79	49.96	49.00	51.13	48.54	48.63
TiO_2	1.72	1.27	1.33	1.15	0.61	2.98	1.31	1.11
Al_2O_3	16.62	17.27	15.78	16.42	27.49	15.24	15.51	15.79
Fe_2O_3	8.95	8.67	9.05	8.09	0.73	10.69	8.36	8.41
MnO	0.17	0.16	0.18	0.15	0.04	0.19	0.15	0.13
MgO	7.16	7.40	7.89	8.55	0.59	6.07	10.39	10.43
CaO	9.71	10.15	10.65	10.96	14.69	8.56	10.18	10.27
Na_2O	4.92	3.85	3.13	3.00	4.26	4.54	3.36	3.15
K_2O	0.18	0.75	0.09	0.19	0.22	0.15	0.19	0.18
P_2O_5	0.42	0.19	0.16	0.21	0.20	0.50	0.16	0.13
L.O.I.	1.15	1.55	1.27	1.38	2.25	1.07	1.43	1.31
Total	99.22	101.01	99.24	100.05	100.05	101.22	99.58	99.54
Ni	113	126	93	131	12	67	191	185
V	204	203	230	209	44	373	162	157
Cr	237	324	366	379	20	161	374	391
Zr	220	106	100	108	705	294	66	67
Y	36	32	29	26	78	58	22	22
Nb	8	5	5	7	19	10	4	5
Ce	43	28	31	19	122	53	22	17
Rb	3.7	22.5	3.3	7.6	1.5	5.0	8.3	1
Sr	283.7	194.6	139.5	205.5	1058.4	182.7	156.5	142.6
Ba	176	127	141	125	49	336	91	90
Zr/Y	6.1	3.3	3.4	4.1	9.0	5.1	3.0	3.0

A:3:2 Trace element data for crustal rocks

	LIZARD COMPLEX		OX MOUNTAINS										
			Drill cores										
	Man of War gneiss MW1	Lizard Head Series LH6a	KS1A	KS1C	KS1G	KS1F	4/79/3/1	4/79/3/2	4/79/3/3	4/79/3/4	4/79/3/5	4/79/3/6	4/79/3/8
Ni	4	42	27	55	303	102	10	29	56	73	44	38	17
V	56	121	69	178	111	59	55	142	248	197	139	103	72
Cr	15	140	49	173	563	79	87	152	308	459	197	110	66
Zr	148	118	178	162	16	106	228	162	99	80	153	249	244
Y	37	26	20	30	15	15	23	25	28	38	28	21	20
Nb	6	15	9	14	4	7	11	13	14	17	11	8	6
Ce	56	74	51	33	12	39	26	32	47	38	34	46	26
Rb	16.0	64.9	73.4	100.1	208.6	120.8	1.4	2.2	20.3	14.4	2.2	2.6	3.8
Sr	700.7	237.6	482.1	452.1	125.9	582.3	154.6	163.3	166.2	120.0	151.5	166.8	158.5
Ba	499	532	583	491	109	682	19	58	157	148	50	27	14
Zr/Y	4.0	4.5	8.9	5.4	1.1	7.1	9.9	6.5	3.5	2.1	5.5	11.9	12.2

	OX MOUNTAINS SEDIMENTS																SEDIMENTS					
	Whole-rocks																					
	4/79/9	4/79/13	4/79/14	OX/22	81/1	81/2	81/3	81/4	81/8	81/9	81/10	81/14	81/15	NC1	NC2	EIR5	BT1	GF1	GF2	ARC2	ARC1	AGV-1
Ni	58	92	132	49	20	17	32	58	51	53	67	47	102	22	69	41	5	33	52	26	23	23
V	166	307	214	293	147	64	71	82	139	153	93	125	118	48	174	119	73	125	110	112	110	121
Cr	404	211	240	146	72	43	66	100	114	123	100	118	148	52	132	103	35	86	75	64	61	12
Zr	120	139	119	117	420	149	365	216	181	175	219	166	199	280	174	157	240	233	268	173	174	235
Y	32	45	27	31	54	61	47	29	42	39	30	36	32	27	36	34	24	32	36	37	31	24
Nb	22	24	15	13	20	15	15	18	19	19	17	21	16	13	18	17	10	19	18	13	12	16
Ce	121	69	31	40	145	43	55	63	99	96	62	101	69	58	80	84	46	93	51	71	60	63
Rb	5.9	24.1	5.2	15.9	83.2	64.0	41.5	95.2	165.4	191.4	110.6	181.2	138.2	38.8	161.4	156.1	54.1	124.1	109.3	70.1	78.6	
Sr	146.4	97.7	90.3	99.4	24.6	79.0	55.6	55.7	53.0	46.7	84.7	137.1	84.6	59.8	79.7	155.5	55.1	123.2	73.5	144.7	157.1	
Ba	118	220	212	297	662	446	326	455	798	789	608	803	541	237	632	545	537	575	470	375	507	1185
Zr/Y	3.8	3.1	4.4	3.8	7.8	2.4	7.8	7.5	4.3	4.5	7.3	4.6	6.2	10.4	4.8	4.6	10.0	7.3	7.4	4.7	5.6	

REFERENCES

D.H.M. Alderton, J.A. Pearce and P.J. Potts (1980) Rare earth element mobility during granite alteration: Evidence from south west England. Earth planet. Sci. Letts. 49, 149-165.

D.T.Aldiss (1981) Plagiogranites from ocean crust and ophiolites. Nature, 289, 577-578.

C.J. Allegre and D.B. Othman (1980) Nd-Sr isotopic relationship in granitoid rocks and continental crust development: a chemical approach to orogenesis. Nature, 286, 335-342.

C.R. Allen (1975) The petrology of a portion of the Troodos Plutonic Complex, Cyprus. Unpublished Cambridge University Thesis.

J.G. Arth (1976) Behaviour of trace elements during magmatic processes - A summary of theoretical models and their applications. Jour. Research U.S. Geol. Survey vol. 4,1 41-47.

J.G. Arth and G.N. Hanson (1975) Geochemistry and origin of the early Precambrian crust of north eastern Minnesota. Geochim. Cosmochim. Act. 39, 325-362.

J.G. Arth, F. Baker, F. Peterman, Z.E. Friedman (1978) Geochemistry of the gabbro-diorite-tonalite-trondhjemite suite of south west Finland and its implications for the origin of tonalitic and trondhjemitic magmas. J. Petrol. 19, 289-316

J.L. Anderson and R.L. Cullers (1978) Geochemistry and evolution of the Wolf River Batholith, A late precambrian Rapakivi massif in north Wisconsin, U.S.A. Precam. Res, 7, 287 -324.

J.R. Andrews, W.E.A. Phillips and M.A. Molloy, (1978) The metamorphic rocks of part of the north Central Ox Mountains inlier of Counties Sligo and Mayo. J. Earth. Sci. R. Dubl. Soc. 1, 173-94.

T.A. Auge and S. Roberts (1982) Petrology and geochemistry of some chromitiferous bodies within the Oman ophiolite OFIOLIITI, 7, 133-154

J.W. Baker (1969) Correlation problems of unmetamorphosed Precambrian rocks in Wales and South East Ireland. Geol. Mag., 106, 246-259.

J.P.N. Badham and G.A. Kirby (1976) Ophiolites and the generation of ocean crust: data from the Lizard Complex, Cornwall. Bull. Soc. geol. France, 7, 885-888

D. Bamford, K. Nunn, C. Prodehl and B. Jacob (1978) LISPB - IV. Crustal structure of northern Britain. Geophys. J.R. Astron. Soc., 52:43-60.

A.J. Barber and M.D. Max (1979). A new look at the Mona Complex (Anglesey, North Wales) J. Geol. Soc. Lond., 136, 407-432.

A.J. Barber, M.D. Max and P.M. Bruck (1980) Geologists' Association - Irish Geological Association Field Meeting in Anglesey and south eastern Ireland, 4-12 June 1977. Proc. Geol. Ass. 92, 269-92.

R.P. Barnes and J.R. Andrews(1981) Pumpellyite - actinolite grade metamorphism in south Cornwall. Proc. Ussher Soc. 5, 139-146

R.P. Barnes and J.R. Andrews (in press) Metamorphic evidence for the cold emplacement of the Lizard Complex. J. Geol. Soc. Lond.

R.D. Beckinsale and R.S. Thorpe (1979) Rubidium-Strontium whole rock isochron evidence for the age of metamorphism and magmatism in the Mona Complex of Anglesey. J. Geol. Soc. Lond., 136, 433-39.

G.M. Bennison and A.E. Wright (1970) The Geological History of the British Isles. (Arnold).

F.Y. Bokhari and J.D. Kramers (1981) Island arc character and late Precambrian age of volcanics at Wadishwas, Hijaz, Saudi Arabia: geochemical and Sr and Nd isotopic evidences, Earth. Planet. Sci. Lett., 54, 409-422.

T.G. Bonney (1877) On the serpentine and associated rocks of the Lizard District, with notes on the chemical composition of some rocks in the Lizard District by W.H. Hudleston. Q.J. Geol. Soc. Lond., 33, 884 - 982.

N.L. Bowen (1928). The Evolution of the Igneous Rocks. Princeton University Press.

G.W. Brass (1976) The variation of the marine $^{87}Sr/^{86}Sr$ ratio during Phanerozoic time; interpretation using a flux model. Geochim: Cosmochim Acta, 40, 721-730.

J.C. Brindley (1973) The Structural Setting of the Leinster granite, Ireland. Sci. Proc., Royal Dublin Soc. Series A. Vol. 5, 27-36.

A.V. Bromley (1973) The sequence of emplacement of basic dykes in the Lizard Complex, South Cornwall (abstract). Proc. Ussher Soc., 2, 508.

A.V. Bromley (1976) A New Interpretation of the Lizard Complex, South Cornwall, in light of the ocean model. J. Geol. Soc. Lond., 132.114.

M. Brook, D. Powell and M.S. Brewer (1977) Grenville events in Moine rocks of the Northern Highlands, Scotland. J. Geol. Soc. Lond., 133, 489-496.

M. Brook, M. Brewer and D. Powell (1976) Grenville age for rocks in the Moine of North-Western Scotland. Nature, Lond. 260, 515-517.

C. Brooks, S.R. Hart, A. Hofmann and D.E. James (1976) Rb-Sr mantle isochrons from oceanic regions. Earth Planet. Sci. Lett. 32, 51-61.

M. Brooks and J.S. Doody (1981) A report on recent seismic refraction surveys in the Lizard area. Abst. Tectonic Studies Group Meeting.

M. Brown (1982) The Petrogenesis of the St. Malo. Migmatite Belt, Armorican Massif, France with Particular Reference to the Diatexites. N. Jb. Miner. Abh. 135, 48-74.

P.M. Bruck and P.J. O'Conner (1977) The Leinster Batholith: Geology and Geochemistry of the Northern Units. Geol. Surv. Ireland Bull. 2. 107-141.

S.R. Carter, N.M. Evensen, P.J. Hamilton and R. K.O'Nions. (1978). Neodymium and Strontium Isotope evidence for crustal contamination of continental volcanics, Science, 200, 743-747.

E.N. Cameron (1975). Post-cumulus and sub-solidus equilibration of chromite and co-existing silicates in the eastern Bushweld Complex. Geochim. Cosmochim. Acta. 39, 1021-1033.

C. Chauvel, A.W. Hofmann and N.T. Arndt (1983) New evidence for early mantle depletion from Nd isotopes of greenstones. (Abstr) Terra Cognita, 3, 129.

R.S. Chase (1969) Basalt from the axial trough of the Red Sea, In: Hotbrines and recent heavy metal deposits in the Red Sea; a geochemical and geophysical account. E.T. Degens and D.A.Ross (Eds.) New York: Springer-Verlag, 122-128.

W.R. Church (1969) Eclogites. In: Basalts, H.H. Hess (Ed.) Wiley-Interscience, 755 - 98.

J.A.P. Clayburn (1981) Age and petrogenetic studies of some magmatic and metamorphic rocks in the Grampian Highlands. Unpublished Ph.D. Oxford.

R.S. Cohen and R.K. O'Nions (1982) The lead, neodymium and strotium isotopic structure of ocean ridge basalts. J.Petrol. 23, 299-324

R.G. Coleman, D.G. Hadley, R.G. Fleck, C.T. Hedge and M.M. Donato, (1979). The Miocene Tihama Asir Ophiolite and its bearing on the opening of the Red Sea, In: Evolution and Mineralisation of the Arabian-Nubian Shield, 1, Al-Shanti (Ed.), 173-186, Pergamon Press, N.Y.

D. Cummings and G.E. Schiller (1971) Isopach map of the earth's crust. Earth. Sci. Rev. 7, 97-125.

A.E. Curral and W.E.G. Taylor (1965) Geological history of the Slieve Camph Mountains, Co. Mayo. Proc. R. Ir. Acad. 638, 131-165.

D.J. DePaolo (1980) Crustal growth and mantle evolution: inferences from models of element transport and Nd and Sr isotopes. Geochim, Cosmochim, Acta, 44, 1185-1196.

D.J. De Paolo (1981a) A neodymium and strontium isotopic study of the Nesozoic calc-alkaline granitic batholiths of the Sierra Nevada and Peninsular Ranges, California. J. Geophys. Res., 86, 10470-10488.

D.J. DePaolo (1981b) Neodymium isotopes in the Colorado Front Range and crust-mantle evolution in the Protezozoic. Nature, 291, 193-196.

D.J. DePaolo (1981c) Trace element and isotopic effects of combined wallrock assimilation and fractional crystallisation. Earth Planet. Sci. Lett. 53, 189-202.

D.J. DePaolo and G.J. Wasserburg (1976a) Inferences about magma sources and mantle structure from variations of $^{143}Nd/^{144}Nd$. Geophs. Res. Lett., 3, 743-746.

D.J. DePaolo and G.J. Wasserburg (1976b) Nd-isotope variations and petrogenetic models. Geophys. Res. Lett., 3, 249-252.

D.J. DePaolo and G.J. Wasserburg (1979) Sm-Nd age of the Stillwater Complex and the mantle evolution curve for neodymium. Geochim. Cosmochim. Acta, 43, 999-1008.

B. Deruelle, R.S. Harmon and S. Moorbath (1983) Combined Sr-O isotope relationships and petrogenesis of Andean volcanics of South America. Nature , 302, 814.

H.J.B. Dick (1977) Partial melting in the Joshephine peridotite, I, The effect on mineral composition and the consequence for geobarometry and geothermometry. Am. J. Sci., 277, 801-832.

M.H. Dodson (1976) Kinetic processes and thermal history of slowly cooling solids. Nature, 259, 551.

M.H. Dodson and D.C. Rex (1971) Potassium-argon ages of slates and phyllites from South-west England. Q.Jnl. Geol. Soc. Lond., 126, 465-499.

K.M.J. Downes (1974) The geology and geochemistry of the Ordovician volconics of Co. Waterford and south-west Co. Wexford. (Unpubl. Ph.D. thesis, Trinity College, Dublin.)

H.J. Duyverman, N.B.W. Harris, C.J. Hawkesworth (1982) Crustal accretion in the Pan African: Nd and Sr isotope evidence from the Arabian Shield. Earth and Planet. Sci. Lett., 59, 315-326.

P.C. England (1978) Some thermal considerations of the Alpine metamorphism - Past, Present and Future. Tectonophysics, 46, 21-40.

J.S. Flett (1946) Geology of the Lizard and Meneage. Mem. Geol. Surv. Gt. Br. 359.

J.S. Flett and J.B. Hill (1914) The Geology of the Lizard and Meneage. Mem. Geo. Surv. U.K., 2nd ed. H.M.S.O.

S. Fourcade and C.J. Allegre (1981) Trace elements behaviour in granite Genesis: A case study. The Calc-Alkaline Plutonic Association from the Querigut Complex (Pyrenees, France). Contrib. Mineral Petrol 76 : 177-195.

P.W. Francis, R.S. Thorpe, S. Moorbath, G.A. Kretzschmar and M. Hammill (1980) Strontium isotope evidence for crustal contamination of calc-alkaline volcanic rocks from Cerro Galan, north west Argentina. Earth Planet. Sci. Lett. 48, 257-267.

F.A. Frey (1969) Rare earth abundances in a high temperature peridotite intrusion. Geochim. Cosmochim. Acta. 33, 1429-1477.

F.A. Frey (1983) Rare earth element abundances in upper mantle rocks. In: Rare Earth Element Geochemistry P.Henderson, (Ed.) Elsevier, 153 - 203.

F.A. Frey and M.A. Prinz (1978) Ultramafic inclusions from San Carlos, Arizona: petrology and geochemical data bearing on their petrogenesis. Earth Planet. Sci. Lett., 38, 129-176

F.A. Frey, B.W. Chappell and S.D. Roy (1978) Fractionation of rare-earch elements in the Tuolumne Intrusive series, Sierra Nevada batholith, California. Geology, 6. 239-242.

F.A. Frey, D.H. Green and S.D. Roy (1978) Integrated models of basalt petrogenesis: a study of quartz tholeiites to olivine melilites from South Eastern Australia utilising geochemical and experimental petrological data. J. Petrol. 19, 463-513.

N.H. Gale, R.D. Beckinsale and A.J. Wadge (1980) Discussion of a paper by McKerrow, Lambert and Chamberlain on the Ordovician, Silurian and Devonian time scales. Earth. Planet. Sci. Lett., 51, 9-17.

I.G. Gass, D.I.J. Mallick and K.G. Cox 1973. Volcanic islands of the Red Sea. J. Geol. Soc. Lond. 129, 275-310.

P.W. Gast, (1968) Trace element fractionation and the origin of tholeiitic and alkaline magma types. Geochim. Cosmochim. Acta., 32, 1057-1086.

W. Gibbons (1983) Stratigraphy, subduction and strike-slip faulting in the Mona Complex of North Wales - a review. Proc. Geol. Ass. 94, 147-163.

E.D. Goldberg (1965) Minor elements in seawater. Chemical Oceanography, Vo. 1, Riley and G. Skirrow (Eds.), Academic Press, New York, 164-165.

S.L. Goldstein and R.K. O'Nions (1981) Nd and Sr isotopic relationships in pelagic clays and ferromanganese deposits. Nature, 292, 324-327.

G. Grau, B. Leveque, A. Marot, J.L. Joron and R. Capdevila (1983) Komatitics from French Guyana : Sm-Nd age and REE geochemistry (Abstr.) Terra Cognita, 3, 130.

C.M. Graham (1976) Petrochemistry and tectonic significance of Dalradian metabasalts of the S.W. Scottish Highlands. J.Geol.Soc.Lond.132,61-84.

A.M. Graham and B.G.J. Upton (1978) Gneisses in diatremes, Scottish Midland Valley:petrology and tectonic implications. J.Geol.Soc.Lond.,135,219-228.

D.H. Green (1964)a The petrogenesis of the high-temperature peridotite intrusion in the lizard area,Cornwall.J.Petrol. 5,134-88.

D.H. Green (1964)b The metamorphic aureol of the peridotite at Lizard,Cornwall.J.Geol.Soc.Lond.72,543-63

D.H.Green (1964)c A re-study and re-interpretation of the Lizard peninsula,Cornwall.In Present views of some aspects of the Geology of Cornwall and Devon. Roy.Geol.Sci.Corn., Commen.Vol.87-114.

E.Greenly (1919) The Geology of Anglesey.Mem.Geol.Surv.U.K. Lond.

M.C.Gupta and R.D.Macfarlane (1970) The natural alpha radioactivity of Samarium.J.Inorg.Nucl.Chem.32,3425-32.

A.N. Haliday, W.E. Stephens and R.S. Harmon 1980 Rb-Sr and O isotopic relationships in 3 zoned Caledonian granitic plutons, Southern Uplands, Scotland: evidence for varied sources and hybridization of magmas. J. Geol. Soc. Lond. 137, 329-348.

P.J.Hamilton,N.M.Evensen,R.K.O'Nious,H.S.Smith and A.J.Erlank (1978) Sm-Nd dating of Onverwacht Group volcanics,southern Africa,Nature,279,298-300.

P.J.Hamilton,N.M.Evensen,R.K.O'Nions and J.Tarney (1979) Sm-Nd systematics of Lewisian gneisses:implications for the origin of granulites.Nature,277,25-28.

P.J.Hamilton,R.K.O'Nions and N.M.Evensen (1977) Sm-Nd dating of Archaean basic and ultrabasic volcanics.Earth.Planet.Sci. Lett .,36,263-268.

P.J.Hamilton,R.K.O'Nions and R.J.Pankhurst (1980) Isotpe evidence for the provenance of some Caledonian granites. Nature,287,279-284.

P.J.Hamilton,R.K.O'Nions,N.M.Evensen,D.Bridwater and J.H. Allart (1978) Sm-Nd isotopic investigations of the Isua supracrustals,West Greenland:implications for mantle evolution. Nature,272,41-43.

G.N.Hanson (1977) Geochemical evolution of the suboceanic Mantle. J.Geol.Soc.Lond.134,235-254.

G.N.Hanson (1978) The application of trace elements to the Petrogenesis of igneous rocks of Granite composition. Earth. Planet.Sci.Lett.38,26-42.

W.J.Harrison and B.J.Wood (1980) An Experimental Investigation of the Partitioning of REE between Garnet and Liquid with reference to the role of Defect Equilibria.Contr.Miner. Petrol.72,145-155.

S.R.Hart (1981) Diffusion compensation in natural silicates. Geochim.Comochim.Acta.45.279-293.

S.R.Hart and C.Brooks (1980) Sources of Terrestrial basalts: In:Basaltic Volcanism of the Terrestrial Planets, Lunar and Planetary Institute, Houston.

C.J.Hawkesworth (1982) Isotope characteristics of magmas erupted along destructive plate margins.In: Andesites (Ed) R.S.Thorpe.Wiley, 549 - 71.
C.J.Hawkesworth and P.W.C. van Calsteren (1983) Radiogenic isotopes- some geological applications.In:REE Geochemistry (Ed) P.Henderson, 375 - 421.

C.J.Hawkesworth and M.Powell (1980) Magma genesis in the Lesser Antilles island arc. Earth.Planet.Sci.Lett.51,297-308.

C.J.Hawkesworth,J.D.Kramers and R.M.G.Miller (1981) Old model Nd ages in Namibian Pan-African rocks. Nature,289,278-282.

C.J.Hawkesworth,R.K.O'Nions and R.J.Arculus (1979) Nd and Sr Isotope geochemistry of island arc volcanics,Grenada,Lesser Antilles. Earth.Planet.Sci.Lett.45,237-248.

C.J.Hawkesworth,M.Hammill,A.R.Gedhill,P.van Calsteren and G.Rogers (1982) Isotope and trace element evidence for late-stage intra-crustal melting in the High Andes. Earth.Planet. Sci.Lett. 58,240-254.

C.J.Hawkesworth,R.K.O'Nions,R.J.Pankhurst,P.J.Hamilton and N.M.Evensen (1977) A geochemical study of island arc and back arc tholeiites from the Scotia Sea. Earth.Planet.Sci. Lett.36,253-262.

C.J.Hawkesworth,M.J.Norry,J.C.Roddick,P.E.Baker,P.W.Francis and R.S.Thorpe (1979) $^{143}Nd/^{144}Nd$, $^{87}Sr/^{86}Sr$, and incompatible element variations in calc-alkaline andesites and plateau lavas from South America.Earth.Planet.Sci.Lett.42,45-57.

P.Henderson (1975) Reaction trends shown by chrome spinels of the Rhum layered intrusion. Geochim.Cosmochim.Acta.39, 1035-1044.

P.Henderson and P.Suddaby (1971) The nature and origin of the chrome-spinels in the Rhum layered intrusion. Contrib. Mineral.Petrol. 33,21-31.

P.J.Hooker,P.J.Hamilton,R.K.O'Nions (1981) An estimate of the Nd isotopic composition of Iapetus seawater from ca. 490 Ma metalliferous sediments.Earth.Planet.Sci.Lett.56, 180-188.

F.J.Humphries and R.A.Cliff (1982) Sm-Nd dating and cooling history of Scourian granulites , Sutherland. Nature,295,515.

S.B.Jacobsen and G.J.Wasserburg (1979)a Nd and Sr isotopic study of the Bay of Islands Ophiolite Complex and the evolution of the source of MORB.J.Geophys.Res. 84,7429-7445.

S.B.Jacobsen and G.J.Wasserburg (1979)b The mean age of crustal reservoir. J.Geophys.Res.84,7411-7427.

S.B.Jacobsen and G.J.Wasserburg (1980) Sm-Nd isotopic evolution of chondrites. Earth.Planet.Sci.Lett.50,139-155.

B.Jahn,G.Gruau and A.Y.Glikson (1982) Komatiites of the Onverwacht Group, S.Africa:REE Geochemistry,Sm/Nd Age and Mantle Evolution. Contrib. Mineral.Petrol.80,25-40.

D.E.James (1971) Andean crustal and upper mantle structure. J.Geophys.Res.76,3246-3271.

D.E.James (1982) A combined O,Sr,Nd and Pb isotopic and trace element study of crustal contamination in central Andean lavas,1.Local geochemical variations. Earth.Planet. Sci.Lett.57,47-62.

R.J.Jamieson (1980) Ophiolite emplacement as recorded in the dynamothermal aureole of the St.Anthony complex ,N.W. Newfoundland. In: Proc.Int.Ophiolite Symp.Cyprus,1979 (Ed) Panayiotou,620-627.

R.W. Kay and P.W. Gast 1973. The Rare Earth content and origin of alkali-rich basalts. J. Geol. 81, 653-682.

G.A.Kirby (1978) Layered gabbros in the Eastern Lizard, Cornwall,and their significance. Geol.Mag. 115,199-204.

G.A.Kirby (1979) The petrochemistry of rocks of the Lizard Complex,Cornwall. Unpubl.Ph.D. thesis Univ. of Southampton.

G.A.Kirby (1979) The Lizard complex as an ophiolite. Nature,282,58-61.

A.Kröner,R.E.Jacob and M.Halpern (1978) Rb-Sr geochronology in favour of polymetamorphism in the Pan African Damara belt of Namibia (South West Africa) Geol. Rundschau.67,688-705.

C.H.Langmuir,J.F.Bender ,A.E.Bence,G.N.Hanson and S.R.Taylor. Petrogenesis of basalts from the Famous Area: Mid-Atlantic Ridge.Earth.Planet.Sci.lett.36,133-156.

R.St.J.Lambert,J.A.Winchester and J.G.Holland (1981) Comparitive geochemistry of pelites from the Moinian and Appin group (Dalradian) of Scotland. Geol.Mag.118,477-490.

G.G.Lemon (1952) The Moinian inlier of Rosses Point ,near Sligo,Eire. Geol.Mag. 89,124-128.

G.G.Lemon (1971) The Precambrian rocks of the N.E.Ox Mountains Eire. Geol.Mag.108,193-272.

C.A.Locke (1980) Geophysical investigation of Caledonian Granites within a regional classification. Unpubl.PhD. Open University.

C.B.Long and M.D.Max (1977) Metamorphic rocks in the S.W.Ox Mountains Inlier ,Ireland; their structural compartmentation and place in the Caledonian orogen. J.Geol.Soc.Lond.133,413-432.

C.D.Longman,B.J.Bluck and O.van Breeman (1979) Ordovician conglomerates and the evolution of the Midland Valley . Nature,280,578-581.

M.Loubert and C.J.Allegre (1982) Trace elements in orogenic lherzolites reveal the complex history of the upper mantle. Nature,298,809-814.

M.Loubet,N.Shimizu and C.J.Allegre (1975) Rare Earth Elements in Alpine Peridotites. Contrib.Mineral.Petrol.53,1-12.

G.W. Lugmair and K. Marte (1978) Lunar initial $^{143}Nd/^{144}Nd$: differential evolution of the lunar crust and mantle. Earth Plant. Sci. Lett., 39, 349-357

G. Mahood and W. Hildreth (1983) Large partition coefficients for trace elements in high-silica rhyolites. Geochim. Cosmochim Acta, 47, 11-30.

G. Manhes, J.F. Minster and C.J. Allegre (1978) Comparative unranium-thorium-lead and rubidium-strontium study of the Saint Severin amphoterite: consequences for early solar system chronology. Earth Planet. Sci. Lett., 39, 14-24.

J.M. Martin and M. Meybeck (1979) Elemental mass-balance of material carried by major world rivers. Marine Chem. 7, 173-206.

M.D. Max (1976) The pre-palaeozoic basement in south eastern Scotland and the southern uplands fault. Nature. 264, 485.

M.T. McCulloch and B.W. Chappell (1982a) Nd isotopic characteristics of S- and I- type granites. Earth Planet. Sci. Lett., 58, 51-64.

M.T. McCulloch and W. Compston (1981) Sm-Nd age of Kambalda and Kanowna greenstones and heterogeneity in the Archaean mantle. Nature, 294, 322-327.

M.T. McCulloch and G.J. Wasseburg (1978) Sm-Nd and Rb-Sr chronology of continental crust formation. Science. 200, 1003-1011.

M.T. McCulloch, R.J. Arculus, B.W. Chappell and J. Ferguson (1982). Isotopic and geochemical studies of nodules in Kimberlite have implications for the lower continental crust. Nature, 300, 166-169.

M.T. McCulloch, R.T. Gregory, G.J. Wasserburg and M.P. Taylor (1980). A neodymium, strontium, and oxygen isotopic study of the cretaceous Saamail Ophiolite and implications for the petrogenesis and seawater-hydrothermal alteration of oceanic crust. Earth Planet. Sci. Lett., 46, 201-211.

W.S. McKerrow and L.R.M. Cocks (1976) Progressive faunal migration across Iapetus Ocean. Nature, 263, 304 - 306.

W.S. McKerrow, R. St.J. Lambert and V.E. Chamberlain (1980) The Ordovician, Silurian and Devonian time scales. Earth Planet. Sci. Lett., 51, 1-8.

S.M. McLennan and S.R. Taylor (1982) Geochemical constraints on the growth of the continental crust. J. Geol., 90, 347-361.

S.M. McLennan, B.J. Fryer, G.M. Young (1979) Rare earth elements in Muronian (lower Proterozoic) sedimentary rocks: composition and evolution of the post-Kenoran upper crust. Geochim. Cosmochim. Acta. 43, 375-388.

M.A. Menzies, D. Blanchard, J. Brannon and R. Korotev (1977) Rare earth geochemistry of fused ophiolitic and alpine lherzolites II: Beni Bouchera, Ronda and Lanzo. Contrib. Mineral. Petrol. 64, 53-74.

J.C.C. Mercier and A. Nicolas (1974) Textures and fabrics of Upper-Mantle Peridotites as illustrated by xenoliths from Basalts. J. Pet., 16, 454-487.

J.C.C. Mercier (1976) Single-pyroxene geothermometry and geobarometry. Am. Min., 61, 603-615.

J.C.C. Mercier (1980) Single pyroxene thermobarometry. Tectonophysics, 70, 1-37.

J.A. Miller, D.H. Matthews and D.G. Roberts (1973) Rock of Grenville Age from Rockall Bank. Nat. Phys. Sci. 246, 61.

S. Moorbath (1978) Age and isotopic evidence for the evolution of continental crust. Phil. Trans. R. Soc. Lond., A288, 401-413.

M.D. Muir, G.M. Bliss, P.R. Grant and M. Fischer (1979) Palaeontological evidence for the age of some supposedly Precambrian rocks in Anglesey, North Wales. J. Geol. Soc. Lond., 136, 61-4.

N. Nakamura 1974 Determination of REE, Ba, Fe, Mg, Na and K in carbonaceous and ordinary chondrites. Geochim. Cosmochim. Acta, 38, 757-773.

J.E. Nielson Pike and E.C. Schwarzman (1976) Classification of textures in ultramafic xenoliths, J. Geol. 85, 49-61.

M. Obata (1976) The solubility of Al_2O_3 in orthopyroxene in spinel and plagioclase peridotites and spinel pyroxenite. Am. Mineral. 61, 804-816.

P.J. O'Connor and P.M. Burck (1978) Age and Origin of the Leinster Granite. J. Earth Sci. R. Dubl. Soc. 1, 105-113.

R.K. O'Nions, N.M. Evensen and P.J. Hamilton (1979) Geochemical modelling of mantle differentiation and crustal growth. J. Geophys. Res., 84, 6091-6101.

R.K. O'Nions, P.J. Hamilton and N.M. Evensen (1977) Variations in $^{143}Nd/^{144}Nd$ and $^{87}Sr/^{86}Sr$ ratios in oceanic basalts. Earth Planet. Sci. Lett., 34, 13-22.

R.K. O'Nions. P.J. Hamilton and P.J. Hooker (1983) A Nd isotope investigation of sediments related to crustal development in the British Isles. Earth. Plant. Sci. Lett. 63, 229-240.

R.K.O'Nions, S.R. Carter, R.S. Cohen, N.M. Evensen and P.J. Hamilton (1978) Pb, Nd and Sr isotopes in oceanic ferromanganese deposits and ocean floor basalts. Nature. 273, 435-438.

J.P. Patchett, N.H. Gale, R. Goodwin and M.J. Humm (1980) Rb-Sr whole-rock isochron ages of late Precambrian to Cambrian igneous rocks from southern Britain. J. Geol. Soc. Lond., 137, 649-56.

R.J. Pankhurst and R.T. Pidgeon (1976) Inherited isotope systems and the source region pre-history of early Caledonian granites in the Dalradian series of Scotland. Earth Planet. Sci. Lett., 31, 55-68.

R.J. Pankhurst, J.R. Andrews, W.E.A. Phillips, I.S. Sanders and W.E.G. Taylor (1976) The age and structural setting of the Slieve Gamph Igneous Complex, Co. Mayo, Eire. J. Geol. Soc. Lond., 132, 327-34.

D.A. Papanastassiou and G.J. Wasserburg (1969) Initial strontium isotopic abundances and the resolution of small time differences in the formation of planetory objects. Earth Planet. Sci. Lett., 5, 361-376.

J.A.Pearce (1982) Trace element characteristics of lavas from destructive plate boundaries.In: Andesites (Ed) R.S Thorpe, Wiley, 525 - 48.

J.A.Pearce (1983) Role of the sub-continental lithosphere in magma genesis at active continental margins.In:Continental Basalts and Mantle Xenoliths (Eds) C.J.Hawkesworth and M.J. Norry. (Shiva), 230 - 49.

J.A.Pearce and J.R.Cann (1974) Tectonic setting of basic volcanic rocks determined using trace element analysis. Earth Planet. Sci. Lett. 19,291-303.

J.A.Pearce and M.J.Norry (1979) Petrogenetic implications of Ti,Zr,Yand Nb variations in volcanic rocks. Contrib.Mineral. Petrol. 69,33-45.

Z.E.Peterman,C.E.Hedge and H.A.Tourtelot (1970) Isotopic composition of strontium in seawater throughout Phanerozoic time. Geochim.Cosmochim. Acta. 34 ,105-120.

W.E.A. Phillips,C.J.Stillman and T.Murphy (1976) A Caledonian plate tectonic model. J.Geol. Soc Lond. 132,579-595.

W.E.A. Phillips, W.E.G. Taylor and I.S. Sanders (1975) An analysis of the geological history of the Ox Mountain inlier. Scient. Proc. R. Dubl. Soc. 5A, 311-329.

R.T. Pidgeon and M. Aftalion (1978) Cogentic and inherited zircon U-Pb systems in granites: Palaeozoic granites of Scotland and England. In Crustal evolution in northwest Britain and adjacent regions. (Eds. Bowes and Leake), 183 - 220.

D.J. Piepgras and G.J. Wasserburg (1980) Neodymium isotopic variations in Seawater. Earth Plant. Sci. Lett. 50, 128-138.

D.J. Piepgras, G.J. Wasserburg and E.J. Dasch (1979) The isotopic composition of Nd in different ocean masses. Earth Planet. Sci. Lett., 45, 223-236.

R. Powell (1978) The thermodynamics of pyroxenes geotherms. Phil. Trans. Roy. Soc. Lond., A288, 457-469.

C. Pride and G.K. Muecke (1982) Geochemistry and origin of Granitic Rocks, Scourian Complex, N.W. Scotland. Contrib. Min. Petrol. 80, 379-385.

Pugh and Winslow, 1967 The analysis of Physical Measurements. Addison-Wesley.

P.Richard,N.Shimizu and C.J.Allegre (1976) $^{143}Nd/^{146}Nd$, a natural tracer : an application to oceanic basalts, Earth. Planet. Sci. Lett. 31,269-278.

I.S. Sanders (1979) Observations on eclogite- and granulite-facies rocks in the basement of the Caledonides. In: The Caledonides of the British Isles - reviewed. Geol. Soc. Lond. 97-100.

L.D. Sanders (1955) Structural observations on the south-east Lizard. Geol. Mag., 92, 231-40.

J.G. Schilling (1971) Sea-floor evolution: rare-earth evidence. Phil. Trans. R. Soc. Lond., A, 268, 663-706.

M.P. Searle, S.J. Lippard, J.D. Smewing and D.C. Rex. (1980)

Volcanic rocks beneath the Semail Ophiolite Nappe in the northern Oman mountains and their significance in the Mesozoic evolution of Tethys. J. Geol. Soc. Lond., 137, 589-604.

R.M. Shackleton (1954) The structure and succession of Anglesey and the Lleyn Peninsula. Advmt. Sci. Lond., 11, 106-8.

R.M. Shackleton (1969) The Precambrian of North Wales. In (A. Wood, ed:) The Precambrian and Lower Palaeozoic rocks of Wales. University of Wales Press, Cardiff, 1-22.

J.W. Shearton, A.C. Skinner and J. Tarney (1973) The geochemistry of the Scourian gneisses of the Assynt district, in: The Early Precambrian of Scotland and Related rocks of Greenland, R.G. Park and J. Tarney (eds.), Univ. Keele, 13-30.

J.G. Spray (1982) Mafic segregations in ophiolite mantle sequences. Nature, 299, 524-528.

R.H. Steiger and E. Jager (1977) Subcommission on geochronology: convention on the use of decay constants in geo- and cosmo- chronology. Earth Planet. Sci. Lett., 36, 359-362.

C.J. Stillman and C.T. Williams (1978) Geochemistry and Tectonic setting of some Upper Ordovician Volcanic Rocks in East and Southeast Ireland. Earth Planet. Sci. Lett. 41, 288-310.

C.J. Stillman, K. Downes and E.J. Schiener (1974) Caradocian Volcanic activity in east and south-east Ireland. Sci. Proc. R. Dublin Soc. 5A, 87-98.

P. Strogen (1974) The sub-Palaeozoic basement in central Ireland. Nature vol. 250, 562.

D.F. Strong, R.K. Stevens, J. Malpas and J.P.N. Badham (1975) A new tale for the Lizard. Pro. Ussher Soc., 3, 252.

M.T. Styles and G.A. Kirby (1980) New investigations of the Lizard Complex, Cornwall, England and a discussion of an Ophiolite model. Proceedings International Ophiolite Symposium Cyprus 1979, 517-526.

J. Tarney (1976) Geochemistry of Archean high-grade gneisses, with implications as to the origin and evolution of the Precambrian crust. In: The Early History of the Earth, B.F. Windley (Ed.) Wiley, Lond. 405-417.

J. Tarney and B.F. Windley (1977) Chemistry, thermal gradients and evolution of the lower continental crust. J. Geol. Soc. Lond., 134, 153-172.

M. Tatsumoto, (1978) Isotopic composition of lead in oceanic basalt and its implication of mantle evolution. Earth. Planet. Scil. Lett., 38, 63-87.

M. Tatsumoto, D.M. Unruh and G.A. Desborough (1976) U-Th-Pb and Rb-Sr systematics of Allende and U-Th-Pb systematics of Orgueil. Geochim. Cosmochim. Acta, 40, 617-634.

H.P. Taylor (1980) The effects of assimilation of country rocks by magmas on $^{18}O/^{16}O$ and $^{87}Sr/^{86}Sr$ systematics in igneous rocks. Earth. Planet. Sci. Letts., 47, 243-254.

S.R. Taylor and S.M. McLennon (1981) The rare earth element evidence in Precambrian sedimentary rocks: implications for crustal evolution, in: Precambrian Plate Tectonics, A. Kroner (ed.), Elsevier, Amsterdam, 527-548.

M.F. Thirlwall (1982) Systematic variation in chemistry and Nd-Sr isotopes across a Caledonian calc-alkaline volcanic arc: implications for source materials. Earth Planet. Sci. Lett., 58, 27-50.

M. Thoni, R.G. Miller and R.K. O'Nions (1983) Nd-siotopic study of British river sediments and particulates from the W. Atlantic (Abstr.) Terra Cognita, 3, 132.

R.S. Thorpe, P.W. Francis and R.S. Harmon (1981) Andean andesites and crustal growth. Phil. Trans. R. Soc. Lond., A.301, 305-320.

R.S. Thorpe, P.W. Franci and L.O'Callaghan (in press). Relative roles of source composition, fractional crystallization and crustal contamination in petrogenesis of Andean volcanic rocks. Phil. Trans. R. Soc. Lond.

R.S. Thorpe, R.D. Beckinsale, P.J. Patchett, J.D.A. Piper, G.R. Davies and J.A. Evans (in press). Crustal growth and late Precambrian-Palaeozoic plate tectonic evolution of England and Wales. J. Geol. Soc.

A.G. Tindle (1982) Petrogenesis of the Loch Doon Granitic intrustion, Southern Uplands of Scotland. Ph.D. Thesis Open University.

A.G. Tindle and J.A. Pearce (1981) Petrogenetic modelling of in situ fractional crystallization in the Zoned Loch, Doon Pluton, Scotland. Contrib. Mineral Petrol. 78, 196-207.

A.G. Tindle and J.A. Pearce (In Press) Assimilation and Partial Melting of Continental Crust: evidence from the mine alogy and geochemistry of autoliths and xenoliths. Lithos

S.R. Taylor and S.M. McLennan (1981) The composition and evolution of the continental crust: rare earth element evidence from sedimentary rocks. Phil. Trans. R. Soc. Lond., A301, 381-399.

B.G.J. Upton, P. Aspen and N.A. Chapman (1983) The upper mantle and deep crust beneath the British Isles: evidence from inclusions in volcanic rocks. J. Geol. Soc., 140, 105-122.

B.G.J. Upton, R. Aspen, A.M. Graham and N.A. Chapman (1976) Pre-Palaeozoic basement of the Scottish Midland Valley. Nature, 260, 517-8.

O. van Breemen and C.J. Hawkesworth (1980) Sm-Nd isotopic study of garnets and their metamorphic host rocks. Trans. R. Soc. Ed. 71, 97 - 102.

O. van Breemen, A.N. Halliday, M.R.W. Johnson and D.R. Bowes (1978) Crustal additions in late Precambrian times. In: Crustal evolution in northwestern Britain and adjacent regions. 81 - 106.

J.R. Vearncombe (1980) The Lizard Ophiolite and two phases of suboceanic deformation. In: Proceedings International Ophiolite. Symposium Cyprus 1979, ed. A. Panayiotou 527-537.

J. Veizer and W. Compston (1974) $^{87}Sr/^{86}Sr$ composition of seawater during the Phanerozoic. Geochim. Cosmochim. Acta, 34, 105-120.

G.J. Wasserburg, S.B. Jacobsen, D.J. De Paolo, M.T. McCulloch and T. Wen, (1981) Precise determination of Sm/Nd ratios, Sm and Nd isotopic abundances in standard solutions. Geochim. Cosmochim. Acta, 45, 2311-2324.

B.L. Weaver and J. Tarney (1980) Rare earth geochemistry of Lewisian granulite- facies gneisses, north west Scotland: Implications for the petrogenesis of the Archean lower continental crust. Earth. Planet. Sci. Lett., 51, 279-296.

B.L. Weaver and J. Tarney (1981) Lewisian gneiss geochemistry and Archean crustal development models. Earth. Planet. Sci. Letts., 55, 171-180.

P.R.A. Wells (1977) Pyroxene thermometry in simple and complex systems. Contrib. Mineral, Petrol, 62, 129-139.

D.J. Whitford, W. Compston and I.A. Nicholls (1977) Geochemistry of late Cenozoic lavas from eastern Indonesia: Role of subducted sediments in petrogenesis. Geol. 5, 571-575.

D.J. Whitford, I. A. Nichols and S.R. Taylor (1979) Spatial variations in the geochemistry of quaternary lavas across the Sunda Arc in Java and Bali. Contrib. Min. Petrol. 70, 431-356.

D.J. Whitford and P.A. Jezek (1982) Isotopic constraints on the role of subducted sialic material in Indonesian Island-arc magmatism. Geol. Soc. of America Bullet. v.93, 504- 513.

G.V. Wilson (1918) Preliminary notes on volcanic rocks in north west Ayrshire. Trans. Geol. Soc. Glasgow, 16, 86-99.

J.A. Winchester, R.G. Park and J.G. Holland (1980) The Geochemistry of Lewisian Semipelitic Schists from the Gairloch District, Western Ross. Scott. J. Geol. 16, 165-179.

J.A. Winchester, R. St. J. Lambert and J.G. Holland (1981) Geochemistry of the western part of the Moinian assemblage Scott. J. Geol. 17, 281-294.

T.J. Wolery and N.H. Sleep (1976) Hydrothermal circulation and geochemical flux at mid-ocean ridges. J. Geol. 84, 249-258.

D.A. Wood, S.L. Joron, M. Trevil, M. Norry and J. Tarney (1979) Elemental and Sr Isotope variations in basic lavas from Iceland and the surrounding ocean floor. Contrib. Mineral. Petrol. 70, 319-339.

D.S. Wood (1974) Ophiolite, melange, blueschists and ignimbrites: early Caledonian subduction in Wales? In (R.H. Dott and R.H. Shaver, eds.) Modern and Ancient Geosynclinal sedimentation. Spec. Publ. Soc. Econ. Paleont. Mineral. Tulsa, 19, 334-44.

M. Wood and G.D. Nicholls (1973) Precambrian stromatolitic limestones from Northern Anglesey. Nature (Phys. Sci.), Lond., 24, 65 - 68.

B.W.D. Yardley, C.B. Long and M.D. Max (1979) Patterns of metamorphism in the Ox Mountains and adjacent parts of Western Ireland. In: The Caledonides of the British Isles - reviewed. 1979 Geological Society of London, 369 - 74.

D. York (1969) Least squares fitting of a straight line with correlated errors. Earth Planet. Sci. Lett., 5, 320-324.

A. Zindler, C. Brooks, N.T. Arndt and S. Hart (1978) Nd and Sr isotope data from Komatiitic and tholeiitic rocks of Munro Township, Ontario. 4th Int. Conf. Geochron. Cosmochron. Isotope Geol., 469-471.